New Technology for Longwall Ground Control

Proceedings: U.S. Bureau of Mines Technology Transfer Seminar

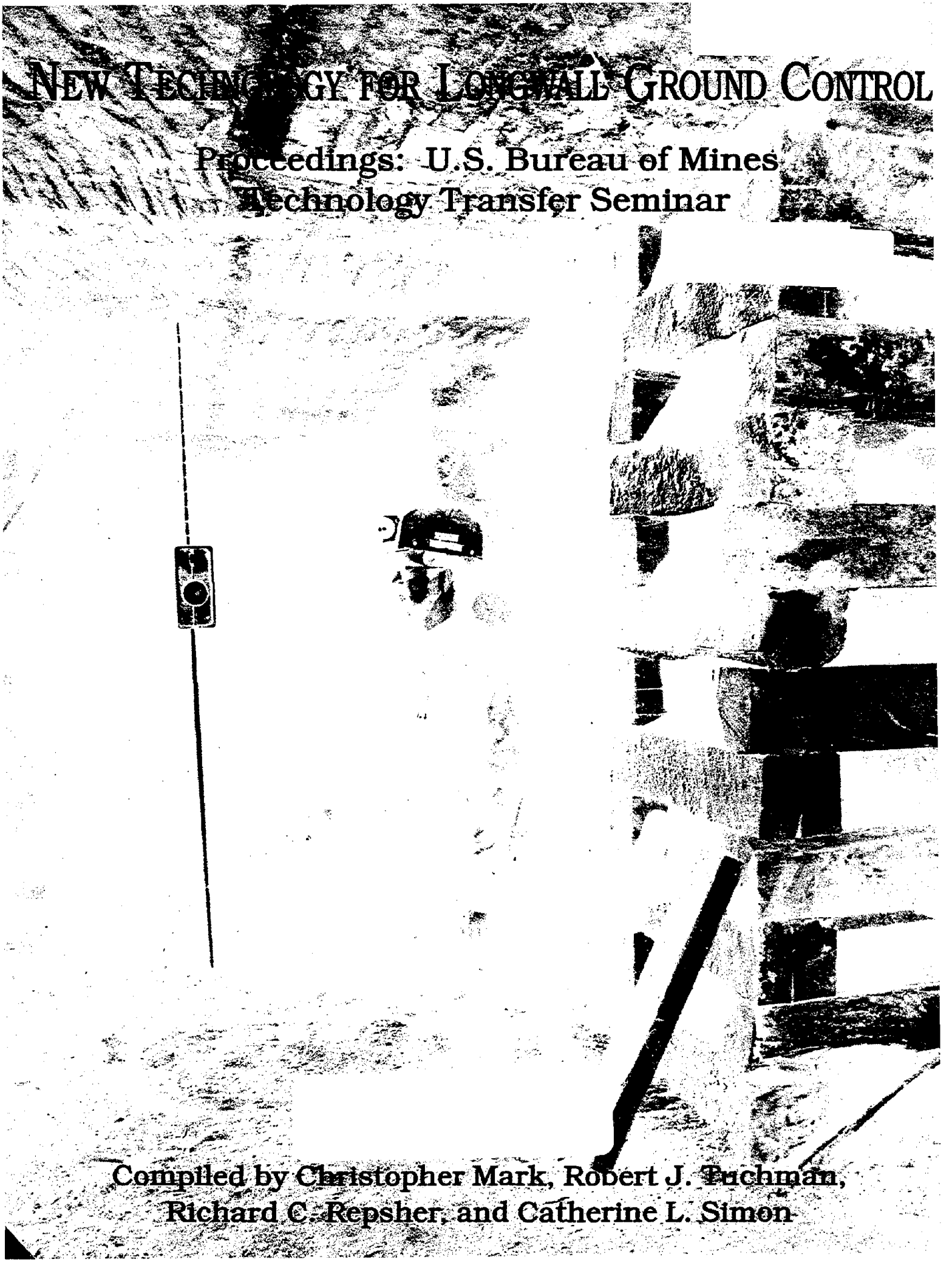

Compiled by Christopher Mark, Robert J. Tuchman, Richard C. Repsher, and Catherine L. Simon

Special Publication 01-94

New Technology for Longwall Ground Control

Proceedings: U.S. Bureau of Mines Technology Transfer Seminar

Compiled by Christopher Mark, Robert J. Tuchman, Richard C. Repsher, and Catherine L. Simon

UNITED STATES DEPARTMENT OF THE INTERIOR
Bruce Babbitt, Secretary

BUREAU OF MINES

Cover Photograph: The U.S. Bureau of Mines has developed highly practical technologies for maintaining effective ground control in the hazardous tailgate entries of longwall mining systems, which will significantly improve the safety of the Nation's underground mineworkers. *(Photo: Alan A. Campoli, Pittsburgh Research Center, U.S. Bureau of Mines)*

For sale by the Superintendent of Documents, U.S. Government Printing Office
Washington, D.C. 20707

CONTENTS

UNIT OF MEASURE ABBREVIATIONS USED IN THIS REPORT

cm	centimeter	m^2	square meter
cm^2	square centimeter	mA	milliampere
d	day	mi	mile
ft	foot	min	minute
GPa	gigapascal	mm	millimeter
h	hour	MPa	megapascal
in	inch	mt	metric ton
in^2	square inch	mV	millivolt
kg	kilogram	N	newton
km	kilometer	N/m	newton per meter
kN	kilonewton	pct, %	percent
kPa	kilopascal	psi	pound (force) per square inch
lb	pound	s	second
lbf	pound force	st	short ton
lb/ft	pound per foot	V	volt
m	meter	°	degree

Reference to specific products does not imply endorsement by the U.S. Bureau of Mines.

NEW TECHNOLOGY FOR LONGWALL GROUND CONTROL

Proceedings: U.S. Bureau of Mines Technology Transfer Seminar

**Compiled by Christopher Mark,[1] Robert J. Tuchman,[2]
Richard C. Repsher,[3] and Catherine L. Simon[4]**

ABSTRACT

This proceedings volume contains papers presented at the U.S. Bureau of Mines (USBM) technology transfer seminars on New Technology for Longwall Ground Control. These seminars were conducted in Washington, PA, on April 12, 1994, and Denver, CO, on May 10, 1994. The papers herein describe several new, highly practical USBM technologies now available for ground control in longwall mines, including the Coal Mine Roof Rating (CMRR), cable bolts, the MULSIM/NL numerical model, and the Wood Crib Performance Model. Other significant topics addressed include longwall panel layout, coal pillar design, horizontal stress in longwall mines, roof support selection for gate entries, and ground control monitoring.

[1]Mining engineer, Pittsburgh Research Center, U.S. Bureau of Mines, Pittsburgh, PA.
[2]Writer-editor, Pittsburgh Research Center, U.S. Bureau of Mines, Pittsburgh, PA.
[3]Staff engineer, Div. of Health, Safety, and Mining Technology, Research Directorate, U.S. Bureau of Mines, Washington, DC.
[4]Editor, Office of Technology Transfer, Research Directorate, U.S. Bureau of Mines, Washington, DC.

INTRODUCTION

By Christopher Mark[1] and Richard C. Repsher[2]

Longwall mining has revolutionized the coal industry in the United States during the last 20 years. In 1973, primitive longwalls accounted for only 3% of the Nation's underground coal production (*2*).[3] Today, 75 longwall mines produce more than 40% (*6-7*). This remarkable record was achieved through the rapid development of all aspects of longwall technology. The radically different mining designs, equipment, and production rates utilized by longwalls challenged the U.S. Bureau of Mines (USBM) to develop new solutions for ground control, dust control, methane gas control, and other health and safety concerns.

A major thrust of ground control research has been to improve the stability of longwall gate entries. Gate entries are the lifelines through which mineworkers, supplies, and ventilating air reach the longwall working face, and they are the escape routes needed by miners in case of an emergency. They must remain operational despite the heavy abutment loads resulting from longwall mining. A gate entry blocked by a roof fall constitutes a major safety hazard to miners, as well as a substantial expense for the mine operator.

This proceedings volume describes a number of new, extremely practical USBM technologies now available for gate entry ground control. The papers herein encompass a wide range of issues, including panel layout, coal pillar and entry design, mine roof support, and ground control monitoring strategies. They discuss proven techniques, not just theories, and they focus on how to implement them. Two other significant concerns in longwall ground control—coal mine bumps and face support—are addressed in other USBM publications (*1, 3-5*).

The papers by Mark/Chase/Molinda and by DeMarco address the conventional and yielding approaches to longwall pillar and entry design. The Analysis of Longwall Pillar Stability (ALPS) design method is already widely used throughout the coal mining industry for sizing conventional longwall pillars, but there has been some uncertainty as to the appropriate stability factor to employ with it. The new research presented here shows that tailgate performance also depends on mine roof quality—weaker roof needs larger pillars. The Coal Mine Roof Rating (CMRR) has been developed by the USBM as a simple technique for measuring roof quality, and recommendations are presented for utilizing the CMRR to select the proper ALPS stability factor, entry width, and primary support density. Yield pillar designs are an attractive alternative for many deep-cover, bump-prone, and multiple-seam applications. A survey of the experience of western U.S. longwall mines with yielding pillar systems is presented, together with a review of many years of USBM research. The results highlight the importance of pillar width-to-height ratio, roof quality, and support to the performance of yield pillar systems.

Several new concepts for the design of longwall panels are presented in the papers by Mark/Mucho and by Zipf. Horizontal stress is shown to be widespread in U.S. coalfields, and its significant effects on longwall ground control are documented. A stress map of the United States is presented, along with a compilation of underground stress measurements from U.S. coal mines and simple field procedures for determining local stress fields. Recommendations are also given for minimizing the effects of horizontal stress through panel orientation, panel sequencing, mining direction, roof support, and stress relief. MULSIM/NL is a powerful three-dimensional computer program tool for stress analysis of complex mine layouts and multiple-seam interactions. Recommendations for material properties for use in the program are provided, along with several examples that illustrate MULSIM/NL's application to longwall panels.

Roof support in longwall gate entries is the subject of three other papers in this proceedings volume. Longwall mines in the United States develop more than 1,700 km (1,000 mi) of longwall gate entries each year, and primary roof support is provided by the approximately 5 million roof bolts installed annually. Signer describes procedures developed by the USBM to evaluate roof bolt performance in different geologic environments. The field instrumentation used and some preliminary results leading toward the development of scientific design recommendations are also described. Wood cribbing, the subject of the paper by Barczak/Gearhart, has been the traditional supplemental support for longwalls, especially in tailgate entries. Remarkably little engineering currently goes into wood crib

[1]Mining engineer, Pittsburgh Research Center, U.S. Bureau of Mines, Pittsburgh, PA.

[2]Staff engineer, Div. of Health, Safety, and Mining Technology, Research Directorate, U.S. Bureau of Mines, Washington, DC.

[3]Italic numbers in parentheses refer to items in the list of references at the end of this introduction.

design, considering that the material cost alone for tailgate support in the United States exceeds $25 million annually. The Wood Crib Performance Model described by Barczak/Gearhart matches the stiffness, stability, and strength of the crib structure with the expected rock mass behavior. It can be used to help determine a crib design and employment spacing that will provide optimum support. Cable bolts, discussed by Tadolini/Gallagher, represent an innovative departure from traditional support concepts. Widely used in metal mines and foreign longwalls, they offer significant advantages with regard to materials handling and ventilation in addition to ground control. Resin-grouted cable bolt technology is now available for wide application in U.S. mines. This technology is described here, along with some quite favorable field results.

The remaining two papers address the use of ground control monitoring in longwall mines. Maleki describes techniques that have been used, including measurements of roof deformation, crosshole seismics, and stress measurements. He provides examples to illustrate how the rate of roof sag, changes in seismic velocity, and location of stress concentrations can be used to infer structural stability. A major impediment to widespread monitoring in the past is that it has been highly labor-intensive. Computerized minewide monitoring systems have now made routine, real-time ground control monitoring achievable. The McDonnell/Cox/Dunford paper discusses three examples of the use of minewide monitoring, along with the instrumentation and techniques for acquisition, analysis, and display of geostructural data from longwall operations. It appears certain that the future will witness increasing use of this technology.

Longwall mining now constitutes the predominant underground mining method in many major coal-producing areas of the United States, including the Pittsburgh Coal Seam in the northern Appalachian Mountains, the Herrin (No. 6) Coal Seam in Illinois, the Blue Creek Coal Seam in Alabama, and the western coalfields. The highly useful USBM ground control technologies presented in this proceedings volume will help longwall mines provide a safer underground working environment for their mineworkers, optimize daily operations, and avoid the costly mistakes that still occur. In other regions, notably the southern Appalachians, longwalls have been less successful. Ground control has forced at least two longwalls in the southern Appalachians to close, and all other longwalls in the area have experienced significant ground control problems. Improved ground control engineering could be the key that makes the continued expansion of longwall mining possible.

REFERENCES

1. Barczak, T. M. Examination of Design and Operation Practices for Longwall Shields. USBM IC 9320, 1992, 14 pp.

2. ____. The History and Future of Longwall Mining in the United States. USBM IC 9316, 1992, 26 pp.

3. Barczak, T. M., D. E. Schwemmer, and C. L. Tasillo. Practical Considerations in Longwall Face and Gate Road Support Selection and Utilization. USBM IC 9217, 1989, 22 pp.

4. Campoli, A. A., T. M. Barton, F. C. Van Dyke, and M. Gauna. Mitigating Destructive Longwall Bumps Through Conventional Gate Entry Design. USBM RI 9325, 1990, 38 pp.

5. Haramy, K. Y., and J. D. McDonnell. Causes and Control of Coal Mine Bumps. USBM RI 9225, 1988, 35 pp.

6. Merrits, P. C. 1993 U.S. Longwall Census. Coal, Feb. 1993, pp. 26-35.

7. U.S. Department of Energy, Energy Information Administration (EIA). Coal Production 1992. DOE/EIA-0118(92), Oct. 1993, 112 pp.

DESIGN OF LONGWALL GATE ENTRY SYSTEMS USING ROOF CLASSIFICATION

By Christopher Mark,[1] Frank E. Chase,[2] and Gregory M. Molinda[2]

ABSTRACT

Successful longwall mining requires a stable tailgate entry. Gate entry performance is influenced by a number of geotechnical and design factors, including:

- Pillar size and pillar loading;
- Roof quality;
- Floor quality;
- Entry width;
- Artificial support (primary and secondary).

This paper describes a comprehensive, practical design methodology based on statistical analysis of a nationwide database of longwall ground control experience.

Geotechnical surveys were conducted by U.S. Bureau of Mines (USBM) researchers at 44 U.S. longwall mines, and underground observations of site geology, entry conditions, and support design were recorded at each mine. The observations were combined with discussions with mine personnel to identify 69 longwall gate entry designs as satisfactory, unsatisfactory, or borderline. Only conventional longwall designs, in which the pillars are expected to carry the full abutment loads, were included in the database. Designs that employed yield pillars only were excluded.

The case histories were characterized using five descriptive parameters. Pillar design was described by the Analysis of Longwall Pillar Stability Factor (ALPS SF). A major new contribution is the Coal Mine Roof Rating (CMRR), a rock mass classification system that quantifies the structural competence of bolted mine roof. Other rating scales were developed for primary support, secondary support, and entry width.

Statistical analyses indicated that in 84% of the case histories the tailgate performance could be predicted correctly using only ALPS and the CMRR. Most of the misclassified cases fell within a very narrow borderline region. The analyses also confirmed that primary support and gate entry width are essential elements in successful gate entry design. The relative importance of the floor and of secondary support could not be determined from the data.

Based on these results, a simple equation was developed to guide the design of longwall pillars and gate entries:

$$\text{ALPS SF}_R = 1.76 - 0.014\ \text{CMRR},$$

where ALPS SF_R = ALPS SF suggested for design.

Guidelines for entry width and primary support density, as related to the CMRR, are also provided.

[1]Mining engineer.
[2]Geologist.
Pittsburgh Research Center, U.S. Bureau of Mines, Pittsburgh, PA.

INTRODUCTION

During the past decade, longwall mining has become the predominant mining method at large underground coal mines. Average face productivity has nearly quadrupled and now stands near 2,400 clean tons per unit shift. In 1991, 76 longwall mines accounted for nearly 40% of all U.S. underground coal production. (*3, 6, 8*).[3]

Ground control has been an important element in improved longwall performance. Fifteen years ago, there were no reliable guidelines for designing either gate entries or chain pillars. Tailgate failures occurred frequently, and the literature of the time describes many instances when roof falls, floor heave, or pillar sloughage impeded face advance and ventilation. The safety implications of tailgate blockages were further underscored by the Wilberg Mine disaster in 1984, and regulations introduced by the U.S. Mine Safety and Health Administration (MSHA) in 1988 required that roof control plans address the issue of maintaining safe travelways on the tailgate side of the longwall (30 CFR 75).

Responding to the need for better conditions, ground control researchers focused initially on the design of longwall chain pillars. Many mines had found by trial and error that tailgate conditions could improve significantly when pillar sizes were increased. Data published by Mark (*4*) confirmed the correlation between pillar design and tailgate stability. Of 46 case histories of unsatisfactory tailgate designs, only 1 occurred when the ALPS SF was greater than 1.3.

While the various pillar design formulations proposed during the 1980's built upon this correlation, it was also evident that pillar design is not the *only* factor affecting tailgate stability. Indeed, experience and common sense strongly suggest that roof quality and entry support also play a significant role. As Wilson noted, studies conducted as early as the 1960's had concluded that "whether or not the stress [from an extracted longwall panel] will influence a roadway depends more on the strength of the rocks which surround the roadway itself than on the width of the intervening pillar" (*2*).

The study described in this paper began with the hypothesis that tailgate performance is determined by six factors:

- Pillar design and loading;
- Roof quality;
- Floor quality;
- Entry width;
- Primary support;
- Supplemental support.

The study examined the relative importance of these parameters and developed a design methodology for gate entries, not just pillars. The approach was to analyze actual longwall mining experience.

The sections that follow describe how the data were collected and how the necessary rating scales were derived.

DATA COLLECTION

Data for the study were collected during a series of mine visits conducted between October 1988 and June 1992. A total of 44 mines were included, representing approximately 55% of all U.S. longwall mines in operation during the time period. The mines were selected to represent a geographic and geologic cross-section of the U.S. longwall experience. Every State with an operating longwall except Ohio was included (figure 1).

At each mine, information was collected through underground geotechnical surveys and discussions with mine personnel. The underground surveys documented geology, support, and gate entry conditions. Standardized data sheets were used to record rock mass properties observed in underground exposures, usually roof falls and/or overcasts. Other data sheets were used at coalbed and floor exposures, and at the headgate and tailgate corners of the longwall.

The discussions with mine personnel focused on past experience with gate entry ground control. Panels in which conditions had been satisfactory were identified, as were locations where conditions were unsatisfactory. Where conditions were considered unsatisfactory, the steps taken by management to prevent reoccurrence were documented.

[3]Italic numbers in parentheses refer to items in the list of references at the end of this paper.

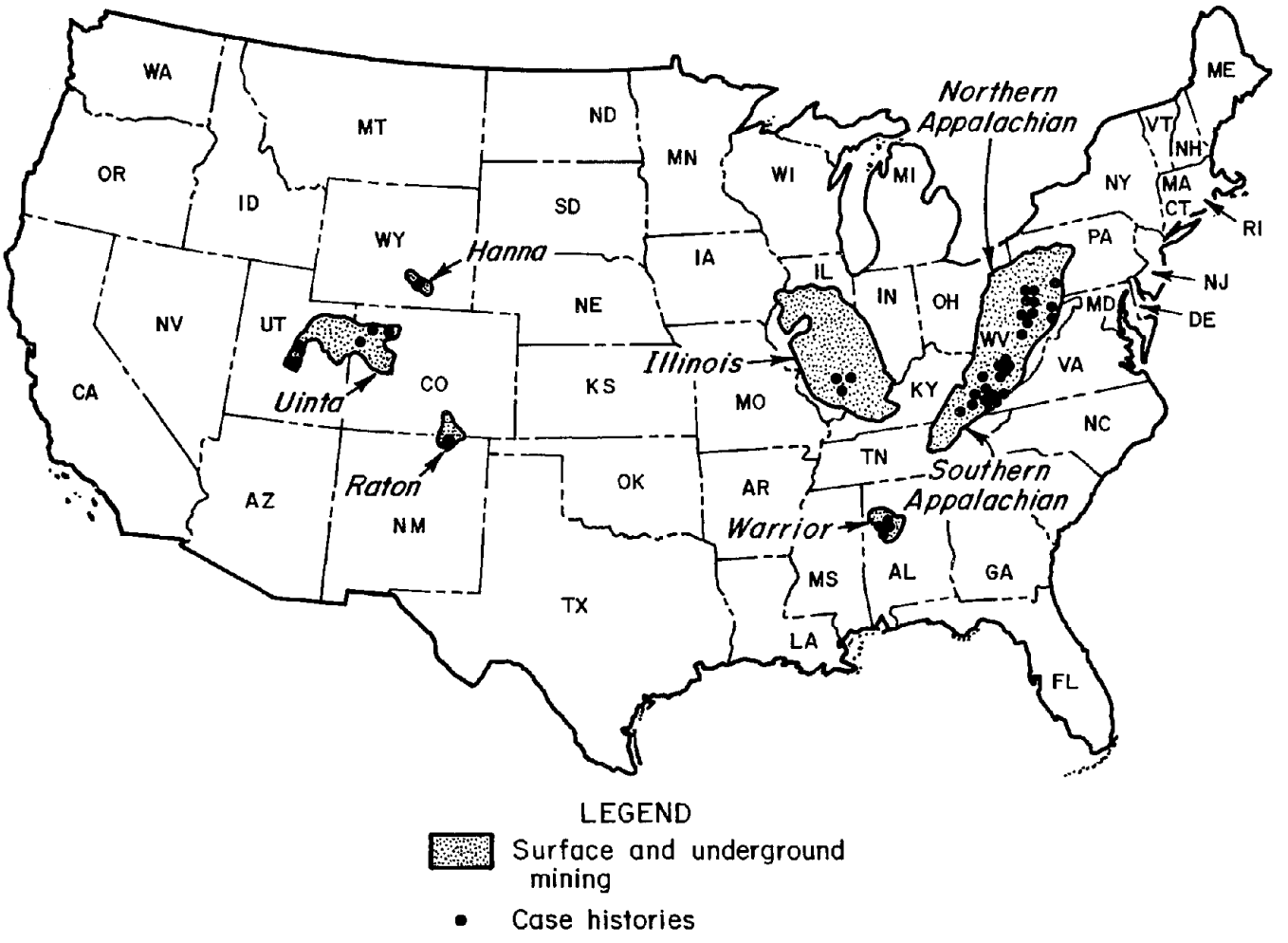

Figure 1.—Location of geotechnical surveys conducted by USBM ground control researchers.

DESCRIPTION OF THE DATABASE

A total of 62 individual longwall case histories were distilled from the data. The database was limited to conventional designs where the pillars were sized to carry the full abutment loads (5). Total yielding pillar designs were excluded. Each complete case history was defined by approximately 50 individual data fields, which were in turn used to define 7 summary variables. The first of these variables is Design Performance, which is the "outcome" or "dependent" variable in the analysis. The other six are "explanatory" or "dependent" variables. Tables 1 and 2 summarize the information included in the longwall tailgate performance case history database.

DESIGN PERFORMANCE

The case histories were each classified as "satisfactory" (30 cases) or "unsatisfactory" (32 cases). Unsatisfactory conditions almost always included roof deterioration and falls, although floor heave and pillar sloughage were often cited as well. To be classified as unsatisfactory, a case had to meet one of four criteria:

- Management changed the pillar design or the entry support in response to the poor tailgate conditions (25 cases).
- The panel was abandoned owing to poor conditions (2 cases).
- Unacceptable conditions developed in the areas of deepest cover (2 cases).
- Several falls above the bolt anchorage occurred in the tailgate, resulting in tailgate blockages and significant longwall delays (3 cases).

Satisfactory cases, in contrast, were those in which—

- The design was used for at least three successive panels;

Table 1.— Unsatisfactory tailgate case histories

State and seam	ALPS Stability Factor	Coal Mine Roof Rating	Entry width, m	Primary Support Rating	Secondary Support Rating
Alabama:					
Blue Creek	0.96	49	6.2	0.50	0.16
Do	0.94	49	6.2	0.28	0.75
Do	0.85	49	6.2	0.15	0.27
Do	0.44	49	6.2	0.18	0.16
Colorado:					
D Seam	1.02	51	5.5	0.31	0.44
Wadge	0.45	62	5.8	0.15	0.50
Kentucky:					
Harlan	0.42	63	5.5	0.26	1.14
Lower Elkhorn	0.66	85	6.2	0.19	0
Taggart	0.41	54	6.2	0.15	0.53
Warfield	0.92	56	6.2	0.12	0.27
New Mexico:					
Left Fork	0.52	31	5.5	0.25	0.88
Pennsylvania:					
Pittsburgh	0.81	39	5.2	0.30	0.66
Pittsburgh	0.90	46	5.2	0.22	0.38
Pittsburgh	1.02	34	5.2	0.26	0.41
Utah:					
Castlegate	0.28	80	5.2	0.21	0.67
Castlegate	0.41	80	5.2	0.21	0.67
Wattis	0.41	69	6.2	0.15	0.66
Virginia:					
Jawbone	0.80	54	5.8	0.23	0.15
Lower Banner	1.58	45	6.3	0.21	0.21
Pocahontas No. 3	0.36	78	6.2	0.15	0.25
Taggart	0.63	58	5.5	0.30	0.38
West Virginia:					
Campbell Creek	0.75	38	5.8	0.19	0.33
Do	0.75	52	5.8	0.21	0.25
Do	0.62	38	5.8	0.19	0.25
Do	0.58	58	5.8	0.15	0.31
Do	0.72	52	5.2	0.23	0.25
Eagle	0.62	60	5.7	0.20	0.13
Pittsburgh	0.93	39	4.8	0.20	0.33
Pittsburgh	0.99	38	4.2	0.09	0.24
Pittsburgh	1.24	38	4.2	0.09	0.24
Upper Freeport	0.89	44	5.2	0.26	0.25
Wyoming:					
Hanna	1.01	43	5.5	0.29	0

Do. Same as above.

Table 2.— Satisfactory tailgate case histories

State and seam	ALPS Stability Factor	Coal Mine Roof Rating	Entry width, m	Primary Support Rating	Secondary Support Rating
Alabama:					
Blue Creek	1.18	49	6.2	0.18	0.16
Do	1.14	49	6.2	0.50	0.16
Do	1.16	49	6.2	0.28	0.37
Do	1.16	70	6.2	0.10	0.06
Colorado:					
E Seam	0.50	77	5.8	0.18	0.75
Illinois:					
Herrin No. 6	1.33	49	4.6	0.15	0.37
Do	1.33	49	4.6	0.28	0.37
Do	1.38	49	4.9	0.26	0.15
Kentucky:					
Alma	1.42	56	6.2	0.12	0.50
Elkhorn No. 2	0.85	85	6.2	0.19	0
Do	0.78	85	6.2	0.19	0.25
Taggart	0.92	54	6.2	0.15	0.20
Pennsylvania:					
Lower Kittanning	1.72	56	5.5	0.20	0.18
Pittsburgh	1.18	34	5.2	0.26	0.41
Pittsburgh	1.23	41	4.8	0.24	0.35
Pittsburgh	1.61	39	5.2	0.30	0.66
Pittsburgh	1.40	34	5.2	0.26	0.41
Virginia:					
Dorchester	1.21	45	5.8	0.23	0.12
Jawbone	0.91	65	5.8	0.23	0.30
Jawbone	1.03	65	5.8	0.23	0.30
Pocahontas No. 3	0.63	78	6.2	0.15	0.25
West Virginia:					
Campbell Creek	0.79	58	5.8	0.15	0.31
Do	0.86	67	5.8	0.15	0.31
Eagle	0.90	50	5.2	0.23	0.23
Eagle	1.04	60	5.7	0.20	0.13
Pittsburgh	1.27	38	4.2	0.50	0.38
Pittsburgh	1.38	39	4.8	0.20	0.33
Pittsburgh	0.87	38	4.2	0.50	0.38
Pittsburgh	1.77	46	4.2	0.20	0.19
Upper Freeport	1.59	44	5.2	0.26	0.30

Do. Same as above.

- Tailgate blockages were very rare or nonexistent; *and*
- Good conditions, with minimal delays attributable to ground control, were reported.

In some instances, a single, satisfactory case represents as many as 50 extracted panels. Where the depth of cover varied, the deepest cover was used to characterize the satisfactory case. Because previous studies had indicated that failures were very rare when the ALPS SF exceeded 1.3, no cases were included where the ALPS SF exceeded 2.0. Figure 2 shows the regional distribution of the satisfactory and unsatisfactory designs.

PILLAR DESIGN

Pillar design was characterized using the ALPS SF. The ALPS SF is defined as:

$$\text{ALPS SF} = \frac{\text{Estimated load-bearing capacity of pillar system}}{\text{Estimated load applied to pillars at tailgate corner}} .$$

The estimated load-bearing capacity is determined by the width-to-height ratios and the total load-bearing area of the pillars composing the pillar system. The estimated load is determined by the depth of cover, the panel width, and the extraction ratio within the gate entry system. Details on calculation of the ALPS SF have been published elsewhere (*4-5*). The distribution of the ALPS SF within the database is shown in figure 3.

Although data were collected at each site on the cleat, bedding, and other structural characteristics of the coal seams, no attempt was made to determine the in situ coal strength. As discussed elsewhere (*4*), there is little evidence that coal strength significantly affects tailgate entry performance.

ROOF QUALITY

One of the keys to the success of this research was the development of the CMRR as a quantitative measure of the structural competence of coal mine roof. The CMRR weighs the importance of the geotechnical factors that determine roof competence and combines these values into a single rating on a scale from 0 to 100. Three significant contributions of the CMRR are that it—

- Focuses on the characteristics of bedding planes, slickensides, and other discontinuities that determine the structural competence of sedimentary coal measure rocks.
- Applies to all U.S. coalfields and allows a meaningful comparison of structural competence even where lithologies are quite different.
- Treats the bolted interval as a single structure, while considering the contributions of the different lithologic units that may be present within it.

The field data necessary for calculation of the CMRR are typically obtained from underground exposures of the roof strata in roof falls or overcasts. The following features of the roof rock are observed:

- Shear strength of discontinuities (roughness and cohesion);
- Intensity of discontinuities (spacing and persistence);
- Strength and weatherability of the rock;
- Presence of a strong bed within the bolted interval;
- Number of beds within the bolted interval;
- Quality of the rock overlying the bolted interval;
- Quantity of groundwater inflow.

Full details on the collection of field data and the determination of the CMRR are presented in reference (*7*).

The CMRR of the roofs observed at the longwalls varied from a low of 30 to a high of 85. Within this range, three broad classes of roof emerged as follows:

- *Weak* roof (CMRR<45): Roof typically consisting entirely of low strength 56 MPa (<8,000 psi), closely bedded, jointed, and/or slickensided rocks, usually shales and coals.
- *Moderate* roof (45<CMRR<65): Bolted interval usually contains at least one competent unit, typically a siltstone or strong shale, i.e., at least 0.6 m (2 ft) thick containing few bedding planes or other discontinuities.
- *Strong* roof (CMRR>65): Bolted interval typically contains at least one very competent, massive bed, at least 1 m (3 ft) thick that exceeds 56 MPa (8,000 psi) in strength, usually a sandstone or limestone.

Figure 4 shows the geographic distribution of the CMRR in the database. It can be seen that mines in the northern Appalachians (Pennsylvania, Maryland, and northern West Virginia) were characterized primarily by *weak* roof. Mines in Illinois and Alabama had mainly *moderate* roof, and in Utah the roof was usually in the *strong* category. In the other two regions—the southern Appalachians (Virginia, eastern Kentucky, and southern West Virginia) and in Wyoming-Colorado-New Mexico—the roofs were distributed among all three classes.

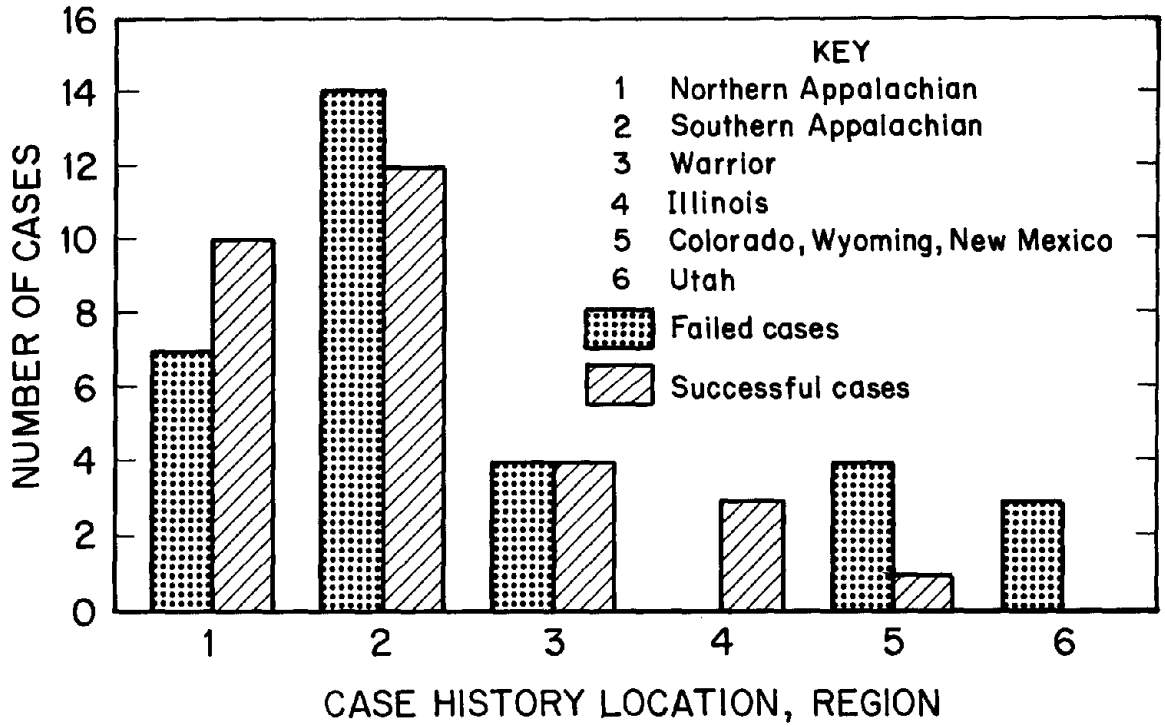

Figure 2.—Case location distribution.

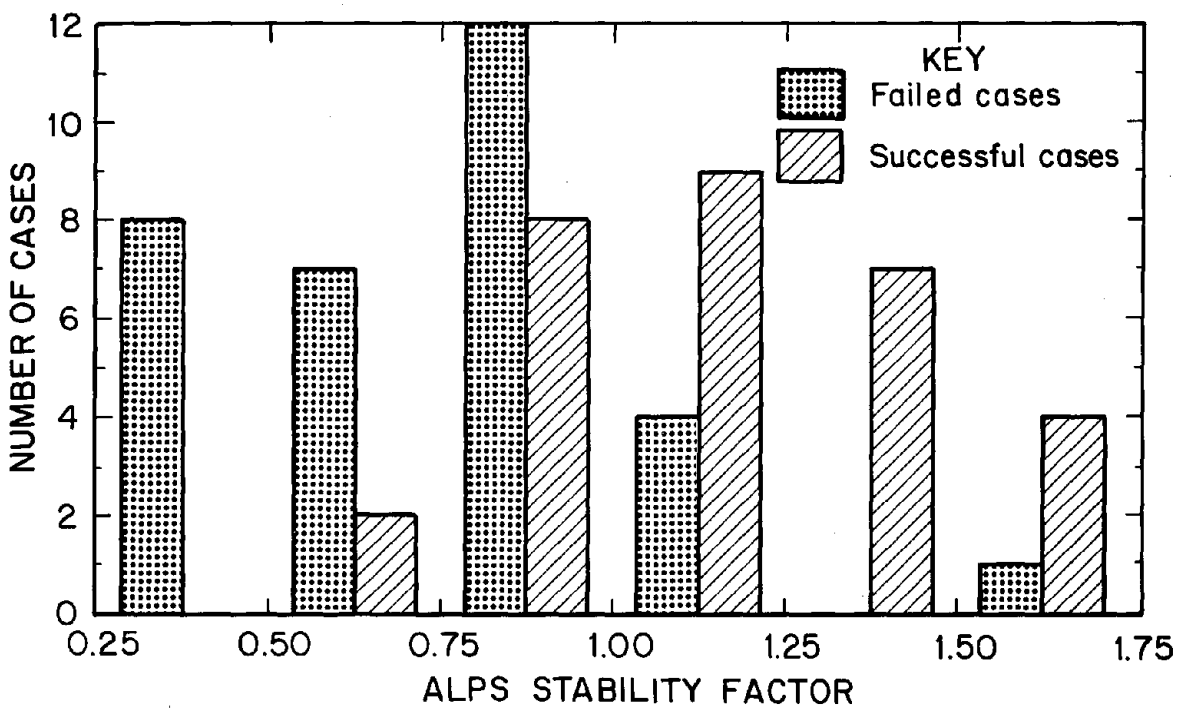

Figure 3.—ALPS SF distribution.

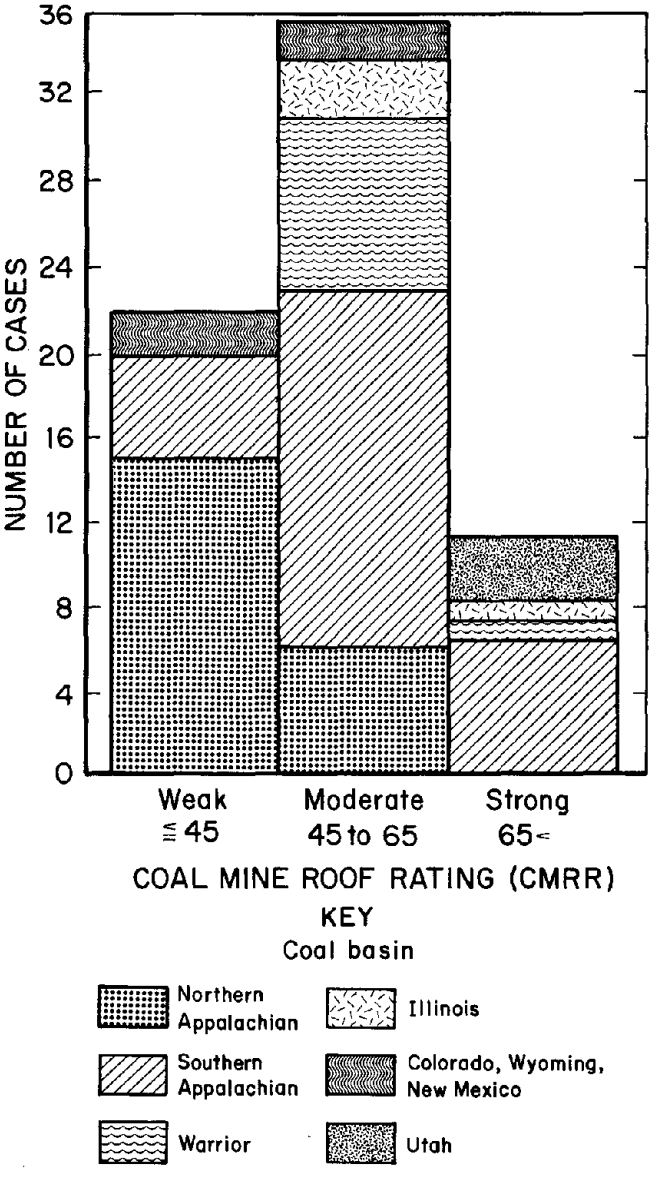

Figure 4.—CMRR distribution.

ENTRY WIDTH

No rating system needed to be developed to characterize entry width. For consistency, the entry width used in the analysis is as-mined, without considering the effects of rib sloughage. The range of entry widths within the database is shown in figure 5.

PRIMARY SUPPORT

A wide variety of primary (roof bolt) support fixtures and patterns were used in the longwall mines studied. Data collected underground included the type of bolt, bolt length and diameter, bolting pattern, plate type and dimensions, and additional support (mats, headers, mesh, etc.). The Primary Support Rating (PSUP) used in the analysis was developed as a rough measure of roof bolt density:

$$PSUP = \frac{Lb * Nb * Db}{Sb * We * 84}, \quad (1)$$

where Lb = Length of the bolt (m),

Nb = Number of bolts per row,

Db = Diameter of the bolts (mm),

Sb = Spacing between rows of bolts (m),

and We = Entry width (m).

In other words, the PSUP increases if the length of the bolts, the bolt diameter, or the number of bolts in a row increases. It is reduced if the entry width or the spacing between rows is increased. PSUP treats all bolts equally, without attempting to pass judgment on the relative reinforcement value of different types of fixtures. Figure 6 shows the distribution of PSUP in the database.

SECONDARY SUPPORT

The most common type of secondary support used in the tailgates, by far, was wood cribbing. Concrete fibercrete cribs were used in only one case, and in three cases no secondary supports were installed. The Secondary Support Rating (SSUP) is a rough measure of the volume of wood installed per unit length of the tailgate:

$$SSUP = \frac{Nc * Lc * Wc}{Sc * 0.3}, \quad (2)$$

where Nc = Number of rows of cribs installed,

Lc = Length of the crib blocks (m),

Wc = Width of the crib block (as installed, m),

and Sc = Center-to-center between cribs in each row (m).

The SSUP increases if more rows or cribs are installed or if the length or width of the crib blocks is increased. It is reduced if the spacing between cribs is increased. Figure 7 shows the distribution of SSUP.

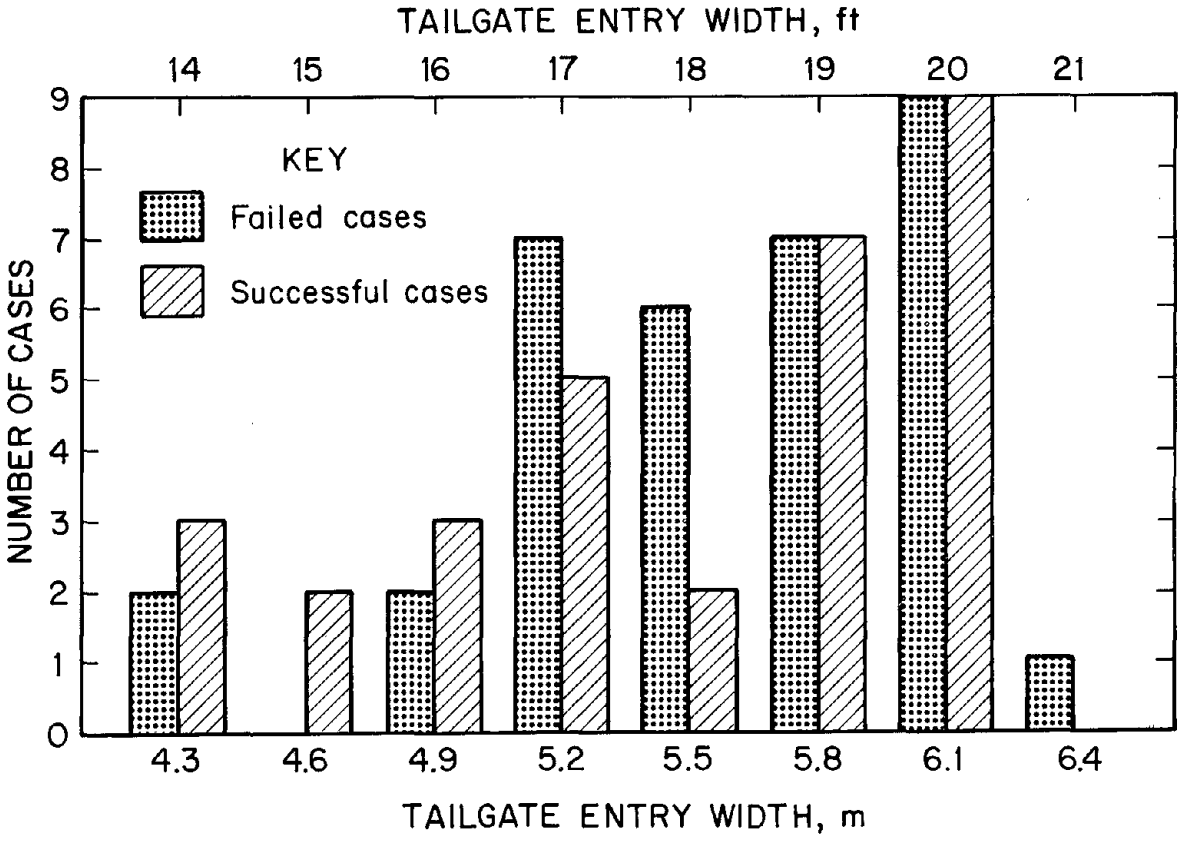

Figure 5.—Tailgate entry width distribution.

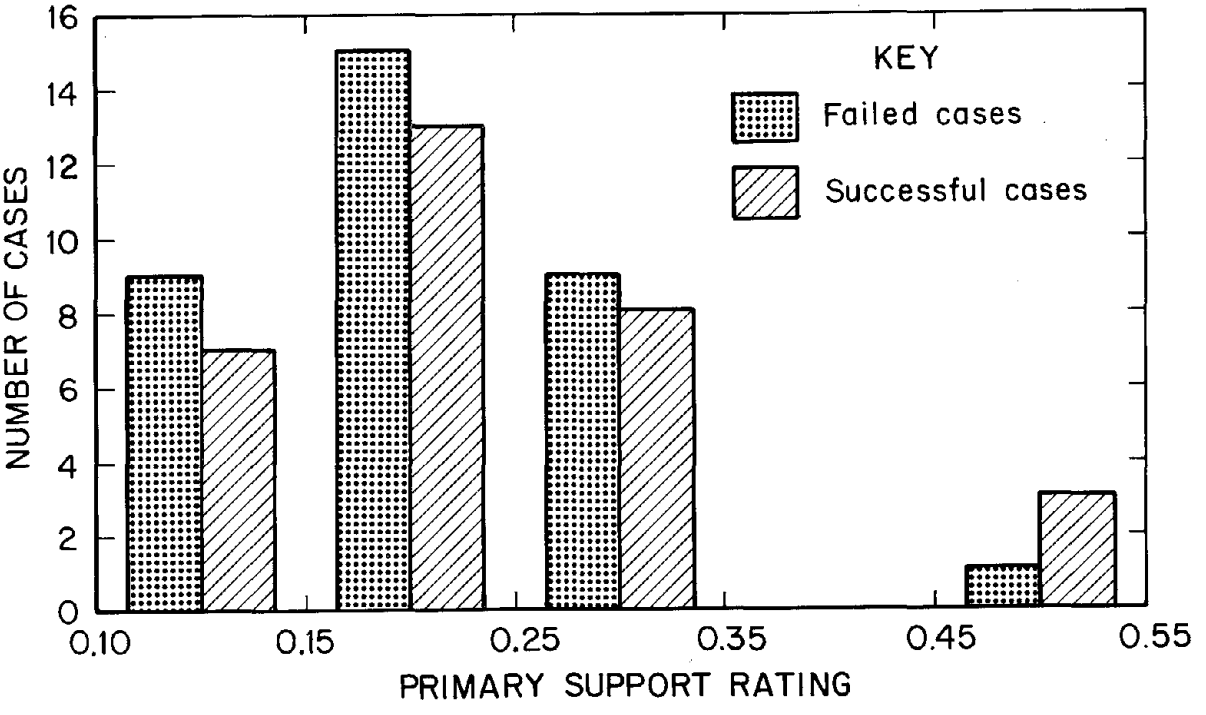

Figure 6.—Primary support distribution.

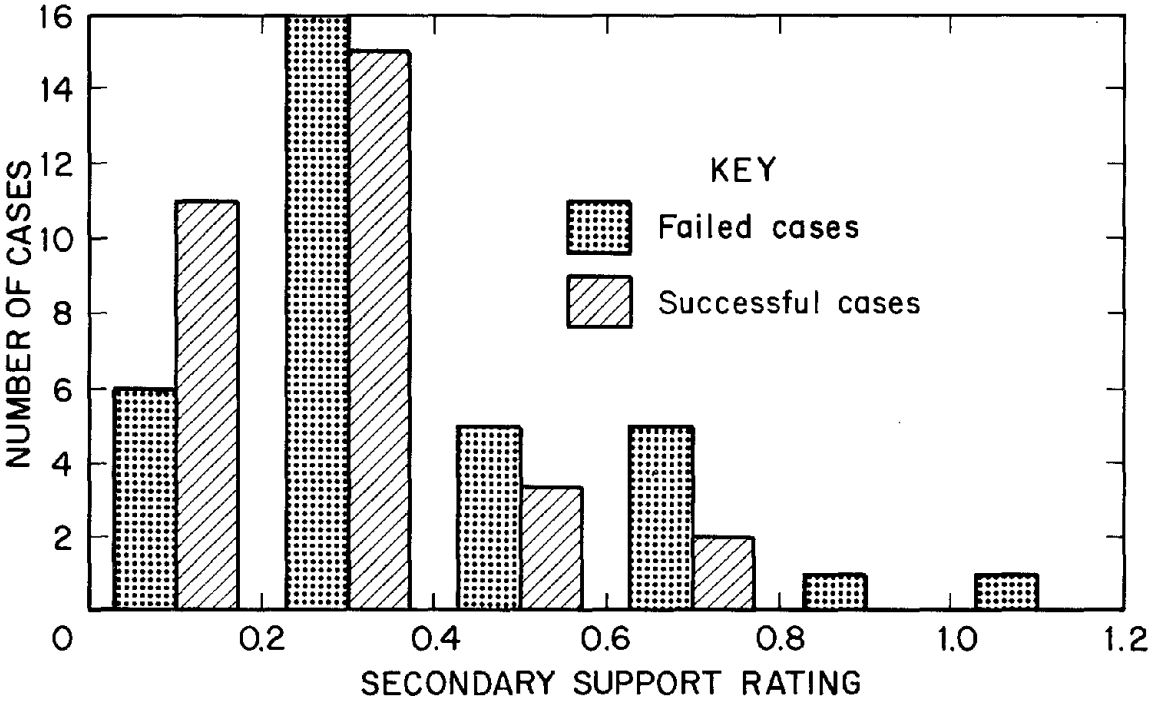

Figure 7.—Secondary support distribution.

FLOOR QUALITY

Characterizing the floor presented special difficulties. While attempts were made to collect data on the lithology and structure of the mine floors, good underground exposures were often unavailable. The floor has received relatively little research attention, so not all of the important information may have been collected. In the end, it was not possible to construct a meaningful floor rating system from the data available, and the floor could not be included in the analyses.

STATISTICAL ANALYSIS

The goals of the statistical analysis were to—

- Determine which parameters are significantly related to tailgate entry performance.
- Classify each case history as a success or failure using a predictive model (or classification rule) based on those parameters.
- Develop an equation that can be used in design.

The statistical technique of discriminant analysis was employed. Discriminant analysis is a regression method that classifies observations into two populations. The statistical package SPSS was used in all computations.

The first step was to determine which variables were significant predictors of tailgate entry performance. Using a significance level of "alpha" = 0.05, only two variables, ALPS SF and CMRR, were included in the model. The discriminant equation was calculated as

$$Z = 4.10\ (\text{ALPS SF}) + 0.057\ (\text{CMRR}) - 6.83, \quad (3)$$

where Z = discriminant.

When the discriminant (Z) value of a case is greater than zero, tailgate conditions are predicted to be satisfactory, whereas unsatisfactory conditions are predicted when Z is less than zero.

Equation 3 can be rearranged to relate ALPS SF to CMRR:

$$\text{ALPS SF} = 1.67 - 0.014\ \text{CMRR}. \quad (4)$$

The model represented by equations 3 and 4 successfully identified all but 11 cases, for an overall success rate of 82%. The misclassifications were evenly divided between satisfactory and unsatisfactory designs. Figure 8 shows the complete database, with equation 4 represented as the discriminant equation.

While equation 4 could be used directly in design, a more conservative equation that reduced the misclassification rate for unsatisfactory designs might be more appropriate. Moreover, it is evident from figure 8 that most of the misclassifications fall very near the discriminant equation. By designating a borderline region in which the outcome is uncertain, the total number of misclassifications is reduced to three, for an overall misclassification rate of 5%. The upper bound of the borderline region is shown in figure 8 as the design equation:

$$\text{ALPS SF}_R = 1.76 - 0.014\ \text{CMRR}, \qquad (5)$$

where ALPS SF_R is the ALPS SF suggested for design.

The lower bound of the borderline region is defined by equation 6:

$$\text{ALPS SF} = 1.58 - 0.014\ \text{CMRR}. \qquad (6)$$

The three remaining misclassifications can perhaps be explained by exceptional conditions. The two unsatisfactory cases that fell within the region of predicted satisfactory designs were also the only unsatisfactory cases in which *no* secondary support was installed in the tailgate. Conversely, the misclassified satisfactory case used significantly more than the average amount of artificial support.

Numerous other statistical analyses were performed on the complete data set on subsets. The most significant, and initially surprising, result was that including additional variables in the model did not improve the predictive capacity. The explanation is that primary support and entry width are correlated with the CMRR and the ALPS SF at a statistically significant level of "alpha" = 0.05. Figure 9 shows the correlation between entry width and the CMRR. Of the 14 mines with *weak* roof (CMRR≤45), all but 1 employed entries no more than 5.5 m (18 ft) wide. Conversely, of 20 mines with CMRR>55, 19 used entry widths that were 5.5 m (18 ft) or wider. It appears that mine operators have "naturally" adapted to weaker roof by using narrow entries. A similar, though less pronounced, correlation between primary support and the CMRR is evident in figure 10.

None of the predictive models presented thus far have included supplemental support. This is because the unsatisfactory case histories in the database tended to use more supplemental support than did the satisfactory cases (see figure 7). The positive correlation between unsatisfactory conditions and heavy supplemental support arises because the installation of more cribbing is often the only available means of trying to save a troubled tailgate. In other words, the level of SSUP was often a consequence, not a cause, of the outcome. As a result, when SSUP was forced into a predictive model, the implication was that tailgate conditions would *improve* as tailgate support was *decreased*. Such a conclusion would obviously be incorrect. The inability of the data to help determine the role of supplemental support in tailgate performance points to a limitation of the back calculation method. The data suggest, however, that installing more supplemental support is not usually a satisfactory substitute for an adequate pillar design.

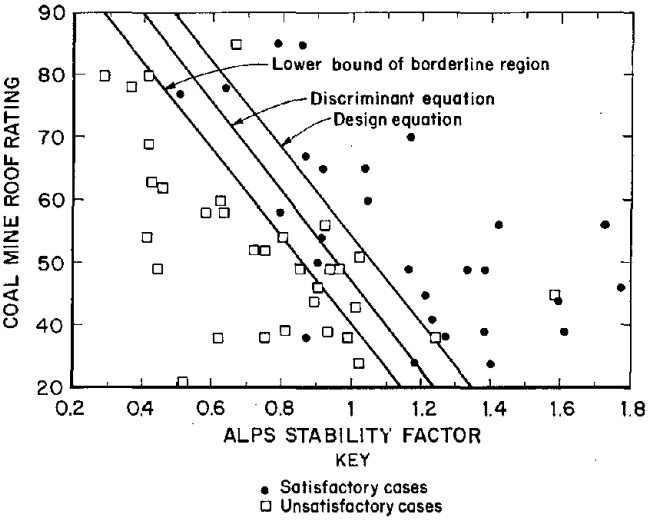

Figure 8.—Scatter plot of case histories.

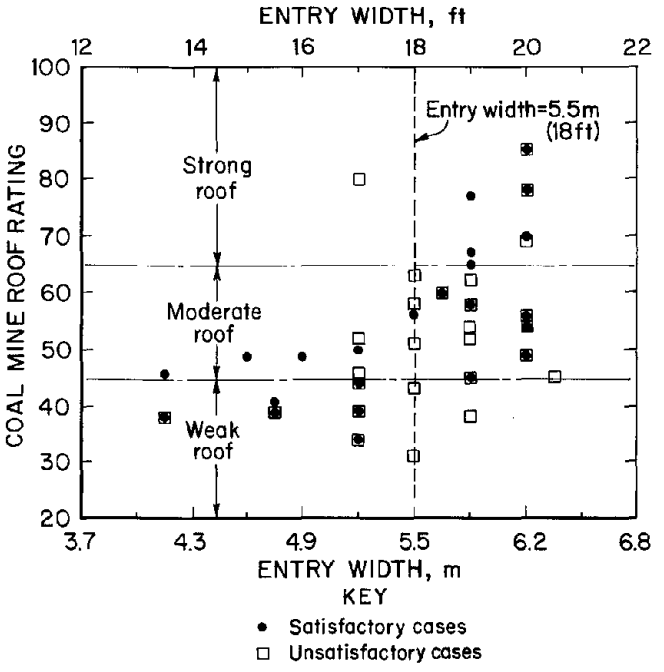

Figure 9.—Entry width versus CMRR.

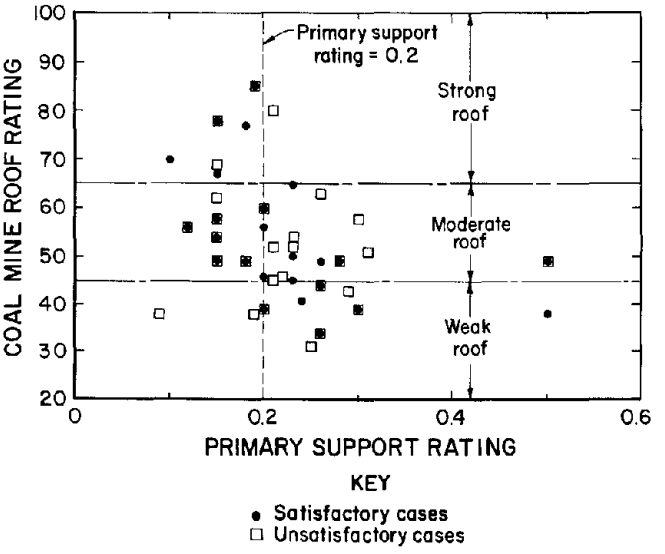

Figure 10.—Primary support versus CMRR.

GUIDELINES FOR GATE ENTRY DESIGN

For practical design, the most significant conclusions from the study are:

- The three key design elements determining tailgate performance are *pillar sizing*, *entry width*, and *primary support*.
- Gate entry design *must* be based on the roof quality.

The first step is to evaluate roof conditions. If nearby underground exposures are available, the CMRR may be determined directly. The CMRR may also be estimated from core logs, although detailed procedures for determining the CMRR from core are still being developed. The complete CMRR database, containing more than 100 observations from throughout the U.S. coalfields, is also available as a further aid in estimating the CMRR (*7*). In most instances, however, it is probably sufficient to place the mine roof into one of the three categories described above: *strong* (CMRR > 65), *moderate* (45 < CMRR < 65), or *weak* (CMRR < 45).

The next step is to use ALPS to determine the pillar size. Single copies of the ALPS computer program may be obtained by sending one double-sided, double-density diskette to: Christopher Mark, U.S. Bureau of Mines, Pittsburgh Research Center, Cochrans Mill Rd., P.O. Box 18070, Pittsburgh, PA 15236-0070.

Given the appropriate CMRR, ALPS SF for use as the design criterion can be obtained using equation 5. The research indicates that achieving the proper ALPS SF is essential to tailgate performance. For *weak* roof, an ALPS SF of 1.3 appears appropriate, while in *strong* roof an ALPS SF of 0.7 should perform adequately. Other aspects of pillar design, including the number of entries and the widths of the individual pillars, may be determined by ventilation or other operational considerations.

Finally, the entry width and the primary support may be estimated from what has been successful in the past. In *weak* roof, it appears that the entry width should be less than 5.2 m (17 ft), as shown in figure 9. Longer bolts, typically at least 1.8 m (6 ft), also appear appropriate to achieve a PSUP of 0.25. In *strong* roof, entries of 6.2 m (20 ft) and a PSUP of 0.15 appear to be adequate. While the study was not successful in defining the necessary secondary support, the indications are that if the other criteria are met, no more than a moderate level of cribbing should be necessary.

Suggested design guidelines for three typical roof conditions are summarized in table 3.

Table 3.—Suggested gate entry design guidelines for three typical roof conditions

	Weak roof (CMRR = 35)	*Moderate* roof (CMRR = 55)	*Strong* roof (CMRR = 75)
Suggested ALPS SF	1.3	1.0	0.7
Entry width, m (ft)	4.3 (16)	5.8 (19)	6.2 (20)
Primary Support Rating	0.25	0.2	0.15

CONCLUSIONS

A comprehensive study of tailgate performance was conducted at 44 U.S. longwall mines. Statistical analysis of the data indicated that performance could be accurately predicted by the ALPS and the CMRR. The analysis also indicated that entry width and primary support are important, but they were not explicitly included in the predictive model because they were highly correlated in practice with the CMRR. The importance of floor quality and secondary support could not be determined from this data set.

The gate entry design methodology that resulted from the study should be a valuable aid to longwall mine planners. It is the first design methodology to focus on the tailgate entry itself, rather than on the chain pillars. More importantly, it is based on the scientific interpretation of the ground control experience obtained at more than one-half of all U.S. longwalls. The method thus makes the wealth of U.S. longwall experience available in a practical form.

This paper also illustrates the power of the empirical, back calculation approach in deriving practical solutions to complex ground control problems. The CMRR makes a critical contribution by providing a meaningful, quantitative measure of the structural competence of bolted mine roof. Both back calculation and the CMRR can be expected to figure prominently in future USBM ground control research.

REFERENCES

1. Afifi, A. A., and V. Clark. Computer-Aided Multivariate Analysis. Lifetime Learning Publications, 1984, Belmont, CA, 458 pp.

2. Carr, F., and A. H. Wilson. A New Approach to the Design of Multi-Entry Developments for Retreat Longwall Mining. Paper in Proceedings of the 2nd Conference on Ground Control in Mining, Morgantown, WV, 1982, pp. 1-21.

3. Combs, T. H. Longwall Productivity Dips 2% From 1990 Record. Coal, Feb. 1993, pp. 36-37.

4. Mark, C. Analysis of Longwall Pillar Stability (ALPS): An Update. Paper in Proceedings of the Workshop on Coal Pillar Mechanics and Design. USBM IC 9315, 1992, pp. 238-249.

5. Mark, C. Pillar Design Methods for Longwall Mining. USBM IC 9247, 1990, 52 pp.

6. Merrits, P. C. 1993 U.S. Longwall Census. Coal, Feb. 1993, pp. 26-35.

7. Molinda, G. M., and C. Mark. Coal Mine Roof Rating (CMRR): A Practical Rock Mass Classification for Coal Mines. USBM IC, 1994, in press.

8. U.S. Department of Energy, Energy Information Administration (EIA). Coal Production 1991. DOE/EIA-0118(91), p. 35.

YIELDING PILLAR GATE ROAD DESIGN CONSIDERATIONS FOR LONGWALL MINING

By Matthew J. DeMarco[1]

ABSTRACT

With the ever present pressures to both expedite longwall gate road development and optimize panel entry stability, the use of yield pillars, either alone or in combination with larger, stiff abutment pillars, has become a topic of considerable interest worldwide. To help provide mine operators with a clearer understanding of the successful application of yielding gate road systems, this paper summarizes western U.S. longwalling experiences with yield pillar design, artificial support installation, entry configurations, and the general degree of gate stability achieved for various mining settings. Additionally, the concepts of the "critical pillar" and "optimum-time-to-yield" are discussed, and a brief qualitative analysis of a limited database is presented that demonstrates a potentially high correlation between a number of mining parameters and the stability performance of the yielding entry system. Preliminary conclusions drawn from this cursory evaluation include the following:

- No successful yield pillar designs were achieved in settings where the Coal Mine Roof Rating (CMRR) (5)[2] was less than 50 (on a scale of 0 to 100).
- No successful yield pillar designs employed width-to-height ratios (w/h) greater than 5.
- Mining depth and floor quality are largely insignificant where the performance of yielding designs are concerned, but greatly influence whether a critical pillar design will bump violently or damage roof and floor members due to pillar punching.

While U.S. Bureau of Mines (USBM) research continues to develop a proven, comprehensive design methodology for yielding gate road systems, this report serves as a summary reference in support of the emerging acceptance of yield pillar usage in U.S. longwalling.

INTRODUCTION

The design of safe, productive longwall entry systems in difficult mining conditions has long been a subject of contention among labor, regulatory, and mine operator groups in the Western United States. It has only gained national attention since the Wilberg Mine disaster in 1984 near Orangeville, UT, which involved the controversial use of a two-entry, yield pillar gate road design. In fact, deep, multiseam, severely bump-prone mining conditions and the highly competitive western U.S. coal market have, for nearly 3 decades, made the design of successful, high-performance gate road systems an engineering priority, *critical* to the economic survival of the mine. To overcome these unique mining conditions, full-yielding gate road systems—those solely employing yield pillars—have been routinely used in a majority of the longwall operations in the Wasatch Plateau and Book Cliffs coalfields of central Utah, where abutment pillar gate road systems have largely failed to effect bump-free, economically feasible

[1]Mining engineer, Denver Research Center, U.S. Bureau of Mines, Denver, CO.

[2]Italic numbers in parentheses refer to items in the list of references at the end of this paper.

mining. Several mines in New Mexico, Colorado, and Alabama have also utilized this gate design option and variations thereof to minimize any number of ground control problems without seriously impacting required productivity. By far, the two most common ground control applications of yielding pillar systems are for (1) the mitigation of severe pillar bumps, most commonly experienced in the tailgate entries, and (2) the abatement of destructive, high-stress concentrations surrounding remnant gate road pillars, which seriously affect entry stability during close-proximity, multiseam mining.

A majority of western U.S. longwalls are currently multiple-seam mining operations or plan to be in the near future. Many of these mines are subject to massive sandstone canyon-and-mesa overburden conditions (figure 1), relatively strong roof and floor strata (figure 2), and mining depths routinely ranging over 450 m (1,500 ft)—currently approaching 900 m (3,000 ft) at one mine in central Utah. As a result, western longwallers have experienced among the worst pillar/panel bump and seam interaction problems found in U.S. underground coal mining within the last 30 years.

To cope with these severe mining conditions, the use of stiff, load-concentrating abutment pillars in gate developments was largely abandoned in favor of the less rigid, load-shedding yielding pillar. As these pillars gradually and nonviolently yield, the strata immediate to the entry system are allowed to deform, creating a "softened" zone around the entry system. Weakening the pillar supports and surrounding rock mass transfers high abutment loads away from the entry system onto the adjacent panel(s) and minimizes the load-concentrating potential of the remnant gate pillars during subseam mining.

Additional applications of yielding gate designs include the control of floor heave, cutter roof (an example of horizontal stress-related problems), and less commonly, subsidence problems. Although the performance record has not reflected a marked improvement in ground stability in every case, sufficient success has been achieved by some of the industry's most productive mines to warrant a growing interest in the level of safety that yielding systems may afford operations in other U.S. coal regions.

In addition to ground control, yielding gate systems offer some very distinct advantages over full abutment pillar designs where mining economy is concerned. For example, rapid advancements in support, shearing, and face haulage technologies over the past few years have placed an enormous strain on the ability of development to keep pace with longwalling. Yielding systems require less crosscut development and may marginally improve place-mining efficiency where extended cuts are allowed. Reduced entry development and advantages in miner move efficiency may also be realized for various configurations employing both yield and abutment pillars. Support, labor, and capital equipment costs may also be minimized by less overall development. Once developed, improvements to gate stability in difficult or multiseam mining conditions translate into less nonscheduled face downtime, recently estimated by one western longwall engineer to average over $350 per minute for a ~9,000-metric-ton (10,000-U.S.-short-ton) per 8-h shift operation.

Nevertheless, as promising as the yielding gate system appears to be, the acceptance of this design option continues to be most greatly hindered by (1) the lack of a proven design methodology that quantifies the performance potential of the entire yielding gate road system, coupled with (2) the somewhat frequent occurrence and severity of failed "misapplications" within the limited experience base attained thus far.

To date, a number of design methods have been developed for these specialized gate systems, but they typically focus on pillar sizing alone and fail to address gate performance once the pillar has yielded. As a result, on-site engineers have primarily relied upon the trial-and-error refinement of traditional pillar designs used within the local mining community. While this "technology transfer" process has worked fairly well within specific western U.S. coal districts, failure to recognize that gate performance depends greatly on such factors as the quality of the immediate roof strata and installed support systems has also resulted in several unsuccessful attempts to import a design from one coal region to another. With relatively few mines utilizing this gate design option in recent years, the consequences of misapplying and/or poorly designing yielding pillar gate roads can only encourage industrywide skepticism and misunderstanding. Today, for example, it is largely held that full-yielding systems are *limited* to the difficult mining conditions found in the West, that extensive secondary tailgate support is required at a minimum, and that multientry systems (more than two) simply provide inferior, unacceptable levels of gate stability performance. As will be illustrated later, yielding gate road systems, and particularly yield pillars in abutment-yield gate configurations, have a much broader application potential in many U.S. coalfields than is currently believed.

Regardless of existing perceptions, the challenge of gate development keeping pace with rapidly expanding longwall production capabilities has driven mine operators to minimize both pillar sizes and the number of entries mined. As a result, interest in this design option has been largely mandated by these economic concerns, and now the engineering questions surrounding ground control and operations need to be answered. To assist mine operators in addressing the ground control/gate design aspects of yielding pillar gate systems, this paper presents a general overview of what has been learned thus far from western U.S. mining experiences over the past decade. More specifically, the fundamental concepts of design viability (under which circumstances yielding gates might be appropriate), timing of pillar yielding, and the "critical" pillar are

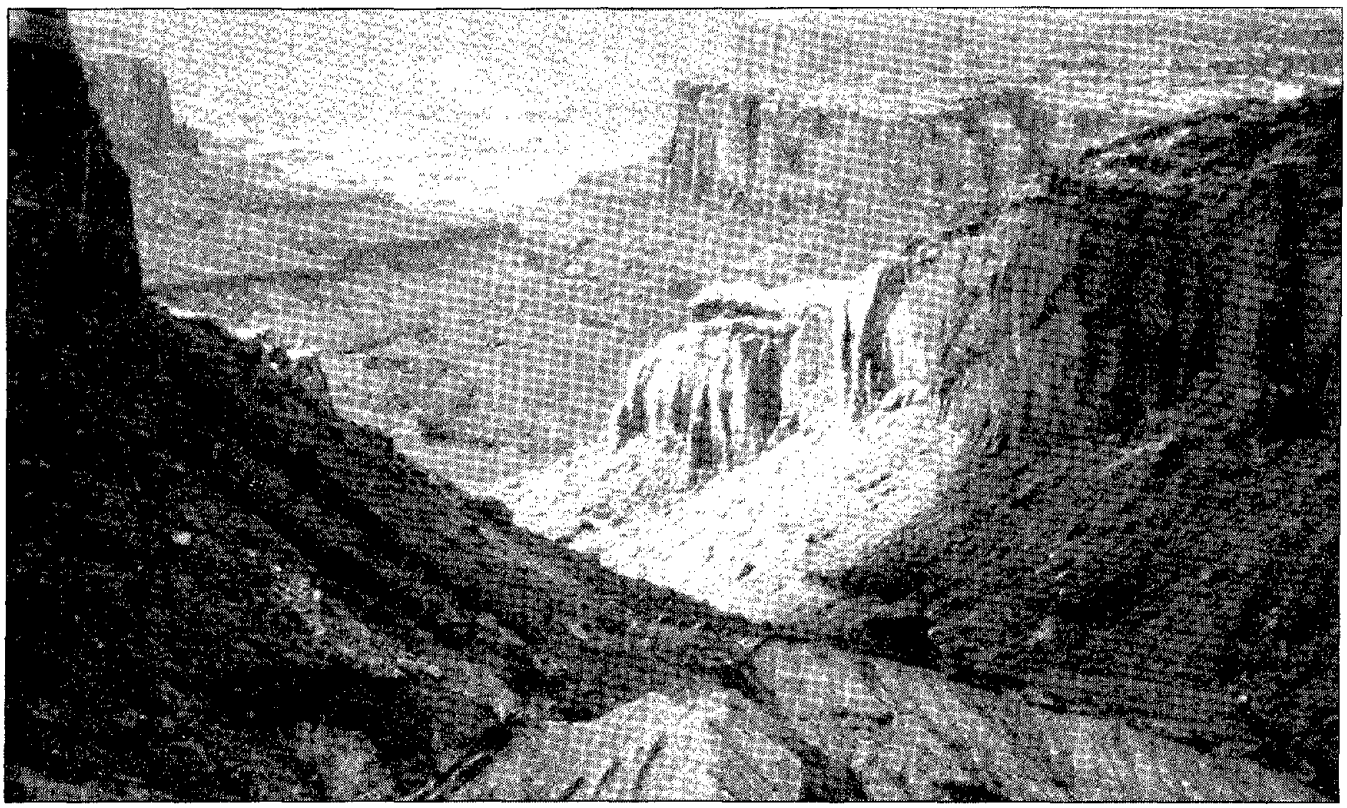

Figure 1.—Canyon and mesa topography common to the coalfields of central Utah.

Figure 2.—Typical strong roof strata sequence, found in many western U.S. mines, comprised of fine-grained sandstones, siltstones, and strong mudstones.

discussed in the context of an approach for designing yielding gate systems. A brief, informal analysis of several successful and unsuccessful attempts to use yielding designs in recent years as related to roof and floor quality, pillar dimensions, and mining depth is also presented. While USBM research continues to develop a proven, comprehensive design methodology for yielding gate road systems, this paper serves as a summary reference in support of the emerging acceptance of yield pillar usage in U.S. longwalling.

ASSESSING THE VIABILITY OF YIELDING GATE ROAD SYSTEMS

With respect to ground control, the viability of yielding gate designs for any particular mining property is a function of the strength or supportability of the immediate mine roof, lateral continuity of both the roof and floor strata, and mining depth. In lieu of being able to currently quantify this relationship mathematically, the basic concept is most simply illustrated in figure 3. Three boundaries—the left, lower, and right sides of the "viable" region—essentially define the following basic requirements of a potentially viable yielding pillar gate design for any specific mining property.

1. Does sufficient overburden exist to effectively initiate the timely yielding of the minimum pillar size required by the U.S. Mine Safety and Health Administration (MSHA) and/or mine operations?

Most important to the successful implementation of a yielding gate system is *using pillars that yield.* Although this requirement appears obvious, perhaps the most common factor in unsuccessful cases is the use of pillars that do not yield sufficiently to effectively redistribute pillar/entry loads to the surrounding panel abutments. The stabilizing, load-reducing qualities of the yielding design are instead replaced by severe roof, floor, pillar, and panel instabilities driven by the concentration of high abutment loads across the entry system.

Failure to achieve pillar yielding in moderate to deep settings is generally a design-related problem involving pillar oversizing or attempts to customize the timing of pillar yield to accommodate marginal ground conditions (discussed in more detail in the next section). Conversely, pillar yielding in relatively shallow operations (the left side of the "viable" region in figure 3), may be unavoidably restricted by both the minimum pillar width allowed and the minimum overburden depth then required to initiate timely yielding.

Based on an informal survey of many western U.S. operations, the smallest pillar width deemed operationally feasible, as well as allowed without an MSHA exemption, is 6.1 m (20 ft), and in some cases no smaller than 9.1 m (30 ft). Most of the operations queried used two-entry systems, so it may be possible to utilize smaller widths for the adjacent pillars in multientry applications. Experience with pillar sizes less than 6.1 m (20 ft), used in conjunction with abutment pillars and/or in thin-seam settings where rib stability is not a problem, suggests this is a feasible consideration.

2. Is the mine roof quality sufficient to withstand potentially large entry deformations without the use of excessive artificial support?

Yielding gate systems by definition involve significant entry deformations ranging from several centimeters to over a meter depending on the height of the opening, width of the gate, caving characteristics, support type, pillar behavior, etc. The ability of the immediate, supported interval of roof strata to withstand the bending and shearing stresses that accompany pillar yielding is paramount to achieving gate stability throughout panel mining. Weak strata in the immediate mine roof can be tolerated with the use of wire or plastic mesh if the unit is not too thick, but competent strata must comprise the majority of the bolted interval. Unconsolidated, highly structured, weak, thinly bedded roofs, without adequate support, are destined for failure in yielding systems (figures 4-5). Some allowance for roof weaknesses can be made depending on

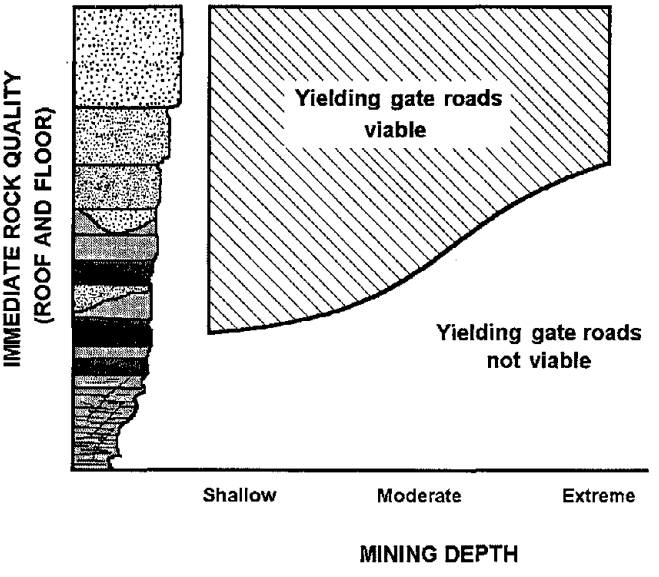

Figure 3.—Conceptual relationship between immediate roof quality, mining depth, and the potential viability of a yielding gate road system.

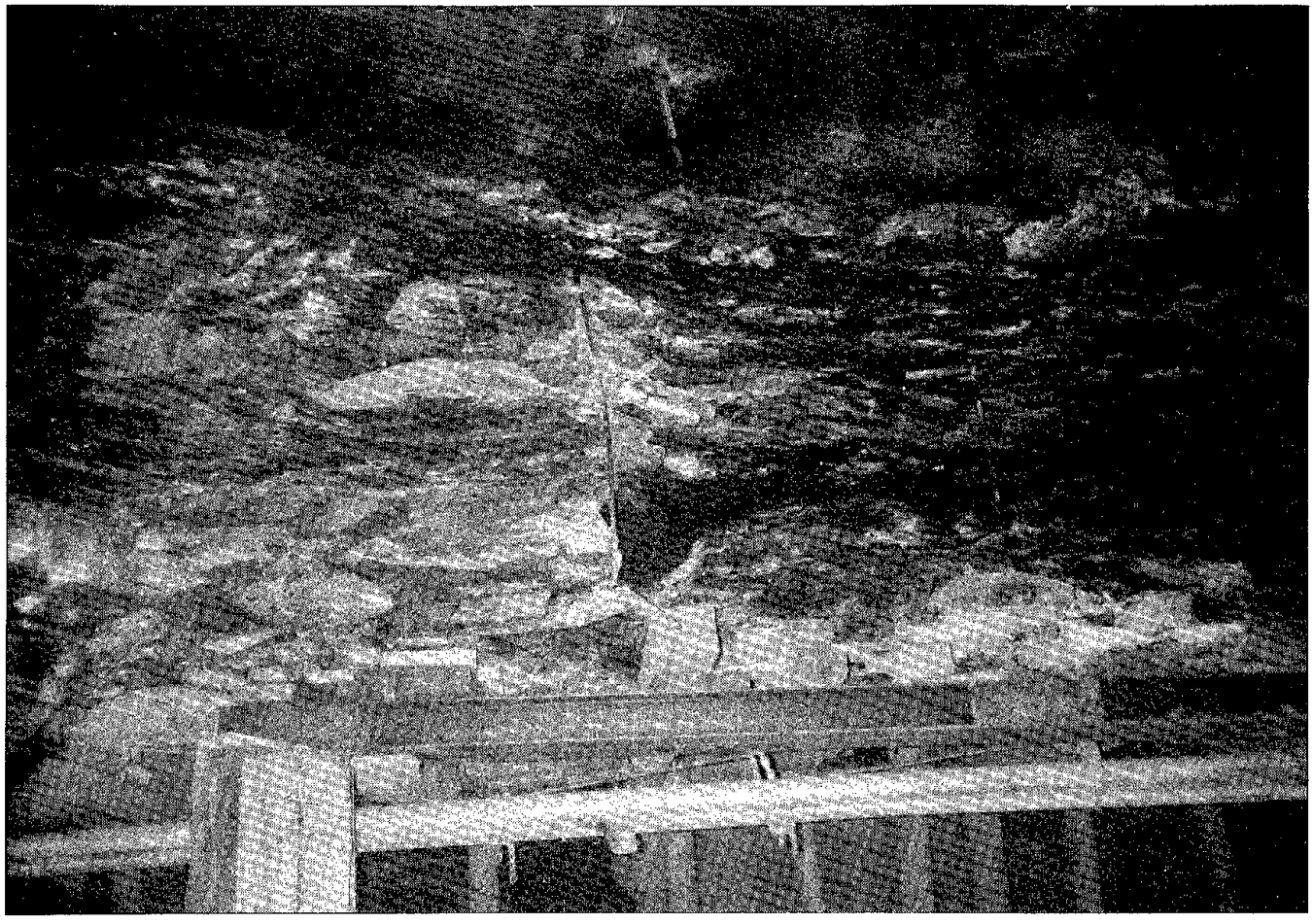

Figure 4.—Weak, unconsolidated, highly laminated roof sequence that is not conducive to successful applications of yielding gate road designs.

the amount and type of support to be used, persistence of weak roof zones along the gate, and perhaps the stand time required of the opening (mostly due to panel lengths). In general, however, additional (heavy) support should not be viewed as an alternative for making yielding systems viable in marginal conditions; the risk of failure is high.

As mining depths increase, the quality of the bolted roof necessary to ensure gate stability should also improve to accommodate potentially higher and more sudden gate deformations. Although it can be argued that yielding of the gate pillars and softening of the immediate few meters of overlying roof strata essentially isolate the entry system from overburden loading, the potential for higher abutment loads at greater depth is not a subject best left to theory. Abutment loading mechanisms, both ahead of the face and along the caving gob, are not easily characterized for nonyielding gate systems, let alone the more complex yielding systems.

Consideration should also be given to strong mine roof conditions where the possibility of sudden loads being imparted to partially yielded pillars exists during first face passage. Strong, stiff roof units (beds, channels, etc.) can effectively bridge small gate widths (typical of two-entry designs) prior to first panel mining, thereby shielding the entry system from a majority of the overburden loading necessary to initiate full pillar yielding. Once the face passes, removing a primary support abutment for the gate road roof strata, the full weight of the panel side abutment is imparted to the partially yielded coal pillar. The result is commonly severe pillar bumping and/or damage to the immediate headgate floor near the face. In this case, the roof is sufficient to withstand considerable entry deformation, but may actually contribute to serious pillar and floor instabilities if pillar yielding is significantly impeded.

The USBM-developed CMRR, described later, is an efficient, practical rock mass classification system that the mine design engineer can employ to assess the structural integrity and supportability of the mine roof when considering yielding gate designs (*5*).

3. Is the floor quality sufficient to not engender problems related to specific roof conditions and mining depths?

Although mine roof quality is by far the most important factor affecting entry stability once pillar yielding has begun, the quality of the floor can create two extreme circumstances in which yielding entry systems become hazardous under otherwise viable roof conditions. First, in moderate, yet supportable roof conditions, where delayed pillar yielding (using a larger pillar) is being considered to minimize total roof deformations, the floor must be strong enough to resist pillar punching. Weak floor strata cannot withstand sustained loading from highly loaded pillars, resulting in serious, progressive entry heave and, occasionally, sudden, violent failures of the immediate floor strata (figure 6). Second, in strong roof conditions, the floor must not be so strong that pillars cannot be designed small enough to ensure nonviolent yielding and still meet operational and mining law requirements.

4. Is the mining depth so great or complicated by unique seam conditions that a yield pillar cannot be developed?

This situation (illustrated by the right side boundary of the "viable" region in figure 3) has only been partially demonstrated by one U.S. mine in recent years. In this case, mining depths approaching 900 m (3,000 ft) and high gas concentrations within the seam produced severe face bumping in gate development drivages, forcing the mine to use an advancing longwall system. Although the inability to develop panel entries was not the direct result of a failed yield pillar design, the existence of an application limit was nevertheless demonstrated. This limitation does not appear to be of immediate concern in today's longwall industry, but will certainly impact future operations as mining proceeds to greater depths in search of quality deposits. To date, correlations between gate performance and such factors as widely ranging, sudden changes in overburden depth, seam dip, and extreme mining depth have been inconclusive. These topics will be addressed in more detail when a much larger database has been compiled.

Aside from these most basic considerations, there are many additional factors that influence whether a yielding gate design is actually appropriate for a particular mine setting or not. Factors such as the number of entries to be used (total gate span), pillar sizes, entry spans, types of supports, cavability of the gob, geologic anomalies, etc., all influence the potential success of these designs as well, as they do any type of gate configuration. However, the historical experience base with yielding gate systems in the United States is fairly limited and often does not clearly define the boundaries of success/failure for the many possible cases that could exist. Nevertheless, completing this first step in the design process can roughly estimate the success potential of a yielding pillar design as high, marginal (risky), or low (extremely risky) and, more importantly, is an absolute requirement to avoid the oversights common to available yield pillar design methods.

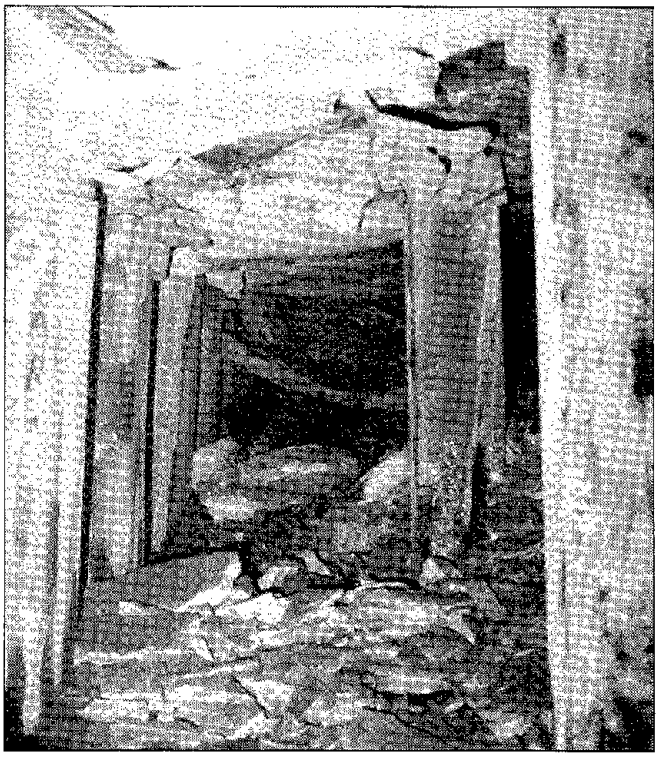

Figure 5.—Poorly laminated, minimally supported mine roof typically cannot withstand the deformations of yielding gate designs.

Figure 6.—Severe floor heave resulting from improper pillar design.

YIELDING GATE ROADS: SOME PRACTICAL CONSIDERATIONS

Despite the fact that a thorough design methodology does not currently exist for the yielding gate road *system*, past experiences with this design option in the United States have given a good deal of insight into its successful application, as well as some of the key concepts governing its use. Until proven guidelines are available for defining appropriate mining conditions for successful applications, one should consider the following characteristics common to many western U.S. experiences when further evaluating the viability of yielding gate designs for a specific property.

PILLAR SIZING

Pillars are generally 6 to 9 m (20 to 30 ft) wide in 1.8 to 3.0 m (6 to 10 ft) seams (w/h ratio of 3 to 5) and are typically intended to yield shortly after development or with the approach of the first panel face at depths averaging around 455 m (1,500 ft). In practice, measurements of pillar load histories (*2*) suggest that *full* yielding seldom occurs until after first panel mining is well outby and the majority of the peak side abutment has been attained. Although substantial, sometimes slightly increasing loads are often seen within the pillar core region long after first face passage, it is clear from elevated load measurements taken within the adjacent panel that the maximum load-bearing capacity of the pillar has been surpassed and a yielding gate system is in place. Aside from the various stages and degrees of loading during mining, the rate of pillar yielding is a function of such factors as coal strength, seam height, pillar and entry width, and roof and floor strata properties. The influence of each, or a combination, of these parameters varies considerably with conditions. For example, strong, unstructured coal confined by massive sandstone roof and floor members has been encountered by at least one western U.S. mine in recent years, where a 9-m (30-ft) pillar design failed to yield properly under 365 m (1,200 ft) of mesa-forming sandstone strata, which resulted in consecutive, violent pillar bumps as second panel mining approached. A much smaller pillar might have yielded under these conditions; however, as previously noted, it is both mining law and the general consensus among western mine operators that 6 m (20 ft) is a minimum limit based on operational feasibility considerations (power center storage, face equipment manipulation, place-mining scheduling, etc.). Likewise, larger pillars have been used, up to 14 m (45 ft) wide, with the intention of early yielding, but significant problems have been reported owing to inconsistent pillar yielding along the gate length (*2*).

The database of case history experience described later in this report indicates that no successful yield pillar designs were achieved with w/h ratios >5. Although the database compiled for this discussion is quite limited, it does represent the general experiences of most western U.S. mines employing yielding pillar systems.

Critical Pillars

Where the use of pillars with w/h ratios greater than 5 is concerned, the concept of the *"critical pillar"* has often governed the performance experienced. A critical pillar can most simply be defined as one that is too large to yield sufficiently, resulting in load transfer to nearby panel abutments, yet remains too small to fully support panel abutment loads safely. Figure 7 illustrates the relationship of the critical pillar to both appropriate applications of the yield and abutment pillar gate systems. The horizontal axis represents the minimum performance standard that separates a successful system from an unsuccessful application. The curve is an idealistic representation of how the level of confidence in a design passes from working abutment systems to working yielding systems, passing through the critical pillar zone along the way.

An important aspect of this concept is the rate at which a successful gate design can become unsuccessful. For abutment pillar systems, changes in performance are generally more gradual, and are witnessed by the onset of minor floor heave, an increase in audible coal popping and minor bumping, and increased frequency in roof-related problems. These changes generally develop more slowly

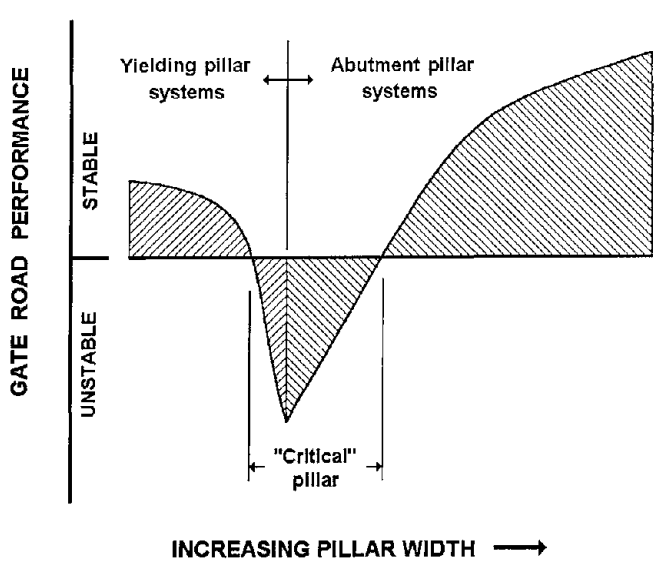

Figure 7.—Conceptualization of the "critical pillar" relationship showing the transition from successful yield pillar systems, through unsuccessful critical designs, to successful abutment pillar systems.

since pillar sizes are not typically subject to drastic downsizing at operations using this design option; nor do mining conditions typically change quickly enough to affect the full definition of the critical pillar on a design that has worked well for several panels. Conversely, for yield pillar applications the difference between a fully successful yielding gate and the worst possible critical pillar conditions can often be measured in a matter of a few meters of additional pillar width.

A USBM study currently underway in Utah involving pillar sizes ranging from 9 to 17 m (30 to 55 ft) under cover depths approaching 900 m (3,000 ft) has already witnessed the extremes over this relatively short range of pillar sizes, and first panel mining has only recently passed the largest of the pillars being investigated. At this time, the 17-m (55-ft) design has bumped violently in the headgate just after passage of the first face. The 9-m (30-ft) pillars, still 600+ m (2,000+ ft) outby the face, have exhibited signs of sufficient yielding to inhibit this type of pillar failure entirely, as considerable past experience at this mine would also support. Although pillar bumping subsided as face advance has temporarily moved under more moderate cover, it is very likely that renewed bumping will occur in the pillars ranging 12 to 15 m (40 to 50 ft) once the second panel face approaches.

This study graphically emphasizes the importance of keeping pillar sizes small enough to yield at all times. Increasing yield pillar widths to accommodate deepening cover, in the same manner abutment pillar widths may be increased, is a notion to be avoided. The very nature of the yielding gate road—the softening of the localized ground mass—makes the degree of entry stability attained largely independent of mining depth once pillar yielding has been achieved. Maintaining this weakened zone around the panel entry system is paramount to gate stability.

It cannot be overemphasized that increasing the pillar width toward the critical pillar range only invites the full weight of the overburden to be imparted upon a gate system that cannot possibly support it. As a result, critical pillars are to be considered *extremely* bump-prone (figures 8-9), even at shallow depths when strong mine roof and floor conditions exist. Unlike the abutment-to-critical pillar transition, where coal bumps are generally first witnessed in the tailgate, the yield-to-critical pillar transition provides for severe bumping in the headgate entries immediate to the face. In settings not readily conducive to pillar bumping, prolonged loading of the gate pillars will certainly result in severe roof, floor, and/or rib instabilities (figure 10), requiring extensive supplemental support along the entire tailgate entry at a minimum (figures 11-12), if gate closure can be avoided at all.

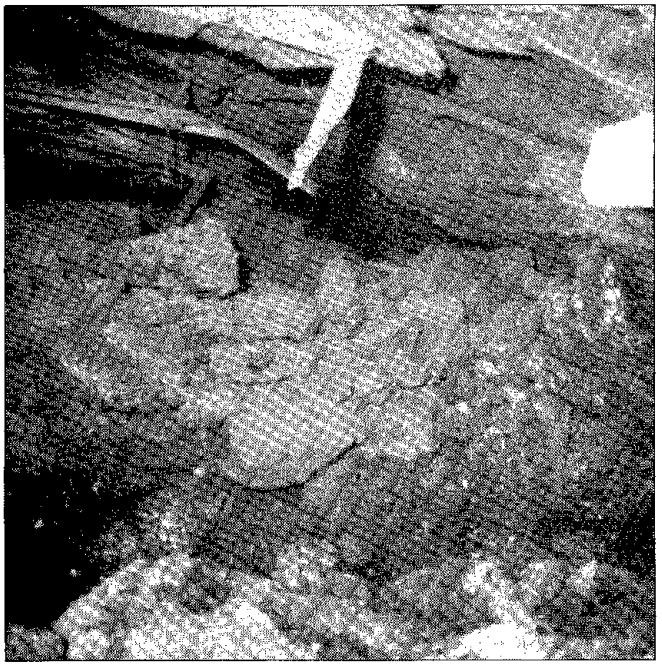

Figure 8.—Critical pillar bump at the tailgate corner.

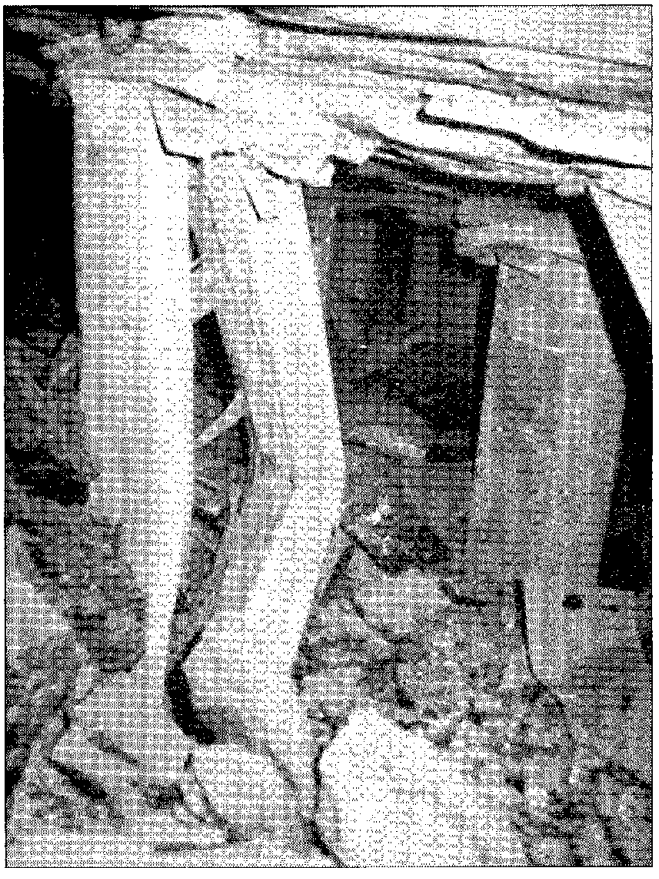

Figure 9.—Critical pillar bump near the headgate corner.

Figure 10.—Severe rib failures accompanying floor heave conditions in a critical pillar application.

Figure 11.—Intensive mine roof support used to control entry closure in a critical pillar tailgate setting.

Figure 12.—Additional example of tailgate support requirements when critical pillar is used.

Timing of Pillar Yielding

The ability to reliably design pillars to yield at specified points in mining would greatly increase the utility of this gate design option, but at the same time would require a much better understanding of ground response to pillar yield than currently exists. Timed yielding would be most beneficial in cases where a yielding system is deemed desirable for any number of reasons (bumps, multiseam, subsidence issues, etc.), but poor mine roof conditions necessitate minimizing entry deformations to ensure gate stability. For example, delaying pillar yielding until late in the mining cycle, or even until gob isolation, may minimize tailgate roof strains to within stable limits and still relieve stress transfer problems when mining subjacent seams.

However, the risks associated with attempting to customize designs to account for marginal or weak ground conditions as a function of mining advance are considerable. In weak conditions, where pillar yielding is designed to occur with the onset of second panel face approach, or after, during isolation in the gob, the risk of inducing bumps may be low, but critical pillar sizes are likely to create detrimental roof and floor conditions. Conversely, yielding too early in weak ground will undoubtedly encourage severe roof falls ahead of the face. The greatest risks are often when attempting to customize designs in moderate ground conditions to yield later in mining. Here, both roof and floor failures and severe pillar bumping can become serious issues, with little margin for design error.

ARTIFICIAL SUPPORT

Primary tailgate support varies greatly depending on the quality and continuity of the roof strata. Strong roof conditions generally warrant little more than conventional, planned bolting. Moderate roof quality typically requires a higher-cost primary support system commonly consisting of high-strength combination bolts and straps, angle bolting, slings or trusses, and steel mesh installed during bolting, not during cribbing. Generally, poor mine roof quality cannot be effectively supported without the use of multiple-support systems, as has been the case in a number of western U.S. mining experiences.

Longwalls are currently operating in the United States under poor roof conditions with yielding pillar gate designs, but tailgate stability is marginal on a day-to-day basis, with occasional entry closures immediate to the face-end responsible for significant delays in mining. In such cases, the performance of the support system is typically less than effective regardless of the type or quantity installed. A promising type of support for improving moderate roof performance, and possibly some weak roof situations, is the cable bolt. The USBM is currently conducting research to determine the effectiveness of this support in holding the severe loads often witnessed in tailgate roof strata.

Wire or plastic mesh, generally installed during gate road advance or with tailgate cribbing, is a standard practice to control the inevitable roof rash occurring within the first few centimeters of the immediate roof. In cases where roof quality is above average and minimal deterioration is anticipated, mesh installation can be done during cribbing and may be limited to lightweight plastic varieties. Marginal roof conditions require strong, steel mesh bolted tightly against the roof to inhibit progressive strata failures (figure 13). Particular care should be taken to adequately mesh along the tailgate panel roof-ribline, as this will be a difficult area to control when at the face-end.

Secondary support is critical to the success of most yielding systems, primarily those with moderate roof conditions, and generally consists of double-row, soft-wood cribbing to accommodate large deformations and provide a protected escapeway. Four-point cribbing is often preferred for its softer, consistent response to entry deformations, but nine-point cribbing is not uncommon when conditions warrant (figure 14). As roof qualities weaken, approaching the point where yielding systems should be re-evaluated for their effectiveness, it is not unusual to see solid wood packs begin to replace the larger nine-point cribs. In extreme conditions, various steel-set systems have been trialed for their effectiveness (figure 15), but abandoned due to cost.

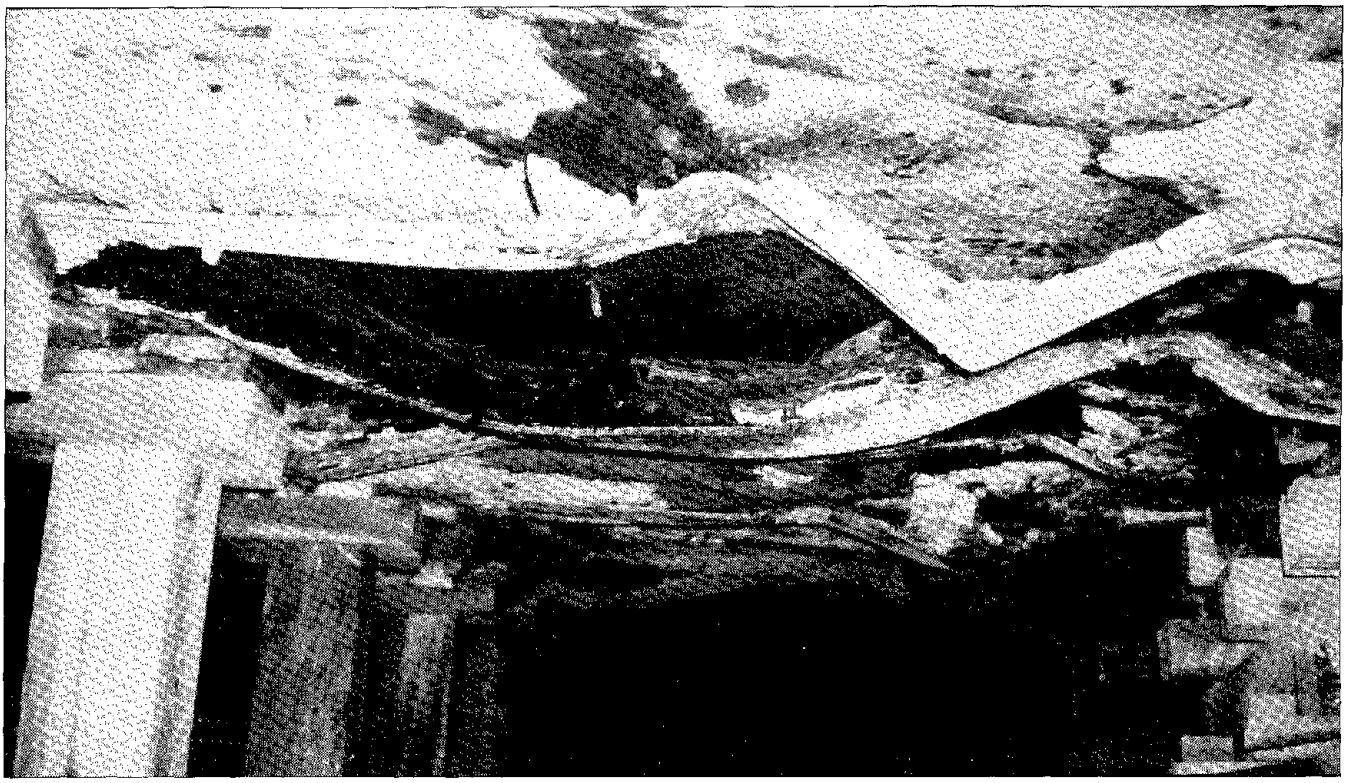

Figure 13.—Insufficient support system for holding weak, poorly laminated roof.

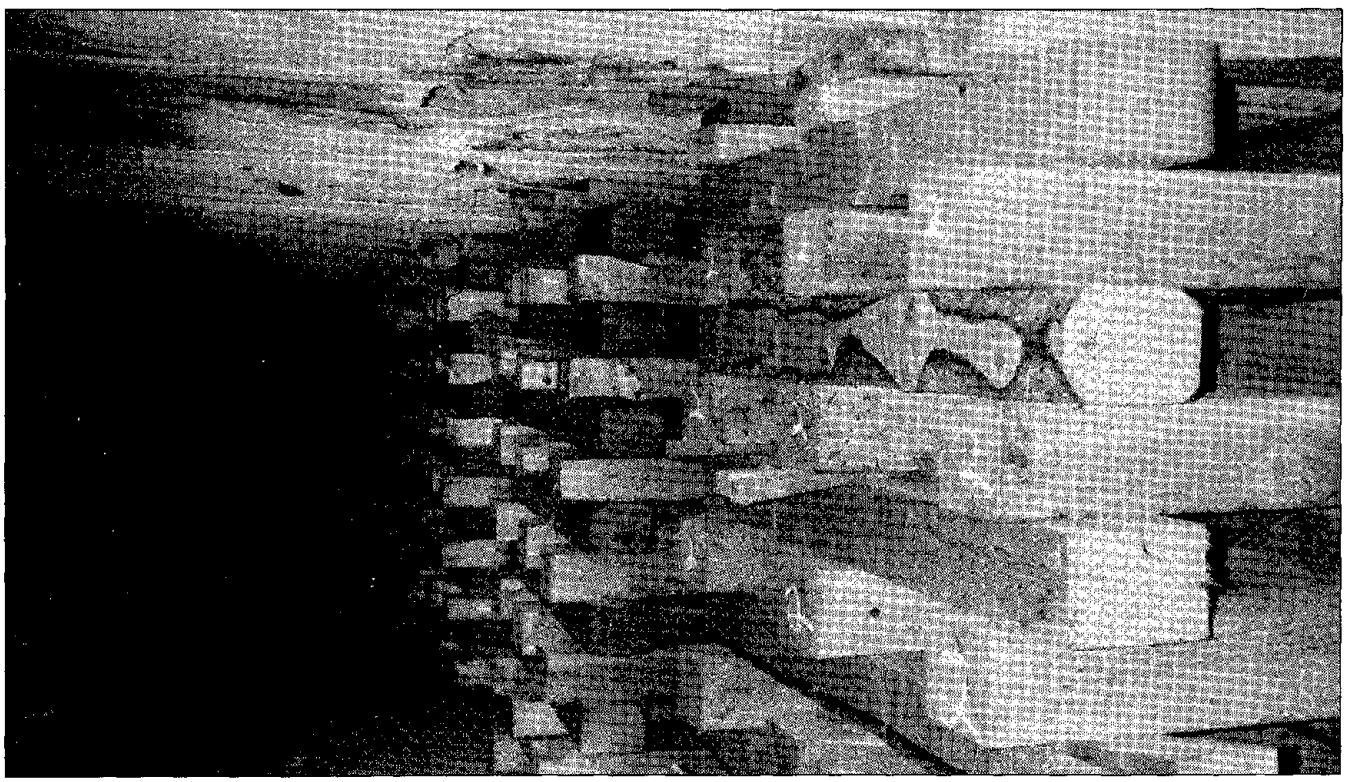

Figure 14.—Nine-point cribbing application in a yielding gate road.

Figure 15.—Steel-set support system, which is no longer used except in the most severe conditions.

Stiff supports, such as concrete donut cribs and "Big John" timbers, are generally incompatible with the substantial entry closures found in yielding systems, often inducing localized roof and/or floor problems or failing early in the mining cycle. Incorporating "soft" elements within the stiff support structure has been successful in some cases at getting the best of both worlds, i.e., soft enough to survive the initially high entry closures common to yield pillar systems, yet stiff enough to effectively support the mine roof once it has relaxed over the gate (figure 16). Customizing stiff supports in this manner is not a simple engineering task, however, and requires regular design modification to address changing ground conditions.

ENTRY CLOSURE

Entry closure for yielding systems is often considerably greater than that typically experienced in abutment- or yield/abutment-pillar systems. However, where strong roof and moderate/strong floor conditions prevail, primary support is well engineered, and the pillars are designed to yield properly, tailgate entries may actually experience relatively minor degrees of closure, with the most noticeable effects witnessed within 30 to 60 m (100 to 200 ft) of the face. At one of the deepest western operations, where mining depth has progressed from 455 m (1,500 ft) to nearly 915 m (3,000 ft), little or no change in cribbing practices has been required to support the relatively strong roof strata present across most of the property. Closures of less than 5% of the entry height after first-panel mining are common at this operation, reaching 10% to 15% with second face approach. Despite the routine use of double-row cribbing at this and other local operations, significantly less cribbing could likely be used with little or no impact to entry stability. To this end, several western operations are currently experimenting with lower-density crib patterns and new types of yieldable supports that can be employed less frequently and somewhat more inexpensively.

In mines where the roof is weaker, greater degrees of entry closure should be anticipated due to bed separations (sag) and failed strata migrating into the entry. Recent observations in one operation under poor roof (weak, highly laminated stack rock conditions) showed tailgate closures averaging 35% in a 1.8- to 2.4-m (6- to 8-ft) seam, with closures often reaching as high as 50% within 60 m (200 ft) of the second panel face. Detached strata well above the bolt horizon was clearly responsible for these excessive crib deformations.

Excessive entry closure becomes a major concern where MSHA-mandated minimum escapeway dimensions come into play, where face-end/tailgate junction blockages can become problematic, and where restricted ventilation problems may be encountered as panel lengths are significantly increased.

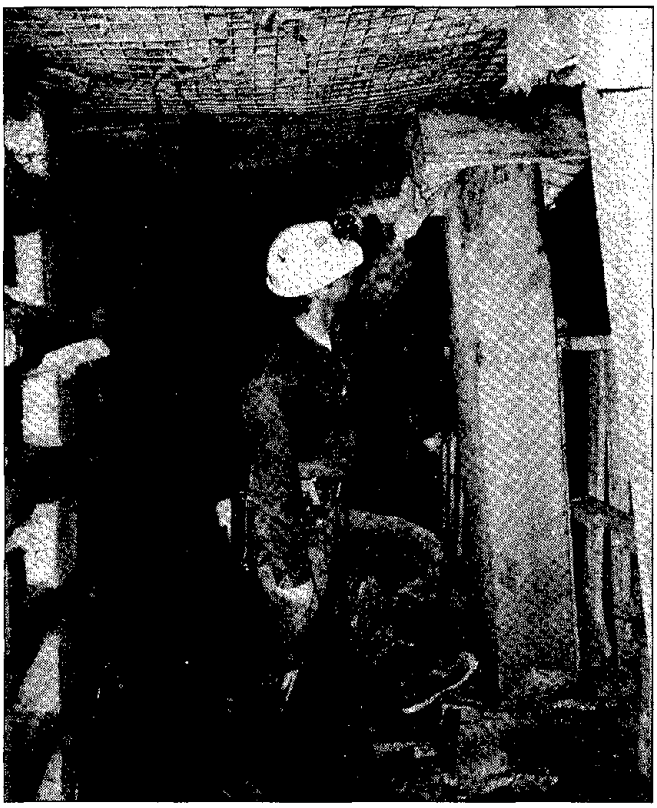

Figure 16.—Capped "Big John" timber allows additional entry closure to occur before failure of the support.

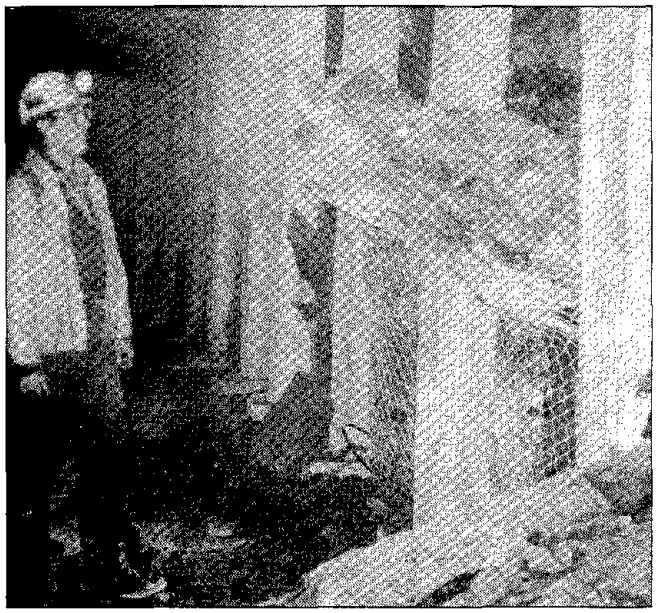

Figure 17.—Although generally successful in controlling rib sloughage, fencing methods must account for rib toppling in high seams.

RIB STABILITY

Extensive pillar rib sloughage is to be expected, particularly along the entire length of the tailgate, and is commonly treated with wire mesh or some form of fencing. Artificially confining the rib to help control sloughage, a practice often used by mines employing abutment pillar gate designs, has been used successfully in several situations. Generally, however, the volume of rib material moving into the entry is too great to rely solely on rib bolting or doweling. Entry cribbing alone usually provides a sufficient barrier to retard excessive rib migration into the entry, as long as a closely spaced pattern is maintained. Some form of fencing, such as plastic mesh or chain link, has also proved to be very effective when used with a variety of entry supports (figure 17). Where entry heights approach or exceed 3 m (10 ft), the problems of rib slabbing (toppling into the entryway) and crib damage (rollout due to rib loading) often require further support measures.

NUMBER OF ENTRIES

Theoretically, two-entry systems should outperform three-entry systems based on the principle that the less ground opened up the better. This assertion was emphasized by Carr, where in an analysis of the applications of yield pillars at the Jim Walter Resources, Inc., mines in central Alabama, he states, "The general application of the yield pillar principle is limited to a two-entry yield pillar system. A good spanning main roof is essential if three- or four-entry systems are required." (*1*, p. 176). This has generally been true in western U.S. mines as well and certainly applies to all multiseam applications (i.e., where abutment structures overlay the current gate road system).

Gate loading can be shown to be higher with the wider multientry spans at various points in the mining process, but no definitive reason exists to rule out multientry gates in all conditions. For example, a three-entry full-yielding system is currently being successfully used in a Utah operation under low cover conditions (< 180 m (< 600 ft)) to effect improved ground control during subseam mining. Also, at a nearby operation, adequate entry conditions have been recently observed in three-entry end-panel-section bleeder systems at depths reaching nearly 610 m (2,000 ft) (*2*).

PILLAR BUMP APPLICATIONS

Gate road systems employing yield pillars, whether alone or in conjunction with abutment pillars, are highly recommended design options for all longwall operations experiencing or anticipating coal bump events in the headgate and/or tailgate entries. Fully yielded pillars simply cannot store the strain energy that drives the dynamic explosiveness of coal bumps, thereby effectively eliminating their occurrence altogether. The historical record of successful longwalling in western U.S. mines,

which presently include some of the most productive operations in the world, would certainly be greatly abbreviated were it not for the bump mitigation attributes of yielding gate systems.

Nevertheless, while it is true that tailgate pillar bumps in yielding entry systems are virtually nonexistent in western U.S. operations today (critical pillar bumping in the headgate, however, remains a serious problem), legitimate concerns have been raised regarding the influence these gate designs may have on end-panel face bumps. Because overburden loads are largely diverted away from the softened groundmass about the entry system and onto the nearby, stiffer panel abutments, one can reasonably conclude that the frequency and severity of face bumps near the tailgate will also increase. This has not been the experience of most western operations, however, suggesting that the degree of face bumping induced by the yielding entry system is a function of numerous mining parameters.

In moderate roof and floor conditions, where the coal strength and seam structure accommodates yielding, peak side-abutment loads are typically lower and more evenly distributed within the tailgate panel periphery. Early pillar yielding maximizes total panel loading before the arrival of the face, which furthers the development of the yield zone within the panel ribline. The deeper the yield zone, the less likely small-scale bumping along the tailgate ribline is to occur or become a frequent problem. Also, the peak stress abutment within the panel will be further minimized and, thereby, less of a contributing factor to face bumping.

This supposition was recently supported at a western operation where panel drilling along the tailgate delineated the yield zone at 9+ m (30+ ft) within the ribline. Face bumping was minimal and did not appear to be related to the side abutment as much as to the rate of face advance. This suggests that, for this particular operation, face bumping occurs when the rate of mining overtakes the peak face abutment and is not the result of using a yielding gate system.

The existence of a deep yield zone does not, however, preclude the occurrence of large-scale bump events. It only indicates a tendency for the seam to yield nonviolently, rather than confine high, bump-prone stresses at or near the face/ribline.

In particularly strong roof and floor settings, where the coal strength and lack of seam structure inhibits yielding around mine openings, yielding gate designs may very well enhance face/panel bumping by enabling a greater expanse of intact roof to cantilever off the panel ribline. The confinement offered by the roof and floor strata typically minimizes the depth of yielding that occurs within the panel rib and concentrates the abutment loads within a relatively short distance of the panel edge.

Where these types of conditions exist over a significant portion of the panel, an abutment-yield system is an alternative worth considering. The yield pillar would not only act as a bump-proof gate support, but also serve as a "bump curtain," shielding the tailgate escapeway from the possibility of explosive abutment pillar failures. Where these conditions are of limited extent (e.g., localized sand channels in most western mines) and a full-yielding gate system is desired, a minimum number of entries is recommended to reduce the span of the cantilevering strata and the resultant abutment load imparted to the tailgate corner of the panel.

MOVING TOWARD A DESIGN METHODOLOGY

Addressing the general performance standard in a *quantitative* manner requires a specific design criterion that discriminates success/failure in terms of available engineering parameters. For example, the traditional concept of the safety factor is commonly used by many engineering design criteria to express the relationship between the operating environment and the functional requirements of the structure being designed. However, this concept works most easily in mine design applications when static conditions prevail, or can be assumed for reasonably few points in the mining process, and considerable simplification of the setting parameters can be tolerated. As previously discussed, the yielding gate environment is far from static, and the interrelationship of setting elements does not readily lend itself to simplification in the context of a *deterministic* approach to gate design. This is emphasized by the current lack of a methodology or set of guidelines for the design of the integrated pillar-entry-support yielding gate system.

Fortunately, as described by Mark, "deterministic methods are not the only ones for the solution of complex ground control problems" (*3*). In support of this, he describes the method of *back-analysis* as it was applied to the refinement of the empirically based abutment pillar gate road design methodology called Analysis of Longwall Pillar Stability (ALPS) (*4*). Essentially, back-analysis determines significant relationships between specific parameters describing a large database. In the case of Mark's most recent application, analysis of design data from a total of 69 longwall case histories found a significant correlation between mine roof quality and the ALPS stability factor (*4*). This correlation allows longwall planners to estimate the required pillar sizes at operations utilizing abutment pillar gate designs after making a quantitative evaluation of the roof quality.

The remainder of this paper describes preliminary back-analysis of yielding pillar designs, employing a database of 15 case histories representing 10 mines. The cases were evaluated to determine if any apparent relationships could be identified between readily available mining parameters that could be used to define the success or failure potential of specific designs. The database used in this evaluation was considered too small to attempt to draw mathematical relationships for a success/failure criterion, yet the results indicate the promise of back-analysis techniques in providing such a criterion once a sufficient database is collected.

DESCRIPTION OF THE DATABASE

Of the 15 cases, 6 were considered satisfactory and 9 were considered unsatisfactory examples of yield pillar usage. Only three cases involved multientry (more than two) applications. All of the mines evaluated operate within the Utah, Colorado, and New Mexico coal regions, with depths ranging from roughly 200 to 900 m (650 to 3,000 ft). Generally, each satisfactory case history represents many applications of that particular design across the property, while each unsatisfactory case represents as few as a single application. The final analysis involves only a few mining parameters (listed in table 1), including pillar width-to-height ratio, mining depth, roof quality rating (CMRR), and floor quality rating. Although the ratings are fairly subjective, as described next, the correlation indicated by these parameters is notable.

Case History Success/Failure Performance Determination

The case histories were objectively described as being either *satisfactory* or *unsatisfactory* based on a general performance criterion largely patterned after that employed by Mark (*4*). Some additional considerations have been added to Mark's criteria that are more specific to yield pillar gate designs.

To be considered *unsatisfactory*, a case history had to meet any one of the following criteria:

- Pillar design and/or entry support was significantly changed in response to poor ground conditions in either the headgate or tailgate entries.
- The panel was abandoned owing to intolerable gate road ground conditions.
- Unacceptable conditions were encountered in areas of poor roof and/or floor quality.
- Pillar bumps had been reported, regardless of severity, timing, location, or frequency.
- Significant face-end bumping occurred that could be attributed to the yielding gate system.
- There were significant longwall delays attributable to ground conditions in the headgate and tailgate entries, most commonly experienced as tailgate closures.

To be considered *satisfactory*, a case had to meet *all* of the following criteria:

- The design was used for at least three successive panels, *or* proven site-specific design guidelines had been established based on a substantial record of yield pillar performance.
- Tailgate blockages were rare or nonexistent and of minimal extent.
- Good ground conditions, with minimal delays attributable to ground control, were reported.

Discriminating between degrees of gate performance is relatively clear-cut where critical pillars are concerned, but becomes much more difficult for cases involving yield pillars in marginal ground conditions. The immediate, severe pillar and entry loading conditions imposed when critical pillars are mistakenly employed typically engender among the worst ground conditions found in U.S. longwalling. The failure to achieve complete, nonviolent pillar yielding in a timely manner is often readily apparent in the form of severe pillar bumping, roof punching and shearing, and/or floor heave. Conversely, when pillar yielding is achieved as planned in marginal-quality roof and/or floor settings, and particularly at lower cover depths, factors such as mining rate, and amount and type of roof support can complicate the distinction between satisfactory and unsatisfactory performance for a given case history. Owing to the limited database available, the influence of these factors may not be fairly represented in all cases where failed yield pillar applications are concerned.

Roof Quality Rating

Roof qualities were quantified using the CMRR recently developed by Molinda and Mark (*5*). This rock mass rating system for coal measure rocks provides a weighted evaluation of the overall quality of the roof strata within the bolted horizon, considering such parameters as discontinuity intensity and shear strength, unit rock strength, weatherability, number and sequencing of beds, and the presence of groundwater inflows. The individual roof quality ratings are expressed on a scale of 0 to 100 and fall within three broad classes described by the developers:

- *Weak* roof (CMRR < 45): Roof typically consisting entirely of low-strength 56 MPa (<8,000 psi), closely bedded, jointed, and/or slickensided rocks, usually shales and coals.

Table 1.—Data set for yield and critical pillar analyses

Mine, entries,[1] pillar type,[2] performance[3]	Mining depth, m	Pillar width, m	Seam height, m	Pillar w/h ratio	Coal Mine Roof Rating[4]	Floor rating (FR)[5]	$CMRR^2 \times FR$ (×100)	$CMRR^2 \times FR \times w/h$ (×1,000)
Mine A:								
2E, YP, S	550	9.1	2.4	3.8	75	4	225	86
Mine B:								
2E, YP, S	550	9.1	2.4	3.8	80	4	255	97
Mine C:								
2E, YP, S	455	9.1	2.4	3.8	60	2.5	90	34
3E, CP, U	455	16.8	2.4	6.9	60	2.5	90	62
Mine D:								
3E, YP, S	245	9.1	3.0	3.0	55	3	90	27
Mine E:								
2E, YP, S	855	9.1	2.1	4.3	80	3.5	225	96
2E, YP, U	730	9.1	2.1	4.3	50	3	75	32
2E, CP, U	855	16.8	2.1	7.9	80	3	190	152
Mine F:								
2E, CP, U	355	9.1	2.1	4.3	75	6	340	145
2E, CP, U	490	15.2	2.1	7.1	75	6	340	240
Mine G:								
2E, CP, U	150	9.1	2.4	3.8	33	2	20	8
Mine H:								
3E, YP, U	245	12.5	2.1	5.9	38	1	15	9
Mine I:								
3E, YP, S	550	7.6	2.1	3.6	70	3	145	53
Mine J:								
2E, YP, U	490	9.1	2.1	4.3	[6]33	5	55	23
2E, CP, U	490	24.4	2.4	10.0	[6]75	5	280	281

[1]2E refers to 2-entry systems, 3E to 3-entry systems.
[2]YP refers to yield pillar, CP to critical pillar.
[3]Performance is either satisfactory (S) or unsatisfactory (U).
[4]On a scale of 0 to 100.
[5]On a scale of 0 to 6.
[6]Estimated from previous on-site investigation.

- *Moderate* roof (45<CMRR<65): Bolted interval usually contains at least one competent unit, typically a siltstone or strong shale, i.e., at least 0.6 m (2 ft) thick containing few bedding planes or other discontinuities.
- *Strong* roof (CMRR>65): Bolted interval typically contains at least one very competent, massive bed, at least 1 m (3 ft) thick that exceeds 56 MPa (8,000 psi) in strength, usually a sandstone or limestone.

CMRR ratings for most western U.S. operations are generally found to be high, over 70 in most cases. Yet, the database used in this analysis includes several examples of roof qualities appraised much lower, including three estimated in the 30's range. With the exception of two values that were estimated by the author, based on proximity to known CMRR data points, all of the roof quality data were acquired from the developers of the CMRR (*4*).

Floor Quality Roofing

In the absence of a method to rate floor qualities similar to that of the CMRR, a very subjective rating was applied to available floor data for each mine in the database. Based on the general categories of weak, moderate, and strong, a scale of 0 to 6 was applied that allowed some discrimination as to how weak or strong the floor was from site to site. While future evaluations will attempt to more accurately describe this parameter, it is worth noting that the floor largely does not influence the outcome of the relationship between satisfactory and unsatisfactory designs *as long as the pillars yield.* The floor does play a significant role, however, when the pillars do not yield—the critical pillar failure modes discussed earlier.

QUALITATIVE DATA ANALYSIS

It was determined that a relationship between mining depth and the multiplied product of w/h, CMRR^2, and the floor rating provided a very descriptive discrimination between the performance attributes of each case history within the database. Two perspectives on this relationship relative to the database shed considerable light on the potential for back-calculation to provide a very useful design tool for yielding gate systems in much the same way it has been used for abutment pillar systems. The first considers just those cases where pillar yielding was actually achieved, while the second considers the distinctions between those cases where the application failed.

Considering just those cases where pillar yielding was achieved, shown in figure 18, a clear distinction between satisfactory and unsatisfactory performance can be seen, with an apparent trend also indicating the need for a higher CMRR with increased mining depth to ensure success. While this plot suffers the already admitted failings of limited data, the implied trends coincide with the basic ideas presented in figure 3. It should be noted that the presented relationship is largely independent of the floor rating since pillar yielding largely minimizes the occurrence of floor instabilities.

Considering just those cases that were determined to be unsatisfactory, shown in figure 19, a distinction begins to

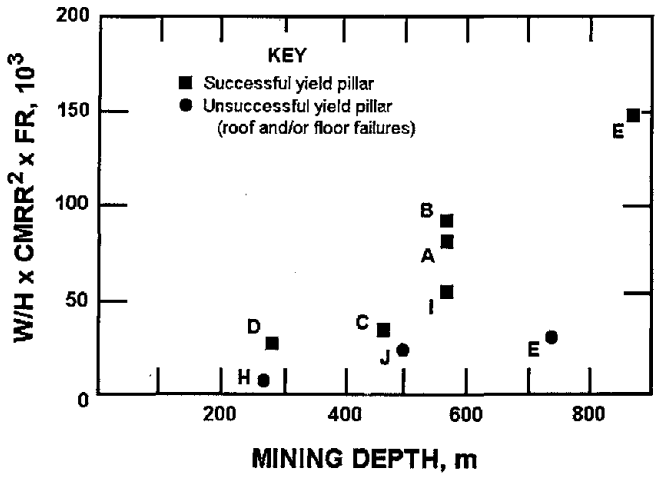

Figure 18.—Rock quality/pillar size ratio relationship versus mining depth with respect to successful and unsuccessful yielding gate road system case histories. Mines A through E and H through J are listed in table 1 and represent those cases where the pillar actually yielded. W/H = pillar width-to-height ratio; CMRR = Coal Mine Roof Rating; FR = floor rating.

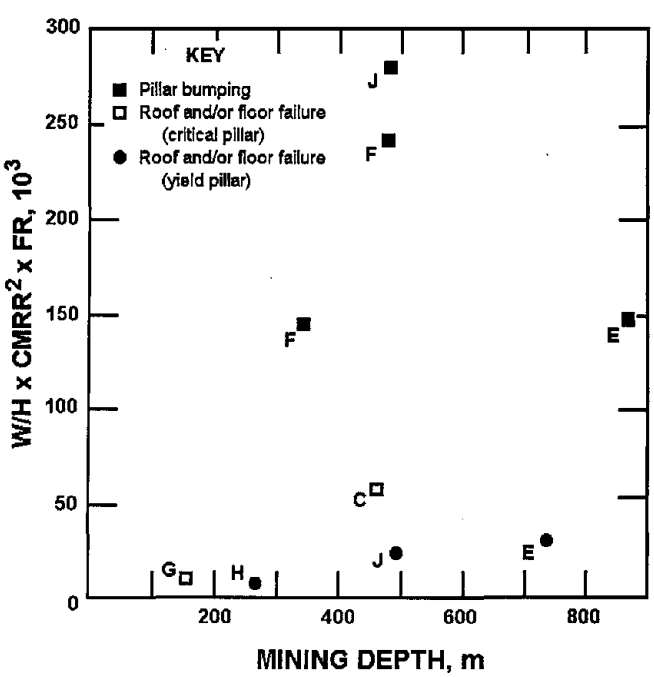

Figure 19.—Rock quality/pillar size ratio relationship versus mining depth with respect to three forms of unsuccessful designs: yielded pillar in weak ground, critical pillar in moderate-weak ground, and critical pillar in strong, bump-prone ground. W/H = pillar width-to-height ratio; CMRR = Coal Mine Roof Rating; FR = floor rating.

emerge between the types of failures to be experienced by inappropriate applications. For weak roof and floor conditions where the pillars actually yielded, the observed failure mode was generally massive roof instabilities (mines E, H, and J). Where the pillars did not yield adequately in both weak to moderate strata conditions, the observed failure modes were dominated by both massive roof and floor instabilities (mines C and G). The worst conditions were experienced at mine C, which also happens to be the deepest of the two experiences given in this database. Although not shown (since it was not evaluated as a separate case history), mine D reported floor problems at cover depths less than 180 m (600 ft), where adequate pillar yielding was not occurring as planned. Finally, where the pillars did not yield under strong strata conditions, entry failure was solely due to explosively severe pillar bumping (mines E, F, and J). In several cases, numerous tailgate stoppings were blown out, and the travelway along the tailgate was closed for varying lengths of time. Mine F was forced to abandon longwalling in two panels largely because of pillar bumping and eventually closed owing to both severe gate road and face bumps. Mine E experienced bumping in the headgate pillars shortly after first face passage.

SUMMARY

Yielding pillar gate road systems have been shown through historical practice to be viable considerations when deep, bump-prone and/or multiseam mining conditions are present. It can also be shown, however, that this gate design option is not solely limited to difficult mining settings, but may be used very effectively in moderately shallow mining conditions as well. The greatest hurdles facing the routine, successful application of these gate road systems appear to be (1) the lack of a proven design methodology that quantifies the performance potential of the entire yielding gate road system, coupled with (2) the frequent occurrence and severity of failed applications within the limited experience base attained thus far.

USBM research is currently attempting to address these deficits in design capabilities and the database of experience through both on-site evaluations and reviews of the historical performance record. Utilizing the proven techniques of back-analysis, particularly in light of the promise that the preliminary analysis presented herein has engendered in this evaluation approach, it is conceivable that very specific methodologies for the application of full-yielding gate road designs may be developed for a broad spectrum of applications in the not-too-distant future.

REFERENCES

1. Carr, F. Ten Years' Experience of the Wilson/Carr Pillar Sizing Method at Jim Walter Resources, Inc. Paper in Proceedings of the Workshop on Coal Pillar Mechanics and Design. USBM IC 9315, 1992, pp. 166-179.

2. DeMarco, M. J., L. R. Barron, and R. O. Kneisley. Comparative Analysis of Longwall Gate Road Designs in Four Deep, Bump-Prone Western U.S. Coal Mines. Paper in Proceedings of the 12th Conference on Ground Control in Mining, ed. by S. S. Peng (Morgantown, WV, Aug. 3-5, 1993). Dept. of Min. Eng., WV Univ., Morgantown, WV, 1993, pp. 104-113.

3. Mark, C. Pillar Design Methods for Longwall Mining. USBM IC 9247, 1990, 53 pp.

4. Mark, C., and F. E. Chase. Gate Entry Designs for Longwalls Using the Coal Mine Roof Rating. Paper in Proceedings of the 12th Conference on Ground Control in Mining, ed. by S. S. Peng (Morgantown, WV, Aug. 3-5, 1993). Dept. of Min. Eng., WV Univ., Morgantown, WV, 1993, pp. 76-83.

5. Molinda, G.M. and C. Mark. The Coal Mine Roof Rating (CMRR): A Practical Rock Mass Classification for Coal Mines. Paper in Proceedings of the 12th Conference on Ground Control in Mining, ed. by S. S. Peng (Morgantown, WV, Aug. 3-5, 1993). Dept. of Min. Eng., WV Univ., Morgantown, WV, 1993, pp. 92-103.

LONGWALL MINE DESIGN WITH MULSIM/NL

By R. Karl Zipf, Jr.[1]

ABSTRACT

MULSIM/NL, developed by the U.S. Bureau of Mines (USBM), is a three-dimensional boundary-element-method computer program for stress analysis of coal mines. The PC-based program computes stresses throughout a mine. Engineers can then judge whether the stress levels are acceptable and, if not, adjust the mine layout accordingly. Users need material properties for coal, gob, and surrounding rock mass. In this paper, tables give suggested values for Young's modulus of the rock mass and suggested input parameters for strain-hardening gob, and figures give suggested input parameters for strain-softening coal. Different approaches are discussed for assigning material properties in MULSIM/NL models, namely: (1) uniform, (2) confinement, (3) width-to-height (w/h) ratio, and (4) combined. An example analysis of a longwall panel shows how to select and assign material properties to a model based on these suggestions. Discussions illustrate how to interpret the stress analysis results. A second example shows the analysis of a longwall panel that lies under old workings. The advantage of MULSIM/NL is that it can analyze complicated mine layouts, including multiple-seam interactions. The stress information provided by MULSIM/NL can help coal mining engineers avoid hazardous ground conditions, expensive repairs, and costly production delays due to inadequate mine planning.

INTRODUCTION TO MULSIM/NL

The USBM seeks to reduce ground control hazards and accidents to underground mineworkers through research on improved mine design. Numerical models provide coal mining engineers with a tool to test their intuition about the stress response of different underground mine layouts. The merits of alternate designs can then be judged from a ground control perspective.

This paper describes the capabilities of MULSIM/NL (*1-2*).[2,3] Next, detailed recommendations for material properties required by the computer program are provided. Finally, several examples illustrate application of MULSIM/NL for stress analysis of longwall panels. These examples illustrate the benefits of using the program in practical coal mine design.

MULSIM/NL uses the displacement-discontinuity approach (*3*) to calculate stresses and displacements around tabular deposits such as coal seams. References *1-3* provide details on the theory and operation of the program. MULSIM/NL can analyze from one to four parallel seams having any orientation with respect to the Earth's surface. These seams must lie far below the surface, since topographic or free surface effects are neglected. The user models each seam with a coarse-mesh grid of blocks (up to 50 by 50) that contains an embedded fine-mesh grid of elements (up to 150 by 150). Figure 1 shows a typical longwall coal mine layout and the modeling grid for a stress analysis using MULSIM/NL. The coarse-mesh blocks cover a large area of a mine layout, while the fine-mesh elements cover a central area where the user wants greater detail.

[1]Mining engineer, Denver Research Center, U.S. Bureau of Mines, Denver, CO.

[2]MULSIM/NL software and documentation are available from the author.

[3]Italic numbers in parentheses refer to items in the list of references at the end of this paper.

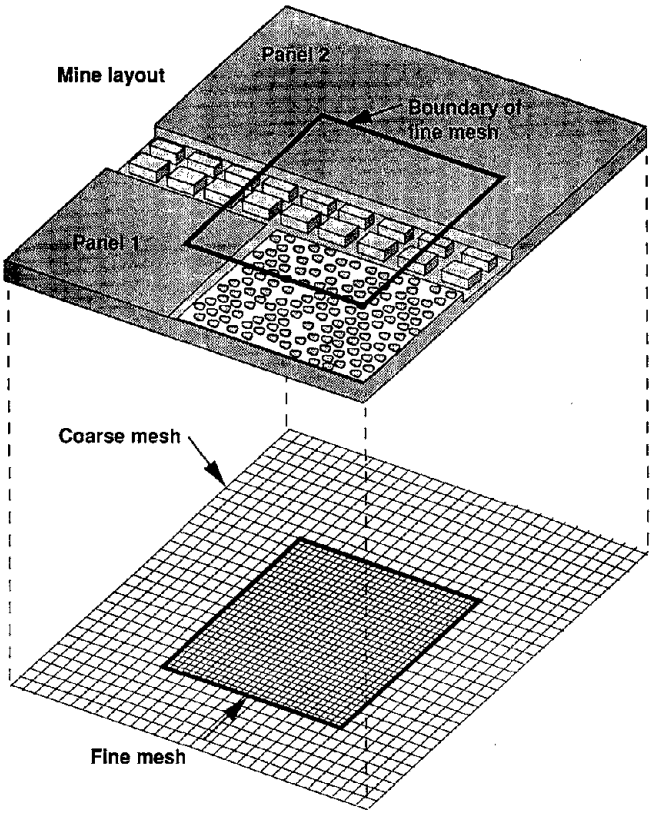

Figure 1.—Typical longwall coal mine layout and modeling grid for a stress analysis using MULSIM/NL.

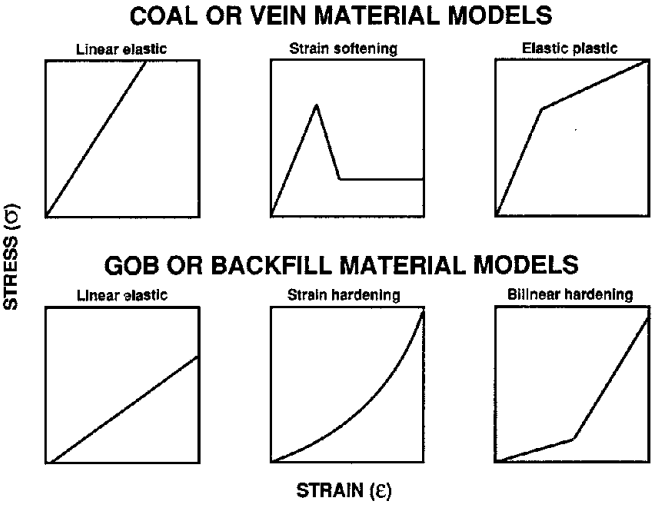

Figure 2.—Stress-strain models for MULSIM/NL.

NONLINEAR MATERIAL MODELS

MULSIM/NL assumes that a continuous, homogeneous, linear elastic rock mass surrounds the seam(s). Unlike prior versions of the program (*3-5*), which assume a linear elastic stress-strain relationship for the in-seam materials, MULSIM/NL now permits various nonlinear material models for the in-seam materials. Figure 2 shows the six models available for the in-seam material: linear elastic for intact seam material (coal), strain softening, elastic-plastic, bilinear hardening, strain hardening, and linear elastic for broken seam material (gob). The first three are intended for the unmined in-seam material, while the latter three are for the broken gob material left in the wake of full extraction mining (*1-2*).

MULTIPLE MINING STEPS AND ENERGY RELEASE CALCULATIONS

MULSIM/NL has a multiple mining step capability to simulate the various stages of mining. With this feature, the user can compute and examine stress and displacement changes between mining steps. Such changes are more comparable to field measurements that usually record stress and displacement changes, as opposed to total, or absolute, stresses and displacements. Based on stress and displacement changes between mining steps, MULSIM/NL computes an energy release rate (ERR) using the derivations of Salamon (*6*). ERR may serve as an indicator of coal mine bump risk (*7*). In addition, MULSIM/NL calculates other strain energy quantities that may serve as indicators of coal mine bump potential (*1, 8*).

INPUT PARAMETERS FOR MULSIM/NL

To conduct a stress analysis with MULSIM/NL, the user must first define the mine geometry of interest to the computer program. The subsequent examples will help to illustrate how this part of an analysis is done. In addition, the user must supply material properties data to the program for the coal, the gob, and surrounding rock mass. Choosing acceptable values for these crucial input parameters will help to ensure that the user obtains a reasonable approximation to the stresses at a particular site.

For the rock mass surrounding the coal seam, the major input parameter required is the Young's modulus. MULSIM/NL assumes that the surrounding rock mass is a linear elastic, homogeneous continuum. Table 1 provides a suggested range of Young's modulus values for different coal measure rocks. The user may have

laboratory measurements of the Young's modulus available. Laboratory-scale values usually exceed field-scale values by a factor of one to four. Typically, the user must decrease a laboratory value by about 50% to obtain the equivalent field-scale value for rock mass modulus.

Table 1.—Suggested values for Young's modulus of rock mass

Major component of rock mass	Range for Young's modulus	
	MPa	psi
Shale	2,000- 6,000	300,000- 900,000
Siltstone	4,000- 9,000	600,000-1,300,000
Sandstone	6,000-12,000	900,000-1,800,000

For the gob left in the wake of full extraction mining, the user must select one of the three different material models available for the gob. The linear elastic and the strain-hardening models are the usual choices. The bilinear hardening model is for special applications. It is highly recommended that the user begin new MULSIM/NL analyses using the linear elastic model. Suggested values for the Young's modulus of the gob might range from 35 to 350 MPa (5,000 to 50,000 psi). After some initial analyses using a linear elastic gob model are complete, the user may want to improve the stress calculations by selecting the more realistic strain-hardening material model for the gob. This model requires three main parameters: an initial tangent modulus, a final tangent modulus, and the vertical stress at that final modulus. Recent laboratory work by Pappas and Mark (*9*) provides a basis for selecting input parameters to the strain-hardening gob model. Table 2 summarizes a suggested range of values for these parameters.

Table 2.—Suggested values for strain-hardening gob model

Parameter	Range	
	MPa	psi
Initial tangent modulus	2- 10	300- 1,500
Final tangent modulus	150-250	20,000-35,000
Final stress	15	2,200

For the coal, the user again has a choice of three different material models: linear elastic, strain-softening, and elastic-plastic. The linear elastic and the strain-softening models are the usual choices. The elastic-plastic model is actually just a special case of the more general strain-softening model. Again, it is highly recommended that the user begin new MULSIM/NL analyses with the linear elastic model. Suggested values for the Young's modulus values of the coal might range from 1,500 to 4,000 MPa (200,000 to 600,000 psi). After some initial analyses using a linear elastic coal model are complete, the user may want to improve the stress calculations by selecting the more realistic strain-softening material model for the coal. This model requires four main parameters: a peak stress and strain, and a residual stress and strain. These parameters define the two points of a strain-softening, stress-strain curve for the coal material as shown in figure 2. Published strength data on full-scale coal pillars provide the basis for selecting these important parameters.

Numerous researchers have created empirical formulas for the strength of coal pillars as a function of the w/h ratio. Bieniawski and van Heerden (*10*) established the linear relationship shown in figure 3 for the peak strength of coal pillars. Recent research by Maleki (*11*) established a

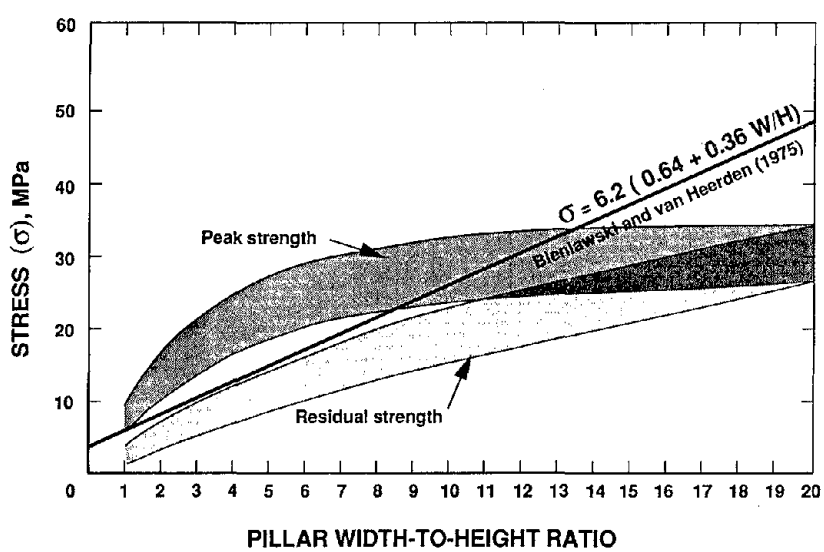

Figure 3.—Strength of coal pillars as a function of width-to-height (W/H) ratio. Peak and residual strengths after Maleki (*11*).

range for the peak and residual pillar strengths as a function of w/h ratio, also shown in figure 3. According to Maleki, the high-strength curve is typical for mines with a large degree of pillar confinement, while the low-strength curve is typical for structurally controlled coal seams with persistent cleats and in-seam contact planes. As shown in figure 4, various researchers (*14-18*) have also contributed data on the postfailure modulus of coal pillars as a function of w/h ratio. By assuming an initial elastic modulus of 2,750 MPa (400,000 psi) and combining the peak and residual strength data of Maleki (*11*) with the postfailure modulus data shown in figure 4, we obtain a set of low-range (figure 5) and a set of high-range (figure 6) strain-softening stress-strain curves for coal that depend on the w/h ratio. Figures 5 and 6 provide a range of suggested values for the peak stress and strain and the residual stress and strain parameters required by the strain-softening material model in MULSIM/NL. Again, the curves shown in figures 5 and 6 are merely suggested places to start. They are based on limited data that exhibit tremendous variance. Whenever possible, the user should obtain site-specific data based on in-mine observations.

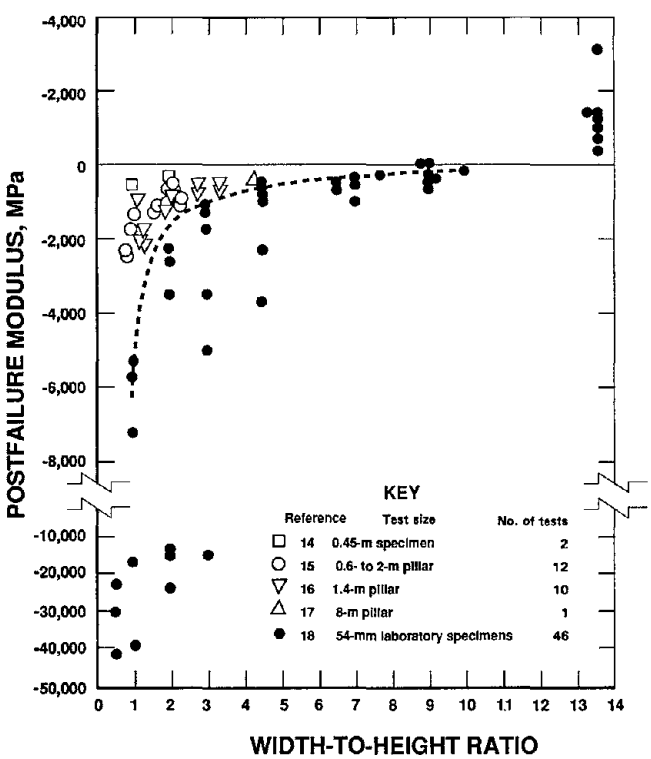

Figure 4.—Postfailure modulus data as a function of w/h ratio.

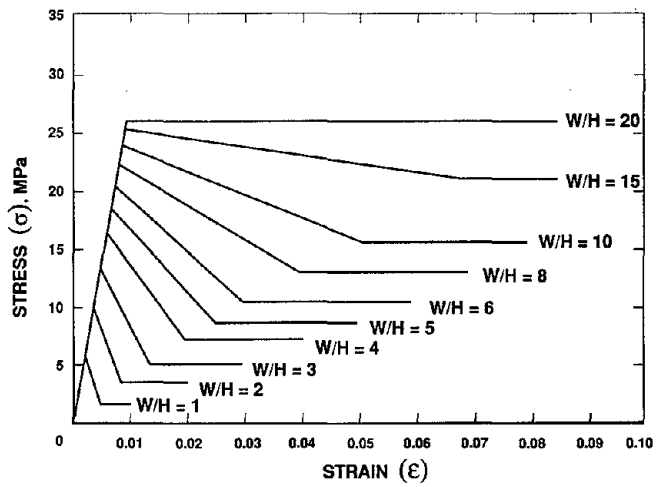

Figure 5.—Suggested strain-softening stress-strain models for MULSIM/NL: low range.

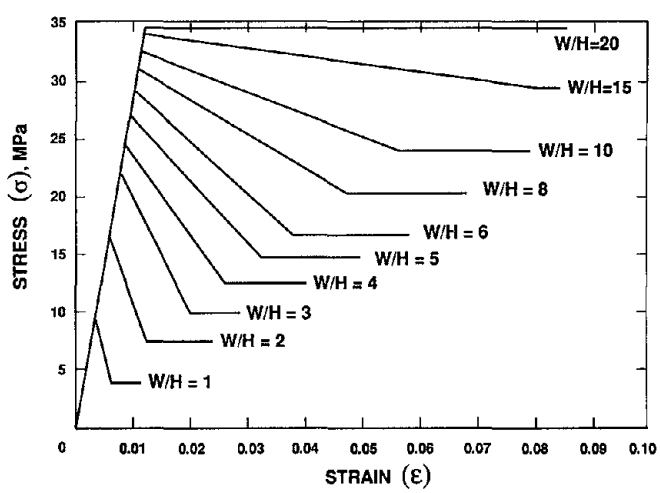

Figure 6.—Suggested strain-softening stress-strain models for MULSIM/NL: high range.

MODELING STRATEGIES WITH MULSIM/NL

In using MULSIM/NL for conducting stress analyses of coal mines, the user must assign material properties to each element in a model. In assigning these properties to the coal elements, four different approaches can be followed: (1) uniform, (2) confinement, (3) w/h ratio, and (4) combined. Figure 7 shows the layout of the headgate area between two longwall panels and indicates how the assignment of material properties defines the mine geometry in a MULSIM/NL model. In the uniform approach shown in figure 7, the same stress-strain curve is applied to a material throughout the mine geometry. In this example, material A is linear elastic coal, and material B is linear elastic gob. However, A could just as well be a strain-softening material, and B could be a strain-hardening material. In any case, properties for coal and gob are uniform throughout the model. The uniform materials approach is usually used for the initial MULSIM/NL stress analyses of a model. Cox and others (*12*) provide an example of this approach using a uniform strain-softening model.

In the confinement approach shown in figure 8, the user assigns different material properties to the elements based on their distance to an opening. Coal elements that are 0 to 3 m (0 to 10 ft) from an opening follow stress-strain curve A, those that are 3 to 6 m (10 to 20 ft) follow stress-strain curve B, and those that are 6 m (20 ft) or more follow stress-strain curve C. This approach accounts directly for the effects of confinement on the strength and postfailure properties of the coal. However, the user should have available stress measurements at various depths into a pillar to help formulate strain-softening stress-strain curves for input. Zipf and Heasley (*7*), Heasley (*8*), Heasley and Zelanko (*13*), and Cox and others (*12*) provide examples of the confinement approach in their analyses using MULSIM/NL.

In the w/h ratio approach shown in figure 9, the user assigns different material properties to entire pillars based on the w/h ratio of the pillar. Thus, the yield pillar with a w/h ratio of 3 follows stress-strain curve A, which is highly strain-softening; the abutment pillar with a w/h

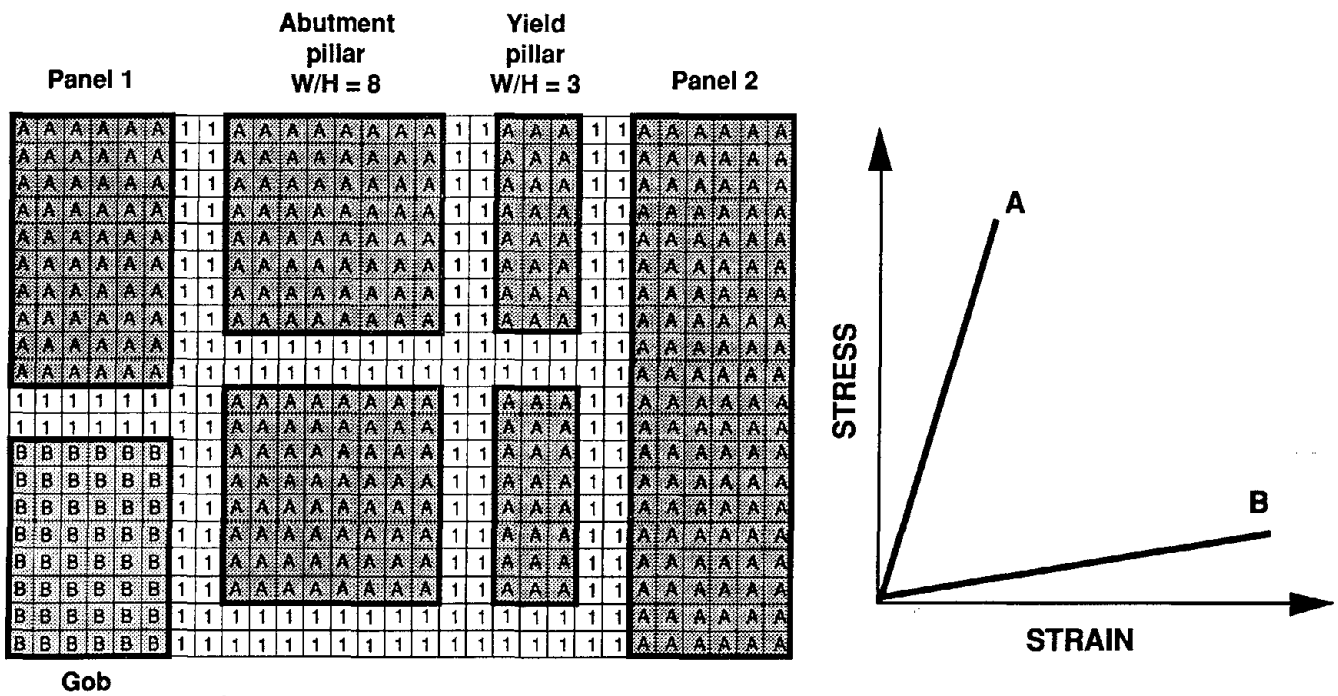

Figure 7.—Uniform approach for material modeling with MULSIM/NL.

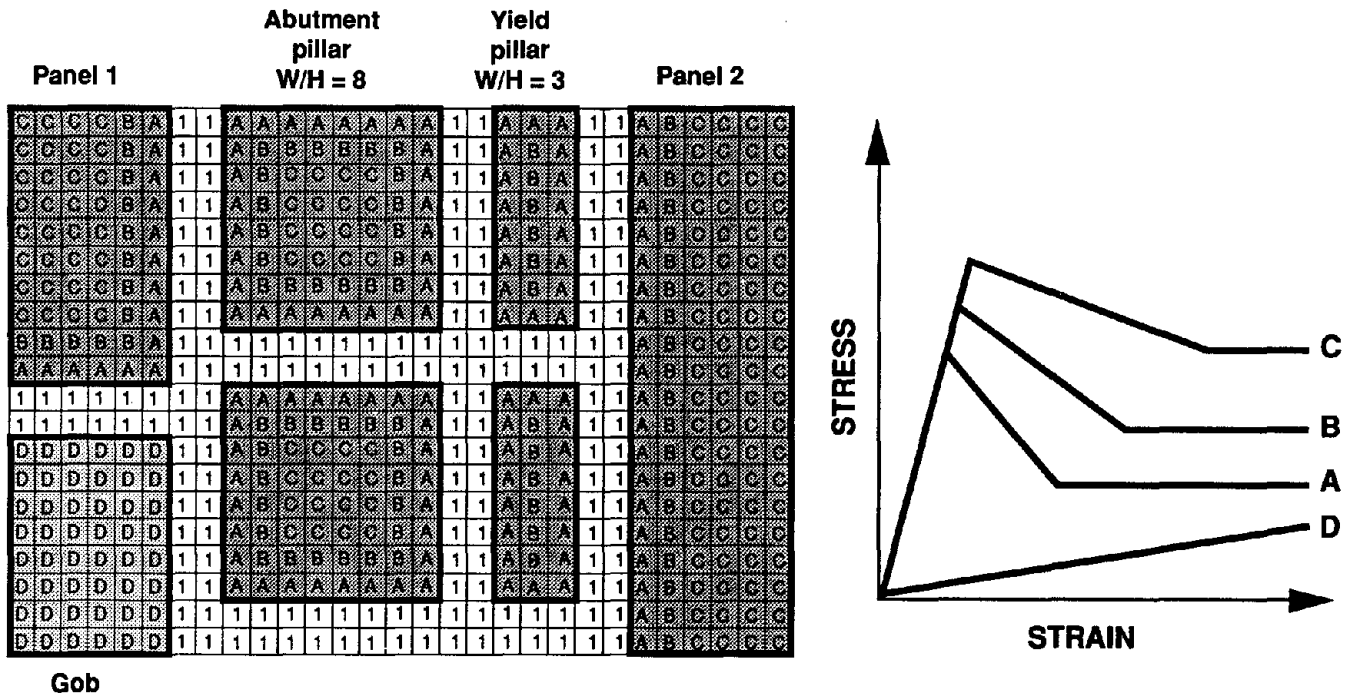

Figure 8.—Confinement approach for material modeling with MULSIM/NL.

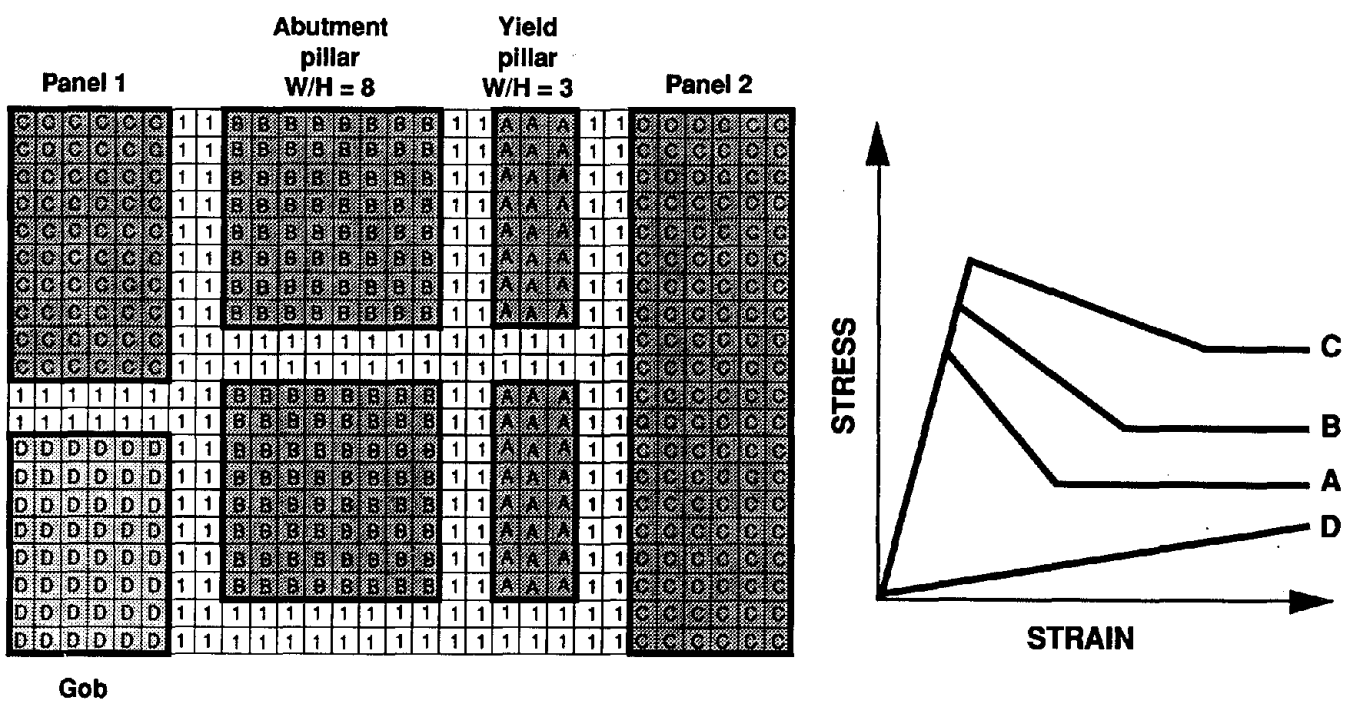

Figure 9.—Width-to-height ratio approach for material modeling with MULSIM/NL.

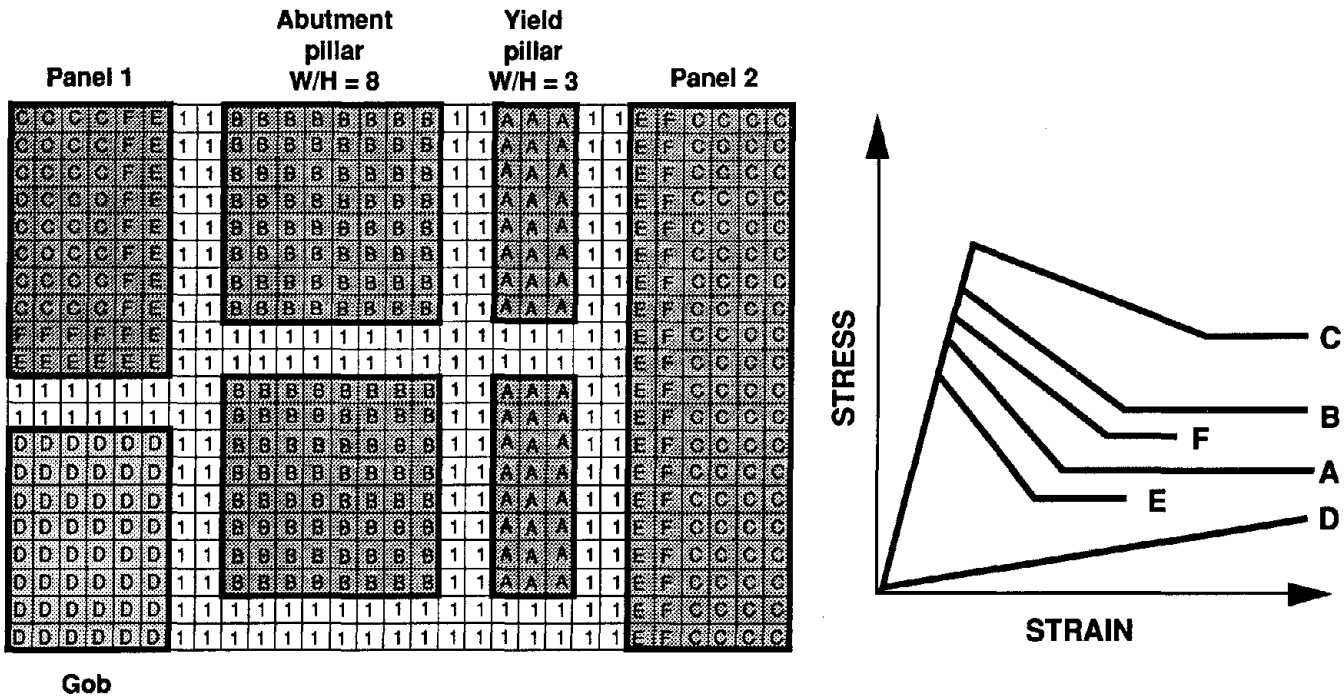

Figure 10.—Combined approach for material modeling with MULSIM/NL.

ratio of 8 follows curve B, which is moderately strain softening; and the solid abutment areas with a w/h ratio greater than 20 follow curve C, which is nearly elastic-plastic. The w/h ratio accounts for the effects of confinement indirectly. The advantage to this approach is the large amount of pillar strength data as a function of w/h ratio that are available. Figures 5 and 6, discussed earlier, provide a range of suggested strain-softening stress-strain curves that depend on w/h ratio. The example analyses provided in this paper illustrate the w/h ratio approach when using MULSIM/NL for stress analysis.

The combined approach shown in figure 10 uses aspects of the confinement and the w/h ratio approaches to assign material properties in a model. One problem with the w/h ratio approach is that it may not work well for pillars with a w/h ratio greater than 20, such as the solid abutment areas around a coal panel. The combined approach overcomes this problem by assigning material properties to solid abutment areas using the confinement approach. Pillars with a w/h ratio less than 20 are still assigned material properties on the basis of their w/h ratio. Therefore, the combined approach tends to bring together the best features of both the confinement and the w/h ratio approaches.

EXAMPLE ANALYSES OF LONGWALL MINES WITH MULSIM/NL

Using MULSIM/NL, an engineer can conduct realistic stress analyses of complex longwall gate road systems, provided that correct material properties are used. Such analyses can help to ensure adequate pillar stability throughout the life of the longwall gate road system. Figures 11, 12, and 13 show computed vertical stresses across complete longwall panels. In these example analyses, mining progresses from left to right. The headgate entries are near the bottom of the model, while the tailgate entries are near the top. All gate road systems use three entries with one 9-m- (30-ft-) wide yield pillar and an abutment pillar that is 18 m (60 ft) square in figure 11, 24 m (80 ft) square in figure 12, and 30 m (100 ft) square in figure 13. Mining occurs at a depth of 300 m (1,000 ft), where the in situ vertical stress is about 7.5 MPa (1,100 psi). Seam thickness is approximately 3 m (10 ft). These MULSIM/NL models show behavior of the gate road pillars at all stages of their life. In the area labeled A in the figures, pillars bear development loads only. In areas B and C, pillars are subject to side abutment loads due to

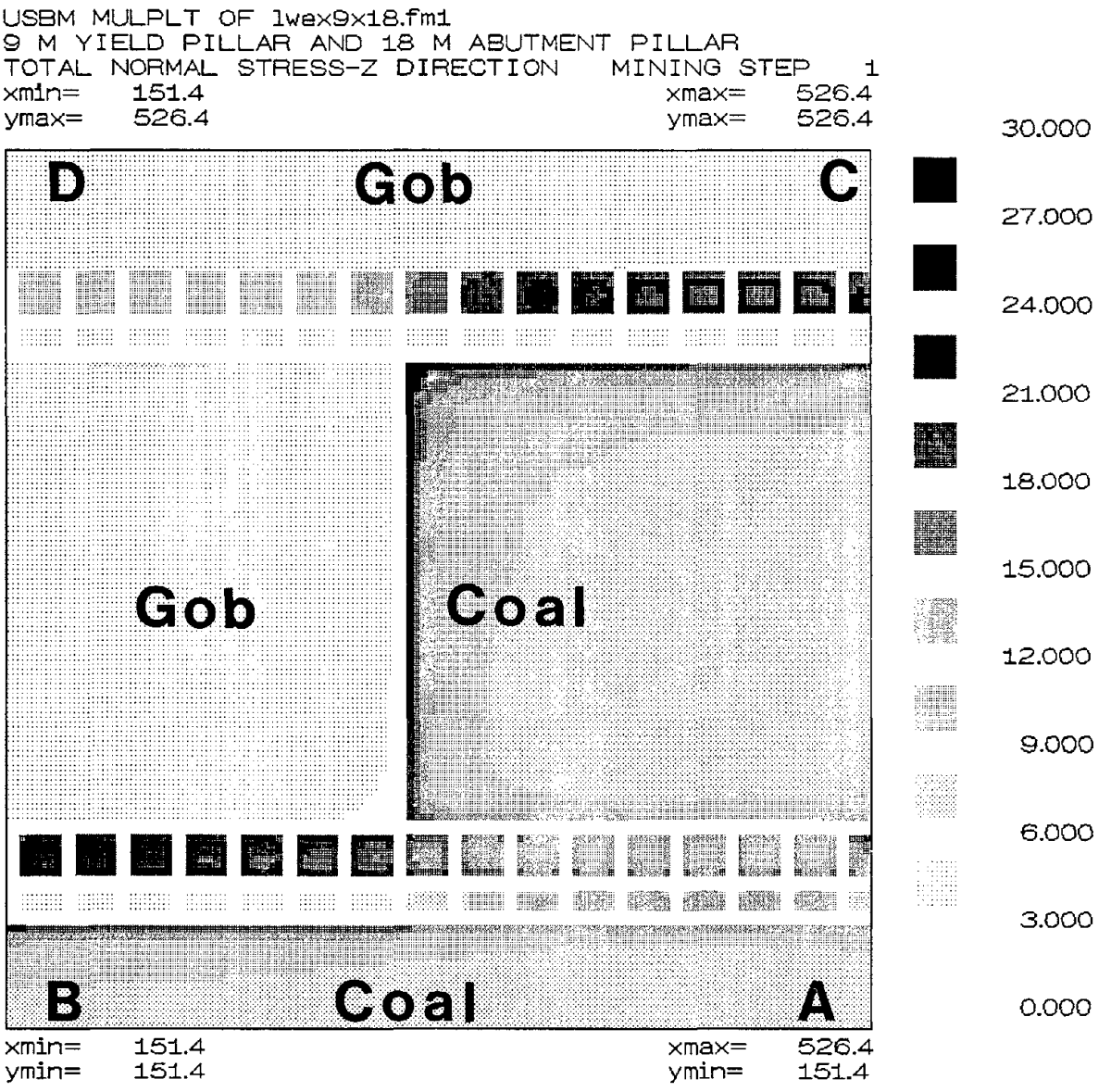

Figure 11.—Computed stresses in MPa across longwall panel with 9-m (30-ft) yield pillar and 18-m (60-ft) abutment pillar. (1 MPa = 145 psi.)

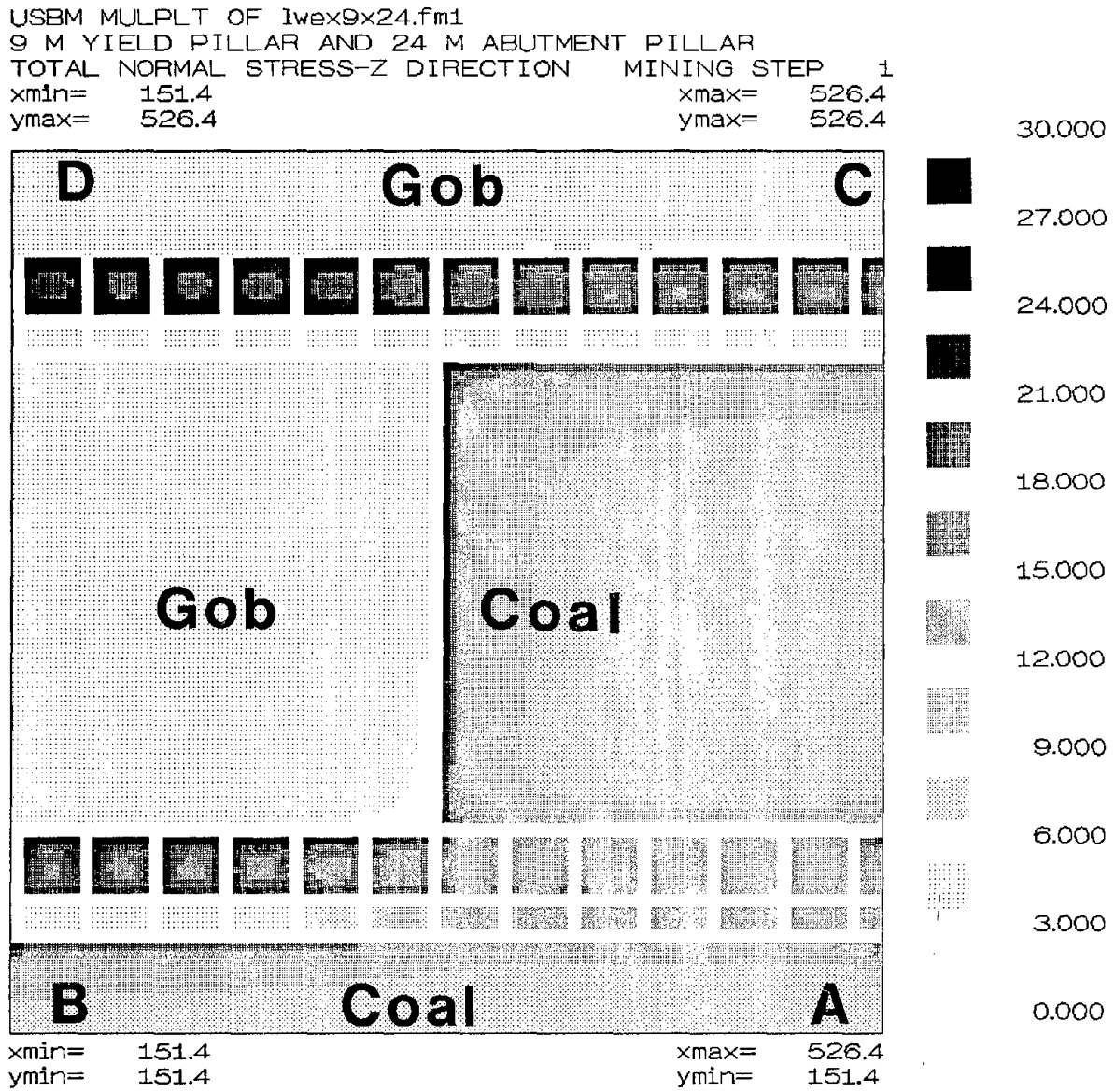

Figure 12.—Computed stresses in MPa across longwall panel with 9-m (30-ft) yield pillar and 24-m (80-ft) abutment pillar. (1 MPa = 145 psi.)

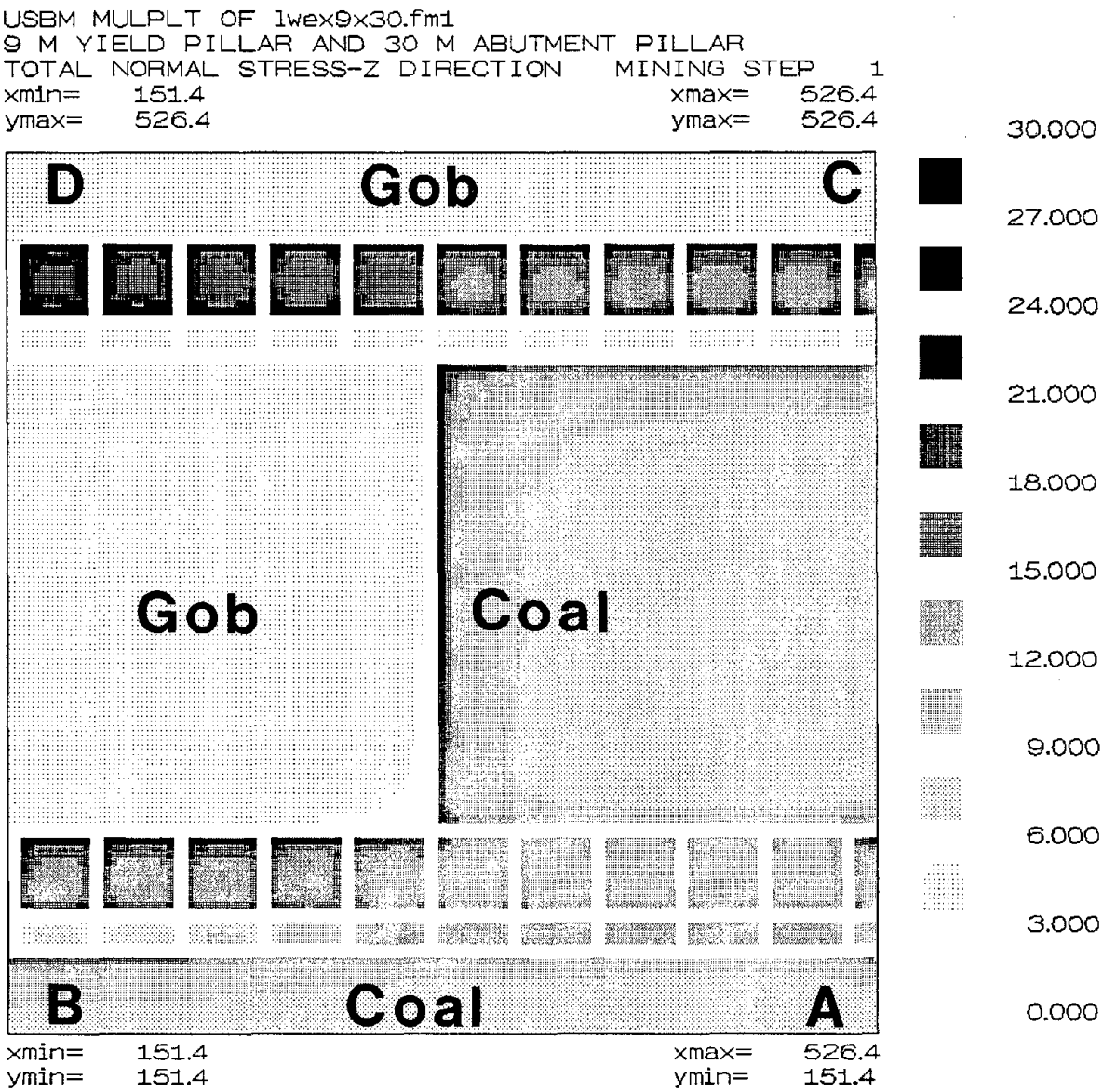

Figure 13.—Computed stresses in MPa across longwall panel with 9-m (30-ft) yield pillar and 30-m (100-ft) abutment pillar. (1 MPa = 145 psi.)

first panel mining. Finally, in area D, pillars experience a second side abutment load due to second panel mining.

MULSIM/NL requires estimates for certain mechanical properties of the coal and the surrounding rock mass. In these analyses, initial elastic modulus of the coal is 2,750 MPa (400,000 psi). Modulus of the rock mass is 10,000 MPa (1,450,000 psi). All analyses use the strain-softening material model for the in-seam coal, which requires an estimate of the peak and residual strength for the coal. Figures 5 and 6 discussed earlier provide a rational means to estimate these strengths as a function of the w/h ratio of the pillar. Table 3 shows the peak and residual strength values for the different pillar sizes used in these analyses.

Figure 11 shows vertical stresses computed by MULSIM/NL for a gate road system using an 18-m (60-ft) abutment pillar with a 9-m (30-ft) yield pillar. On the headgate side, MULSIM/NL shows that the yield pillar begins to fail about 50 m (160 ft) ahead of the face. In other words, the yield pillar has exceeded its peak strength, and the stresses now equal its residual strength. Stresses on the 18-m (60-ft) abutment pillar continue to increase as the longwall face approaches. After the face passes, the abutment pillar begins to fail adjacent to the gob, where stresses have decreased to the residual strength. After first panel mining, in the areas labeled B and C in the figure, MULSIM/NL indicates very high stresses in the core of the abutment pillar. On the tailgate side, the stress calculations show that the 18-m (60-ft) abutment pillar reaches it peak strength about 75 m (240 ft) ahead of the face. In addition, high stress levels exist on the longwall face at the tailgate corner. These stress calculations indicate that the yield pillar fails completely and the abutment pillar fails partially before completion of second panel mining. Therefore, this gate road geometry may be unacceptable.

Figure 12 shows vertical stresses computed by MULSIM/NL for the gate road system using a 24-m (80-ft) abutment pillar with a 9-m (30-ft) yield pillar. With this gate road geometry, the yield pillar fails completely on the headgate side about 30 m (100 ft) after passage of the longwall face. Stresses on the 24-m (80-ft) abutment pillar increase as the longwall face approaches; however, it does not begin to fail as the 18-m (60-ft) abutment pillar did. This pillar remains intact after first panel mining as indicated near areas B and C in the figure. In addition, stress levels on the longwall face at the tailgate corner have decreased because of the larger abutment pillar. As the face approaches on the tailgate side, stresses on the abutment pillar increase. However, unlike the prior case with the 18-m (60-ft) abutment pillar, the 24-m (80-ft) abutment pillar survives after passage of the longwall face. Therefore, this gate road geometry is probably acceptable.

Lastly, figure 13 shows vertical stresses computed by MULSIM/NL for the gate road system using a 30-m (100-ft) abutment pillar with a 9-m (30-ft) yield pillar. With this gate road geometry, the yield pillar fails completely on the headgate side about 130 m (425 ft) after passage of the longwall face. Stresses on the 30-m (100-ft) abutment pillar increase as the longwall face approaches, and as before, it does not fail. This pillar remains intact after first panel mining as indicated near the areas labeled B and C in the figure. Stress levels on the longwall face at the tailgate corner are about the same as with the 24-m (80-ft) abutment pillar. As the face approaches on the tailgate side, stresses on the abutment pillar continue, but it does not fail after passage of the longwall face. Therefore, this gate road geometry is also acceptable, although it is somewhat more conservative than the prior geometry.

One must be cautioned that the accuracy of the stress predictions calculated by MULSIM/NL depends on the material properties selected by the user. The methods for choosing these properties suggested herein are a good place to start; however, the user should always attempt to verify these predictions with field observations and make adjustments accordingly.

Table 3.—Peak and residual strength values for pillars

Pillar type and size	Width-to-height ratio	Peak strength		Residual strength		Figure example
		MPa	psi	MPa	psi	
Yield: 9 m ...	3	15	2,200	5	700	All
Abutment:						
18 m	6	22.5	3,300	10	1,500	11
24 m	8	26	3,800	15	2,200	12
30 m	10	29	4,200	20	2,900	13
Solid coal	NAp	31	4,500	31	4,500	All

NAp Not applicable.

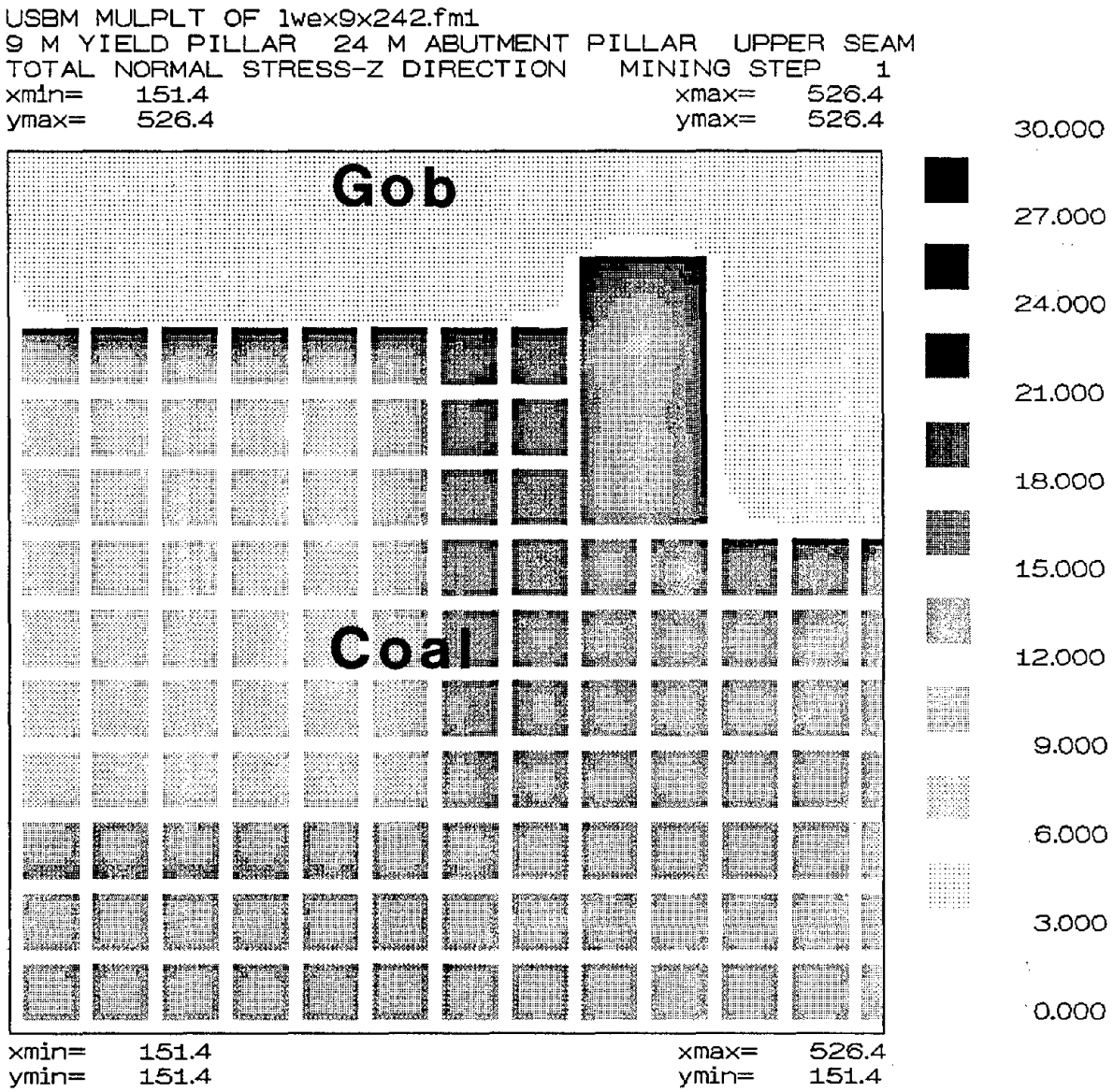

Figure 14.—Computed stresses in MPa across room-and-pillar workings of upper seam. (1 MPa = 145 psi.)

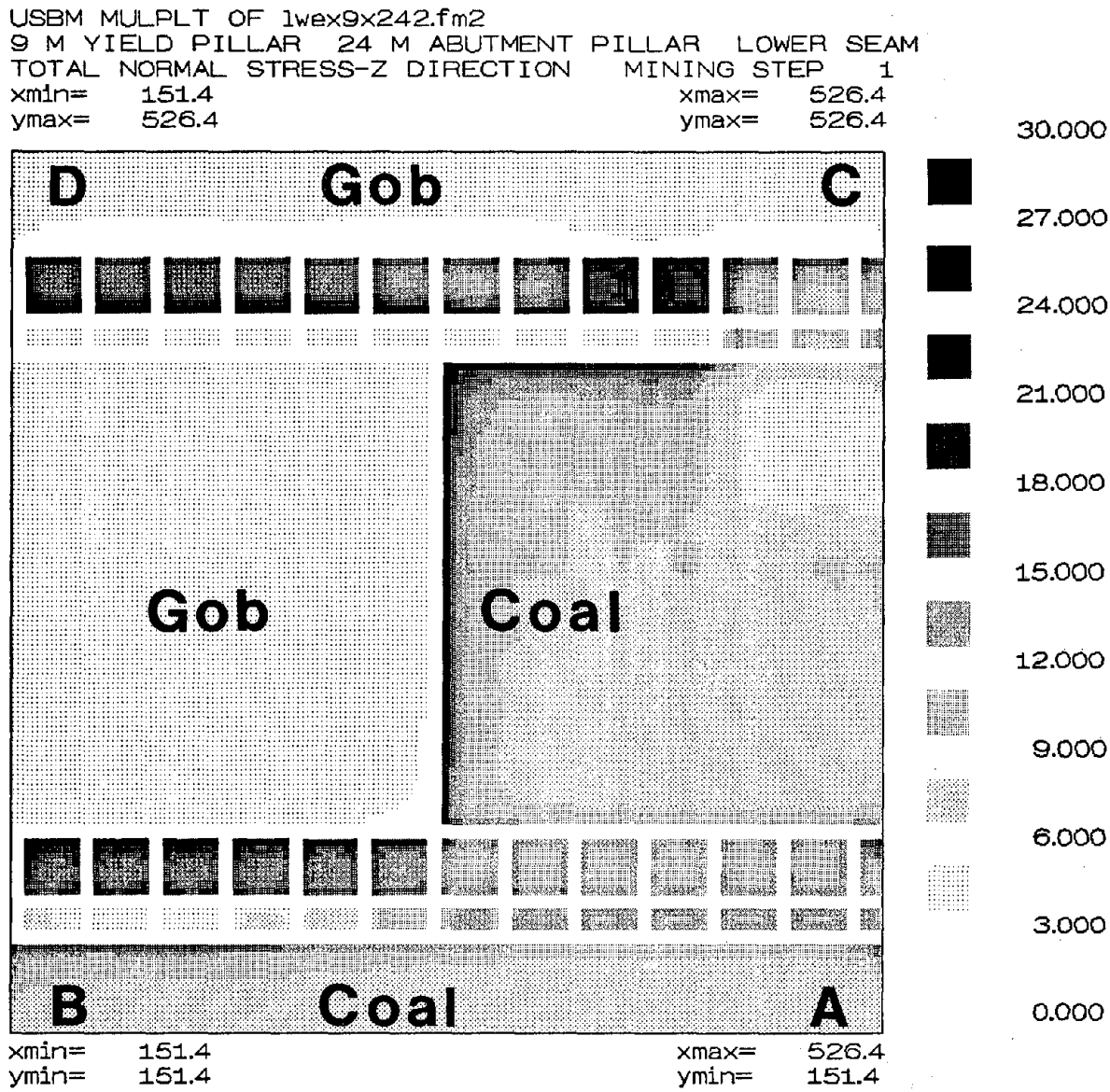

Figure 15.—Computed stresses in MPa across longwall panel of lower seam with 9-m (30-ft) yield pillar and 24-m (80-ft) abutment pillar. (1 MPa = 145 psi.)

The advantage of MULSIM/NL is its ability to analyze stresses for complicated mine geometries and multiple-seam interactions. Figures 14 and 15 illustrate a stress analysis for multiple-seam mining scenarios. Figure 14 shows computed stresses for the upper seam that has been partially extracted with room-and-pillar mining. A large barrier pillar remains adjacent to the gob. Figure 15 shows the stresses on the lower seam, which is 20-m (66-ft) below the upper seam. This longwall mine uses 9-m (30-ft) yield pillars with 24-m (80-ft) abutment pillars and is identical to the operation shown in figure 12. In figure 14, undermining in the lower seam has caused stresses in the upper pillars to decrease. Otherwise, the stress distribution in the upper seam is typical, with higher stresses adjacent to the gob and in the large barrier pillar.

The presence of mining in the upper seam causes numerous changes to the stress distribution in the lower seam. (Figure 12 shows the stresses within this seam without any mining in the upper seam.) In comparing figures 12 and 15, stresses in the headgate pillars and on the headgate side of the longwall panel near areas A and B remain unchanged by the partial extraction in the upper seam. However, the abutment pillars in the tailgate, which lie partially under the gob in the upper seam, show a decrease in stresses. In the area labeled C, figure 12 indicates average abutment pillar stresses of 15 to 18 MPa (2,200 to 2,600 psi), whereas figure 15 shows stresses of 12 to 15 MPa (1,700 to 2,200 psi). The decrease is even more profound in area D. Figure 12, without upper-seam mining, indicates average stresses of about 21 to 24 MPa (3,000 to 3,500 psi), whereas figure 15, with upper-seam mining, shows lower average stresses of about 12 to 15 MPa (1,700 to 2,200 psi).

The presence of the barrier pillar causes many changes to the stress distribution in the lower seam that may affect the mining operations. As seen in figure 15, stresses in the tailgate abutment pillars directly under the barrier pillar have higher stress levels. The stresses in these pillars are identical to those found in figure 12 near area D where the abutment pillars are subject to full-side abutment stresses from both longwall panels. In addition, stresses on the tailgate side of the longwall face are higher than those in the single-seam case. The high stresses under the barrier pillar may cause ground control problems in that section of the tailgate. Extra mine roof support, such as cable bolts or cribs, may be necessary.

SUMMARY

MULSIM/NL, available from the USBM, performs stress analysis of coal mines. As shown in the example analyses, it can calculate realistic stress distributions over a wide variety of complicated longwall mining geometries. These stress distributions can indicate those parts of the mine that have failed and those that remain intact. However, the coal mining engineer must verify the MULSIM/NL predictions against field observations at the mine prior to using the model in new mining areas. The stress analyses provided by MULSIM/NL can help mining companies avoid hazardous ground conditions and costly production delays brought about through inadequate ground control planning.

REFERENCES

1. Zipf, R. K., Jr. MULSIM/NL Theoretical and Programmer's Manual. USBM IC 9321, 1992, 52 pp.

2. ____. MULSIM/NL Application and Practitioner's Manual. USBM IC 9322, 1992, 48 pp.

3. Sinha, K. P. Displacement Discontinuity Technique for Analyzing Stresses and Displacements Due to Mining Seam Deposits. Ph.D. Thesis, Univ. MI, Ann Arbor, MI, 1979, 311 pp.

4. Beckett, L. A., and R. S. Madrid. MULSIM/BM—A Structural Analysis Computer Program for Mine Design. USBM IC 9168, 1988, 302 pp.

5. Donato, D. A. MULSIM/PC—A Personal-Computer-Based Structural Analysis Program for Mine Design in Deep Tabular Deposits. USBM IC 9325, 1992, 56 pp.

6. Salamon, M. D. G. Energy Considerations in Rock Mechanics: Fundamental Results. J. S. Afr. Inst. Min. and Metall., v. 84, No. 8, 1984, pp. 233-246.

7. Zipf, R. K., and K. A. Heasley. Decreasing Coal Bump Risk Through Optimal Cut Sequencing with a Non-Linear Boundary Element Program. Paper in Proceedings of the 31st U.S. Symp. on Rock Mechanics (CO Sch. Mines). A. A. Balkema, Rotterdam, 1990, pp. 947-954.

8. Heasley, K. A. An Examination of Energy Calculations Applied to Coal Bump Prediction. Paper in Proceedings of the 32nd U.S. Symposium on Rock Mechanics (Univ. OK). A. A. Balkema, Rotterdam, 1991, pp. 481-490.

9. Pappas, D. M., and C. Mark. Behavior of Simulated Longwall Gob Material. USBM RI 9458, 1993, 39 pp.

10. Bieniawski, Z. T., and W. L. van Heerden. The Significance of In Situ Tests on Large Rock Specimens. Int. J. of Rock Mech. Min. Sci. Geomech. Abstr., Apr. 1975, v. 12, No. 4, pp. 101-113.

11. Maleki, H. In Situ Pillar Strength and Failure Mechanisms for U.S. Coal Seams. Paper in Proceedings of the Workshop on Coal Pillar Mechanics and Design. USBM IC 9315, 1992, pp. 73-77.

12. Cox, R. M., T. L. Vandergrift, and J. P. McDonnell. Field Test of an Alternative Longwall Gate Road Design. USBM RI, 1994, in press.

13. Heasley, K. A., and J. C. Zelanko. Pillar Design in Bump-Prone Ground Using Numerical Models With Energy Calculations. Paper in Proceedings of the Workshop on Coal Pillar Mechanics and Design. USBM IC 9315, 1992, pp. 50-60.

14. Bieniawski, Z. T., and U. V. Vogler. Load-Deformation Behavior of Coal After Failure. Paper in Proceedings of the 2nd Int. Congr. on Rock Mechanics, ISRM, Belgrade, Yugoslavia, v. 1, 1970, paper #2-12.

15. Wagner, H. Determination of the Complete Load-Deformation Characteristics of Coal Pillars. Paper in Proceedings of the 3rd Int. Congr. on Rock Mechanics, Nat. Acad. Sci., v. 2B, 1974, pp. 1076-1081.

16. Van Heerden, W. L. In Situ Determination of Complete Stress-Strain Characteristics of Large Coal Specimens. J. S. Afr. Inst. Min. and Metall., v. 75, No. 8, 1975, pp. 207-217.

17. Skelly, W. A., J. Wolgamott, and F. D. Wang. Coal Pillar Strength and Deformation Prediction Through Laboratory Sample Testing. Paper in Proceedings of the 18th U.S. Symp. on Rock Mechanics, CO Sch. Mines, Golden, CO, 1977, pp. 2B5-1 to 2B5-5.

18. Das, M. N. Influence of Width/Height Ratio on Post Failure Behavior of Coal. Int. J. Min. and Geol. Engr., v. 4, 1986, pp. 79-87.

LONGWALL MINE DESIGN FOR CONTROL OF HORIZONTAL STRESS

By Christopher Mark[1] and Thomas P. Mucho[1]

ABSTRACT

Horizontal stress is a significant, although often overlooked, factor in ground control in longwall mines. It can be particularly destructive in development and headgate entries, where it can cause persistent compressive-type roof failure called cutter roof, roof guttering, or kink roof. This paper presents the current state of the art in detecting and controlling horizontal stress. The information was collected through detailed site investigations at several eastern U.S. longwall mines, a survey of ground conditions at 50 U.S. longwalls, and an international literature review.

This paper begins with a discussion of the present knowledge of regional in situ stress fields in the United States. A compilation of underground stress measurements from 47 U.S. coal mines is presented. The measurements indicate a persistent trend of high horizontal stresses trending east-northeast to east-west in the Eastern United States. The direction and magnitude of horizontal stress does not appear to be significantly affected by ancient geologic structures in the East, but surface topography may have an important effect. Horizontal stresses in the Western United States are less consistent in direction and are generally lower relative to the vertical stress. These observations are consistent with the regional stress fields identified by the geophysicists of the World Stress Map Project, who have lately presented convincing evidence that the horizontal stresses observed underground are linked to plate-tectonic processes.

Next, experience with horizontal stress in longwall mines is addressed. The paper focuses on the northern Appalachian region, where the effects of horizontal stress have been most evident. Three case histories are described in detail, and the solutions developed are highlighted. Evidence of horizontal stress observed underground in Illinois, Alabama, and the Western United States is also discussed.

The degree of horizontal stress damage to longwall gate entries appears to vary by region and by roof geology. Laminated shale roofs, particularly in the northern Appalachian Mountains and in Illinois, appear to be at the greatest risk. Some simple, in-mine, stress mapping techniques are described. Control techniques discussed include panel orientation, cut sequencing, softened entries, and roof support.

[1]Mining engineer, Pittsburgh Research Center, U.S. Bureau of Mines, Pittsburgh, PA.

INTRODUCTION

Although the role of horizontal stress in ground control has been recognized in U.S. coal mines since at least the early 1970's, its effects and considerations have not been well understood or communicated in many sectors of the mining community. Mines impacted by severe compressive-type roof failure usually become knowledgeable about horizontal stress, but severely affected mines usually have been economically uncompetitive and forced to close. Most of the industry remains unaware, because the effects of horizontal stress may be neither dramatic nor easily differentiated from those of vertical stress. As a result, horizontal stress is seldom a serious consideration in mine design, even when it detrimentally impacts an operation.

The incognizance of the contribution of horizontal stress to opening instability is somewhat perplexing in view of the knowledge that has accumulated about it over the last 20 years. For example, it is widely accepted that the magnitude of the principal horizontal stress, especially at depths less than 800 m (2,600 ft), is often two to three times that of the vertical stress (*22*).[2] Additionally, given the typical rectangular shape of coal mine entries, traditional elastic theory predicts that horizontal stresses would be in close proximity to the immediate roof-and-floor (figure 1).

In longwall mines, the observed effects of horizontal stresses include—

- *Compressive-type roof failures* (commonly called cutter roof, guttering, shear, snap top, pressure cutting, or kink roof). In thinly bedded (laminated) rock, classic cutter roof develops as the progressive layer-by-layer crushing and buckling of individual beds (figure 2).

[2]Italic numbers in parentheses refer to items in the list of references preceding the appendix of this paper.

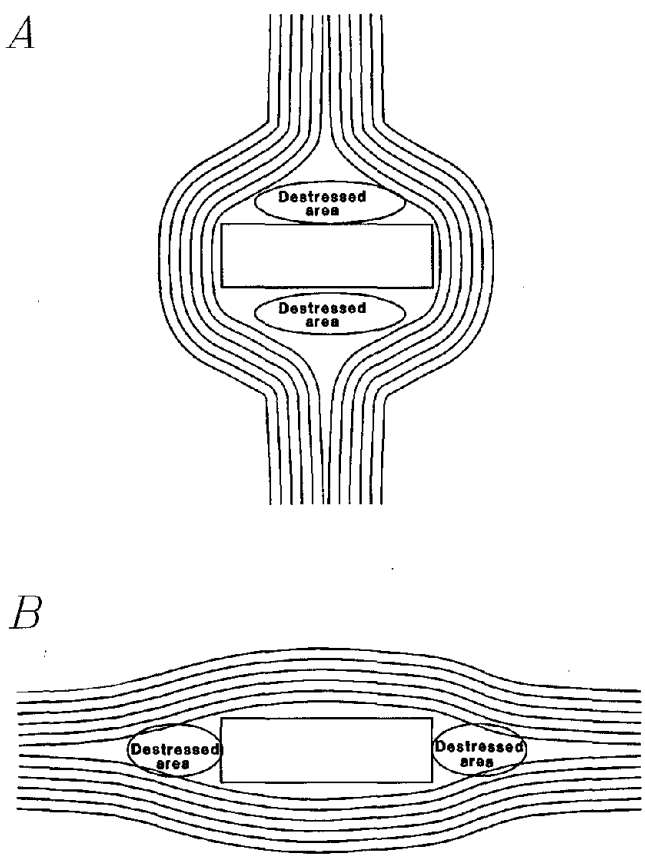

Figure 1.—Conceptualized vertical (*A*) and horizontal (*B*) stress distributions around a mine opening.

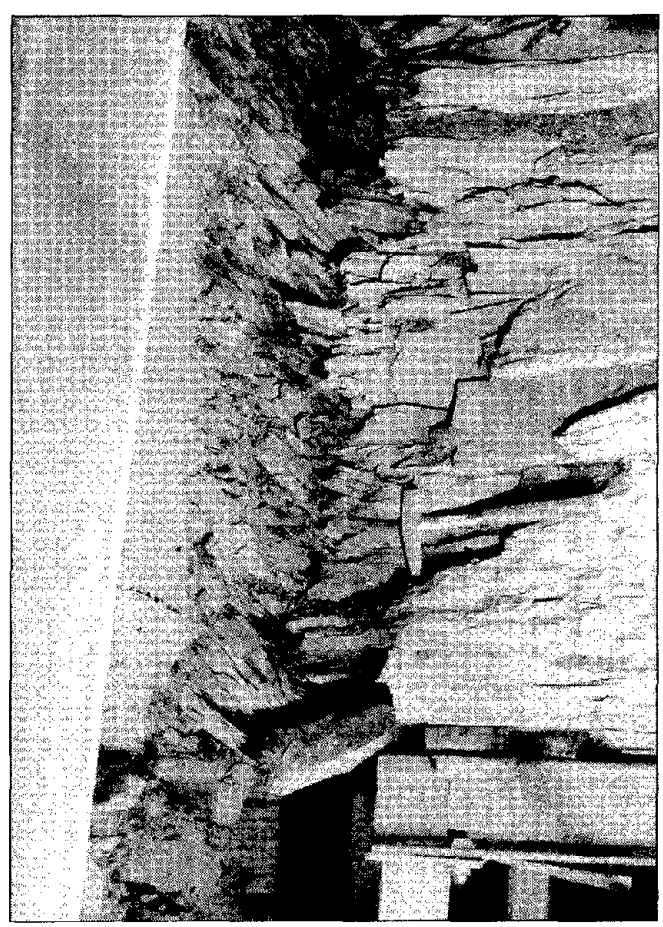

Figure 2.—Cutter roof caused by horizontal stress. *(Photo: Frank E. Chase, Pittsburgh Research Center, U.S. Bureau of Mines)*

• *Directionality of roof falls.* Many horizontal stress fields are distinctly biaxial, with a maximum horizontal stress (σ_H) much greater than the minimum horizontal stress (σ_h). As a result, entries oriented nearly perpendicular to σ_H suffer much greater damage than those oriented parallel.

• *Headgate failures.* In the absence of horizontal stress, headgates are usually less troublesome than tailgates because they are subjected to lower vertical stresses. When headgates are consistently more troublesome, horizontal stress is the most likely cause. Because horizontal stresses cannot pass through the gob left in the wake of longwall mining, the horizontal stresses are relieved in some areas and concentrated in others. These horizontal stress abutment zones are located where a line drawn parallel to the maximum horizontal stress intersects a corner of the longwall panel without passing through the gob (figure 3).

This paper summarizes the current knowledge regarding (1) in situ horizontal stress fields in U.S. coalfields, (2) the prevalence of gate entry instability that is attributable to horizontal stress, and (3) the effectiveness of available control techniques.

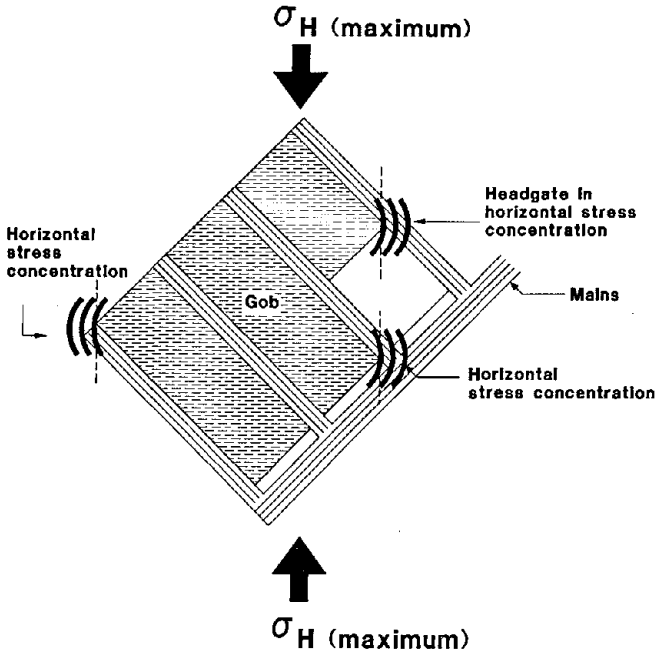

Figure 3.—Horizontal stress concentrations or abutments as a result of retreat mining through the stress field.

HORIZONTAL STRESS FIELDS OF NORTH AMERICA

Evidence that strong horizontal stresses were active in the geologic past is widespread. Mountain chains, thrust faults, and other features are the products of tremendous forces. Present-day earthquakes prove that horizontal stresses are still active. Today, it is widely accepted that horizontal stresses in the Earth's crust are closely linked to the movements and interactions of continental plates. Earlier theories that simply related horizontal stresses to the Poisson's effect have been completely discredited (*31*).

Recent papers by workers associated with the World Stress Map Project (*38, 44-46*) have summarized current knowledge about horizontal stress fields in North America. Their more than 400 data points include hydraulic fracturing stress measurements, overcoring stress measurements, borehole "breakouts" or elongations observed in oil and gas drilling, centerline fractures in oriented core, earthquake focal mechanisms, and fault-slip solutions. Some of these measurements were made at depths as great as 20 km (12 mi), but many were in the 450-1,200 m (1,500-4,000 ft) range.

Using these observations, Zoback and Zoback (*46*) developed the tectonic stress map of the United States shown in figure 4. The stress map divides the continental United States into eight stress provinces, each defined by reasonably uniform horizontal stress orientations and magnitudes (relative to the vertical overburden stresses). The stress provinces are the result of current plate tectonic activity.

The largest stress province, the Mid-Plate, encompasses most of the eastern two-thirds of North America, including all the major eastern coalfields of the United States and Canada. The Mid-Plate stress province is characterized by horizontal stresses that are very consistently oriented northeast to east-northeast, with some rotation toward east-west in the Illinois Coal Basin. The east-northeast stress orientation coincides with current direction of the North American plate as it is being pushed by the expansion of the mid-Atlantic ridge (*46*). The Mid-Plate stress regime is called compressional, because the east-northeast horizontal stress is the major principal stress, while the vertical stress is either the minor or the intermediate principal stress.

The present-day stress field in eastern North America is significantly different from the ancient stress field responsible for the Appalachian Mountains. In fact, the current stress field is "not noticeably affected by faulting or

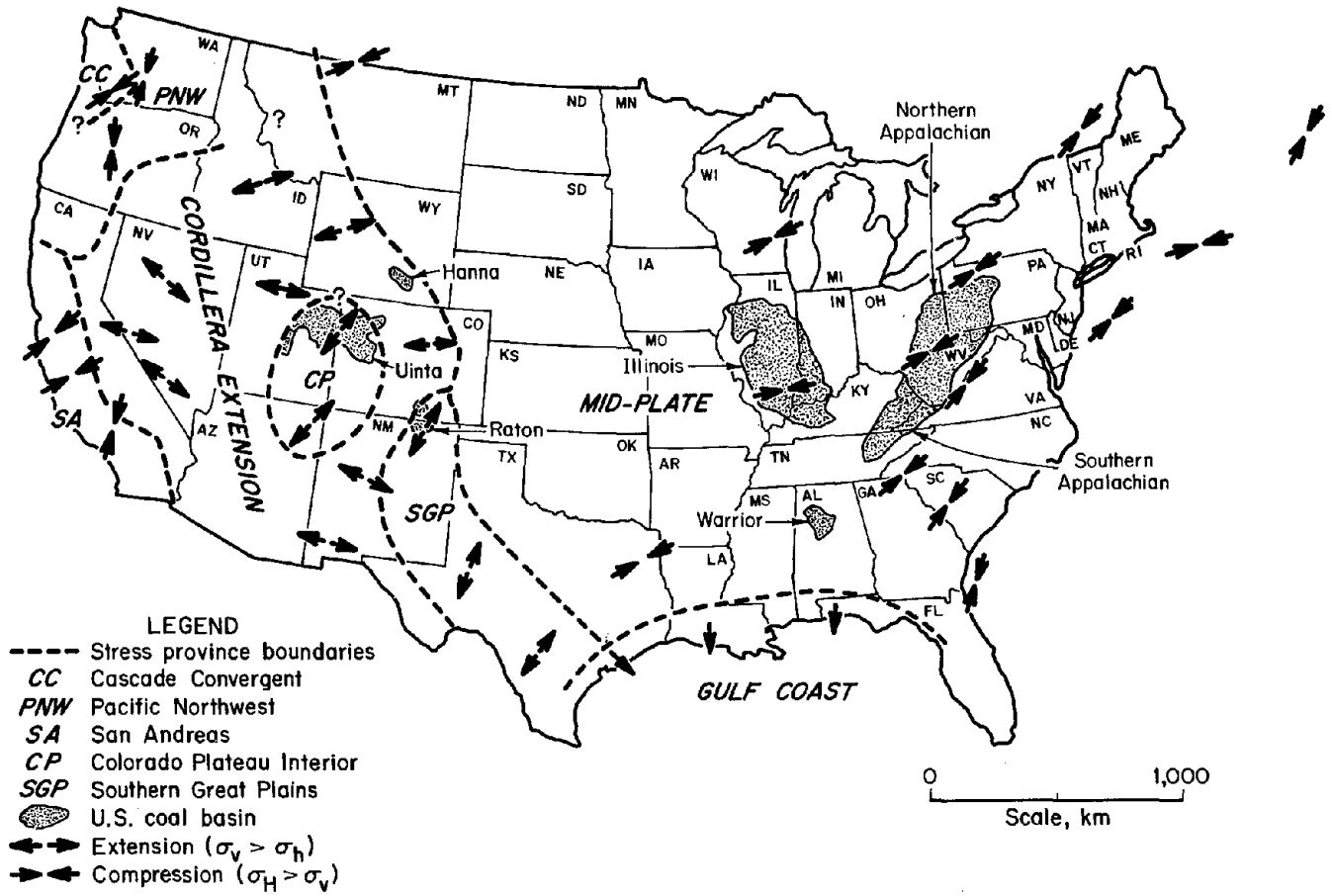

Figure 4.—Eight stress provinces of the continental United States. Arrows indicate the orientation of the maximum horizontal stress. (After Zoback and Zoback (*46*)).

folding on a regional scale" because of its consistency across several geologic and physiographic provinces (*38*). The evidence "that residual stresses from past orogenic events do not appear to contribute in any substantial way to the modern stress field" includes the fact that "the modern ENE orientation is maintained in detail in Pennsylvania through a region where the Appalachian orogenic belt makes a 40 degree bend in strike" (*45*).

In the Western United States, the coalfields lie within three stress provinces: the Colorado Plateau Interior, the Cordillera Extension, and the Southern Great Plains (figure 4). These three stress provinces are called extensional because the vertical stresses equal or exceed the horizontal. The Western United States is an area of high topography, and it is believed that recent uplift is responsible for the development of the extensional stress regimes (*44, 46*). The typical major horizontal stress orientations are west-northwest in the Cordillera Extension province and north-northeast in the Colorado Plateau Interior and the Southern Great Plains provinces, but there are wide local variations in direction and magnitude (*46*). Parts of the eastern Wasatch Plateau-Book Cliffs region are even believed to be characterized by a compressive stress regime, although "the nature of these stresses is not well understood" (*44*).

STRESS MEASUREMENTS IN U.S. COAL MINES

During the past 20 years, a significant number of stress measurements have been conducted in underground coal mines. The appendix to this paper contains a compilation of measurements from 47 mines taken from more than 20 sources. Measurements from the eastern U.S. coal mines are presented in table A-1 in the appendix to this paper, while those from western U.S. coal mines are presented in table A-2.

MEASUREMENTS IN EASTERN U.S. COAL MINES

Table A-1 in the appendix to this paper presents data on stress measurements obtained from 5 coal mines in the northern Appalachian coalfields, 13 from the southern Appalachians, 8 from the Illinois Coal Basin, and 3 from Alabama. Some very clear patterns emerge from the data. In 69% of the measurements from mines in the Appalachian and Warrior Coal Basins, the orientation of maximum horizontal stress falls between N. 80° E. and N. 50° E. (figure 5). In the Illinois Basin, 75% of the measurements indicated that the stress field is rotated toward east-west by approximately 15°. These measurements confirm that the regional east-northeast stress field in the Mid-Plate province is predominant in the eastern U.S. coalfields. The correlation between the measurements and the regional stress field is particularly remarkable, considering that the measurements were made by a wide variety of researchers using a vast range of equipment.

Several explanations may be advanced to explain those measurements that do not conform to the general trend. The most important is perhaps surface topography. Numerous studies have shown that the presence of surface stream valleys can concentrate stresses in the underlying ground (*21*). One recent study (*32*) found that 52% of unstable roof at eight selected mines occurred beneath the bottommost part of stream valleys. Underground mapping, in situ stress measurements, and numerical modeling all indicated that stream valleys strongly interacted with the in situ stress field, sometimes rotating it or even relieving it through thrust faulting. Mines located above drainage, however, may operate in a largely stress-relieved environment. It seems likely that severe surface topography, such as in the southern Appalachians, may often mask the in situ stress field. Some geologic structures, such as faults, may influence local stress fields, but current research indicates that in the Eastern United States, the

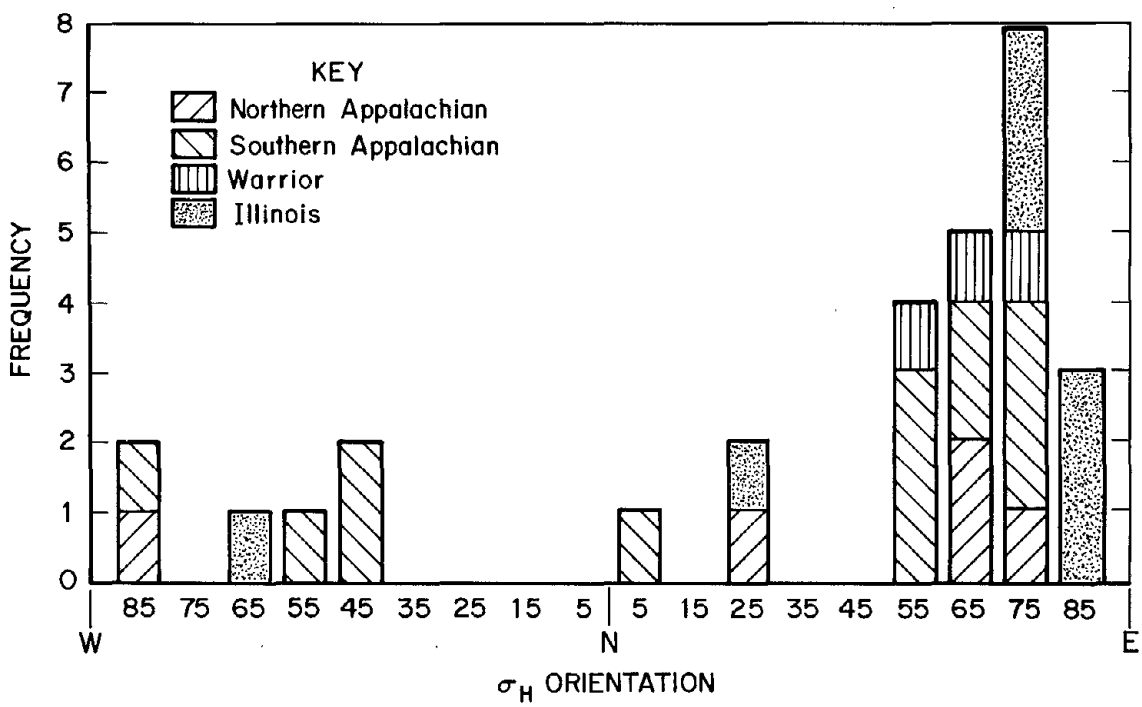

Figure 5.—Orientation of maximum horizontal stress measured in eastern U.S. coal mines.

effect is minimal or nonexistent (*24*). Lastly, errors in measurement may have contributed some inconsistency to the data.

Figure 6 shows that the horizontal stress exceeded the vertical stress in more than 90% of the observations, most often by a factor of two or more. Again, this conforms to the description of the compressional stress regime in the Mid-Plate stress province. Perhaps surprisingly, the seven highest measurements, all in excess of 21 MPa (3,000 psi), are from southern Appalachian coal mines. The measurements may be somewhat biased by the fact that many of them were conducted in mines that had been experiencing a high incidence of stress-related failures. Some of the measurements indicate that stresses may be relieved when the mine is located above the level of drainage. It also appears that, while the magnitude of the horizontal stress continues to increase with depth, the ratio of the horizontal to vertical stress tends to decrease.

MEASUREMENTS IN WESTERN U.S. COAL MINES

Table A-2 in the appendix to this paper presents data on stress measurements obtained from 8 Utah and 10 Colorado coal mines. In the western U.S. coal mines, the trends in stress field orientation (figure 7) are much less clear than for the eastern U.S. mines. Measurements from Colorado mines appear to be fairly randomly distributed, while those from Utah mines indicate some tendency toward the north-northwest trend predicted for the Colorado Plateau Interior stress province (figure 4). Generally, there appears to be much more variation in stress direction from mine to mine and even within individual mines. It seems likely that faults and other geologic structures may be actively influencing local stress fields to a much greater extent than in the East. Many mines are also located near the boundaries between stress provinces.

The magnitude of the horizontal stresses, relative to the vertical stresses, are lower than in the East. As figure 8 shows, in most cases the horizontal stress is almost equal to the vertical stress. Again, this stress ratio is what is expected in the extensional stress regimes prevalent in the western U.S. stress provinces.

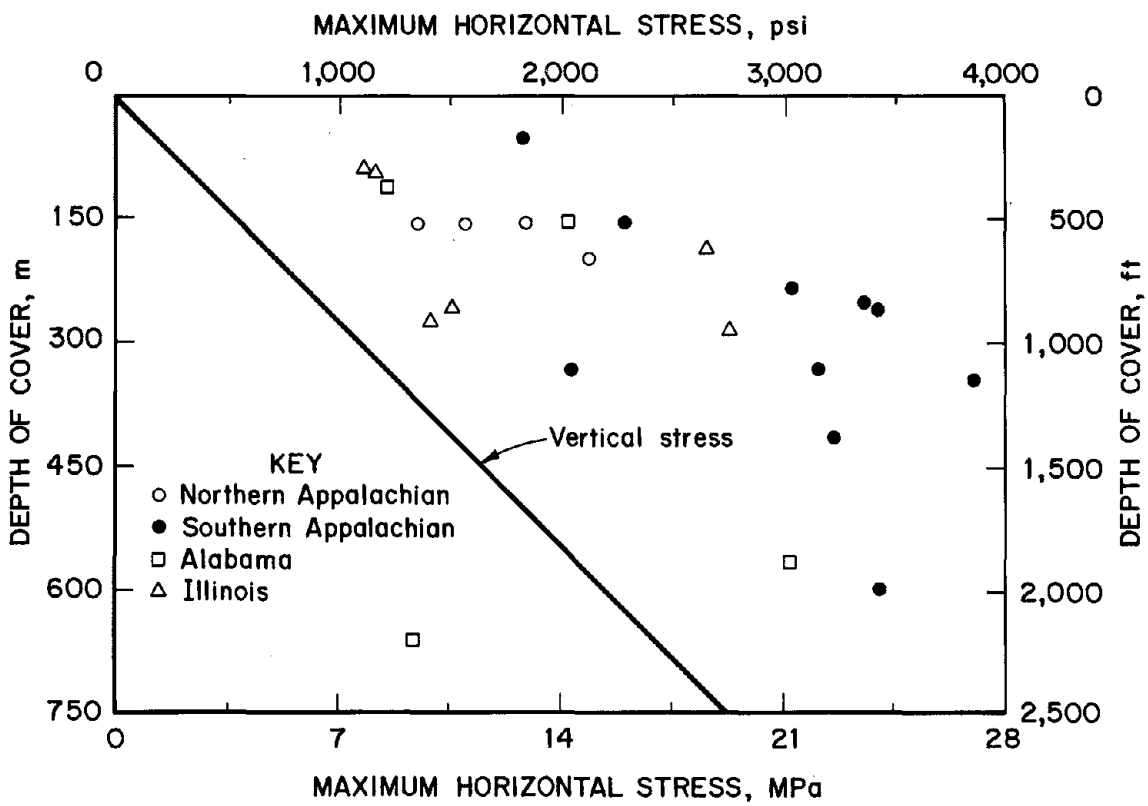

Figure 6.—Relationship of σ_H to depth in eastern U.S. coal mines. Vertical stress (σ_v) shown as .025 MPa/m (1.1 psi/ft).

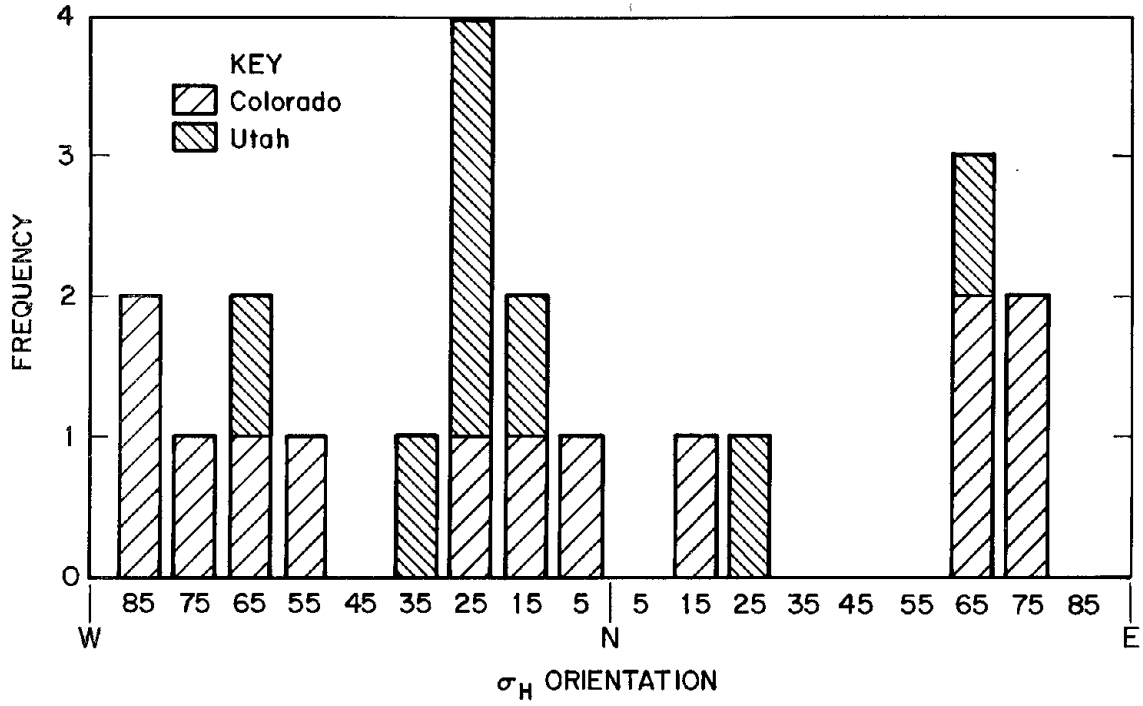

Figure 7.—Orientation of the maximum horizontal stress measured in western U.S. coal mines.

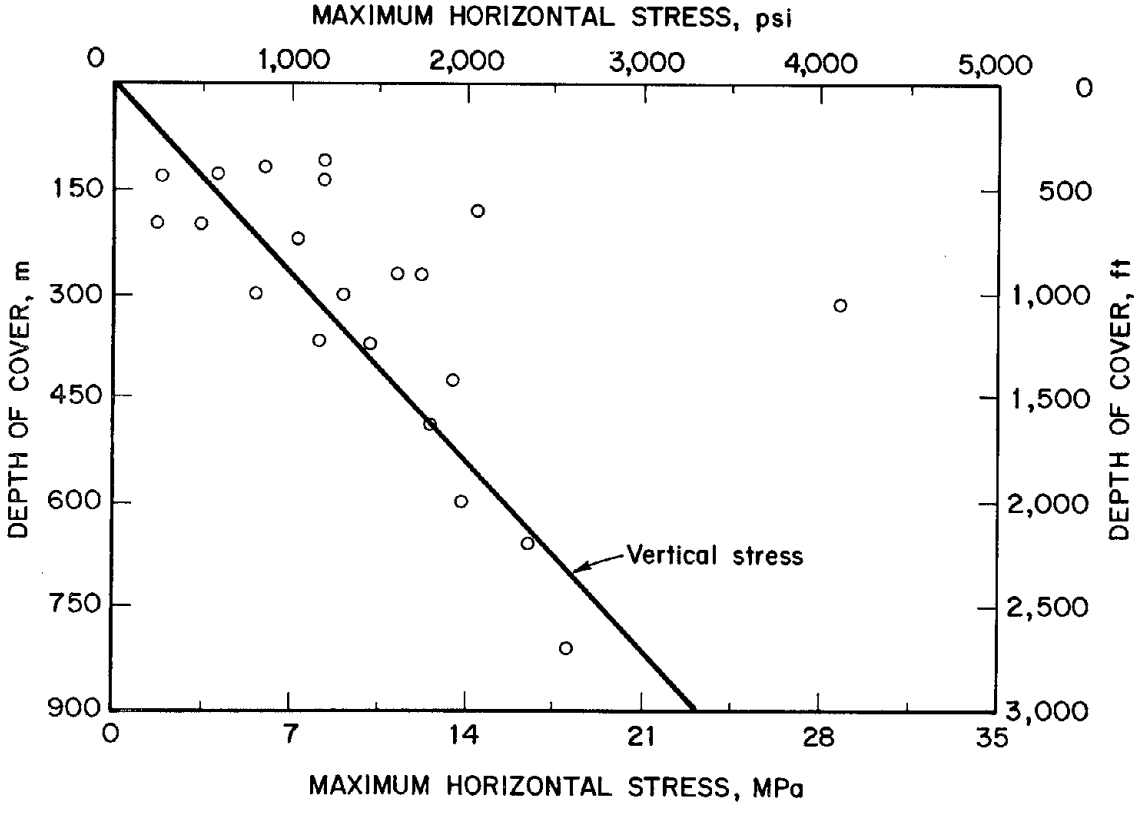

Figure 8.—Relationship of σ_H to depth in western U.S. coal mines. Vertical stress (σ_v) shown as .025 MPa/m (1.1 psi/ft).

LONGWALL MINES AND HORIZONTAL STRESSES

In situ horizontal stresses have been observed to adversely affect longwall mines throughout the world, and they certainly are not new to U.S. coal mines. As early as 1948, Roley (*40*) described a phenomenon he called pressure cutting in the Illinois mines. During the 1970's and 1980's, U.S. Bureau of Mines (USBM) research shed considerable light on the origin and control of cutter roof (*7, 20, 26*). Many of the control technologies now used in Australia and the United Kingdom—including stress mapping, entry orientation, sacrificial entries, and high-strength roof bolts—were pioneered in the United States.

PITTSBURGH COAL SEAM

The Pittsburgh Coal Seam is the most extensively longwalled coalbed in the United States, as well as the most recognized in terms of horizontal stress. Even before the advent of longwall mines, miners had noticed that cutter roof and snap top seemed to occur preferentially in north-south headings. A classic study by Dahl and Parsons in 1972 (*14*) determined that horizontal stress was responsible for these and other directional phenomena, including floor heave, rib spalling, and the formation of tensile cracks.

Based on their prelongwall mining history and some early poor experiences, most mines in the Pittsburgh Coal Seam have oriented their longwall panels nearly east-west. At the 8 Pittsburgh Seam longwall mines composing this study, a total of 157 longwall panels have been extracted during the past 20 years. Of these, 58% were oriented between east-west and N. 70° W. (figure 9). No serious problems attributable to horizontal stress were reported to have occurred on any of these panels, except in crosscuts. Another 29% of the panels had been oriented between N. 70° W. and N. 60° W., with some of these experiencing headgate instability, which will be described in detail later. Only 2 of the 157 panels had been oriented north-south. Both of these experienced conditions so poor that the panels were abandoned before they were completed. Most observers seem to agree that, in general, mine roof falls are much less common now than 20 years ago, particularly in north-south headings. This improvement is often attributed to better roof bolts, which have progressed from mechanical anchors, through fully grouted resin, to the resin-anchored tension bolts used today in most Pittsburgh Seam longwall mines.

Many of the mine officials noted, however, that crosscuts still tended to be troublesome on longwalls and that

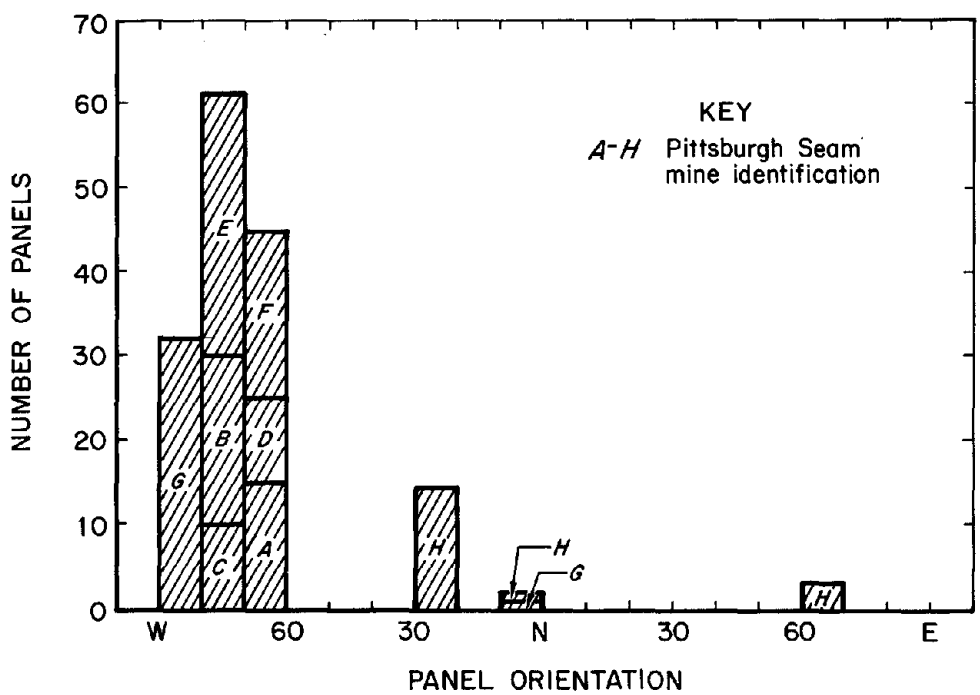

Figure 9.—Orientations of longwall panels in the Pittsburgh Coal Seam.

they usually added extra support in them. At least one mine has experimented with crosscuts oriented at N. 40° E., N. 10° E., and N. 20° W. No significant differences in performance were apparent, although theory predicts that N. 40° E. would be the best for the presumed east-northeast stress field.

Surface stream valleys were correlated with entry stability problems at three of the mines, all in southwestern Pennsylvania. Both east-west and north-south streams were implicated, but the problems appeared to be focused in the north-south headings.

One of the three mines had conducted a program of stress mapping using empty roof bolt holes. Horizontal stress can cause the mine roof to slip along bedding planes, and the movements are observed as offsets in the holes (figure 10). The direction of maximum offset should correspond to the direction of the maximum horizontal stress, while the magnitude of the offsets may be indicative of stress intensity (*37*). It was found that the great majority of the offsets occurred beneath stream valleys and that their orientation ranged between N. 85° E. and N. 80° W. regardless of entry direction.[3]

At the time of the study, only one of the Pittsburgh Seam operations, designated "Mine D", was experiencing serious ground control problems that could be attributed to horizontal stress. In a single year, 10 roof falls had occurred in headgate entries at this mine. Although the mine reported that cutter roof had never been a problem in development headings, the unique pattern and directionality of the headgate instability leaves little doubt that horizontal stress is responsible.

At Mine D, panels have been extracted in both directions back to a set of mains oriented approximately N. 25° E. (figure 11). The headgate problems have all occurred in the "X-Panels," while some "Y-Panels" have experienced problems in the tailgates. The difference in behavior can be explained by a horizontal stress abutment. As figure 11 shows, the horizontal stress abutment moves with the headgate corner on the X-Panels, while the head gates on the Y side remain in the stress shadow provided by the gob.

A detailed look at the behavior of an X-Panel headgate provides further evidence of a horizontal stress abutment (figure 12). As the longwall mines by a crosscut, the

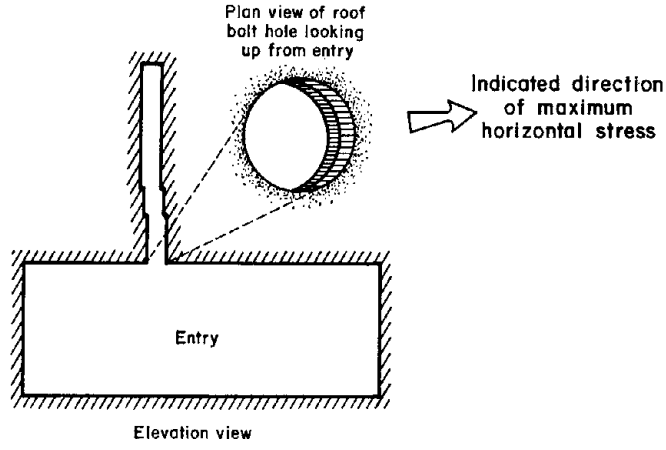

Figure 10.—Empty roof bolt holes used to determine stress orientation (after Parker (*37*)).

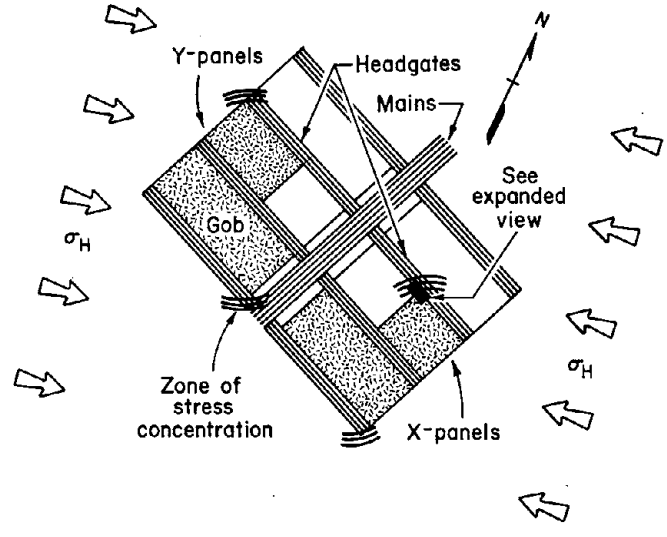

Figure 11.—Horizontal stress concentrations around longwalls at Pittsburgh Seam Mine "D". Expanded view is shown in figure 12.

crosscut roof usually collapses and mining proceeds smoothly for the next 15-18 m (50-60 ft) of longwall face advance. As the longwall subsequently begins to move beyond the stress shadow provided by the crosscut, a cutter begins to develop in the headgate roof along the pillar side. The cutter continues to worsen until the face passes the intersection and the crosscut fails. The entire cycle then repeats.

[3]Mouyard, D. P. Effect of Stress and Geologic Structure on Underground Coal Mines. Unpublished M.Sc. Thesis, WV Univ., Morgantown, WV, 121 pp.

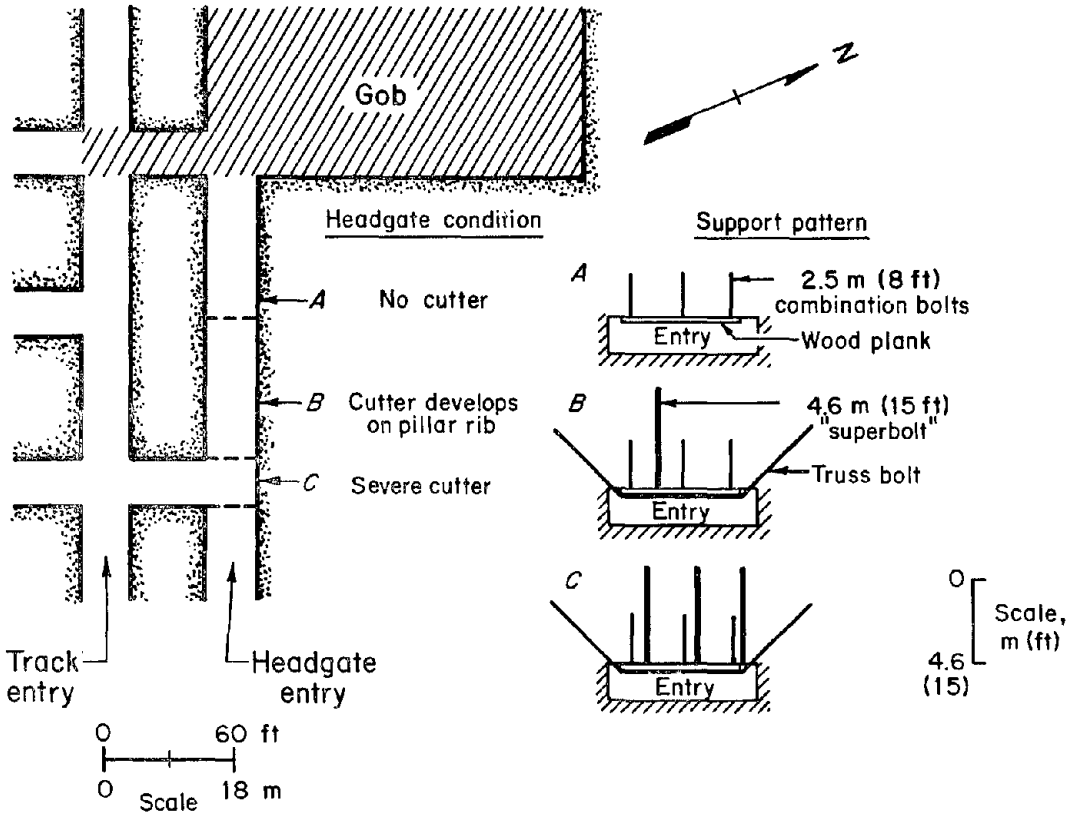

Figure 12.—Sequence of entry failure during longwall face advance at Pittsburgh Seam Mine "D".

Secondary roof bolting has brought the horizontal stress problem under control at Mine D, although at some expense. The primary roof support consists of three, 2.5-m (8-ft) long resin-anchor tension bolts and wood planks on 1.5-m (5-ft) centers. As shown in figure 12, this is all the support necessary in the areas just outby the crosscuts. Starting about halfway between breakthroughs, a heavy-duty truss bolt and a 25-mm (1-in) diameter, 4.6-m (15-ft) long "superbolt" are added between each row of primary support. Finally, in the intersection itself, a truss bolt and three superbolts are installed for each row of bolts.

It is obvious to question why Mine D is unique among the Pittsburgh Seam mines in experiencing horizontal stress problems. Several nearby mines have extracted panels at similar, or even less favorable, orientations and several have employed the same extraction sequence as the X-Panels. One possible explanation is that the magnitude of the horizontal stresses is greater at Mine D or that the stress field there is rotated slightly counterclockwise. Another more likely explanation is geology. In the study, stratigraphic columns were constructed from observations of roof falls at all eight longwall mines (A through H) in the Pittsburgh Coal Seam (figure 13). At the other mines, the immediate roof consisted primarily of drawrock, a rider coal, and/or rash (interbedded shales and coals). At Mine D, both the drawrock and the rider were very thin, and the roof above appeared to consist entirely of finely laminated shale. Laminated shale may be particularly prone to horizontal stress failure because the many closely spaced, smooth, low-cohesion bedding planes greatly reduce rock strength horizontally.

OTHER NORTHERN APPALACHIAN LONGWALL MINES

Mines in the Pittsburgh Coal Seam are not the only northern Appalachian longwall mines affected by horizontal stress. The study found that two operations in the

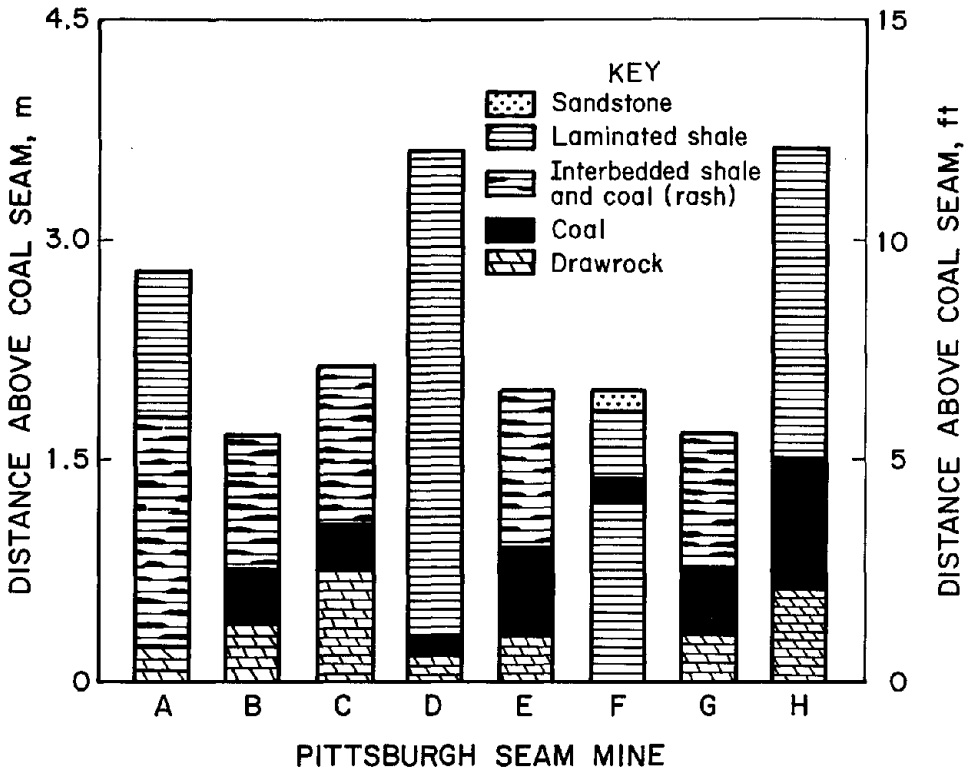

Figure 13.—Roof lithology observed at eight longwall mines in the Pittsburgh Coal Seam.

Freeport Coal Seam—one in Pennsylvania and one in Maryland—displayed indications of horizontal stress. Other examples from the Freeport Seam in Ohio and Pennsylvania can be found in the literature (*7, 27*). However, the two best documented case histories of horizontal stresses in longwalls are from mines working the Lower Kittanning Coal Seam.

The first of these is Kitt Energy Corp.'s Kitt No. 1 Mine, which opened near Philippi, Barbour County, WV, in the late 1970's. Kitt struggled over the years with severe cutter roof and was finally closed in 1987 because a cost-effective solution was not found. The mine has since reopened, but under new owners and without the longwall.

Kitt may be an example of a mine where even the minor horizontal stress exceeds the strength of the roof rock parallel to bedding. The immediate roof over much of Kitt consisted of a highly laminated shale. Several researchers noted that, although the compressive strength of the shale perpendicular to bedding approached 110 MPa (15,000 psi), it was difficult to test because the shale specimens broke so easily along laminations (*30*). Other areas where the roof was a channel sandstone tended to be free of cutters, although roof falls occurred where a cross-bedded sandstone was underlain by less than 1 m (3 ft) of gray shale (*23*).

The mine was designed with entries oriented N. 50° E. and N. 40° W., but running roof falls were common in both orientations. Overcore measurements conducted at Kitt indicated that the maximum horizontal stress was approximately 18 MPa (2,600 psi) oriented N. 66° E. (*1*). Iannacchione and others (*23*) mapped more than 10 km (6 mi) of roof cutters at Kitt and determined that their most common orientation when they occurred away from the rib roof interface was N. 10° E-N. 10° W, indicating a stress field oriented approximately east-west.

The most direct effect of the cutter roof was to slow down development of new longwall panels to unacceptable rates. The roof in the gate entries was often badly damaged by cutters during development, and longwall stresses often caused the roof to collapse. One longwall panel was terminated early owing to roof falls in the headgate in a horizontal stress abutment zone.

Numerous techniques were employed at Kitt to reduce the incidence of roof falls. Mechanical bolts of varying lengths quickly gave way to fully grouted resin bolts, often supplemented by truss bolts. The truss bolts did not seem to prevent cutter roof from occurring, but they were usually able to prevent the broken rock from falling. Mine officials also believed that the several different coal pillar designs that were employed had little observable effect.

The only technique that appeared to be fully successful was the sacrificial entry. During the development of one set of gate roads, severe cutter falls developed all along the length of the belt entry. When a new belt entry was driven parallel to the first in the stress shadow of the cave, conditions were excellent. The decision was then made to use the sacrificial entry in an experimental gate road development concept.

The last longwall mined at Kitt was developed with an arched center entry driven 4.6 m (15 ft) high by a U.K. roadheading machine. This entry, driven some 20 m (60 ft) in advance of the outside headings, was supported with unblocked yieldable steel arches so that the mine roof could collapse an additional 3 m (10 ft) to a total height of 8 m (25 ft). A series of stress measurements was conducted to determine the extent of the stress relief generated by the arched entry (*4*). It was found that the zone of stress relief extended at least 25 m (80 ft) from the arched entry (figure 14). Two independent researchers later attempted to reproduce these results using numerical models. Both found that slippage along horizontal bedding planes was necessary to explain the extent of the stress relief (*4-5*).

In an attempt to determine the degree to which horizontal stresses were concentrated by longwall panel extraction, vibrating wire stressmeters were installed in the roof of a crosscut adjacent to a headgate entry (*30*). Figure 15 shows the results from two stressmeters installed within 2 m (6 ft) of the roofline, one of which was oriented parallel to the crosscut and the other perpendicular. The measurements indicated that horizontal stress increased by as much as 7 MPa (1,000 psi) as the face advanced into the intersection. The additional horizontal stress induced the formation of a roof cutter, which in a matter of hours caused the roof in the crosscut to collapse.

Conditions in the headgate protected by the stress-relief entry were excellent and represented the best ever observed at Kitt. The panel also broke all the mine's previous longwall production records. Unfortunately, the expense of the arched entry proved too great to continue on a routine basis.

Another well-documented case history of horizontal stress is BethEnergy Mines, Inc.'s Cambria Slope Mine No. 33 near Ebensburg, Cambria County, PA. Cambria Slope first adopted the longwall technique in the early 1960's, largely in response to difficulties in controlling cutter roof falls (*16*). While conditions improved somewhat in the intervening years, recent development down the flank of a syncline toward deeper cover has led to the reemergence of the cutter roof problem.

The predominant shale roof rock at Cambria Slope, like that found at Kitt No. 1 Mine, is quite strong perpendicular to bedding. Again, researchers report that "obtaining and preparing test specimens was difficult because of the

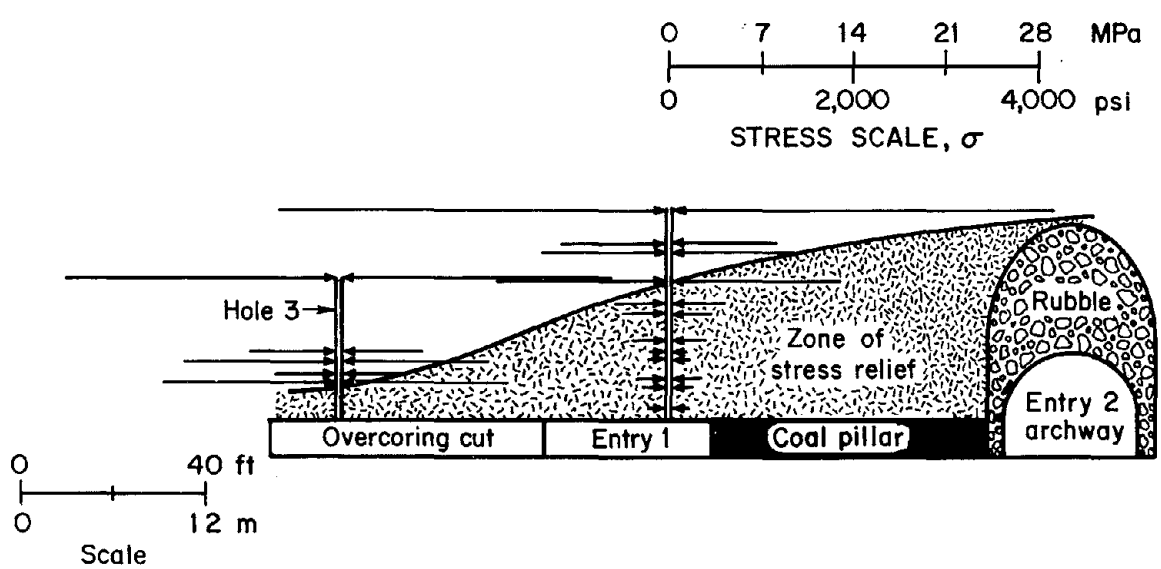

Figure 14.—Measurements of stress relief provided by the arched entry at Kitt No. 1 Mine (after Aggson and Mouyard (*4*)).

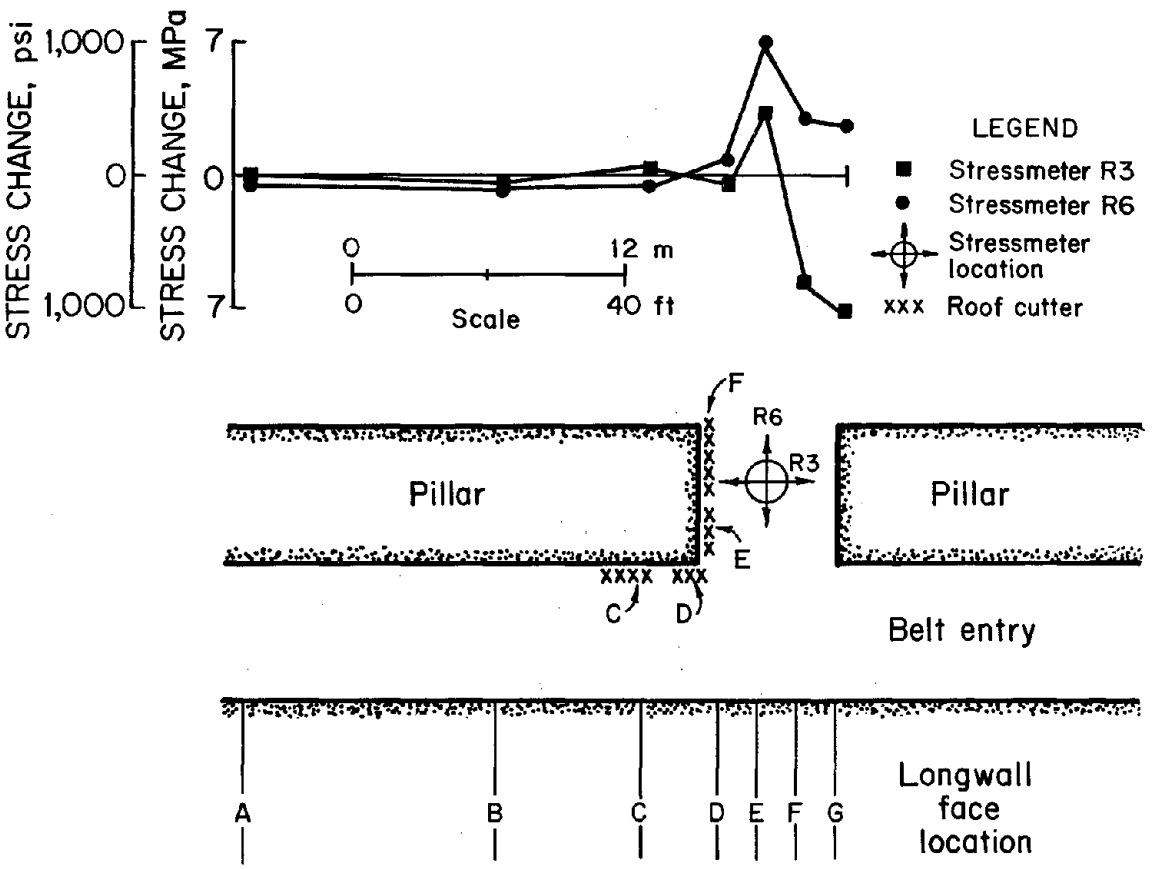

Figure 15.—Measurements of the horizontal stress abutment at Kitt No. 1 Mine near Philippi, Barbour County, WV.

thinly laminated nature of the roof and the weak bonding of these laminations" (25). Roof falls are most common in the gate entries oriented N. 30° E., but also occur in the submain headings.

Primary support for development entries consists of 1.8-m (6-ft) fully grouted resin bolts on 1.5-m (5-ft) centers. In a typical three-entry gate, only the "uphill," or future, headgate entry has been subject to severe cutting. Additional support consisting of steel rails supported by four yielding steel posts has been necessary to carry the broken roof rock. Often, 8 mm (3 in) of downward displacement is recorded on the posts. Apparently, the stress relief provided by this heading is effective in allowing the other two headings to be developed with primary support only. Installing the rails and posts is expensive in terms of material cost, labor, and slowed development rates. Two of the posts also must be removed during longwall retreat to allow the stageloader to pass.

The first part of the solution was to remove the problem from the headgate to the less sensitive center entry. By advancing the center entry 35 to 45 m (120 to 150 ft) ahead, it became the first to contact the stress field (figure 16). The future headgate and tailgate entries were

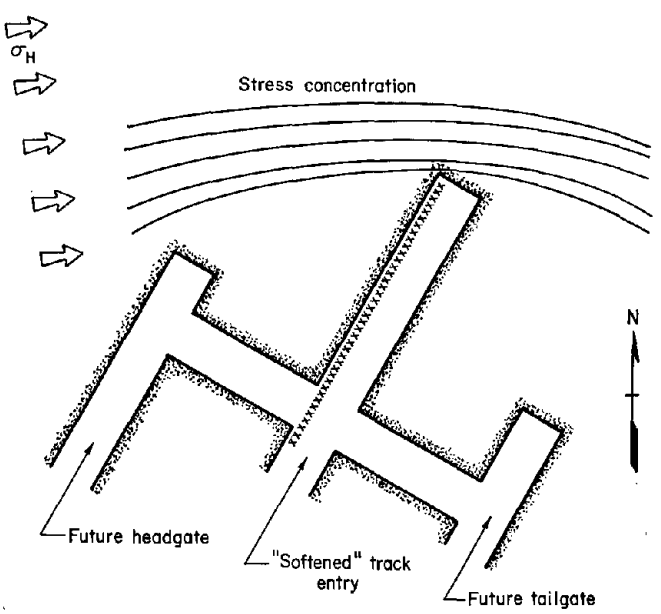

Figure 16.—Softened entry development at Cambria Slope Mine No. 33 near Ebensburg, Cambria County, PA.

stress-relieved. The second problem was to provide more economical support for the softened center heading. Experimentation with different bolting patterns led to a support plan in which the rail and two of the posts were replaced by a truss bolt, two additional resin bolts, and two superbolts. It was found that the superbolts were too stiff, and more reliance had shifted to trusses. It has also proved difficult in practice to keep the center heading sufficiently in advance of the other two.

Cambria Slope also has extensive experience with sacrificial entries. Early observations indicated that entries developed within 90 m (300 ft) of a gob line could be advanced with little difficulty. Caving chambers were later employed, but the technique proved difficult.

ILLINOIS COAL BASIN

In the Illinois Coal Basin, the occurrence of directional roof falls and kink roof have been observed for decades (*40*). Horizontal stress has been acknowledged as the cause, however, for only about the last 10 years. Research conducted at a room-and-pillar operation—Inland Steel's No. 2 Mine (*10, 19*)—appears to have been responsible in large part for the shift in thinking. The roof at Inland No. 2 was described as "highly laminated, with bedding planes [12-37 mm] 0.5-1.5 in apart" (*11*), and for some years the mine led the State of Illinois in total mine roof falls. Through trial and error, some measure of ground control was achieved at Inland No. 2 with high-strength, resin-assisted mechanical bolts. The bolts were installed in a pattern that placed longer bolts near the ribs to suspend the beam created by the center bolts. Entry reorientation to 45° off north-south also proved to be helpful. Some new stress mapping techniques were also proposed, including mapping of striations within roof crush zones and evaluating the appearance of intersection falls (*11*).

Inland No. 2 worked the Springfield (No. 5) Coal Seam, but until recently all of the longwall mines in Illinois have been in the Herrin (No. 6) Coal Seam. The early longwall mines tended to be oriented north-south, and the difference in gate entry conditions between those and others oriented east-west was noted early on. It was also observed, however, that east-west panels were more difficult to cut. As longwall shearing machines became more powerful, cuttability became less of a concern. Nearly all of the panels have been oriented east-west since the mid-1980's. Measures have also been taken to upgrade the roof bolts. Today, resin-assisted mechanical anchors installed with high torques have largely replaced fully grouted resin bolts. It should also be noted that the most troublesome shale roof above the Herrin Seam, the Energy shale, contains many natural discontinuities, but is not noticeably laminated.

SOUTHERN APPALACHIAN COALFIELDS

With few exceptions, longwall mines in the southern Appalachian and Warrior Coalfields have given little notice to horizontal stress. The study found that among the 13 southern Appalachian mines surveyed, panel orientations were evenly distributed across all points of the compass (figure 17). The depth of cover in the southern Appalachians can exceed 600 m (2,000 ft), and the stability problems associated with excessive vertical loading may be overshadowing the effects of horizontal stress. Horizontal stress effects may also be reduced because the roof rock quality is generally higher, and the regional stress field may be extensively reoriented by the rugged surface topography.

High horizontal stresses have been measured in the Beckley and Sewickley Coal Seams near Beckley, WV (*1*). No longwall mines are currently active in either of these seams, but at least one of the longwalls formerly operating there suffered from severe cutter roof in north-south longwall development headings (*41*). Other nearby room-and-pillar operations experienced excessive floor heave caused by horizontal stress (*3*). Of the study mines, two located in south-central West Virginia reported cutter roof beneath surface stream valleys. Some indications of horizontal stress were also observed in several longwall mines near the Virginia-Kentucky border, but the degree to which they influenced stability remained unclear.

WARRIOR COAL BASIN

In Alabama, most longwall mines have been oriented north-south. Coal pillar design for tailgate protection has been the greatest concern at these operations, but recently it has become evident that some of the tailgate difficulties may in fact be related to horizontal stress. Cutters along the panel rib have been a common problem in north-south tailgates, and it has sometimes been necessary to install a second pattern of bolts, biased toward the panel side, as supplemental support before the panels are extracted.

The USBM conducted a geotechnical survey in one Alabama mine and found that roof guttering occurred in nearly 70% of leading entries driven north-south. In contrast, only about 20% of east-west entries or lagging north-south entries experienced guttering. The location of the guttering also depended on the direction of drivage and the location of the box cut (figure 18). It appears that the box cuts contact the horizontal stress field first, damaging the mine roof but providing stress relief for the lagging entries. Tailgate conditions might be improved by adjusting the cut sequence during development.

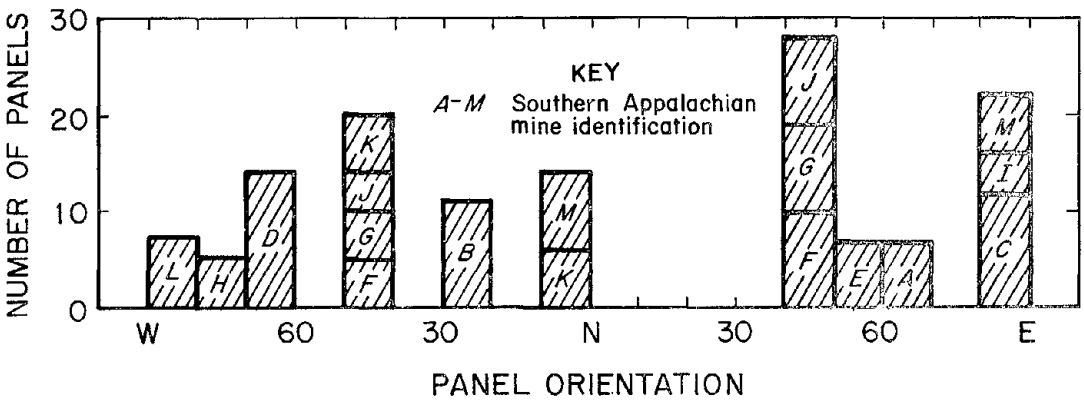

Figure 17.—Orientation of longwall panels at 13 southern Appalachian longwall mines.

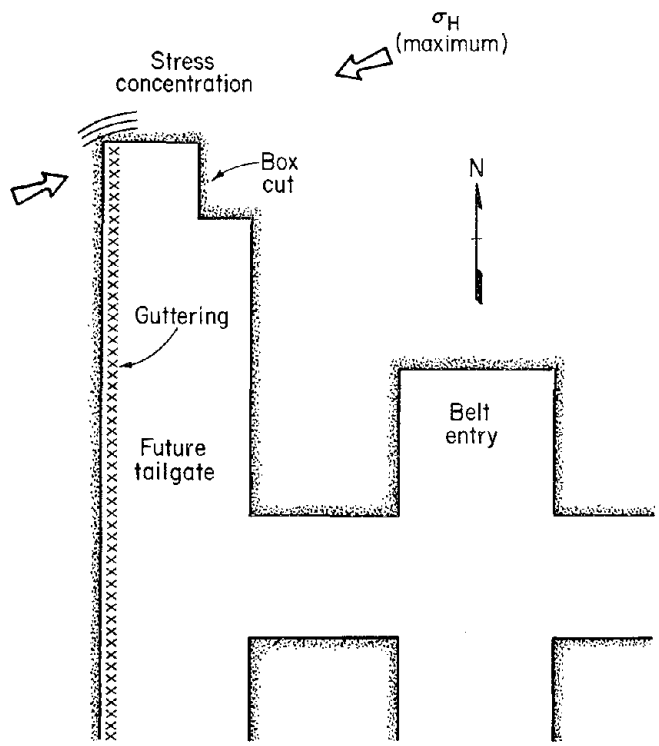

Figure 18.—Development of cutter roof during longwall development in Alabama.

WESTERN U.S. COALFIELDS

Horizontal stress has received relatively little attention in the western U.S. coalfields. Few effects of horizontal stress have been observed at most western U.S. longwall mines probably owing to the relatively low stress levels and the generally strong roof conditions. Horizontal stress cannot be entirely ignored in this region, however. Very troublesome horizontal stress concentrations have developed in the headgate entries at two longwall mines near Scofield, UT, and Rangely, CO. The Utah longwall now uses 3-m (10-ft) long, 25-mm (1-in) diameter bolts to support its headgate. The Colorado longwall relies on trusses and cable slings to back up its primary support. The major horizontal stress is oriented approximately east-west at both mines, indicating that they may be located just outside the boundary of the north-northwest-trending Colorado Plateau Interior stress province.

FOREIGN LONGWALL MINES

In situ horizontal stresses have been observed to adversely affect longwall mines throughout the world. Since the late 1970's, Australian ground control researchers have been actively developing technology for detecting and controlling horizontal stress. Their approach has gained wide acceptance in the United Kingdom, where the trends toward retreat faces, roof bolting, and in-seam drivage of development headings have required fresh approaches to ground control. Today, in some areas of the U.K. coalfields, mine designs must be approved by a strata control engineer based on consideration of the in situ stress field (*39*).

Australian longwall mines typically operate at depths of 350-400 m (1,200-2,000 ft). The horizontal stresses measured there are typically 1.5 to four times the vertical stresses. The region is still experiencing active tectonism. As a result, the stresses observed in mines are often influenced by local structural features, and there is little evidence of a regional stress field. The horizontal stresses are most destructive when the mine roof is laminate rock, consisting of finely interbedded sequences of mudstone,

shale, siltstone, and sandstone (*18*). Massive sandstone roof is reported to be impervious to the effects of horizontal stress.

Horizontal stresses are most disruptive in Australia during development work. Detailed underground surveys, supported by numerical modeling, have shown that the degree of damage is determined largely by the angle between the maximum horizontal stress and the entry. As shown in figure 19, conditions at two mines were found to be better when the angle was less than 30° and worse when the angle was greater than 60°. Australian strata control engineers, therefore, place great emphasis on determining the stress field orientation throughout the mine by stress mapping (*34*).

Perhaps the most significant contributions of Australian research relate to the use of roof bolts for controlling failures induced by horizontal stress. Detailed studies of mine roof behavior and bolt performance indicated that high-strength bolts encapsulated in high-strength resin grouts can be quite effective. Bolt length and pattern are optimized based on field measurements of bolt load and roof movement. For cases in which roof support by bolting alone does not appear feasible, the Australians have developed cable bolting technology as an alternative to standing support (*17*).

Stress control techniques that attempt to modify the stress fields around the mine openings are also employed in Australia. The first of these techniques is entry orientation. Wherever possible, longwall panels are laid out parallel with the maximum stress to minimize the length of drivage in unfavorable directions. It has also been found that once an entry fails, regardless of whether it fully caves, the stress shadow can provide improved ground conditions in parallel headings driven as far as 30-40 m (100-125 ft) away. This principle has been used to optimize drivage sequences for longwall setup rooms and multientry gate systems.

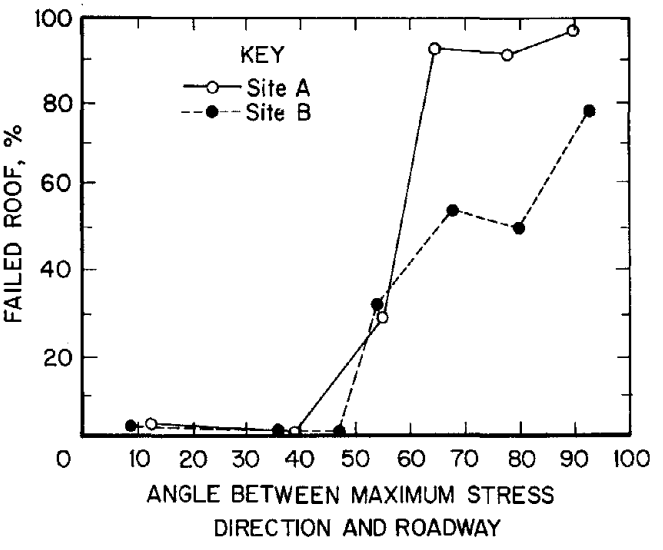

Figure 19.—Relationship between mine roof conditions and angle of roadway to the principal horizontal stress (after Nicholls and Stone (*34*)).

CONTROL OF HORIZONTAL STRESSES

The first step to controlling horizontal stress is to determine its presence and direction. Many of the control techniques require a fairly precise determination of the principal stress direction. The regional stress fields delineated in this paper, particularly the east-northeast stress field in the eastern U.S. coalfields, provide a good starting point. More precise definitions of local stress direction are usually best obtained from stress mapping.

STRESS MAPPING

Horizontal stress manifests itself in a variety of features that can be observed underground (figure 20). Stress mapping is simple and inexpensive, yet can apply to a large area while detecting local changes in orientation due to topography or other effects. While it does not provide the magnitude of the stresses, it can indicate the relative magnitude, especially as related to the strength of the surrounding rock. In situ stress measurements by overcoring can provide more precise information on stress magnitude and orientation, but they are expensive, time-consuming, difficult, and possibly limited in their area of influence.

Table 1 describes the features that should be mapped and the information they provide regarding the horizontal stress field. The USBM is currently refining the stress mapping technique.

Table 1.—Stress mapping features

Feature	Observation noted	Relationship to σ_H
Cutter or kink roof	Location in entry, especially tendency through intersections.	Location in entry gives indication of angle of mining to stress field. In intersections, cutters are aligned with σ_h.
Tensile fractures	Direction	Parallel with σ_H.
Roof potting	Direction of major and minor axes ..	Major axis is parallel with σ_h.
Roof bolt hole offsets	Direction of roof movement	Roof layers move in direction of σ_H.
Shear planes and rock flour	Direction	Planes and rock flour lines are parallel with σ_h.
Striations on roof rock	Direction	Striations are parallel to σ_H.
Roof falls	Location, shape, and appearance ...	Location gives clues as to the general directionality of the stress field. High angular shape usually indicates horizontal stress with stepped shear failures usually predominate on one side.

σ_H = Maximum horizontal stress.
σ_h = Minimum horizontal stress.

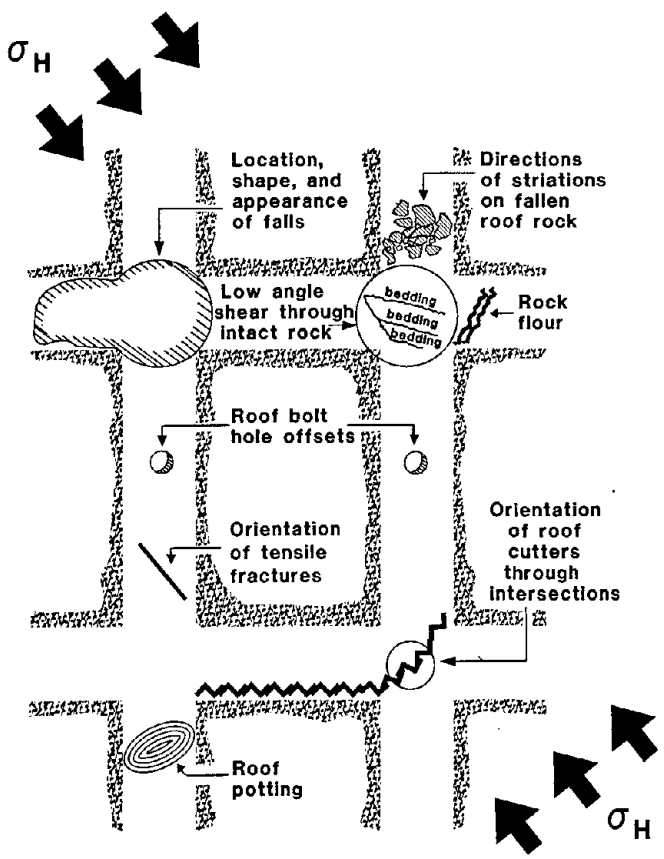

Figure 20.—Summary of underground stress mapping techniques.

The following principles are fundamental to the interpretation of stress mapping results and to the development of many stress control strategies:

1. Less ground damage occurs the more closely the direction of drivage is aligned with the major principal horizontal stress direction.
2. When horizontal stress damage is immediate (occurring with or within hours of initial mining), the leading entry (the first to encounter the stress field) will suffer the most damage.
3. Once ground is damaged by horizontal stress, it will stress-relieve adjacent ground, minimizing or eliminating damage to openings driven within the stress shadow. Gob areas will also create stress shadows.
4. Mining activity also creates areas of stress concentration. These occur where a line drawn parallel to the major horizontal stress contacts the edge of the entry or gob area and are typically zones of maximum roof damage.
5. Where permitted to do so, such as crossing intersections and across openings, major failure features, such as cutters and bottom heave, will try to align themselves with the minimum principal stress. Roof potting and shear failures will try to do this at all times.

PANEL ORIENTATION AND RETREAT DIRECTION/SEQUENCING

Proper mine design is a basic control strategy where horizontal stress is a problem. If possible, longwall mines should be oriented so that the gate entries closely parallel

the maximum horizontal stress. This orientation should provide the best development conditions for the gate roads. If crosscut damage creates problems, angling them in a more favorable direction toward the maximum horizontal stress is often a viable option during longwall development. Additionally, longwall panels create areas of horizontal stress concentration as they retreat into the stress field, as shown in figure 3. These concentrations will fall on either the headgate or tailgate side of a longwall panel and can result in consistent, occasional, or periodic ground control problems in these areas. Aligning the panels with the maximum principal stress will minimize these concentrations.

If mine design dictates that longwall panels must intersect the stress field at an angle exceeding 20° to 30°, their mining sequence should be such that the headgate corner remains within the stress shadow provided by the gob (figure 21). Panels may also be sequenced to locate stress concentrations in noncritical areas.

STRESS SHADOWING AND SACRIFICIAL ENTRIES

Several control techniques employ stress shadowing principles. For example, the least critical entry can be driven into the stress field first, suffer the damage, and provide stress relief for neighboring entries (figure 22). In this softened entry technique, care must be taken to design the mining cycle so that the lead entry always remains in the lead. Otherwise, the protected entries tend to be brought up too rapidly because conditions in the softened lead entry are usually painfully slow and difficult. The width of the coal pillar between the lead entry and the protected entry is also important. Underground measurements have shown that the degree of stress relief decreases with the distance from the softened heading. The extent of the stress shadow is also a function of the height of damage (or softening) in the sacrificial entry, with a higher damaged zone creating a longer shadow. Additionally, the problem of providing effective, rapid, and relatively inexpensive support for a softened entry has not been completely solved. Lastly, if the method is to work consistently, the mine roof in the softened heading must fail as soon as it is exposed. If the failure is delayed, it can eventually develop in one of the "protected" headings instead.

Another variation of this method is to totally sacrifice an entry by installing only enough support to permit initial development, then encouraging failure by driving wider openings, partial pillaring, removing support, etc. Once the sacrificial entry has failed, an adjacent replacement entry can be driven. Good ground conditions can be expected in openings driven near the failed entries. Sacrificial entries may not be routinely practical, but they may have application for shadowing longwall setup and/or bleeder entries when those critical entries must be driven in an unfavorable direction.

MINE ROOF SUPPORT

Roof bolts and other supports have been effective in many instances for horizontal stress control. In the United States, best results have been achieved with high-strength, high-installed-torque, resin-anchored tensionable bolts. The goals of these developments have been to increase support anchorage, increase capacity, and increase installed bolt tension. Additionally, where normal bolt density does not provide sufficient reinforcement to prohibit immediate roof failure, U.S. mine operators usually first opt for longer supports. It may also be desirable to bias the bolts toward the rib where the most roof damage is occurring or to use longer bolts that will anchor outside the cutter zone near the ribs. When these measures do not provide entirely satisfactory results, yielding types of support, such as

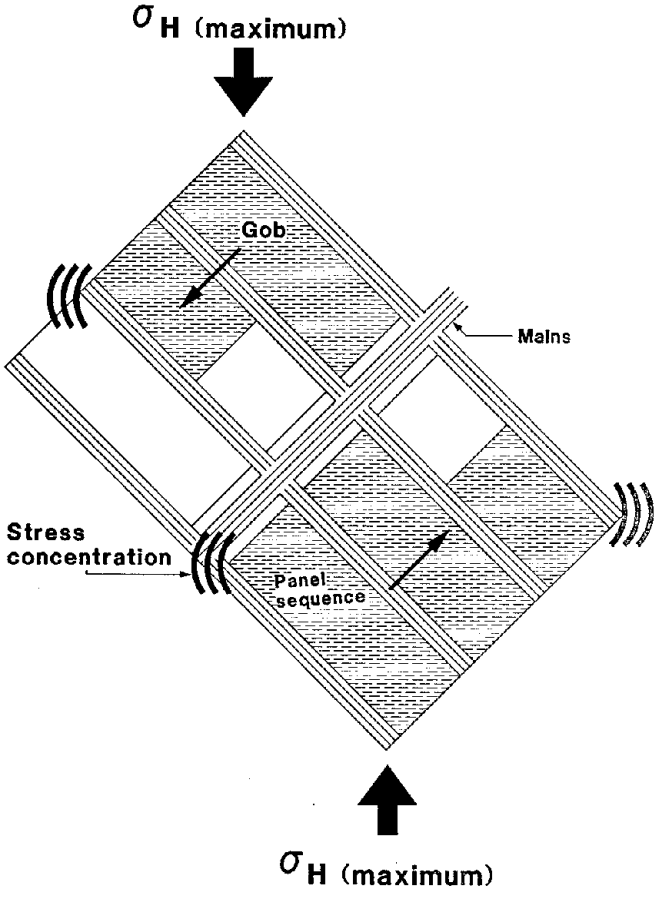

Figure 21.—Use of panel sequencing to stress-relieve headgate entries.

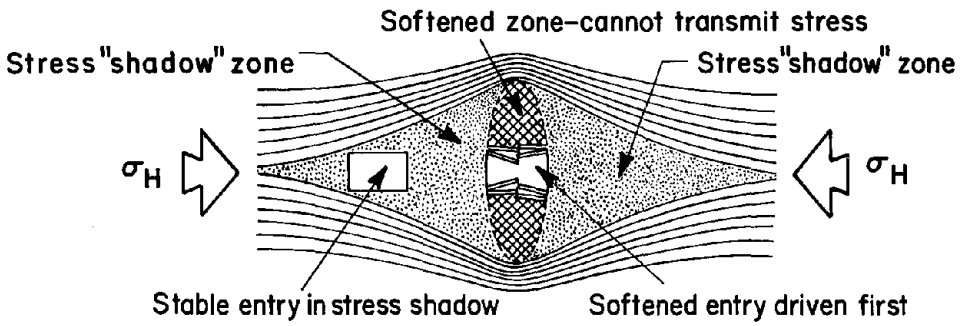

Figure 22.—Development of a stable entry in the stress shadow of a sacrificial entry.

trusses, slings, and standing passive supports, are usually used to contain the failed, very immediate mine roof and use it to provide confinement to the higher strata to prevent total roof collapse.

In Australia and the United Kingdom, where many of the ground control problems are related to horizontal stress, the development of roof support theory and hardware has been aimed at this particular problem. In these countries, the goal is to support the mine roof as quickly as possible with sufficient reinforcement to prohibit strata separation along bedding and interfaces, subsequent deformation, and eventual failure of the laminated roof. As a result, their mining and roof support systems are designed to install fully grouted, tensioned, high-capacity supports as close to the face as possible. As conditions become more difficult to control, these supports are installed in increasing density, often with as many as seven or eight bolts per row. To facilitate better load transfer of the strains of the rock to the support, better support anchorage through reduced hole annulus and stiffer resin is emphasized. The rationale is that fully grouted supports will best resist any lateral movement and high-installed bolt tensions will provide reinforcement to the weak bedding and interface planes of the strata. Fully grouted, torque-tension rebars like those used in the United Kingdom and Australia have not found wide acceptance in the United States.

The USBM is currently investigating a variety of mine roof support systems in different geologic and stress environments. Measurements of roof deformations and bolt loading are being integrated with observations of mine roof quality to help identify the most significant factors affecting roof support performance. The ultimate goal is to develop support selection recommendations for horizontal stress control.

CONCLUSIONS

It appears certain that a horizontal stress field trending east-northeast persists throughout the eastern U.S. coalfields. Measurements indicate that the magnitude of maximum horizontal stress typically exceeds the vertical stress by a factor of two or more. Questions remain regarding the effect of surface topography on stress magnitude and direction. Horizontal stresses in the Western United States are generally lower, but less predictable.

The effects of horizontal stresses have also been observed in longwall mines throughout the United States. Although the greatest stresses have been measured in the southern Appalachian coalfields, the most severely affected mines have usually been in the northern Appalachians and in Illinois. The intensity of horizontal stress damage, however, varies considerably from mine to mine. It appears that the most severely affected mines usually have a highly laminated shale immediate roof. The weakly bonded bedding planes within this type of rock may make it more susceptible to failure when loaded parallel to bedding. Other weak rock types may also be troublesome when subjected to high horizontal stress, but apparently to a lesser extent. Strong roof, such as massive sandstone, does not seem to be affected.

Although the United States has pioneered many of the techniques for identifying and controlling horizontal stress, awareness of the problem remains low. Proper design for horizontal stresses, based on site-specific mapping of the in situ stress field, could significantly improve day-to-day ground control at many longwall installations. Perhaps more importantly, it could forestall major ground control failures that might otherwise occur unexpectedly.

REFERENCES

1. Agapito, J. F. T., S. J. Mitchell, M. P. Hardy, J. R. Aggson, and W. N. Hoskins. A Study of Ground Control Problems in Coal Mines With High Horizontal Stresses. Paper in The State of the Art in Rock Mechanics. Proceedings of the 21st U.S. Symp. on Rock Mechanics (Rolla, MO, 1980), Univ. MO--Rolla, 1980, pp. 820-825.

2. Agapito, J. F. T., S. J. Mitchell, M. P. Hardy, and W. N. Hoskins. Determination of In Situ Horizontal Rock Stress on Both a Mine-Wide and District-Wide Basis (contract J0285020, Tosco Research, Inc., and J. F. T. Agapito & Associates). USBM OFR 143-80, 1980, 174 pp.; NTIS PB 81-139735.

3. Aggson, J. R. Coal Mine Floor Heave in the Beckley Coalbed, An Analysis. USBM RI 8274, 1978, 32 pp.

4. Aggson, J. R., and D. P. Mouyard. Geomechanical Evaluation of a Coal Mine Arched Entry. Int. J. Min. Geol. Eng., v. 6, 1988, pp. 185-193.

5. Ahola, M., and N. P. Kripakov. Analysis of Cutter Roof Using the Boundary Element Method. Paper in Proceedings of the 6th Int. Conf. on Ground Control in Mining. WV Univ., Morgantown, WV, 1987, pp. 107-117.

6. Barron, L. R. Longwall Stability Analysis of a Deep, Bump-Prone, Western Coal Mine—A Case Study. Paper in Proceedings of the 9th Conf. on Ground Control in Mining. WV Univ., Morgantown, WV, 1990, pp. 142-149.

7. Bauer, E. R. Cutter Roof Failure: Six Case Studies in the Northern Appalachian Coal Basin. USBM IC 9266, 1990, 18 pp.

8. Bickel, D. L. Rock Stress Determinations From Overcoring—An Overview. USBM Bull. 694, 1993, 146 pp.

9. Bickel, D. L., and D. A. Donato. In Situ Horizontal Stress Determinations in the Yampa Coalfield, Northwestern Colorado. USBM RI 9149, 1988, 43 pp.

10. Blevins, C. T. Coping With High Lateral Stress in an Underground Illinois Coal Mine. Paper in Proceedings of the 2nd Conf. on Ground Control in Mining. WV Univ. Morgantown, WV, 1982, pp. 137-141.

11. ____. Horizontal Stress Problems in Illinois Basin Coal Mines. Paper in Proceedings of the 3rd Conf. on Ground Control Problems in the Illinois Basin. Southern IL Univ. at Carbondale, 1990, pp. 92-97.

12. Bunnell, M. D., and K. C. Ko. In Situ Stress Measurements and Geologic Structures in an Underground Coal Mine in the Northern Wasatch Plateau, Utah. Paper in Rock Mechanics: Key to Energy Production. Proceedings of the 27th U.S. Symp. on Rock Mech. (Tuscaloosa, AL, 1986), Soc. Min. Eng. AIME, 1986, pp. 333-337.

13. Campoli, A. A., T. M. Barton, F. C. Van Dyke, and M. Gauna. Mitigating Destructive Longwall Bumps Through Conventional Gate Entry Design. USBM RI 9325, 1990, 38 pp.

14. Dahl, H. D., and R. C. Parsons. Ground Control Studies in the Humphrey No. 7 Mine, Christopher Coal Div., Consolidation Coal Co. Soc. Min. Eng. AIME Trans., v. 252, June 1972, pp. 211-222.

15. Dolinar, D. R., J. R. Aggson, and V. E. Hooker. In Situ Stress Distributions and Related Ground Control Problems. Paper in Ground Control in Room-and-Pillar Mining, Soc. Min. Eng. of AIME, 1982, pp. 35-40.

16. Ferguson, P. A. Longwall Mining Systems and Geology. Min. Congr. J., December 1971, pp. 32-35.

17. Gale, W. J., S. Mathews, and M. Fabjanczyk. Strata Control and Rock Reinforcement in Conditions of High Lateral Stress. Paper A8 in Proceedings of the 8th Int. Strata Control Conf., Steinkohlenbergbauverein, Federal Republic of Germany, 1989, 12 pp.

18. Gale, W. J., J. A. Nemcik, and R. W. Upfold. Application of Stress Control Methods to Underground Coal Mine Design in High Lateral Stress Fields. Paper in Proceedings of the 6th Int. Congr. on Rock Mech., Int. Soc. for Rock Mech., 1987, pp. 897-900.

19. Hanna, K., K. Y. Haramy, and D. P. Conover. Effect of High Horizontal Stress on Coal Mine Entry Intersection Stability. Paper in Proceedings of the 5th Conf. on Ground Control in Mining. WV Univ., Morgantown, WV, 1986, pp. 167-182.

20. Hill, J. L., III. Cutter Roof Failure: An Overview of the Causes and Methods for Control. USBM IC 9094, 1986, 27 pp.

21. ____. The Influence of Stream Valleys on Coal Mine Ground Control. Paper in Proceedings of the 7th Int. Conf. on Ground Control in Mining. WV Univ., Morgantown, WV, 1988, pp. 247-258.

22. Hoek, E., and E. T. Brown. Underground Excavations in Rock. Inst. Min. and Metall., London, 1980, 527 pp.

23. Iannacchione, A. T., J. T. Popp, and J. A. Rulli. The Occurrence and Characterization of Geological Anomalies and Cutter Roof Failure: Their Effect on Gateroad Stability. Ch. 24 in Second International Conference on Stability in Underground Mining, ed. by A. B. Szwilski and C. O. Brawner (Lexington, KY, Aug. 6-8, 1984). Soc. Min. Eng. AIME, 1984, pp. 428-445.

24. Ingram, D. K., and G. M. Molinda. Relationship Between Horizontal Stresses and Geologic Anomalies in Two Coal Mines in Southern Illinois. USBM RI 9189, 1988, 18 pp.

25. Khair, A. W., H. U. Lim, and S. J. Jung. An Engineering Approach To Reduce the Cost of Roof Support in a Coal Mine Experiencing Complex Ground Control Problems. Soc. Min. Met. Exp. AIME, preprint No. 90-154, 1990, 5 pp.

26. Kripakov, N. P. Alternatives for Controlling Cutter Roof in Coal Mines. Paper in Proceedings of the 2nd Conf. on Ground Control in Mining. WV Univ., Morgantown, WV, 1982, pp. 142-151.

27. Lizak, J. B., and J. E. Sembourski. Horizontal Stresses and Their Impact on Roof Stability at the Nelms No. 2 Mine. Paper in Proceedings of the 4th Conf. on Ground Control in Mining. WV Univ., Morgantown, WV, 1985, 7 pp. Available from C. Mark, USBM Pittsburgh Research Center, Pittsburgh, PA.

28. Maleki, H. N. Development of Modeling Procedures for Coal Mine Stability Evaluations. Paper in Proceedings of the 31st U.S. Symp. on Rock Mechanics. A. A. Balkema, 1990, pp. 85-92.

29. Maleki, H. N., A. Weaver, and R. Acre. Stress-Induced Stability Problems—A Coal Mine Case Study. Paper in Proceedings of the 32nd U.S. Symp. on Rock Mechanics. A. A. Balkema, 1991, pp. 1057-1064.

30. Mark, C. Analysis of Longwall Pillar Stability. Ph.D. Thesis, PA State Univ., University Park, PA, 1987, 414 pp.

31. McGarr, A. On the State of Lithospheric Stress in the Absence of Applied Tectonic Forces. J. Geophys. Res., v. 93, No. B11, Nov. 10, 1988, pp. 13609-13617.

32. Molinda, G. M., K. A. Heasley, D. C. Oyler, and J. R. Jones. Effects of Horizontal Stress Related to Stream Valleys on the Stability of Coal Mine Openings. USBM RI 9413, 1992, 26 pp.

33. Nelson, J. W., and R. A. Bauer. Thrust Faults in Southern Illinois—Result of Contemporary Stress? Geol. Soc. Am. Bull., v. 98, March 1987, pp. 302-307.

34. Nicholls, B., and I. Stone. Development of Strata Control at Tahmoor Mine. Paper in Proceedings of the Ground Movement and Control Related Coal Min. Symp., Aus. IMM, Illawarra Branch, August 1988, pp. 109-117.

35. Oyler, D. C., A. A. Campoli, and F. E. Chase. Factors Influencing the Occurrence of Coal Pillar Bumps at the 9-Right Section of the Olga Mine. Paper in Proceedings of the 6th Int. Conf. on Ground Control in Mining. WV Univ., Morgantown, WV, 1987, pp. 10-17.

36. Park, D. W., R. L. Sanford, T. A. Simpson, and H. L. Hartman. Rock Characterization and Response in Deep Coal Mine Ground Control. Paper in Proceedings of the Annu. Workshop, Generic Mineral Technology Center for Mine Systems Design and Ground Control, Blacksburg, VA, 1983.

37. Parker, J. Practical Rock Mechanics for the Miner. Part 5: How To Design Better Mine Openings. Eng. Min. J., December 1973, pp. 76-80.

38. Plumb, R. A., and J. W. Cox. Stress Directions in Eastern North America Determined to 4.5. km From Borehole Elongation Measurements. J. Geophys. Res., v. 92, No. B6, May 1987, pp. 4805-4816.

39. Pugh, W. L. Strata Control and Roof-Bolting in Western Area. Min. Eng. (London), June 1988, pp. 584-594.

40. Roley, R. W. Pressure Cutting: A Phenomenon of Coal Mine Roof Failures. Mechanization, v. 12, No. 12, 1948, pp. 69-74.

41. Su, W. H., and S. S. Peng. Cutter Roof and Its Causes. Min. Sci. and Tech., v. 4, 1987, pp. 113-132.

42. Unrug, K. F., G. Herget, and A. Smith. Ground Stresses and Roof Failure in Coal Mine Strata. Paper in Proceedings of the 2nd Int. Conf. on Stability in Underground Mining. Univ. KY, Lexington, KY, 1984, pp. 377-408.

43. Unrug, K. F., and R. S. Mateer. In Situ Stress in Relation to Topography and Major Fracture in Rocks—An Example from Martin County, Eastern Kentucky. Paper in Proceedings of the Conf. on Rock Characterization Techniques (New Orleans, LA, 1986), Soc. Min. Eng. AIME, 1986, pp. 237-244.

44. Wong, I. G., and J. R. Humphrey. Contemporary Seismicity, Faulting, and the State of Stress in the Colorado Plateau. Geol. Soc. of Am. Bull., v. 101, September 1989, pp. 1127-1146.

45. Zoback, M. L. First- and Second-Order Patterns of Stress in the Lithosphere: The World Stress Map Project. J. Geophys. Res., v. 97, No. B8, July 30, 1992, pp. 11703-11728.

46. Zoback, M. L., and M. D. Zoback. Tectonic Stress Field of the Continental United States. Ch. in Geophysical Framework of the Continental United States. Geol. Soc. of America Memoir 172, 1989, pp. 523-539.

APPENDIX—STRESS MEASUREMENTS IN U.S. COAL MINES

This appendix contains tables presenting a compilation of measurements from 47 U.S. coal mines gleaned from more than 20 published sources. Measurements from the eastern U.S. coal mines are presented in table A-1, while those from western U.S. coal mines are presented in table A-2. Nearly all of the measurements were conducted using overcoring techniques. The most popular instrument, used in 80% of the measurements, is the USBM borehole deformation gauge (BDG). The BDG is a mechanical device normally installed in a vertical borehole to measure the stresses in the horizontal plane (*8*). Other devices listed in the tables essentially allow strain gauges to be glued to the rock. Some of these, such as the South African CSIR Triaxial Cell and the more recent Australian CSIRO Hi Cell, can measure three-dimensional stress in a single hole.

Wherever possible, the minewide values of the maximum horizontal stress, its orientation, and the ratio of the maximum to minimum horizontal stress are the values given in the referenced publications shown in the tables. In some instances, data from two or more holes at the same mine were available. Where the results from the separate holes were consistent with each other, the values presented in the tables are averages. In nearly every case, the orientation varied by less than 20° from hole to hole, and the magnitude of the maximum horizontal stress varied by less than 7 MPa (1,000 psi). At five mines (four of which were located in the West), results from separate boreholes were not consistent with each other; these are therefore presented individually. In other cases, the source provided only individual test results. In such instances, values for the hole were calculated as the average of the individual measurements. In some holes, the measured stresses rotated and became more consistent farther up the hole. Here, it was assumed that the lower measurements were influenced by the presence of the mine opening, and these measurements were eliminated from the average.

Because of the difficulties associated with conducting stress measurements, the measurements presented in the following tables are probably of varying quality. In general, the most reliable measurements of far-field stresses are those based on more and deeper tests and on more holes. The experience of the team that performed the tests also plays a significant function, because the techniques are difficult to master.

Table A-1.—Stress measurements from Illinois, Alabama, and northern and southern Appalachian coal mines

Location and mine (or coal seam)	Reference No.	Stress measurement technique[1]	Depth of cover		Maximum test distance into borehole		Number of holes/tests	σ_H maximum horizontal stress		σ_H/σ_h	Orientation of σ_H	σ_H/σ_v[2]
			m	ft	m	ft		MPa	psi			
Eastern Kentucky:												
Hendrix 22	42	BDG	152	500	[3]7.1	23	1/3	15.6	2,257	1.25	N. 66° E.	4.1
Leeco 22	42	NA	NA	NA	7.7	25	1/6	5.1	741	1.48	N. 14° E.	NA
(Coalburg Seam)[4]	43	TRX	91	300	4.9	16	1/7	0.8	122	3.39	([5])	0.4
Do.[4]	43	TRX	91	300	5.2	17	1/7	1.0	142	2.68	N. 75° E.	0.4
(Warfield Seam)	43	TRX	NA	NA	4.3	14	1/4	4.2	613	[5,6]-87.57	N. 80° W.	NA
Western Kentucky:												
Camp No. 2	42	BDG	91	300	7.1	23	1/4	7.9	1,145	1.10	N. 85° E.	3.5
Southern West Virginia:												
Beckley No. 1[7]	2	BDG	335	1,100	4.6	15	2/8	21.6	3,127	1.79	N. 72° E.	2.6
Beckley No. 2[7]	2	BDG	335	1,100	4.0	13	2/NA	14.0	2,026	1.36	N. 49° W.	1.9
Bonny	2	BDG	347	1,140	7.4	24	2/7	26.3	3,815	1.23	N. 57° E.	2.5
Maple Meadows	2	BDG	262	860	7.7	25	5/19	23.3	3,380	1.37	N. 68° E.	3.6
Beckley Mining Co.	2	BDG	253	830	8.0	26	4/22	23.0	3,339	1.33	N. 59° E.	3.7
Olga	35	BDG	419	1,375	4.0	13	3/11	22.1	3,200	1.39	N. 60° E.	2.1
Mine 132	32	BDG	233	765	7.4	24	2/10	20.7	3,000	1.25	N. 47° W.	3.6
Do.	32	BDG	49	160	7.4	24	2/6	12.4	1,800	2.57	N. 59° W.	10.2
Northern West Virginia:												
Kitt No. 1[8]	4, 8	BDG	183	600	[3]4.6	15	3/15	18.1	2,624	1.57	N. 66° E.	4.0
Humphrey No. 7	14	HF	[e]198	[e]650	30.0	100	NA	14.5	2,100	2.33	N. 84° W.	2.9
(Upper Freeport Seam)	42	TRX	152	500	[3]4.6	15	1/4	[9]10.6	1,544	[10]1.98	N. 80° E.[9]	2.8
Virginia:												
(Pocahontas No. 3 Seam)	13	BDG	610	2,000	NA	NA	1/NA	23.4	3,400	2.14	N. 76° E.	1.5
Southwestern Pennsylvania:												
BethEnergy	NA	DST	[e]152	[e]500	9.2	30	3/NA	9.2	1,337	1.27	N. 32° E.	2.4
Ohio:												
Nelms No. 2	27	DST	152	500	1.5	5	1/3	12.5	1,811	4.12	N. 69° E.	3.3
Alabama:												
North River	8, 15	BDG	152	500	3.7	12	1/5	13.9	2,013	10.48	N. 60° E.	3.7
Jim Walter Resources No. 5	36	BDG	671	2,200	4.6	15	NA	9.1	1,323	1.40	N. 78° E.	0.5
Jim Walter Resources No. 7	NA	HI	580	1,875	5.0	16	2/8	21.0	3,010	NA	N. 71° E.	1.5
Illinois:												
NA	33	NA	NA	NA	NA	NA	NA	NA	NA	NA	N. 67° W.	NA
NA	33	NA	NA	NA	NA	NA	NA	22.0	3,191	2.29	N. 76° E.	NA
Wabash	24	BDG	274	900	4.9	16	3/15	9.7	1,400	1.75	N. 83° E.	1.4
Galatia	24	BDG	259	850	4.3	14	3/16	10.3	1,500	3.00	N. 78° E.	1.6
Inland No. 2	10	VWS	283	930	NA	NA	NA	18.8	2,721	3.16	N. 87° E.	2.7
Peabody No. 10	19	BDG	110	360	1.2	4	1/9	8.3	1,207	1.76	N. 73° E.	3.0
Elkhart	8	BDG	84	275	NA	NA	NA	7.6	1,097	1.71	N. 37° E.	3.6

Do. Same as above. NA Not available. [e]Estimated.

[1]BDG = USBM borehole deformation gauge; TRX = CSIR Triaxial Cell; HF = Hydrofracture; DST = CSIR Doorstopper; HI = CSIRO Hi Cell; VWS = Vibrating Wire Stressmeter.

[2]σ_v calculated as .025 MPa/m (1.1 psi/ft) of depth.

[3]Lowest holes apparently influenced by entry, not included in calculation.

[4]Above drainage, near strip pit.

[5]Highly variable.

[6]Minus signifies tension.

[7]Second hole tested 3 years after first.

[8]Two studies, 7 years apart.

[9]Maximum stress nearest horizontal.

[10]Minimum principal stress nearest horizontal.

Table A-2.–Stress measurements from western U.S. coal mines
(Stress measurement technique in all cores was USBM borehole deformation gauge)

Location and mine (or coal seam)	Reference No.	Depth of cover		Maximum test distance into borehole		Number of holes/tests	σ_H maximum horizontal stress		σ_H/σ_h	Orientation of σ_H	σ_H/σ_v[1]
		m	ft	m	ft		MPa	psi			
Utah:											
Sunnyside	8, 15	323	1,060	NA	NA	NA	28.3	4,107	1.25	N. 31° W.	3.5
Utah Fuel	12	[c]274	[c]900	6.2	20	3/NA	[2,3]11.0	1,593	[4]2.41	N. 60° W.[2]	1.3
Do.	12	[c]274	[c]900	6.2	20	3/NA	[2,3]11.9	1,724	[4]3.42	N. 30° E.[2]	1.6
(Upper Hiawatha Seam)	28	NA	NA	NA	NA	NA	NA	NA	2.00	N. 16° W.	1.0
Emery No. 50	8	137	450	NA	NA	NA	8.1	1,177	4.07	N. 22° W.	2.4
Sufco No. 1	8	305	1,000	NA	NA	NA	8.8	1,282	1.55	N. 16° W.	1.2
King No. 4	8	372	1,220	NA	NA	NA	7.9	1,145	2.04	N. 20° E.	0.9
Castle Gate No. 3	6, 8	670	2,200	NA	NA	NA	[5]16.1	2,329	1.19	N. 29° W.	1.0
Colorado:											
Orchard Valley	8	107	350	NA	NA	NA	8.0	1,165	4.27	N. 69° E.	3.0
Do.	8	495	1,625	NA	NA	NA	12.2	1,768	2.89	N. 83° W.	1.0
Coal Basin No. 5	8	305	1,000	NA	NA	NA	5.4	779	1.38	N. 52° W.	0.7
Dutch Creek No. 1	8	823	2,700	NA	NA	NA	17.6	2,554	3.11	N. 29° W.	0.9
Bear Mine	8	381	1,250	NA	NA	NA	9.8	1,419	4.26	N. 69° E.	1.0
Eagle No. 5	9	201	660	4.6	15	1/5	1.6	235	1.27	N. 12° E.	0.4
Do.	9	201	660	4.0	13	2/9	[6]3.2	470	2.83	N. 78° E.	0.6
Apex No. 2	9	128	420	3.4	11	1/5	3.9	567	1.15	N. 86° W.	1.2
Do.	9	128	420	3.7	12	1/4	[6]1.8	257	1.21	N. 19° W.	0.6
Foidel Creek	9	118	387	4.9	16	2/11	[7]5.7	830	1.58	N. 71° W.	2.1
Rienau No. 2	9	224	735	5.2	17	1/5	7.1	1,024	1.71	N. 67° W.	0.7
Deserado	8	184	605	NA	NA	NA	14.1	2,044	1.37	N. 77° E.	3.1
Southfield	29	430	1,410	NA	NA	NA	13.1	1,903	1.47	N. 7° W.	1.2

Do. Same as above. NA Not available. [c]Estimated.
[1]σ_v calculated as .025 MPa/m (1.1 psi/ft) of depth.
[2]Maximum principal stress nearest horizontal.
[3]Three-dimensional stress measured in coal.
[4]Minimum principal stress nearest horizontal.
[5]One hole each in roof-and-floor.
[6]Measured in floor.
[7]Two sites.

CABLE BOLTS FOR LONGWALL GATE ENTRY SUPPORT

By Stephen C. Tadolini[1] and Jamie L. Gallagher[2]

ABSTRACT

Cable supports offer several advantages over traditional secondary support methods. Cable supports enhance stress redistribution to pillars and gob areas, minimize or eliminate timbers and cribs that reduce ventilation capabilities, eradicate material-handling injuries related to the placement of crib supports, and provide a cost-effective alternative to secondary support. The U.S. Bureau of Mines (USBM) has designed and installed cable supports to improve the stability of tailgate and bleeder entries in a western U.S. underground longwall mine. Design and installation techniques are presented for both cement and resin-grouted cable bolt systems. Three case studies discuss the design philosophy, describe measurement instrumentation, and present the quantifiable results to date.

INTRODUCTION

Cable bolts were introduced to the U.S. mining industry in 1970 as a method to reinforce ground prior to mining. Until recently, only four underground U.S. hard-rock mines had used cable supports. In the beginning, discarded wire rope was the preferred choice by most ground control engineers. Today, the basic cable bolt support consists of a high-strength steel cable installed in a 4.1- to 6.4-cm (1.625- to 2.5-in) borehole and grouted with cement. The USBM has also developed the use of resin as an anchorage material in a 2.5- and 3.5-cm- (1- and 1-3/8-in-) diameter hole. Traditional cables have an ultimate strength of 244.7 to 266.9 kN (55,000 to 60,000 lbf) and a modulus of elasticity of about 203.4 GPa (29.5×10^6 psi). Cables are 1.52 to 1.59 cm (0.6 to 0.625 in) in diameter and consist of seven individual wires. Driven by the demand for high capacity and large deformations in coal mine gate roads, "Monster Cables" measuring 1.78 cm (0.70 in) in diameter with a yield strength of 244.7 kN (55,000 lbf) and an ultimate strength of 378.1 kN (85,000 lbf) are being introduced. These cables are placed in a 3.5-cm- (1-3/8-in-) diameter hole. Monster Cable material characteristics provide large amounts of deformation at a high degree of loading and ultimate strength. These steel cables are flexible and can be coiled to a diameter of about 1.2-m (4-ft) for handling. This flexibility is one of the primary advantages of cable supports, since the support length is not limited by the opening height.

For a cable support system to be effective, the loads must be successfully transferred from the rock to the cable through the grout. Laboratory and field investigations have determined that to achieve the ultimate cable capacity of 258.0 kN (58,000 lbf), depending on the water-cement ratio, the top 1.5 m (5 ft) of the cable should be grouted when using a cement product. When resin products are used, 1.2 m (4 ft) of grout will develop the ultimate capacity of the cable. Of course, adequate anchorage should be evaluated on a site-specific basis by performing a standard pull test. Laboratory and field results indicate that at least 6% elongation for the ungrouted portion of the cable can be expected (*1-2*).[3] This permits

[1]Mining engineer.
[2]Geophysical engineer.
Denver Research Center, U.S. Bureau of Mines, Denver, CO.

[3]Italic numbers in parentheses refer to items in the list of references at the end of this paper.

the designer to vary the amount of grouted and ungrouted portion of cable to obtain various degrees of stiffness, depending on the specific strata to be supported.

Gate roads are the most hazardous areas in longwall mines. Keeping the gate road entries stable is a challenging task for the mine engineer. The gate roads provide access and escapeways for the miners, coal transportation, and ventilation (intake and return). Headgates are supported primarily with roof bolts during development mining and, during longwall retreat, generally require secondary reinforcement for a distance outby the face using wooden posts, hydraulic jacks, or spot roof bolts to cope with the front and side abutment pressures caused by mining. Headgate entries must stay unobstructed and completely open, with minimum convergence, for access of personnel and equipment and for coal transport. The tailgates, however, are solely used for return and sometimes for intake air passages and travelways. Much higher ground pressures exist around the tailgate entries, which makes them very difficult to support. Moderate entry closure or partial blockage of the tailgate entry is tolerated. Generally, wood or concrete cribbing materials are used for secondary supports in the tailgate entries. Cribbing patterns and densities are varied to support difficult ground pressures. In 1992, the USBM evaluated the potential for supplementing or replacing conventional headgate and tailgate secondary supports in an underground longwall mine with cement-grouted cables. The results indicated that given the pillar layout and site-specific roof conditions and strengths at the test mine, the use of cable bolt systems was successful in maintaining the longwall tailgate entries (*3*). The successful application of this technology indicated the potential for several mining advantages. A direct benefit of cable systems is the installation of a stiff support system capable of strengthening and reinforcing roof members to transfer high pressures into the main and immediate roof and onto supporting structures away from the periphery of the entries. This will also reduce entry convergence. The indirect benefit of cables is the reduction or elimination of cribs.

A recent analysis revealed that in 1991-92 a total of 734 accidents in U.S. underground mines related to cribbing, timbering, and blocking were reported. The majority of the serious accidents occurred in western U.S. underground longwall mines. This directly relates to the height of the coal seam, which requires the use of ladders to build the cribs with heavy and cumbersome materials (*4-5*). The removal of cribs will also help to minimize the ventilation resistance in air passages, which results in savings in air pressure and increases airflow, while removing gas and dust from the working face more efficiently (*6*). This will create a safer, cleaner environment for underground mineworkers, while reducing mine ventilation costs for the mine operator. Additionally, subject to the availability of a reliable source of quality timber, the amount required to support a single 2,530-m (8,300-ft) gate road with 1.8-m by 20.3-cm by 20.3-cm (6-ft by 8-in by 8-in) crib blocks in a 2.9-m- (9.5-ft-) high opening would be 613 hectares (248 acres) of select-cut prime timber. Eliminating or minimizing crib supports can reduce accidents related to support installation, improve ventilation, and reduce wood consumption.

CABLE SUPPORT DESIGN

Although cables have been used in U.S. hard-rock mines, the design procedure is new for underground coal mines, and applications are significantly different from hard-rock employment. Wire rope and cable supports have been used in Australian coal mines for about 8 years. However, Australian mining methods differ from U.S. methods in that large barrier pillars, approximately 61 to 122 m (200 to 400 ft), are left between two entries, and cables are frequently supplemented with steel arches and beams (*7-8*). The analytical and theoretical approach, ongoing during the investigation, is initially simplistic, but is being constantly modified based on field measurements.

The first step of the design procedure requires detailed data gathering to determine the ground conditions in the underground mining environment. This includes a general estimation of the rock mass quality, the geological structure, and strengths of the immediate and main roof members. This information can be obtained from roof core samples and supplemented with a borescope or camera used in the borehole. Secondly, an estimate of the induced stresses calculated by empirical methods or modeling should be included in the stability analysis. The weight of the rock mass should be expressed per linear meter (foot) of roof for mine entries to determine the required cable spacing. The zone of rock material that must be supported by the cable system can be determined several ways, and design principles are constantly being updated.

The simplest approach is to identify a parting plane where separation above the roof-bolted zone is likely to occur. For the worst-case scenario, it can be assumed that the bolted strata will shear at the pillar boundaries of the opening and that the entire block must be supported by cables as shown in figure 1. The weight of the material can be determined by using the equation

$$F_w = W_e \times H_p \times \gamma, \quad (1)$$

where F_w = weight of the rock per linear meter (foot), N/m (lb/ft),

W_e = effective width of the opening, m (ft),

H_p = distance from the coal mine roof to the parting plane, m (ft),

and γ = average rock density to the parting plane, kg/m^3 (lb/ft^3).

This method is conservative, as it is more likely that the coal pillars will provide additional support to the detached roof structure, forcing the formation of a pressure arch of the failed material. As shown in figure 2, the cables must be capable of supporting only the material within the boundaries of the pressure arch. The height of the arch can be correlated to the vertical and horizontal stresses acting in the immediate mine roof and is believed to increase as the in situ horizontal stress increases. A generally used criterion for determining the height of the pressure arch is that the failure height is 0.5 to 2.0 times the mined seam height, varying with the direction and magnitude of the stress field (*9*). The weight of the material within the arch can be estimated with respect to the opening width and height of the arch by the following equation:

$$F_a = 1/2 \times \pi \times W_e/2 \times H_a \times \gamma, \quad (2)$$

where F_a = weight of the rock within the pressure arch per lineal meter (foot), N/m (lb/ft),

W_e = effective width of the opening, m (ft),

H_a = height of the pressure arch, m (ft),

and γ = rock density, kg/m^3 (lb/ft^3).

The behavior of the pillar under different loading conditions determines the effective opening width W_3, shown in figure 3. Wilson defines the depth of the yield zone as the depth at which the coal strength in the entire pillar is exceeded by the loads imposed; therefore, Wilson's equations can be used to estimate the depth of this yield zone (*10*). Wilson's equations are

$$W = 2\frac{m}{F}\ln\left(\frac{q}{p+p'}\right)_{\text{(rigid roof-floor)}} \quad (3)$$

and

$$W = m\left[\left(\frac{q}{p+p'}\right)^{1/k-1} - 1\right]_{\text{(yielding roof-floor)}}, \quad (4)$$

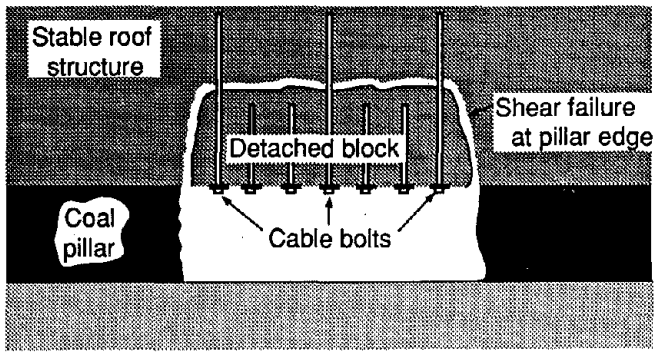

Figure 1.—Detached block failure being supported by cables.

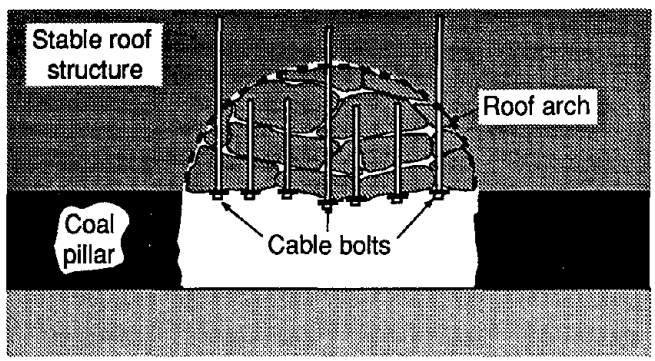

Figure 2.—Formation of a pressure arch of failed mine roof material.

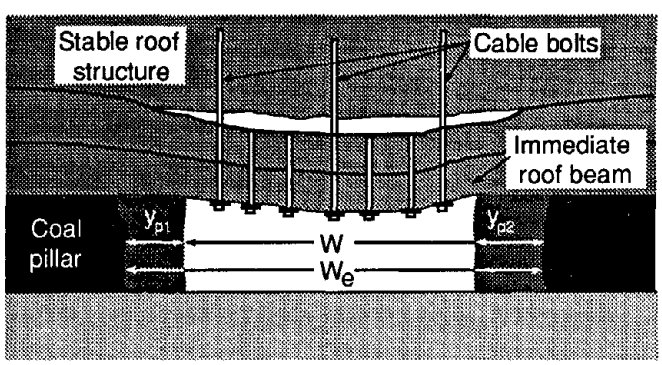

Figure 3.—Formation of a yield zone on the coal pillars. W_e = effective opening width; y_{p1} = yield zone pillar 1; y_{p2} = yield zone pillar 2; W = mined width of the opening.

where W = pillar width, m (ft),

m = seam height, m (ft),

q = overburden load, kN/m^2 or kPa (ton/ft^2),

p = artificial edge restraint (0 kPa (0 ton/ft^2)),

p' = uniaxial strength of fractured coal, 96.4 kN/m^2 (1 ton/ft^2),

k = triaxial factor $\frac{1 + \sin\phi}{1 - \sin\phi}$,

ϕ = angle of internal friction, deg,

and $$F = \frac{k-1}{\sqrt{k}} + \frac{(k-1)^2}{k} \tan^{-1}\sqrt{k}, \quad (5)$$

where $\tan^{-1}\sqrt{k}$ is expressed in radians.

The depth of this yield zone can be calculated or approximated using the chart shown in figure 4. The chart was created using a value of 35° for the angle of internal friction. The W_e can then be calculated by using the following equation:

$$W_e = W + Y_{p1} + Y_{p2}, \quad (6)$$

where W_e = effective opening width, m (ft),

W = mined width of the opening, m (ft),

Y_{p1} = yield zone for pillar 1, m (ft),

and Y_{p2} = yield zone for pillar 2, m (ft).

Once the volume and weight of the material to be supported with cables have been determined, it is possible to determine the number and spacing of the required cables to support the gate road entry. Using a cable capacity of 258.0 kN/cable (58,000 lb/cable) and varying the number of cables across the opening, the best design can be determined for a specific application and operation.

Figure 5 shows a design chart calculated for two, three, and four cables installed for an effective opening width, W_e, of 7.6 m (25 ft) and a material weighing 2,403 kg/m^3 (150 lb/ft^3). For example, drawing a line up from the x-axis, spacing distance along the entry, to the cable number line and going left from that point to the y-axis indicates the thickness of a failed beam member that can be entirely supported with the installed cables. In the example, two, three, and four cables spaced across the width, at 2.1-m (7-ft) spacing along the entry, would have the capacity to support 1.4, 2.0, and 2.7 m (4.5, 6.7, and 8.9 ft) of separated material, respectively.

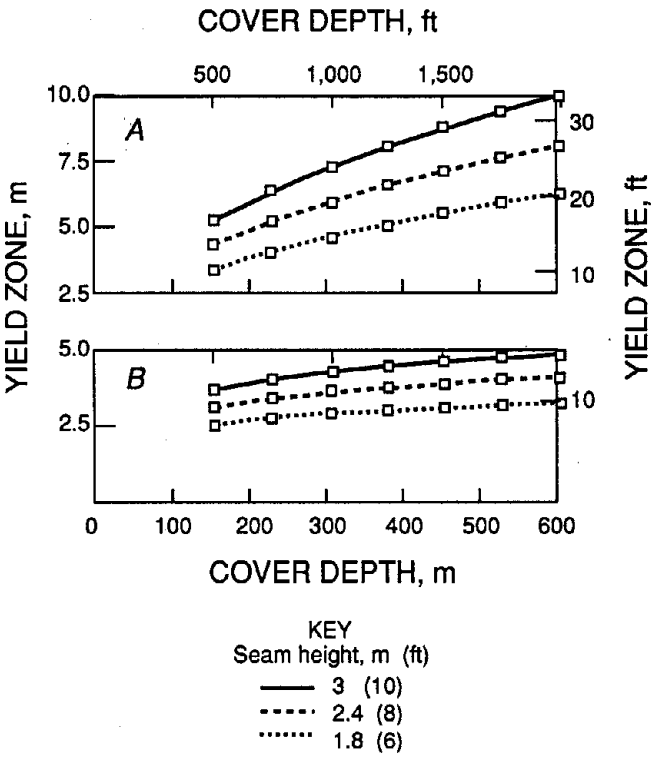

Figure 4.—Design chart to determine the yield zone width in coal pillars. *A*, Yielding roof; *B*, rigid roof.

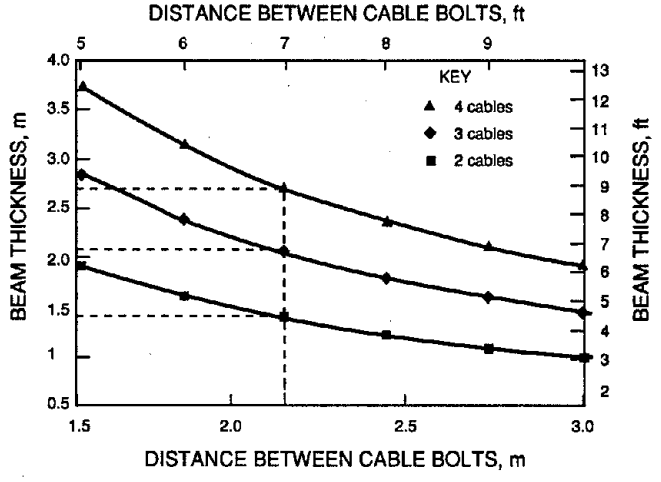

Figure 5.—Cable support design chart where W_e = 7.6 m (25 ft) and γ = 2,403 kg/m^3 (150 lb/ft^3).

INSTALLATION METHODS

Cable supports have been successfully installed using both the "traditional" cement grout and resin grout. Both systems have advantages and disadvantages, but a close examination of both systems indicates that resin-grouted cable bolting is superior for most coal mine applications from a productivity and cost standpoint. However, there may be circumstances where a cement cable system would be preferable. For example, if large voids or washout of the roof rock were present, the concrete would completely fill the voids and develop the required anchorage, whereas the resin would be lost in the voids and may not develop enough anchorage to develop the strength of the cables. Cement grout would also be preferable when a full column of grout is desired to increase the system stiffness. The volume of resin is currently constrained by the diameter of the tubes, and obtaining a full column of resin is extremely difficult.

CEMENT GROUT INSTALLATION PROCEDURES

Cement-grouted cable bolts can be installed at any angle in the rock. To install the cables with concrete grout, the following steps are taken:

1. A hole is drilled, with a diameter of 4.1 cm (1-5/8 in), to a depth of at least 5.1 cm (2 in) deeper than the desired cable length.
2. The cable, with the appropriate retaining anchor, plastic breather tube, and grout tube are inserted into the hole. The breather tube is almost as long as the cable and allows the air being displaced by the grout to escape. Also, when the grout runs out of the tube, this indicates to the cable bolt crew that the hole is filled.
3. Water is sent through the breather tube to flush the hole and clear debris from the breather tube.
4. A plastic grout tube is pushed approximately 45.7 cm (18 in) into the hole.
5. The bottom 20.3 cm (8 in) of the hole is plugged, sealing the area around the cable, grout, and breather tubes. This can be accomplished by stuffing shredded cotton waste material around the tubes or using an expansive foam. The combination of both provides an excellent seal.
6. The hole is then filled with a cement-based grout through the grout tube. The grout commonly used consists of a cement and water mixture at a ratio of 0.35 parts of water to 1 part of cement by weight. Several laboratory studies investigated the effects of water-cement ratios. The strength selected is site-specific and related to the available pumping equipment. The greater the cement-water ratio, the higher the final viscosity. This can be partially overcome by adding a chemical plasticizer, which makes the grout slicker and easier to pump without adversely impacting the final strength.
7. After the hole is filled, the ends of the two tubes are folded over and tied off to prevent the grout from draining.
8. The next day, or approximately 24 h later, the tubes can be cut off to allow the installation of a bearing plate and cable grips. A hydraulic cable jack can be used to tension the cable to the desired preload condition.

A completed cement installation and the required components, without the bearing plate and cable grips, are shown in figure 6.

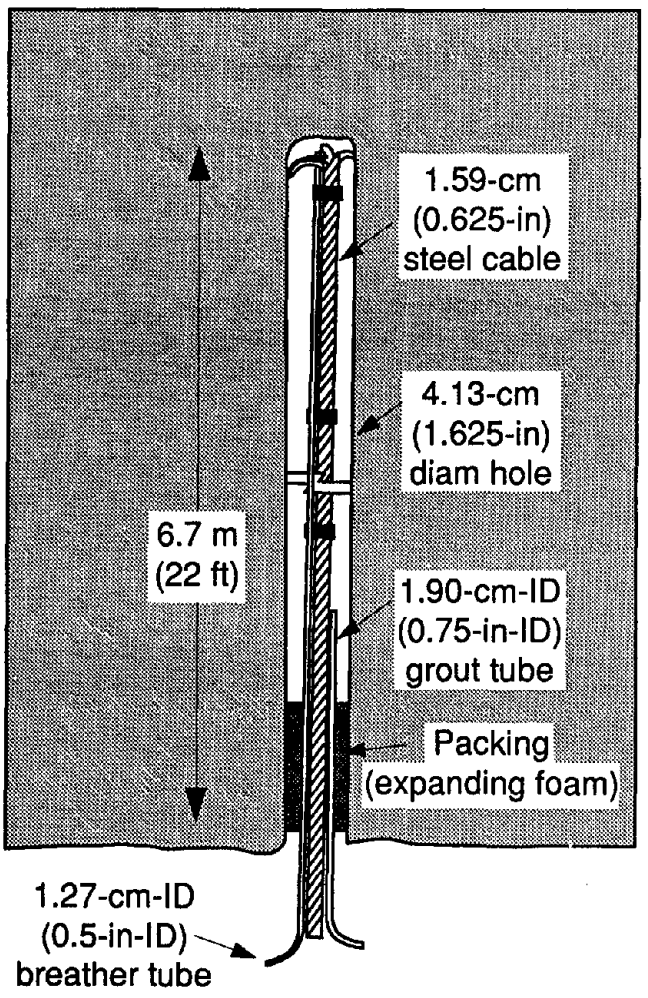

Figure 6.—Components of a concrete-grouted cable support.

RESIN GROUT INSTALLATION PROCEDURES

Resin-grouted cable bolting was initiated in the United States in 1992. Several required installation parameters were identified to make cable bolting with a resin anchorage system as routine as headed rebar. Numerous design evolutions were investigated before resin-grouted cable bolts were fabricated on a production level. An example of the resin-grouted cable bolt used in several USBM investigations is shown in figure 7. Each component (*A* through *E*) serves a specific function that contributes to the overall success of the cable bolt system.

Referring to figure 7, the end of the cables are clamped together using a swedged-on fitting (*A*). This ties all the cable strands together, including the kingwire, which is the center cable strand. The next swedged-on buttons (*B*) serve two functions. First, they provide additional anchorage and resistance to pullout forces. It is extremely difficult, if not impossible, to pull the cable out of the resin when these are imbedded in the borehole. Secondly, the buttons help to mix the resin during placement by forcing it around the tight opening. The turbulence enhances the mixing and helps to detach the cartridge cover. The short button (*C*) generally serves the same functions as the large button and also holds a plastic seal (dam) to restrict the flow of resin down the hole. Laboratory and field results indicate that keeping the resin at the top of the hole can make the difference between adequate or inadequate anchorage for resin-grouted cables. Any resin loss for a critical length of anchorage may allow the cable to pull out of the hole before developing ultimate strength. Because the cables are flexible, they may bend when the back pressure from the resin becomes too great, causing the cable to bend or kink. The cable stiffener rod (*D*) provides stiffness to the bottom portion of the cable to ease the installation of the last 1.2 to 1.5 m (4 to 5 ft) of cable. The length of the stiffener can be adjusted to the mining height and the effective resin column length desired. It eases installation to have the stiffener in the hole before any back pressure causes the cable to bend or kink. Additionally, during the process of mixing the resin, the bearing plates, placed on the cable before installation, tend to spin rapidly. Field observations indicate that this spinning can cause the bearing plate to nick the cable, which may lead to premature failure. The cable stiffener eliminates cable nicking. The final component of the resin-grouted cable bolt system is the installation head or cable nut (*E*). This makes the cable easy to rotate and install with conventional roof bolting machinery. The nut is capable of handling loads in excess of the ultimate bearing capacity of the cable.

Several variations of this system are becoming available. One system of particular interest allows tension to be applied to the cable after the resin has cured. This component is shown in figure 8. High degrees of tension may be

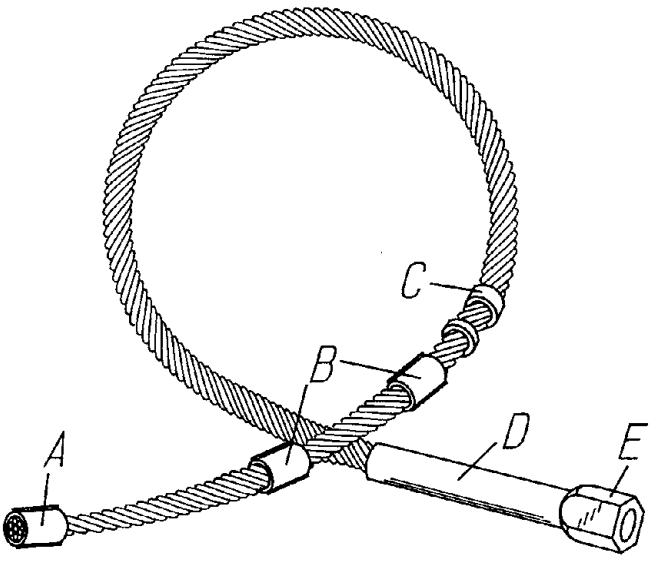

Figure 7.—Specific components of a resin-grouted cable bolt. *A*, swedged-on fitting to tie all cable strands together; *B*, wedged-on buttons for additional anchorages; *C*, short button to hold plastic seal in place; *D*, cable stiffener rod; and *E*, installation head or cable nut.

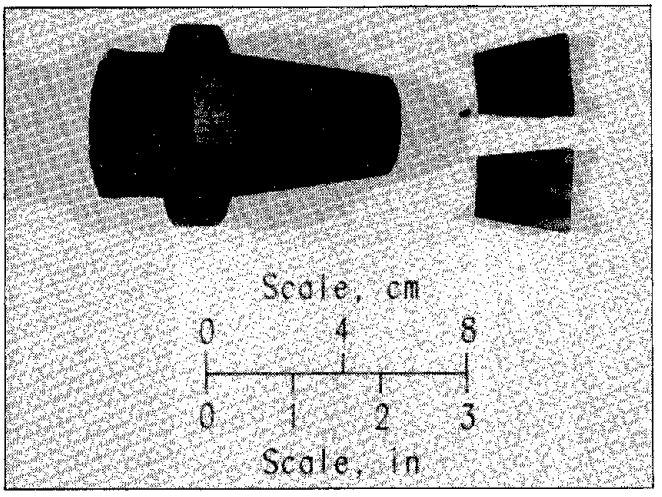

Figure 8.—Tensionable nut for a resin-grouted cable bolt.

an important consideration in a laminated roof material where any separation may lead to progressive-type failures. If a high-tensioned system is desired, it is important to realize that the resulting ultimate support capacity is lowered by the tensioned amount. For example, if the system is pretensioned 44.5 kN (10,000 lb), the remaining capacity of the system to support roof loads is 213.5 kN (48,000 lb). To install the cables with resin grout, the following steps are taken:

1. Drill the prescribed hole 2.5 to 5.1 cm (1 to 2 in) longer than the cable to be installed. The holes can be

drilled with a water or vacuum drilling system. Hole diameters ranging from 2.5 to 3.5 cm (1 to 1-3/8 in) have been used successfully.

2. Place the resin cartridges into the borehole. An installation technique that appears to work well, especially in instances where more than one cartridge of resin is required, is the placement of a faster-setting cartridge at the top of the hole. This permits fast installation, instantaneous anchorage, and immediate support.

3. As the cable is pushed up through the resin cartridges, it is rotated slowly to enhance the mixing of the resin. When the cable is approximately 7.6 to 10.2 cm (3 to 4 in) from the back of the hole, the rotation is increased and the resin is mixed for the total amount of time recommended by the manufacturer. Be careful not to overspin the bolt. The mixing time begins when the cartridges are punctured by the insertion of the cable. Field investigations have revealed that the cable should be rotated counterclockwise. This tends to screw the cable into the hole, getting a positive contact between the bearing plate and the mine roof. While rotating the cable clockwise will pull up the resin, it creates back pressure after the resin has been mixed and the cable is pushed up against the mine roof. When the bolting stinger is removed, the cable relaxes and pushes out of the hole, voiding any plate roof contact that may allow separation and progressive failure to occur.

4. When the resin has been adequately mixed, the cable is pushed up against the mine roof with the full force of the bolter and held in place until the resin has cured. This provides an active bearing plate pressure and pretensions the cable (*11*).

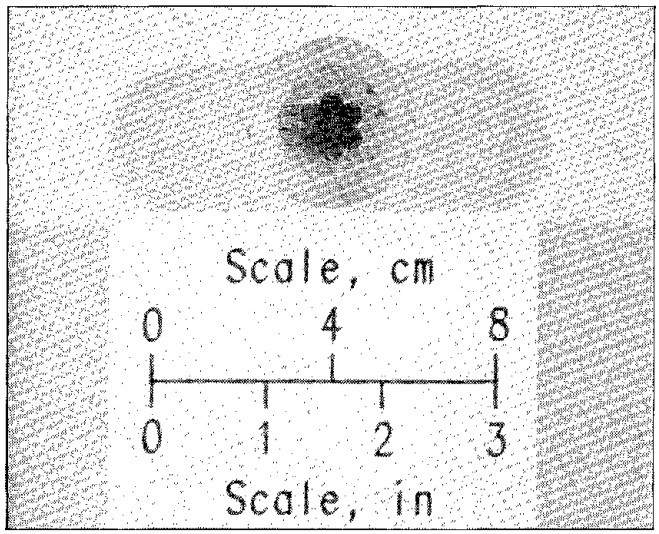

Figure 9.—Cross section of a 1.52-cm- (0.60-in-) diameter cable installed in a 2.5-cm- (1-in-) diameter hole.

5. If a tensionable unit has been installed, the cable is then ready for jacking to a predetermined load using special equipment.

A cross section of a 1.52-cm- (0.60-in-) diameter cable is shown in figure 9. Note the traces of resin around the center strand and tightness against the six outer strands. This demonstrates how resin grout provides an excellent mechanical interlock, creating a high degree of cable anchorage.

FIELD EVALUATIONS

Several long-term field evaluations are underway at underground coal mines. In all of the cases, the cables are being used as secondary support systems in gate roads and bleeder entries. Current work is examining cable supports as primary support as a substitute for intersection trusses, and secondary support fixtures in difficult ground conditions.

CASE STUDY No. 1

Cable supports were installed to assess their effects on the stability of tailgate entries in a western U.S. underground longwall mine. Two entries closest to the longwall panel were supported with high-strength cables installed with cement grout. Instrumentation was used to monitor and assist in the evaluation of the effectiveness of the support system and the general response of the mine openings.

Site Description

The longwall gate roads and the test area are shown in figure 10. The final dimensions of the pillar nearest the panel were 39.6 by 39.6 m (130 by 130 ft), while those of the pillar between entries 2 and 3 were 39.6 m (130 ft) long by 30.5 m (100 ft) wide. With modifications in the intersections, 109.7 m (360 ft) of roadway nearest the longwall panel (entry 1) was supported with 6.7-m- (22-ft-) long cables installed at a 2.1-m (7-ft) spacing. Approximately 76.2 m (250 ft) of the second entry (longwall bleeder entry 2) was supported with 5.5-m- (18-ft-) long cables installed at a 2.1-m (7-ft) spacing, as shown in figure 10. The difference in cable length was attributed to the different loading conditions to which the supports would be subjected as the panel was extracted. The primary support system in the area, installed on initial development, were 1.8-m (6-ft), full-column, resin-grouted

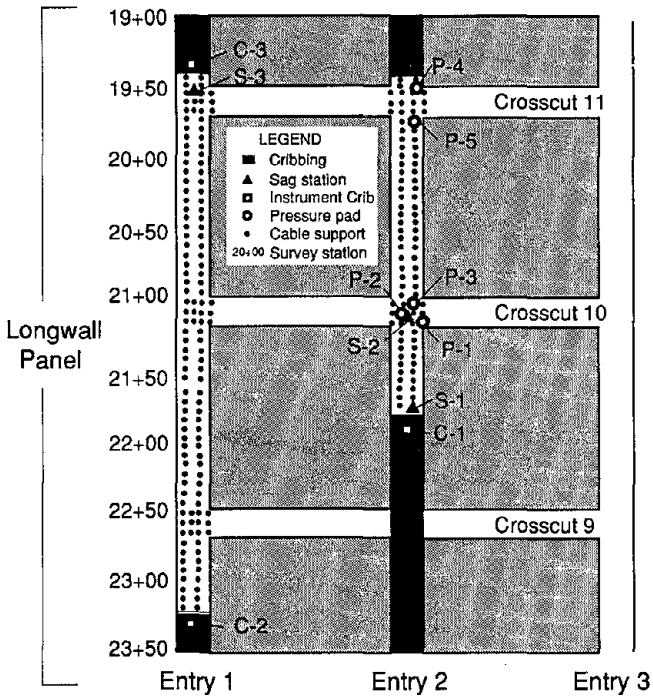

Figure 10.—Gate roads showing the cement-grouted cable test area and instrumentation layout at a western U.S. underground longwall mine.

bolts on a 1.5-m (5-ft) pattern installed with pans and complete wire meshing.

An examination of the mining horizon indicated 4.2 m (14 ft) of minable coal seam, but the gate road entries were driven only 2.9 m (9.5 ft) high. A generalized summary of the immediate mine roof in the area included about 1.1 m (3.5 ft) of top coal overlain by about 0.45 m (1.5 ft) of a silty shale. The roof above the silty shale grades vertically into interbedded units of siltstone, shale, and sandstone. This unit coarsens upward in grain size, with the top portion consisting of sandstone. The thickness of the sandstone in the test area was approximately 4.9 m (16 ft).

Instrumentation

Individual cable loads were monitored with hydraulic U-cells and Goodyear pressure pads. The mine roof behavior was simultaneously monitored with differential magnetic sag stations and closure meters at 7.6-m (25-ft) spacings along the entry axis during the development of the longwall panel to evaluate the response of the immediate and main roofs.

Test Site Results

As the panel was extracted, excessive forward abutments and side loading caused two cables installed near the pillar side of entry 1 to fail at a height of approximately 2.7 m (9 ft). Cable anchorage was strong enough to cause the cable to fail about 0.3 m (1 ft) below the fall of ground. The fall extended at an angle about 6.1 m (20 ft) in front of the face. Face ventilation was never disrupted, and the panel was mined through the fall area without major additional incidence. The mine elected to provide additional supplementary support in the form of two 20.3-cm- (8-in-) diameter timber posts spaced on 1.5-m (5-ft) centers for the remainder of the test area. Five timber posts were instrumented with hydraulic flatjacks to assess their contribution to the total support of the entry. At a distance of about 22.9 m (75 ft) outby the face, the posts began taking load. When the face was approximately 6.1 to 9.1 m (20 to 30 ft) inby, the instrumented posts were carrying an average of 48.9 kN (11,000 lb), which translates to about 1.55 MPa (225 psi) on the timber post. When the face was directly adjacent to the posts, the load reached approximately 124.5 kN (28,000 lb) or 3.86 MPa (560 psi), then failed.

The cable test area in entry 1 was successfully mined through without further incidence of caving or roof falls ahead of the face. Bleeder entry 2 showed only minor signs of loading, and differential roof sag stations indicated insignificant movements or separation in the roof. Given the pillar layout and site-specific roof conditions and strengths at the test mine, the use of cable bolt systems was successful in maintaining the longwall tailgate entries. The installed instrumentation indicated that very little active support can be expected from installed crib systems. Differential magnetic sag stations indicated that roof bed separations, even with the cable support stiff system, still occurred between geological interfaces, which eventually led to loading beyond the designed capacity. Timber posts, installed as additional secondary support in the tailgate entry, were subjected to loads of approximately 124.5 kN (28,000 lb), then failed. The loading on the timber post, while appearing substantial, could have been supported by an additional cable installed in the roof of entry 1. Adding another cable with a 258.0-kN (58,000-lb) capacity in the middle of the entry may have compensated for these extra loads. A three-cable system spaced on 2.1-m (7-ft) centers would have been sufficient to carry the loads generated by the observed roof separation at a height of 2.7 m (9 ft) above the coal seam. This

investigation prompted the mine operator to investigate the effectiveness of cable supports in the bleeder entry behind the next longwall panel start room. The results of this investigation are described in greater detail in reference (*3*).

CASE STUDY No. 2

The first resin-grouted cable test area was established in a longwall bleeder entry immediately behind the panel. A longwall bleeder system is a designated set of special entries developed and maintained as part of the mine ventilation system. These entries are designed to continuously move air-methane mixtures from the gob, away from the active workings, and deliver the mixtures to the return air courses. Because these systems are critical to safe ventilation and provide emergency escapeways, they must be maintained to permit adequate airflow and travel. To accomplish this, most mines elect to install crib supports along the entire length of the bleeder entry system. As an alternative secondary support system, approved by the U.S. Mine Safety and Health Administration, resin-grouted cables were selected to support the bleeder entry.

Site Description

A three-entry system was driven behind the longwall system. The first entry was used as the longwall setup room. The second set of entries were the bleeder entries. The two entries were separated by pillars measuring 57.9 m (190 ft) in length and 45.7 m (150 ft) in width. The 6.1-m- (20-ft-) wide entries were primarily supported with 2.4-m (8-ft) full-column, resin-grouted bolts and steel mesh. The third set of entries, adjacent to virgin coal, resulted in a final pillar dimension of 57.9 m (190 ft) in length and 47.5 m (150 ft) in width. An examination of the mining horizon indicated 4.3 m (14 ft) of minable coal seam, with the entries driven only 2.9 m (9.5 ft) high. A generalized summary of the immediate mine roof in the area included about 0.8 m (2.5 ft) of top coal overlain by about 0.5 m (1.5 ft) of a silty shale. The roof above the silty shale grades vertically into interbedded units of siltstone, shale, and sandstone. This unit coarsens upward in grain size, with the top portion consisting of sandstone. The test area location is shown in figure 11.

Cable System Design

Based on the caving results from a previous panel, the site lithology, and the loading generated on the crib supports in the previous bleeder, a cable system was designed to support the loads generated on the roof when the panel was extracted and the immediate and main roofs caved. The entries were protected by the abutment size pillars,

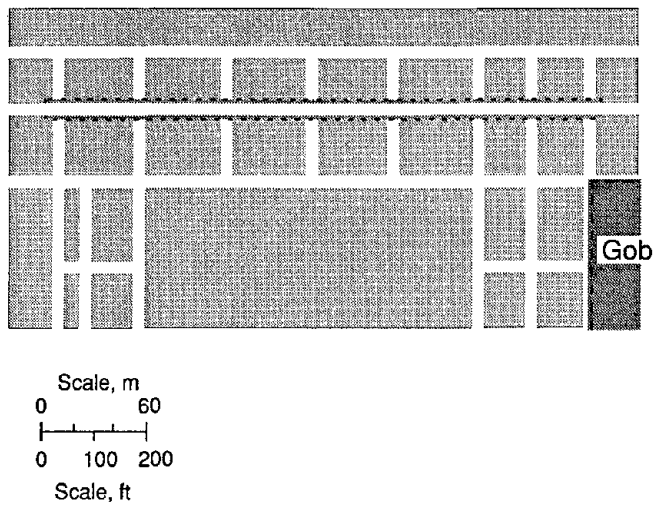

Figure 11.—Bleeder entry configuration and resin-grouted cable test area.

but the transfer of stress over those pillars warranted secondary support to ensure an adequate ventilation and escapeway entry. It was believed that if separation did occur, it would most likely be in the layers of silty shale occurring about 1.2 m (4 ft) up from the roof. Additionally, the interbedded siltstones and shales could separate if the abutment forces became great enough or the immediate roof was lost. Yield zones on the pillars, both calculated and observed in the mine, indicated that the effective roof span would be approximately 7.9 m (26 ft). Considering these facts, the mine operator elected to install a 4.9-m- (16-ft-) long cable, which would intersect the sandstone at 1.8 m (6 ft). The cables were installed with 3.7 m (12 ft) of resin grout to ensure a strong cable anchorage and also to help hold the lower silty shale member intact. The design specified three cables across the entry at a 1.5-m (5-ft) spacing. The cable supports would support a complete roof separation—the worst case scenario—if it occurred at a depth of 2.7 m (9 ft). A cross section of the support system is shown in figure 12. In addition to 15.2- by 15.2-cm (6- by 6-in) bearing plates, the cables and primary support were also installed with "Monster Mats." These are 0.48-cm- (3/16-in-) thick steel pans that are 35.6 cm (14 in) wide and 4.9 m (16 ft) long. The mats provide excellent mine roof support between the cables and maintain any failed material. Mats help prevent unraveling or progressive roof-type failures.

Instrumentation

Hydraulic U-cells were installed throughout the test area on individual cables to determine the actual loading that occurred during various phases of panel extraction. Differential sag stations were installed to monitor any roof separations that occurred in the first entry to establish the

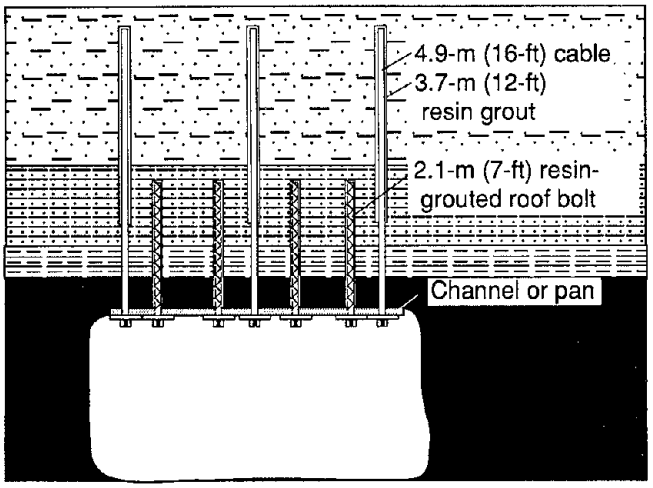

Figure 12.—Cross section showing the primary and cable support spacing and resin grout lengths.

expected failure surface and to estimate the volume of roof material that may have to be carried by the cable supports.

Test Site Results

The test area has been monitored and evaluated 14 times. The panel has been completely extracted, and the adjacent panel is beginning to be mined. The cables will be subjected to higher loads during this period as the adjacent panel creates large spans of unsupported ground. When the immediate and main roofs cave, the support will be subjected to the highest loads. The results of this test area are expected to be published in more detail after the completion of the next panel loads have been measured and evaluated. The cables have performed as expected, with little or no sloughage of the immediate mine roof. The average load measured on the hydraulic load cells was 27.9 kN (6,230 lb) when the face had been completed. The minimum and maximum loads recorded during this same period were 5.6 kN and 129.0 kN (1,250 and 29,000 lb), respectively. The recorded loads were highly variable, with the higher readings mostly related to geologic features that occurred in the supported area.

The mine elected to continue supporting the bleeder system with resin-grouted cables. An additional 2,000 cables have been installed to maintain the bleeder behind the next set of developed panels. These areas have been instrumented to assist in evaluating the long-term stability of the bleeder entries and cable performance.

CASE STUDY No. 3

This last case study describes the most aggressive attempt at installing and evaluating resin-grouted cables for secondary support in a longwall gate road. Cable support systems have been designed and installed to provide stability in a gate road to be utilized for two longwall panels, first as a headgate and then a tailgate.

Site Description

The instrumented test area, approximately 274 m (900 ft) long, was initially supported with 2.1-m (7-ft) full-column resin-grouted bolts. The three-entry system is utilizing a yield-abutment pillar configuration to minimize the pressure on the entries when they become tailgates and to reduce the possibility of coal mine bumps or burst. The final yield pillar dimensions, next to the panel during the second panel mining phase, are 9.8 m (32 ft) wide by 39.6 m (130 ft) long. The final abutment pillar dimensions, designed to absorb the first panel abutment stresses and protect the integrity of the yield pillar, are 30.5 m (100 ft) wide by 39.6 m (130 ft) long. The geology was similar to the bleeder test area with one minor exception: the competent sandstone layer was located about 3.0 m (10 ft) into the roof. However, the laminated materials under this member were competent, and physical property tests indicated a compressive strength of about 103.4 MPa (15,000 psi) for tested specimens.

Cable System Design

After careful analysis of the anticipated pillar behavior and with the experience gained in the first cement-grouted test area, it was decided to test three variations of resin-grouted cables. The test area is shown in figure 13. The secondary supports were 4.9-m- (16-ft-) long, high-strength cable supports installed using three different support concepts. The first 91 m (300 ft) of the designated test area utilized 1.7 m (5 ft 8 in) of resin, leaving approximately 3.4 m (11 ft) of the cable ungrouted. This allowed the cable and the mine roof to yield and relax as abutment loads were redistributed to the gate road. The second area used a 3.7-m (12-ft) equivalent length column of resin, leaving only 1.2 m (4 ft) of the cable ungrouted. This provided a stiffer system that will resist yielding, yet still have enough ungrouted column to allow for separations at the interface between the coal, shale, and interbedded siltstone layers. The third type of support was a tensionable cable system. The cables were installed utilizing 1.7 m (5 ft 8 in) of resin grout and pretensioned using a specially designed jack system to about 35.6 kN (8,000 lb). The tensionable system would help resist any downward movements, but still have enough ungrouted

portion of cable to accept large deformations before reaching the ultimate capacity levels.

All of the cable systems were installed with 15.2- by 15.2-cm (6- by 6-in) bearing plates and Monster Mats. The cables were placed four across the 5.5-m- (18-ft-) wide opening at a spacing of 1.5 m (5 ft). The cables at the ends were installed as closely as possible to the pillar and panel edges and angled at 80°. A cross section of the cable pattern is shown in figure 14.

Instrumentation

The test area was instrumented with 36 hydraulic U-cells and Goodyear pressure pads to evaluate individual cable loading trends and patterns. The mine roof behavior is being evaluated with 12 differential sag stations using magnetic extensometers at critical geologic interfaces. Individual cribs have also been instrumented ahead of the test area to measure the loads and stiffness of the wooden material. Additionally, the pillars and panels were instrumented with borehole pressure cells (BPC's). The BPC's will help evaluate the effects and stresses generated by first panel mining, determine the core of the yield pillar after first panel mining, and provide insight into the effects of a stiff support system on pillar behavior.

Test Site Results

The instrumentation in the test area has been read and evaluated eight times during critical phases of first panel mining. At the conclusion of the first panel mining, the instrumentation indicated that the cables have loaded an average of 24.2 kN (5,450 lb). The minimum recorded cable load was 0 kN (0 lb), where roof dilation has actually caused the cable to unload, while the maximum load was 148.6 kN (33,400 lb) where a localized separation above the primary support has caused the two adjacent cables to support the entire rock mass. The differential sag stations indicate roof separations between the coal and shale interfaces and at the shale and interbedded siltstones, which was expected. Figures 15 and 16 show a portion of the test area before and after the effects of first panel mining. The effects of second panel mining, when the area becomes a tailgate, will be evaluated as the next panel is extracted. The results of this test site are to be published in detail at that time.

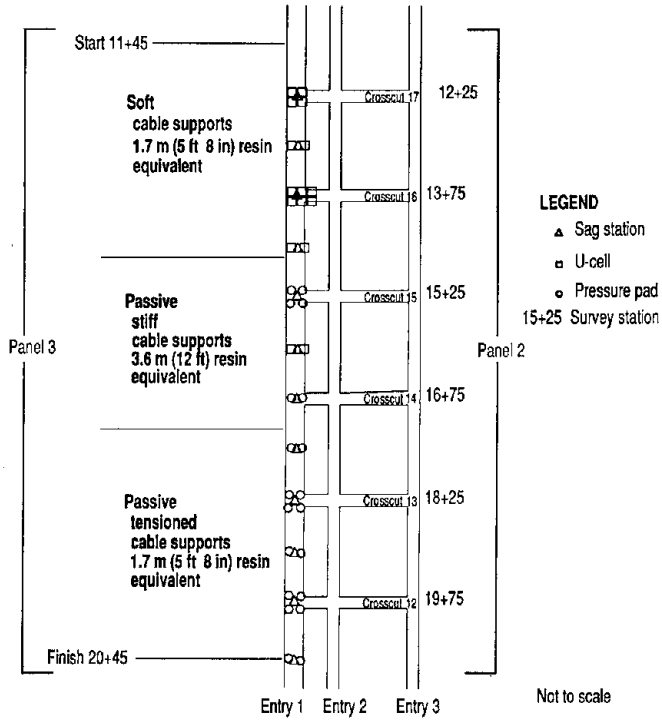

Figure 13.—Test area examining three different types of resin-grouted cable supports and respective instrumentation types and locations.

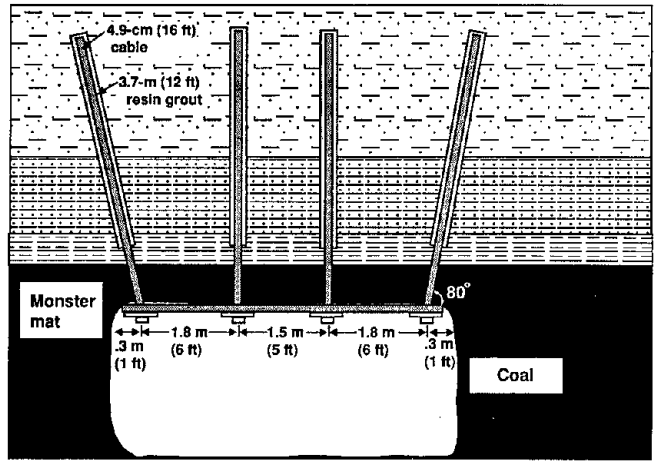

Figure 14.—Generalized cross section of the cable spacing and lengths used in the gate road test areas.

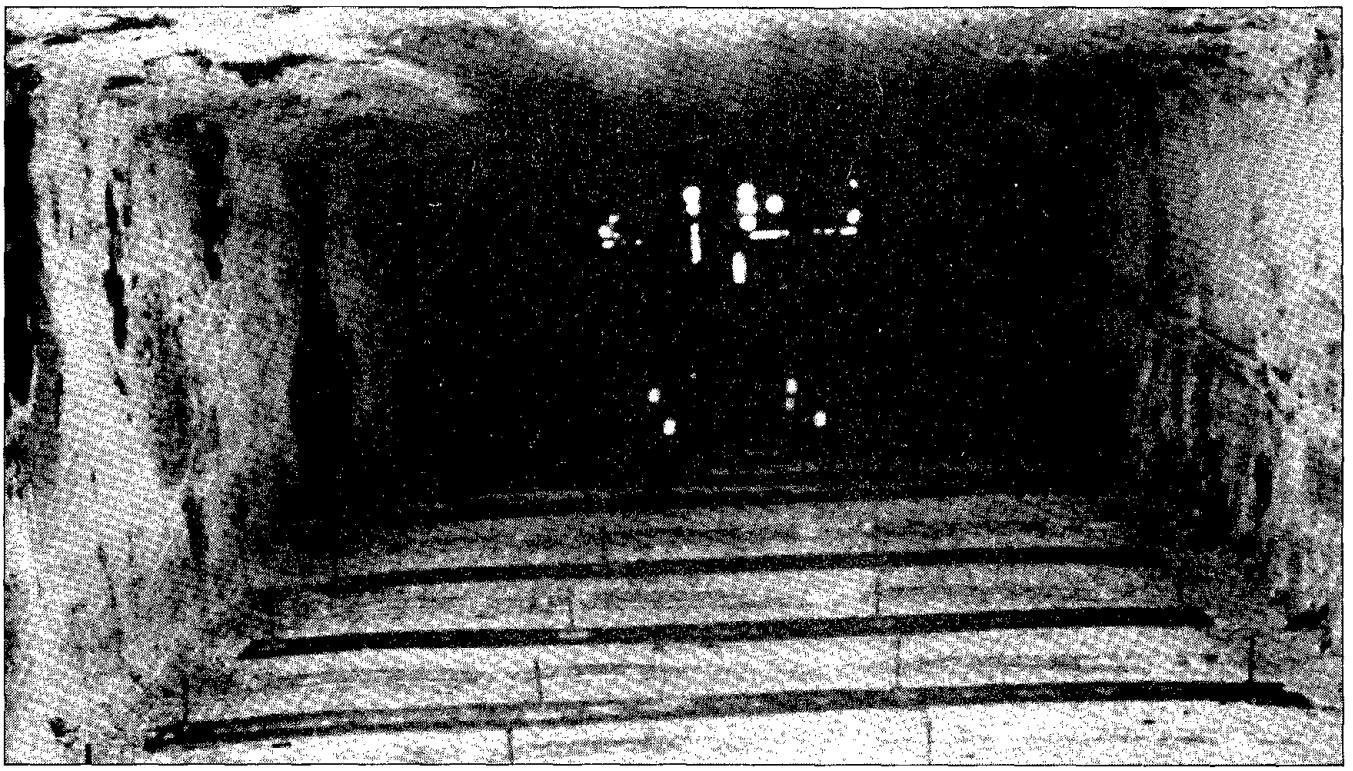

Figure 15.—Resin-grouted cable test area immediately after cable support installation (before first panel mining).

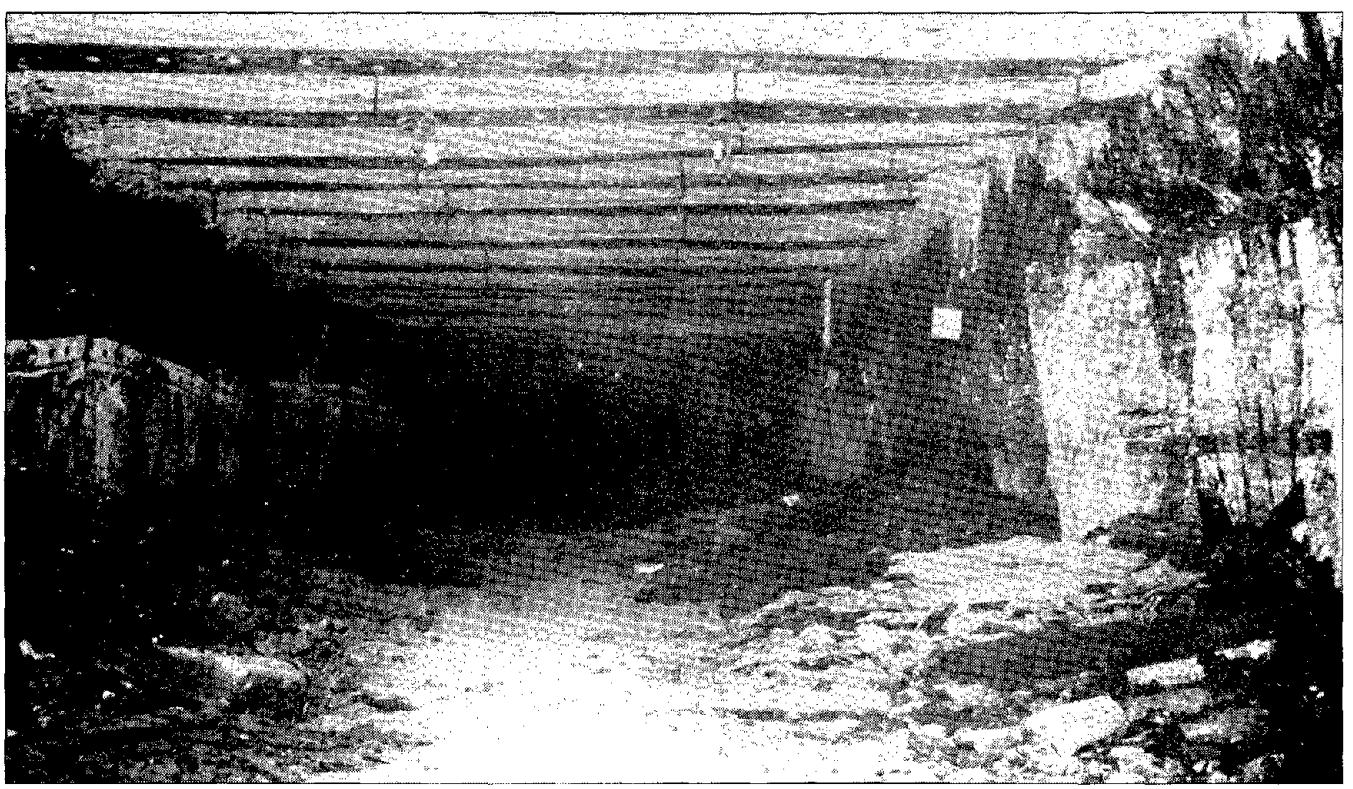

Figure 16.—Resin-grouted cable test area after the first panel has passed and the loads have been redistributed onto the pillars and next panel.

DISCUSSION AND CONCLUSIONS

Cable supports have been successfully installed with both cement- and resin-grouted anchorage systems. Cables have shown their ability to stabilize ground conditions in hazardous underground locations, such as gate roads and bleeder entries. Design principles have been presented to permit initial simplistic cable configurations and spacings. These design schemes will be modified and updated as the results from several ongoing investigations are obtained. USBM personnel, with the assistance of industry, are continuing to examine the effectiveness of cable supports under a wide range of geological and mining conditions. The ultimate goal of this investigation is to provide engineered and economically feasible support designs that will provide safer working areas under diverse and hazardous ground control conditions for the Nation's underground mineworkers.

ACKNOWLEDGMENTS

The authors thank Robert Koch, Senior Engineer, Mountain Coal Co., for his continued support, enthusiasm, and assistance during these investigations.

REFERENCES

1. Goris, J. M. Laboratory Evaluation of Cable Bolt Systems (In Two Parts). 1. Evaluation of Supports Using Conventional Cables. USBM RI 9308, 1990, 23 pp.

2. Goris, J. M. Laboratory Evaluation of Cable Bolt Systems (In Two Parts). 2. Evaluation of Supports Using Conventional Cables With Steel Buttons, Birdcage Cables, and Epoxy-Coated Cables. USBM RI 9342, 1990, 14 pp.

3. Tadolini, S. C., and R. L. Koch. Cable Supports for Improved Longwall Gateroad Stability. Paper in Proceedings of the 12th Conference on Ground Control in Mining, ed. by S. S. Peng (Morgantown, WV, Aug. 3-5, 1993). Dept. of Min. Eng., WV Univ., Morgantown, WV, 1993, pp. 9-15.

4. U.S. Mine Safety and Health Administration, Division of Mining Information Systems, Safety and Health Technical Center, Technical Support, Denver, CO. IR 1207, 1992, p. 16.

5. U.S. Mine Safety and Health Administration, Division of Mining Information Systems. Mine Injuries and Worktime Quarterly, January-June 1993, p. 5.

6. Kadnuck, L. L. Mine Ventilation Enhancement Through Use of Cable Supports (1994 SME Annual Meeting and Exhibit, Albuquerque, NM, Feb. 14-17, 1994). Soc. Min. Eng. AIME, preprint 9436, 1994, pp. 1-4.

7. Gale, W. J. Design Considerations for Reinforcement of Coal Mine Roadways in the Illawarra Coal Measures. Aus. IMM Ground Movement and Control Related to Coal Mining Symposium, August 1986, pp. 82-92.

8. Gale, W. J., and M. W. Fabjanczyk. Application of Field Measurement Techniques to the Design of Roof Reinforcement Systems in Underground Coal Mines. Commonwealth Scientific and Industrial Research Organisation (CSIRO), Australia, 1987.

9. Adler, L., and M. S. Sun. Ground Control in Bedded Formations. Virginia Polytechnic Inst. and State Univ., Research Div., Bull. 28, Mar. 1976, pp. 29-76.

10. Wilson, A. H. A Hypothesis Concerning Pillar Stability. The Mining Engineer, v. 131, No. 141, 1972, pp. 409-417.

11. Tadolini, S. C., and D. R. Dolinar. Thrust Bolting: A New Innovation in Coal Mine Roof Support. Paper in Proceedings of the 10th Conference on Ground Control in Mining, ed. by S. S. Peng (Morgantown, WV, June 10-12, 1991). Dept. of Min. Eng., WV Univ., Morgantown, WV, 1991, pp. 76-84.

FIELD EVALUATIONS OF GROUTED ROOF BOLTS

By Stephen P. Signer[1]

ABSTRACT

Three field tests were conducted by the U.S. Bureau of Mines (USBM) to study the support-rock interaction mechanics of fully grouted roof bolts. Thirty-two instrumented, fully grouted bolts were installed in three different longwall gate roads to measure load changes at various stages of the mining process. Readings were taken during section development and, for sites 1 and 2, as each longwall face passed the test sections.

These studies provided several valuable insights into the behavior of fully grouted resin bolts. In every case, the bolt loads resulting from entry development were greater than what would be produced from simple suspension of the immediate mine roof. As far-field stresses induced by mining activity were transferred to the rock surrounding the entry, the bolts responded by increasing in load. Many sections of the resin-grouted bolts yielded, but none of the bolts came close to the strain necessary to cause failure. The degree of loading seemed to be related to geology and stress fields; i.e., where roofs were weaker and there was more overburden, bolt loads were higher.

This type of instrumented support could be used to monitor problem areas, evaluate loading conditions in the immediate roof with respect to bolt reinforcement and other mining activities, and improve the design selection process for rock reinforcement, resulting in significant improvements in underground mine safety.

INTRODUCTION

A major concern of the coal mining industry is the reinforcement of mine roof to prevent ground failures. One aspect of selecting the proper reinforcement is to evaluate support behavior during the support's working life. Methods to measure bolt tension for ungrouted roof bolts are well established and have been used for many years. The USBM has developed a method to determine loading on grouted roof bolts that will improve the evaluation and selection of this type of support in underground coal mines.

Selection of the type, size, and location of roof rock reinforcement has often been accomplished by trial and error rather than engineering design (Gerdeen and others, 1977; Haas and others, 1976; Unal, 1983). This is due to several factors. Rock behavior around openings can vary dramatically depending on changing geology and stress fields, and determination of rock movements, support load, and stress fields can be very time-consuming and costly, which results in insufficient field data to develop a design methodology. Therefore, the first step in the development of a design methodology is an understanding of support behavior. The benefits to be gained are substantial. Proper design and evaluation procedures could decrease the number of mine roof falls, which would increase both safety and productivity.

This paper presents a brief summary of the USBM's instrumentation methods and field test results using strain gauges to evaluate fully grouted roof bolts. Other methods for the measurement of grouted bolt load have been developed, and substantial laboratory work has been performed (Serbousek and Signer, 1987; Signer, 1990; Signer and Jones, 1990; Signer and others, 1993; Tadolini, 1990; Farmer, 1975). However, the method described herein has proved to be reliable and has led to new insights into the behavior of grouted supports.

[1]Mining engineer, Spokane Research Center, U.S. Bureau of Mines, Spokane, WA.

INSTRUMENTATION

The bolts used in these USBM field tests were standard, grade-60, No. 6 rebar bolts that had been milled with a 6-mm- (1/4-in-) wide by 3-mm- (1/8-in-) deep slot along each side. Strain gauges were installed as shown in figure 1. The instrumented bolts were calibrated in a uniaxial test machine to correlate voltage change to load change. During installation, the bolts were oriented with the strain gauges parallel to the ribs to measure localized bending effects in the mine roof.

Five grade-60 bolts were tested to failure to determine the strength and yield point of the bolt after the slots had been milled. The slotting process reduced bolt strength to an equivalent grade-40 bolt. A typical load-strain curve from one of these tests is shown in figure 2. When the data from the instrumented bolts were reduced, the correlation coefficients from the axial calibrations were used to convert voltage changes to load changes. This process was accurate to ±0.4 kN (±90 lb). When the bolt load levels exceeded the yield point of the steel, voltage readings were converted to strain readings to estimate the degree of plasticity.

The data collection system used for these tests was an Omnidata Polyrecorder 516-C. A completion box was made that provided 5-V excitation and completion resistors for the Wheatstone bridge circuits used to measure strain gauge voltage changes. Various types of sagmeters were installed to measure roof movements. However, the presentation and discussion of those data are beyond the scope of this paper.

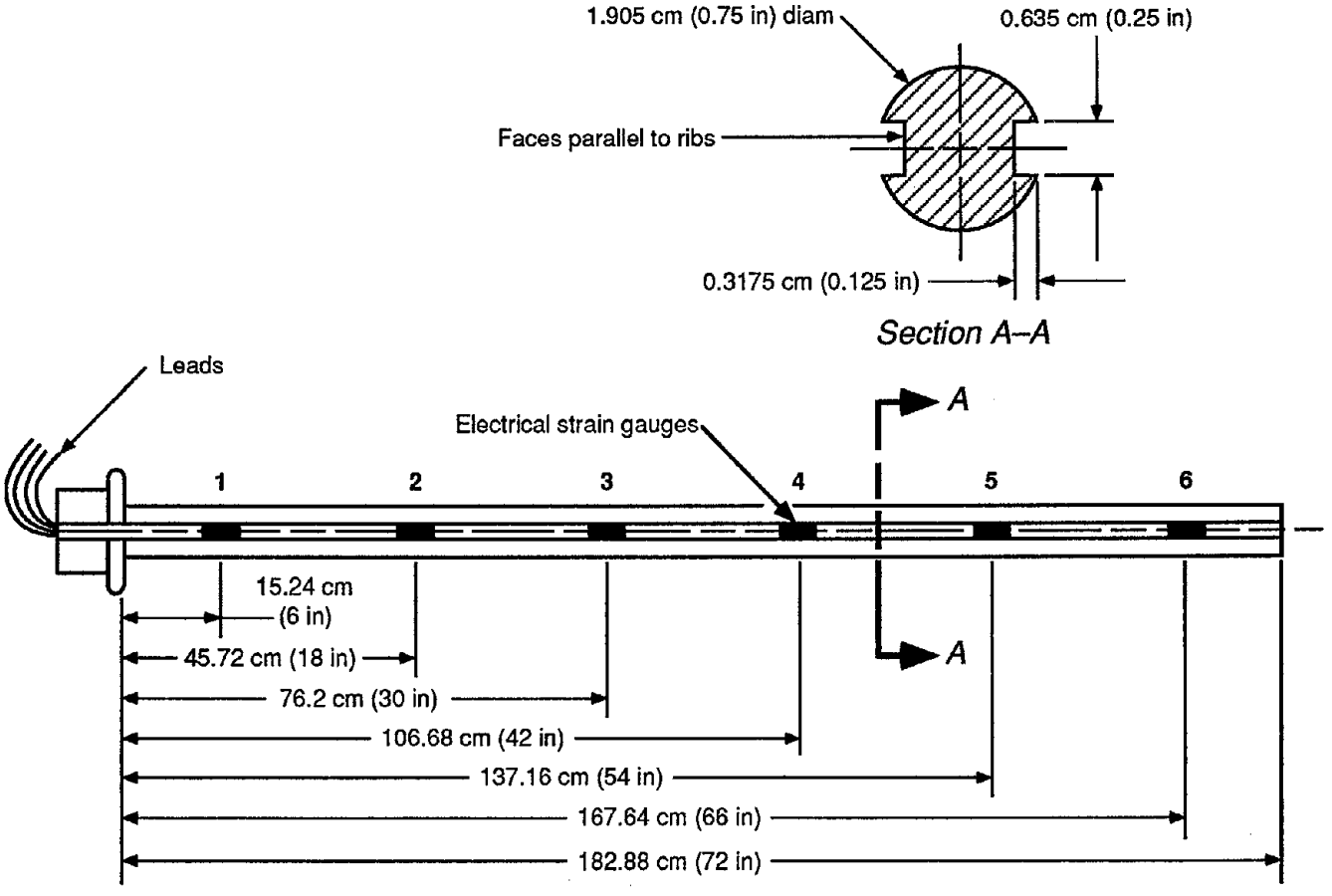

Figure 1.—Instrumented bolt.

FIELD TEST SITES

TEST SITE 1

The first test site was located in a two-entry gate road (figure 3). The coal seam at the test site was approximately 2.5 m (8 ft) thick, and the overburden was between 210 and 240 m (700 and 800 ft) deep. The mine roof was composed of layers of mudstone, very-fine-grained sandstone, and siltstone (figure 4). On the USBM Coal Mine Roof Rating (CMRR) scale of 0 to 100 (Molinda and Mark, 1993), the mine roof has been typically found to be in the 60 to 70 range.[2]

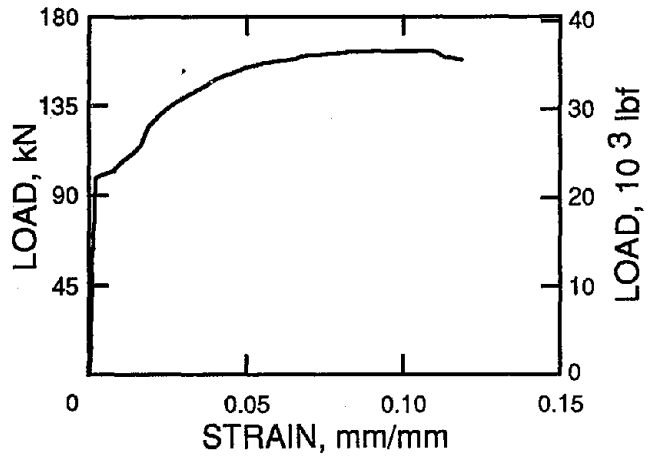

Figure 2.—Typical stress-strain curve for slotted bolt.

Grouted roof bolts 1.8 m (6 ft) long were used as the main roof support in this entry. These bolts were grade-60 steel and spaced in a square pattern approximately 1.2 by 1.2 m (4 by 4 ft), as specified in the roof control plan. Supplemental supports were installed for the gate road. Posts were installed on 1.8-m (6-ft) centers during entry development along the rib adjacent to the second panel, and 1.8- by 1.8-m (6- by 6-ft) cribs were installed on 3.6-m (12-ft) centers along the pillar side of the entry during extraction of the first longwall panel.

Twelve fully grouted instrumented bolts were installed on-cycle and pattern. Eight two-point sagmeters were

[2]Mark, C. Personal communication, 1994.

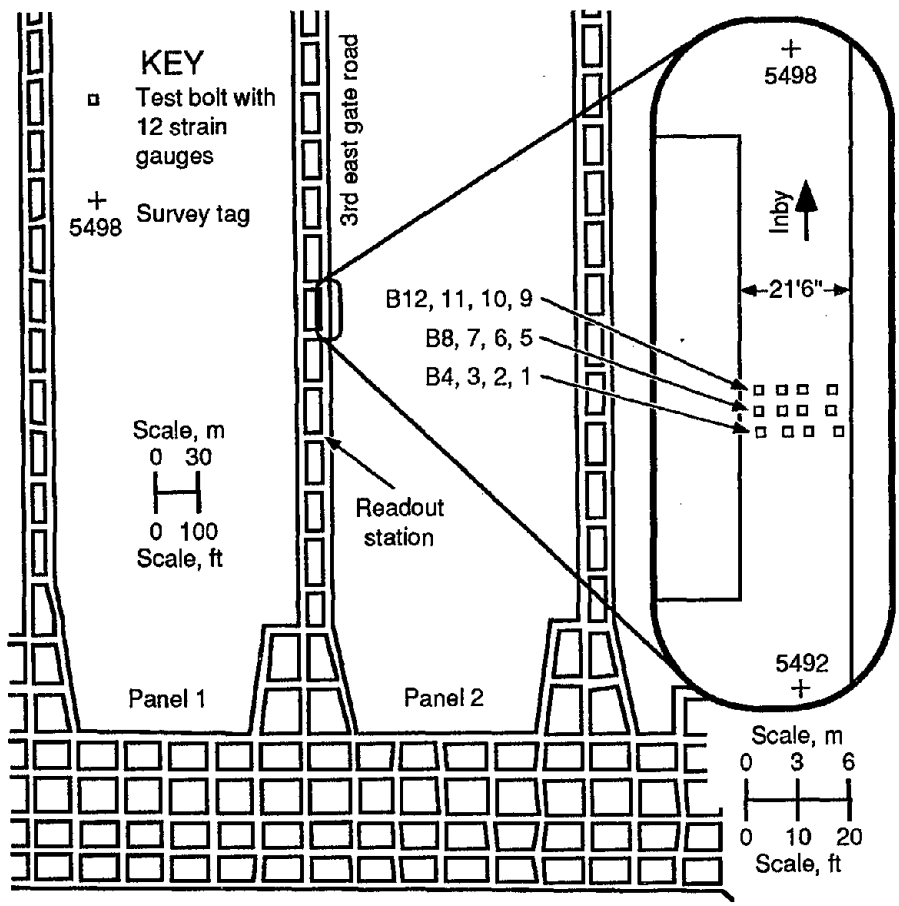

Figure 3.—Test site 1.

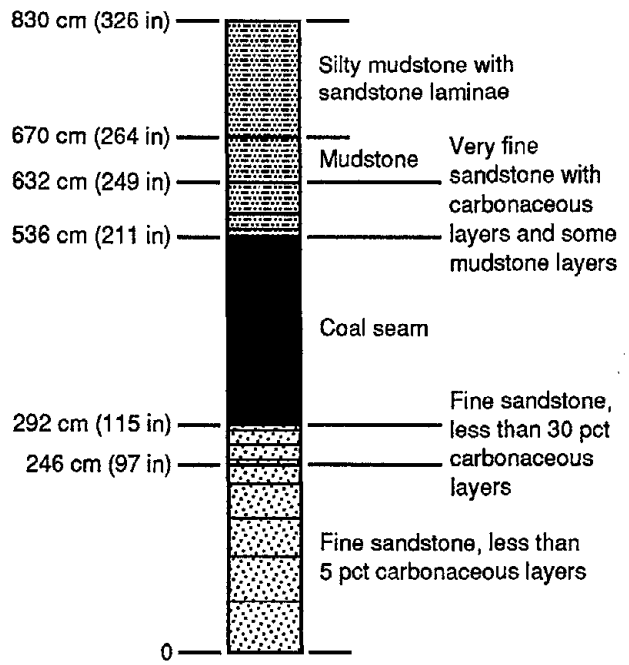

Figure 4.—Geologic column at test site 1.

installed in the roof, and anchors were set at 1.7 and 2.3 m (5.5 and 7.5 ft) to measure roof movements in the bolted strata. Three inspection holes were drilled to a depth of 2.3 m (7.5 ft) to assist in an assessment of the geology of the roof. Wood cribs were installed, with one placed just inby bolts 11 and 12 and the other just outby bolts 3 and 4.

TEST SITE 2

The second test site was located in a four-entry gate road with yield-abutment pillars (figure 5). The overburden at the test site was approximately 670 m (2,200 ft). Figure 6 shows a typical stratigraphic column. A 30-cm- (1-ft-) thick layer of incompetent drawrock overlies the coal seam. The immediate mine roof is formed by a fossiliferous shale that grades into thinly interbedded shales and coals. This seam is overlain by a 30-cm- (1-ft-) thick coal seam. Where the drawrock is thin, it falls during extraction of the coal together with the coal rider seam. The main roof above the rider seam consists of 30 to 60 cm (1 to 2 ft) of competent siltstone overlain by massive sandstone. The instrumented bolts were located in areas where the rider seams remained intact. The CMRR was found to be approximately 50 at the test sites.

The primary support consisted of 19-mm- (3/4-in-) diameter, 1.8-m- (6-ft-) long, grade-40, fully grouted resin bolts, installed five per row with rows on 1.22-m (4-ft) centers. Just prior to the headgate pass, additional rows of resin bolts were installed between each row of primary supports together with wood cribs.

One row of instrumented grouted bolts was installed at midpillar, and one row was installed in a three-way intersection. Detailed maps of the test sites are shown in figure 5. At each site, four instrumented roof bolts and three three-point roof extensometers were installed.

TEST SITE 3

The third test site was in a two-entry gate road as shown in figure 7. The coal seam is approximately 4.3 m (14 ft) thick and has a 16° pitch. The overburden at the test site was approximately 335 m (1,100 ft) deep. The entry was cut approximately 3 m (10 ft) high, and top coal was left on the roof and the floor (figure 8). The top coal was approximately 0.5 m (1.5 ft) thick on the downdip side of the entry and 1.5 m (5 ft) on the updip side. Above the top coal, the immediate roof was a very low-strength carbonaceous mudstone. The CMRR was 35 at this test site.

The primary support consisted of 19-mm- (3/4-in-) diameter, 1.8-m- (6-ft-) long, grade-60, point-anchored (with resin) bolts that were tensioned with a breakaway nut. These bolts were grade-60 steel and were spaced in a square pattern approximately 1.2 by 1.2 m (4 by 4 ft) with four bolts per row. The primary roof control problem is caused by shear failure in the roof; therefore, trusses were also installed as supplementary support at the same time. Two rows of five instrumented grouted bolts were spaced across the entry to compensate for their reduced strength. An extensive system of deflection measurements was installed, but a discussion of this system is beyond the scope of this paper.

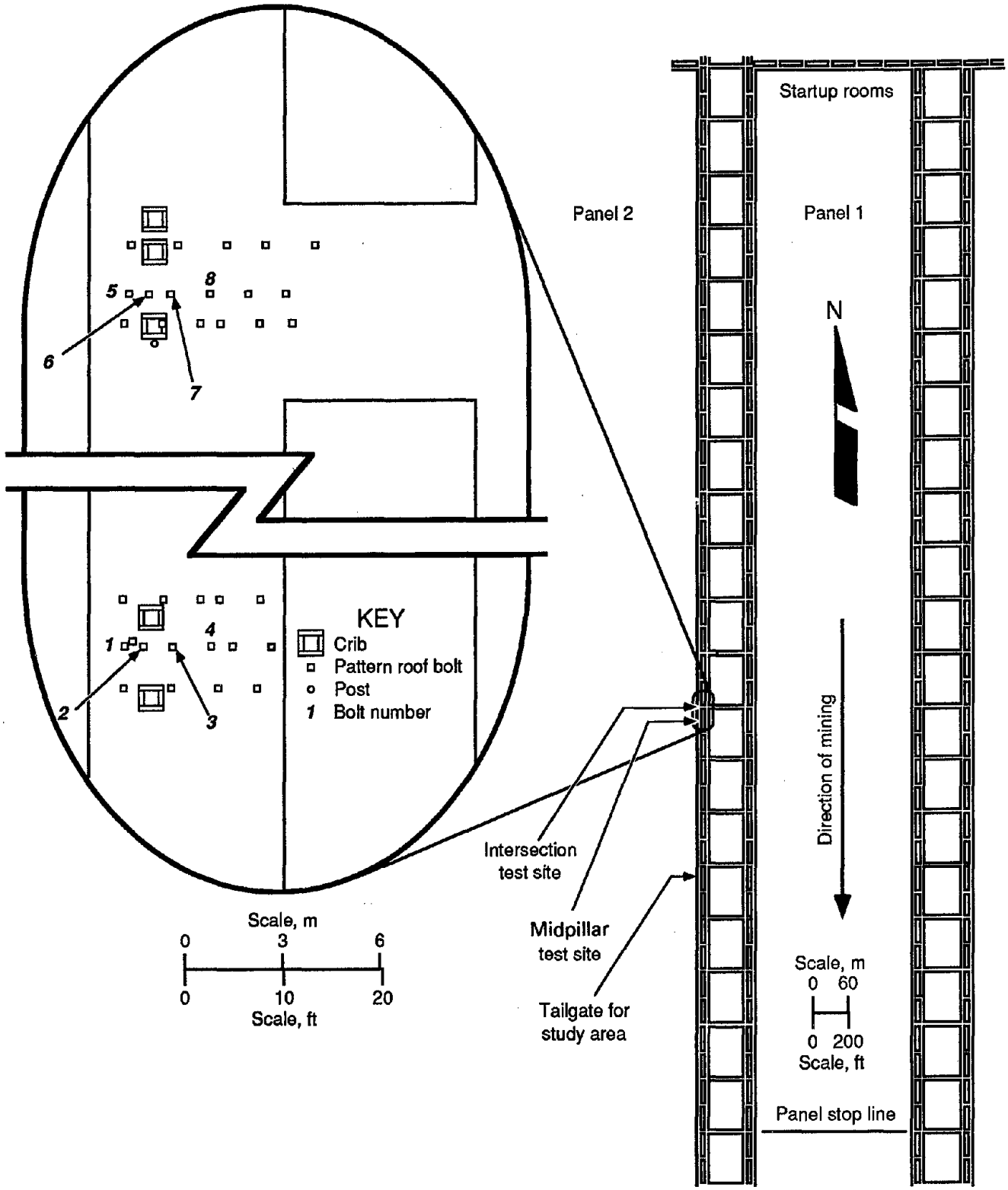

Figure 5.—Test site 2.

RESULTS

At test sites 1 and 2, bolt loads were monitored during entry development and as both longwall panels passed the test sections. The first longwall panel at test site 3 has not yet been mined. Monitoring was conducted daily when mining was active near the test sections and on a regular basis when there was no mining in the vicinity.

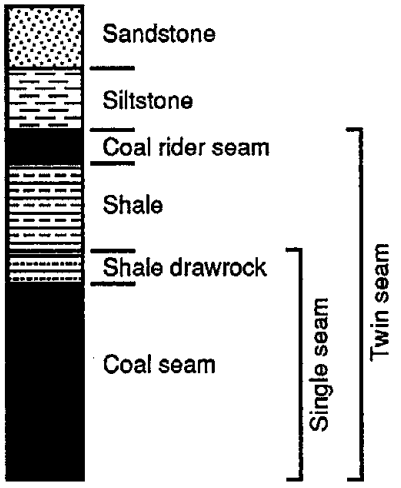

Figure 6.—Geologic column at test site 2.

Figures 9*A*, 10*A*, and 11 show axial bolt loads after the test sections stabilized following section development. Figures 9*B* and 10*B* show bolt loads at test sites 1 and 2 after the pass of the first longwall panel, and figures 9*C* and 10*C* show axial bolt loads when the second longwall face was near the test sections.

TEST SITE 1

Figure 9*A* shows bolt loads 82 days after installation. The highest loads occurred 76.2 cm (30 in) from the bolthead and tapered off toward each end of the bolt. Two bolt sections exceeded the yield point of the steel. The maximum strain was approximately 5,000 microstrain just past the steel yield point, but not yet in the strain-hardening phase. Simple suspension of roof material was

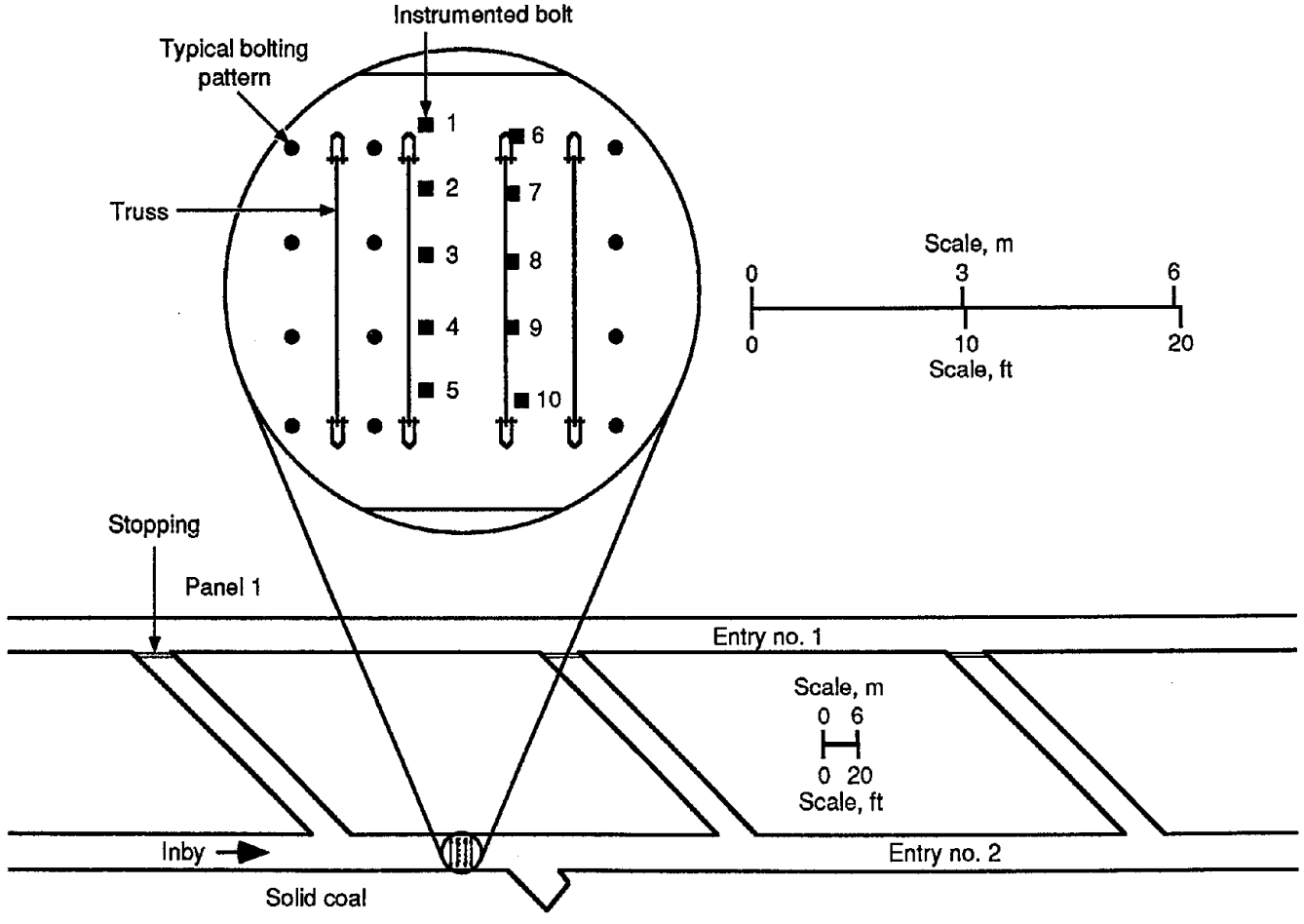

Figure 7.—Test site 3.

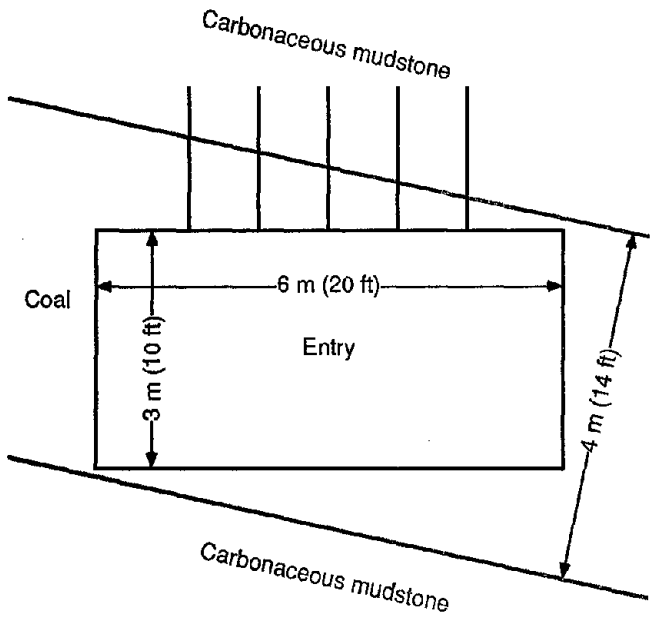

Figure 8.—Cross-sectional view of test site 3.

insufficient to cause these high loads. Loads in the bolt 76 cm (30 in) from the roofline would be approximately 27 kN (6,000 lb) if simple suspension were the sole cause of loading.

After the first longwall panel passed the test site, readings indicated that 75% of the bolts were loaded past the yield point of the steel (fig. 9*B*). This dramatic load increase occurred at every strain-gauged station located 76 cm (30 in) from the bolthead. The bolts that did not load to this high level had posts installed nearby. Strain estimates of the yielded sections indicated that the maximum microstrain was 20,000 and the median microstrain was 7,300. This is well below the approximately 100,000 microstrain necessary to cause failure (figure 2).

Loading of the supports continued after the first face was completely mined and prior to the abutment forces of the second longwall face acting on the test section. As the second longwall face approached the test section, load levels in most of the bolts exceeded the yield point of the steel between the bolthead and 107 cm (42 in) into the roof (figure 9*C*).

The bolts showed adequate anchorage length to develop the full capacity of the steel as indicated by the fact that up to 1.2 m (4 ft) of bolt length had passed the yield point of the steel, but load was still transferred from the bolt to the rock in the remaining 0.6 m (2 ft) of bolt length. Also, none of the instrumented bolts exceeded the ultimate strength of the steel.

TEST SITE 2

Bolt 6 and one station on bolt 8 were lost soon after they were installed. The data in figure 10*A* show high localized loading. Several bolt locations had reached the yield point of the steel. Generally, the maximum load was measured by the gauges located at the 76-cm (30-in) station near the rider seam and main roof interface. At the midpillar site, greater bolts loads tended to develop on the bolts nearest the panel rib. Bolt loads in the intersection were higher than those at the midpillar site.

After the passage of first longwall panel, several bolt locations passed into the strain-hardening phase of the plasticity curve (figure 10*B*). The final days before the tailgate pass of the longwall saw loads increase significantly on nearly every bolt (figure 10*C*). Fifty percent of the strain gauge stations on the resin bolts showed loads in excess of the yield point of the steel. The maximum estimated strain was 60,000 microstrain. In general, bolt loads at test site 2 were higher than those at test site 1.

TEST SITE 3

The bolt loading pattern at test site 3 was greatly influenced by the geometry and geology of the mine entry. A typical roof control problem in these entries is the development of a cutter on the downdip side of the entry that progresses until the immediate roof comes in and rests on the trusses. The bolt loading pattern shows that the bolt sections above the coal interface were more heavily loaded on the downdip side (figure 11). The highest loading occurred within the last 90 cm (3 ft) of bolt length, and on several bolts, yield developed to within 46 cm (18 in) of the end of the bolt. In this weak rock, anchorage may be insufficient and may result in failure at the end of the bolt. The pattern of bolt loading at this site showed that the higher loads occurred farther from the roof line than at test sites 1 or 2.

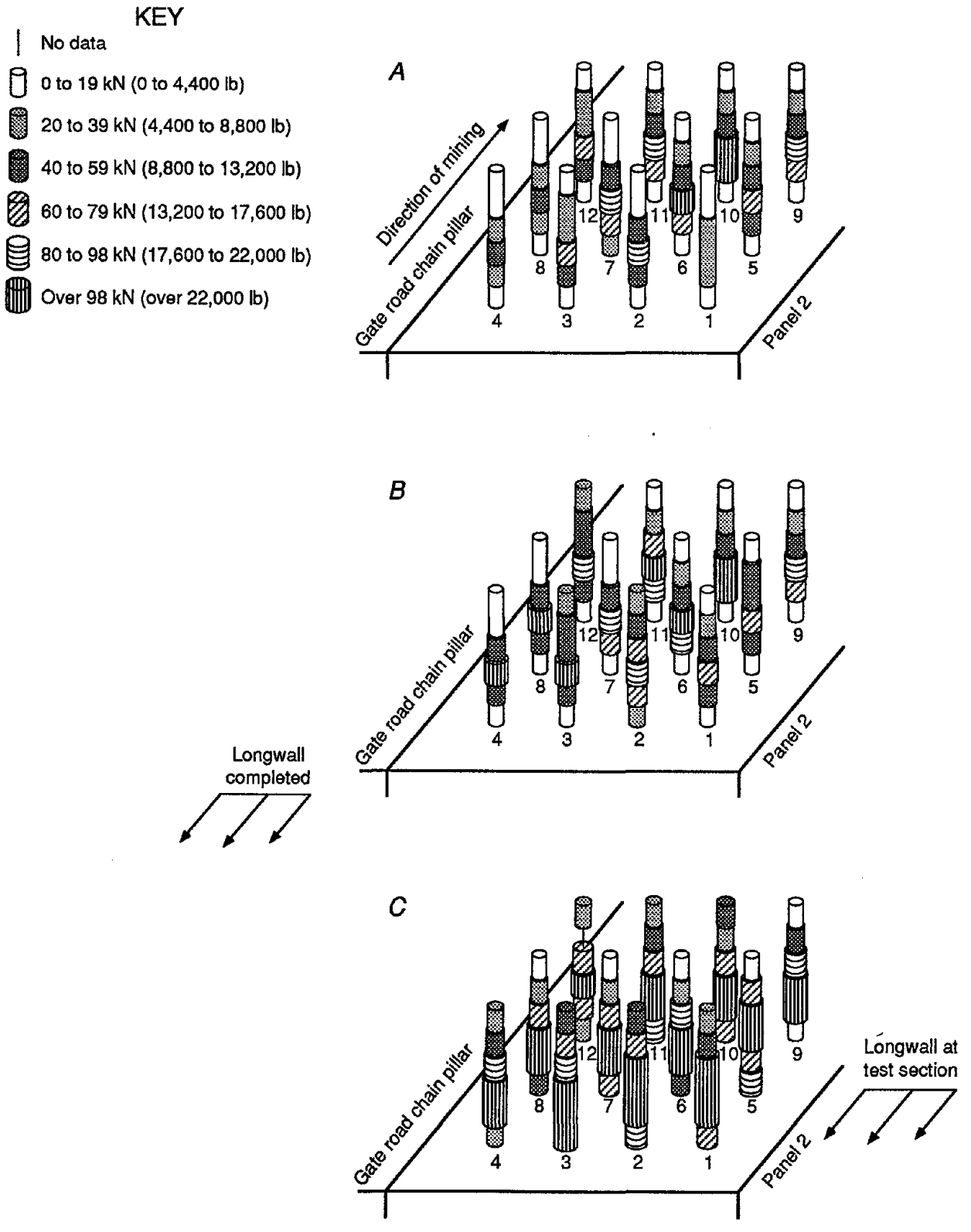

Figure 9.—Axial roof bolt loads at test site 1. *A*, After section development; *B*, after pass of first longwall; *C*, when second longwall is at test site. Numbers indicate bolt numbers.

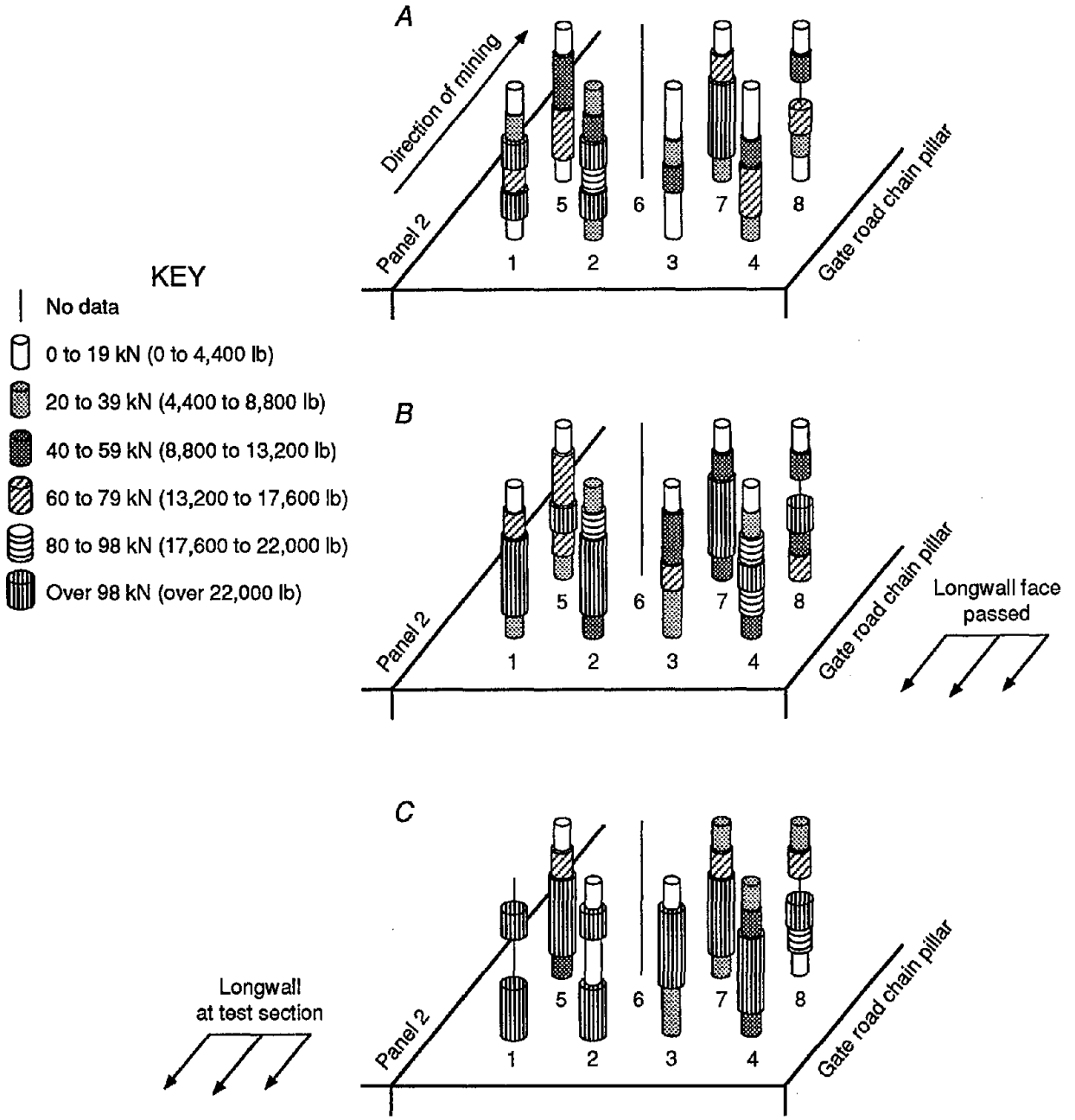

Figure 10.—Axial roof bolt loads at test site 2. *A*, After section development; *B*, after pass of first longwall; *C*, when second longwall is at test site. Numbers indicate bolt numbers.

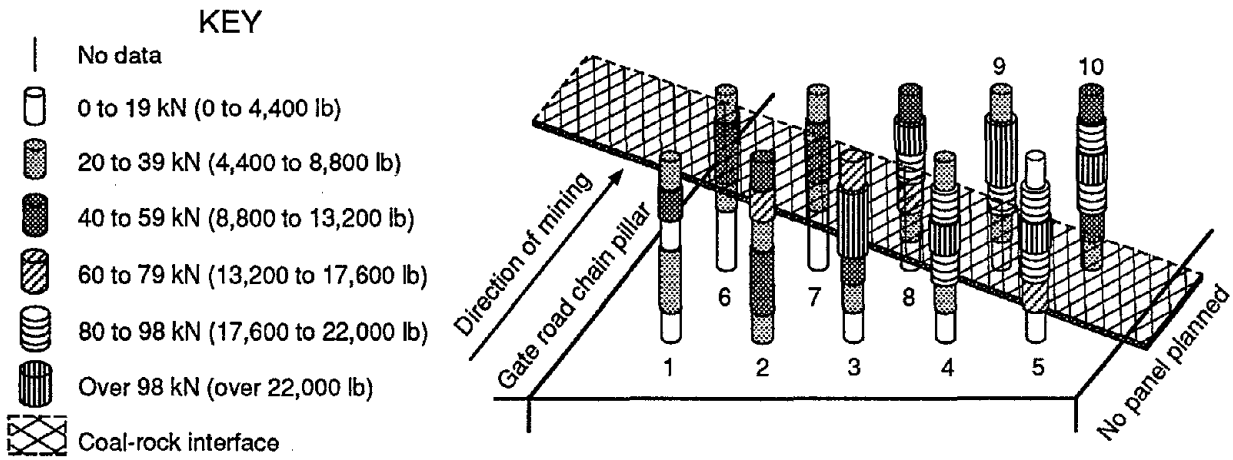

Figure 11.—Axial roof bolt loads at test site 3 after section development. Numbers indicate bolt numbers.

DISCUSSION

Grouted bolts are much stiffer than ungrouted bolts due to their continuous interface with the roof rock. This means that a small amount of rock movement will produce high bolt loads; e.g., in a 30-cm (1-ft) ungrouted section of bolt, less than 0.76 mm (0.03 in) of deflection will cause the bolt to yield. Yield of the steel occurs at approximately 2,000 microstrain, and the strain gauges are functional to approximately 50,000 microstrain. From the laboratory tests on the slotted bolts, it was determined that the ultimate loading of approximately 160 kN (36,000 lb) would be reached at 120,000 to 140,000 microstrain. The highest estimated strain reading was approximately 60,000 microstrain. Open circuits to several of the gauges occurred during the period of the test.

The load in the instrumented bolts increased as a result of stress redistribution around the gate road entries. At all three test sites, the bolt loading was higher than what would result from simple suspension of the roof rock, and in many bolt sections, the load exceeded the yield strength of the steel. The highest load buildup generally occurred above 76 cm (30 in) from the mine roof and was transferred from the bolt to the roof rock in the last 61 cm (2 ft) of bolt length.

Bolt loadings increased significantly after the first longwall panels passed the test sections but before the second longwall panels could generate abutment forces to act on the sections. When the second longwall face was at the test sections, 38% (site 1) and 53% (site 2) of the strain gauges indicated loads exceeding the yield point of the steel. The loading pattern at test site 2 showed that yield sections were farther into the roof than at test site 1. The bolt loading pattern at test site 3 was influenced by the dipping seam and weak roof rock. Even at these extremely high loads, there was enough bolt length to transfer the load from the bolt to the rock and prevent failure.

Table 1 shows the relationship between the CMRR, overburden, number of bolt sections that had passed the yield point, and the average bolt load. The pattern of loading appeared to be influenced by the geology, geometry, and in situ stresses. The lower CMRR's correlate with higher bolt loads. However, the deeper cover at site 2, which is double that at site 3, has an additional effect of producing high localized loads. One effect not taken into account in this paper is the effect of bending on the roof bolts. This mechanism was most pronounced at site 2 and could be a primary cause of localized loads.

Table 1.—Comparisons of bolt loads and site conditions

Site	Coal Mine Roof Rating	Overburden, m	Number of bolt sections yielded, %			Average bolt load, kN		
			Time 1	Time 2	Time 3	Time 1	Time 2	Time 3
1	60-70	210-240	4	10	38	26	36	54
2	50	670	17	29	53	38	56	68
3	35	335	13	NAp	NAp	42	NAp	NAp

NAp Not applicable.

The amount of loading exhibited by these instrumented bolts was much greater than would be produced by simple suspension of the rock from the main roof. Several theories that would explain this behavior include beam, pressure arch, and voussoir arch. In all of these theories, roof bolts interact with the immediate mine roof to form a structural member that carries additional loading imposed by in situ conditions.

SUMMARY

These studies provided several valuable insights into the behavior of fully grouted resin bolts. In every case, the loads were greater than what would be produced from simple suspension of the immediate mine roof. As far-field stresses were transferred to the rock surrounding the entry, the bolts responded by increasing in load. Many sections of the resin-grouted bolts yielded, but none of the bolts came close to the strain necessary to cause failure because of the ductile nature of the steel. The degree of loading appeared to be related to geology and to in situ stresses, with the largest bolt loads occurring in the weakest roof where stress fields were higher. It should also be indicated that despite the extensive yielding of the resin-grouted bolts, major mine roof falls did not develop at any site.

This type of instrumented support can be used to monitor problem areas, evaluate loading conditions in the immediate mine roof with respect to bolt reinforcement and mining activities, and improve the design selection process for rock reinforcement. Therefore, the USBM is currently collecting similar data in a variety of geological and mining environments. This research could result in significant improvements in underground mine safety.

REFERENCES

Farmer, I. W. Stress Distribution Along a Resin Grouted Anchor. Int. J. Rock Mech. Min. Sci. & Geomech., v. 12, 1975, pp. 347-351.

Gerdeen, J. C., V. W. Snyder, G. L. Viegelahn, and J. Parker. Design Criteria for Roof Bolting Plans Using Fully Resin-Grouted Nontensioned Bolts To Reinforce Bedded Mine Roof. Volume I. Executive Summary and Literature Review (contract J0366004, MI Technol. Univ.). USBM OFR 46(1)-80, 1977, pp. 21-28; NTIS PB 80-180052.

Haas, C. J., R. L. Davis, H. D. Keith, J. Dave, W. C. Patrick, and J. R. Strosnider, Jr. An Investigation of the Interaction of Rock and Types of Rock Bolts for Selected Loading Conditions (contract H0122110, Univ. of MO—Rolla). USBM OFR 51-80, 1976, 398 pp.

Molinda, G. M., and C. Mark. A New Coal Mine Roof Rating System (CMRR) Developed for Roof Support and Mine Design. Paper in Proceedings of the 12th Conference on Ground Control in Mining, ed. by S. S. Peng (Morgantown, WV, Aug. 3-5, 1993). Dept. of Min. Eng., WV Univ., Morgantown, WV, 1993, pp. 92-103.

Serbousek, M. O., and S. P. Signer. Linear Load-Transfer Mechanics of Fully Grouted Roof Bolts. USBM RI 9135, 1987, 17 pp.

Signer, S. P. Field Verification of Load Transfer Mechanics of Fully Grouted Roof Bolts. USBM RI 9301, 1990, 13 pp.

Signer, S. P., and S. D. Jones. A Case Study of Grouted Roof Bolt Loading in a Two-Entry Gate Road. Paper in Proceedings of the 9th Conference on Ground Control in Mining, ed. by S. S. Peng (Morgantown, WV, June 4-10, 1990). Dept. of Min. Eng., WV Univ., Morgantown, WV, 1990, pp. 35-41.

Signer, S. P., C. Mark, G. Franklin, and G. Hendon. Comparisons of Active Versus Passive Bolts in a Bedded Mine Roof. Paper in Proceedings of the 12th Conference on Ground Control in Mining, ed. by S. S. Peng (Morgantown, WV, Aug. 3-5, 1993). Dept. of Min. Eng., WV Univ., Morgantown, WV, 1993, pp. 16-23.

Tadolini, S. C. Evaluation of Ultrasonic Measurement Systems for Bolt Load Determinations. USBM RI 9332, 1990, 9 pp.

Unal, E. Development of Design Guidelines and Roof-Control Standards for Coal Mine Roofs. Ph.D. Thesis, PA State Univ., University Park, PA, 1983, 355 pp.

ENGINEERING METHOD FOR THE DESIGN AND PLACEMENT OF WOOD CRIBS

By Thomas M. Barczak[1] and David F. Gearhart[2]

ABSTRACT

Wood cribs are used extensively to stabilize mine openings by providing resistance to deflections of the immediate mine roof and floor and by supporting the weight of unstable rock masses. While the unit costs of these supports are relatively low, their extensive use results in significant costs to coal mine operators. The U.S. Bureau of Mines (USBM) has developed a Wood Crib Performance Model that computes the load capacity of wood cribs as a function of the displacement of the crib structure induced by mine roof and floor convergence. This permits comparison of the loading characteristics of various crib constructions and enables systems to be designed with consideration of the load conditions imposed by the mine environment. The design method matches the stiffness, strength, and stability of the crib structure with expected rock mass behavior to determine a crib design and employment spacing that will provide the lowest cost support.

INTRODUCTION

Combinations of roof bolts, cribs, posts, and beams are often used to stabilize mine openings to provide a safer underground environment for mineworkers. Roof bolts and cribs are used most often. Crib supports are simple in design, with a material cost of less than $70 per meter of height, but their extensive use results in significant costs to coal mine operators. One mine operator estimates that $1 million is spent annually in crib construction for support of its longwall gate roads.[3]

As part of the USBM's program to reduce underground hazards to mineworkers through the development of improved ground control technologies, researchers conducted full-scale tests of crib support systems in the 13,350-kN (3-million-lb) mine roof simulator at the USBM's Pittsburgh Research Center (figure 1). The results obtained permit a comparison of wood crib performance and have led to the development of a Wood Crib Performance Model that predicts the force-displacement behavior of wood cribs. The model can accurately predict the performance of cribs where the type of wood, timber dimensions, and construction configuration are varied. This model will assist the mine operator in selecting the optimum crib design and employment strategy to safely stabilize its mine openings at minimal cost.

[1]Research physicist, Pittsburgh Research Center, U.S. Bureau of Mines, Pittsburgh, PA.

[2]Project engineer, SSI Services, Inc. Pittsburgh, PA.

[3]Private communications with mine operators.

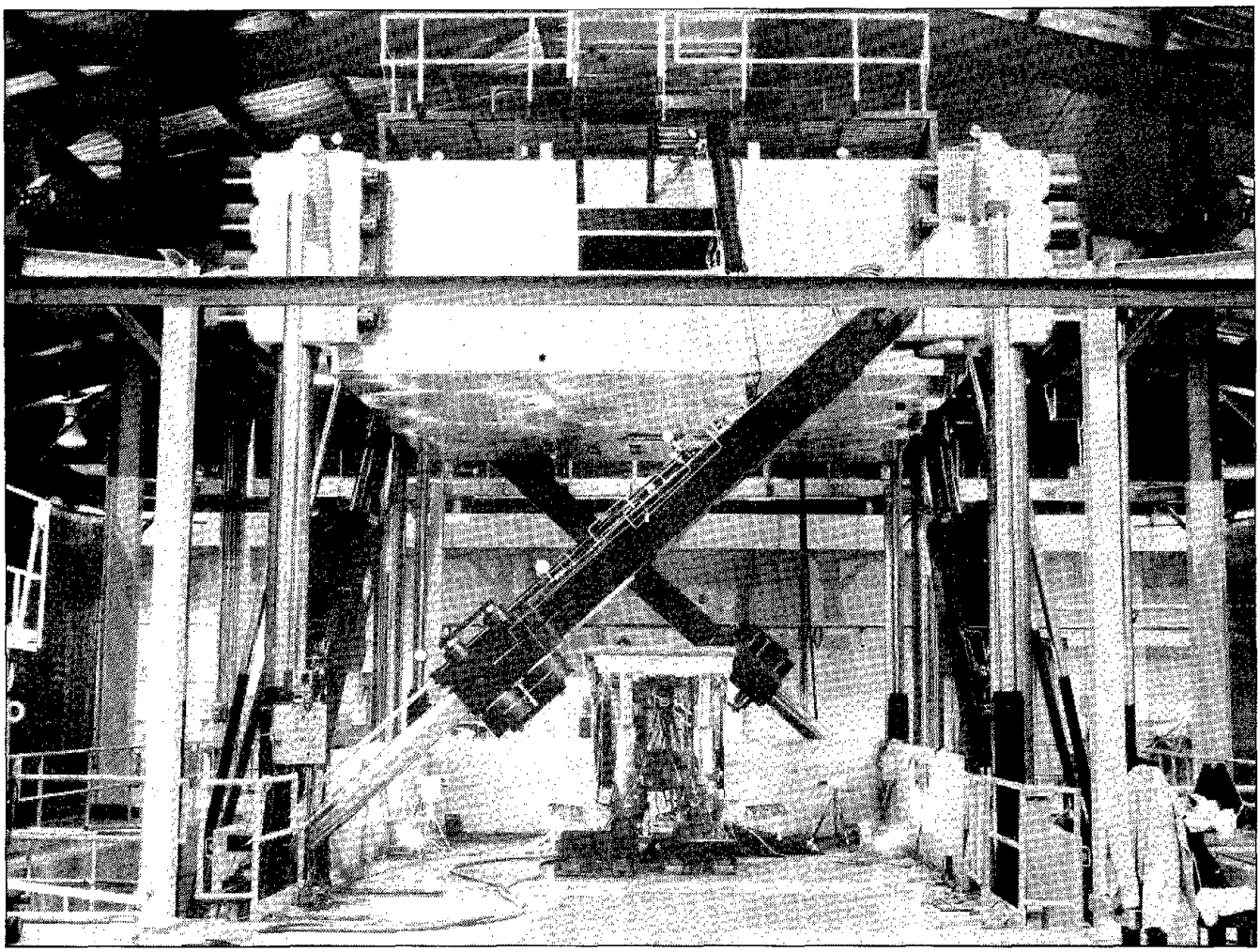

Figure 1.—Mine roof simulator at the USBM's Pittsburgh Research Center, where researchers conducted full-scale tests of crib support systems.

SUPPORT CONSTRUCTION AND LOADING BEHAVIOR

Wood cribs are constructed from layers of two or more parallel timbers. Each successive layer is placed perpendicularly to the previous layer to form an open-box arrangement, as shown in figure 2. Subsequent layers are stacked until the entry height is reached. The configuration is described by the number of timbers per layer. Two-timber-per-layer construction (2×2) is used most often to minimize unit costs. Timber lengths typically range from 76.2 to 152.4 cm (30 to 60 in).

The force-displacement relationship for a wood crib follows a distinct pattern, as shown in figure 3 (*1-2*).[4] Two regions of proportional behavior are followed by a region of nonlinear behavior. Initially, the crib is stiff and the resistive force increases quickly as a linear function of displacement. This phase describes elastic wood behavior and occurs during the initial 5-pct strain. The crib stiffness then decreases as the wood yields during linear plastic deformation. Plastic deformation occurs up to 25- or 30-pct strain. Beyond 25- or 30-pct strain, the crib exhibits nonlinear behavior that depends on the stability of the structure. The force will increase if the crib is stable, whereas the force will decrease if the structure is unstable.

[4]Italic numbers in parentheses refer to items in the list of references preceding the appendixes of this paper.

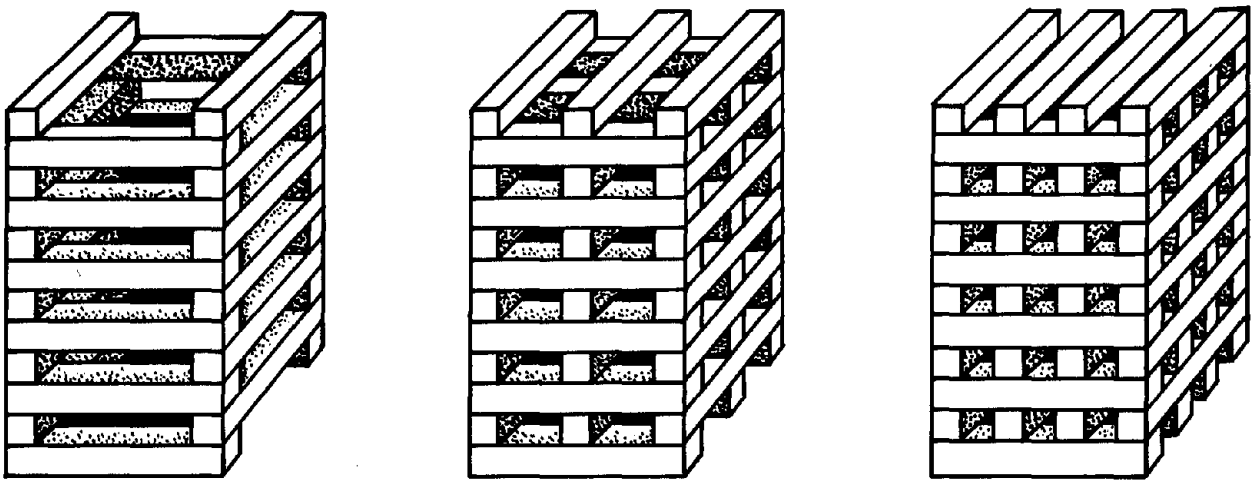

Figure 2.—Wood crib configurations.

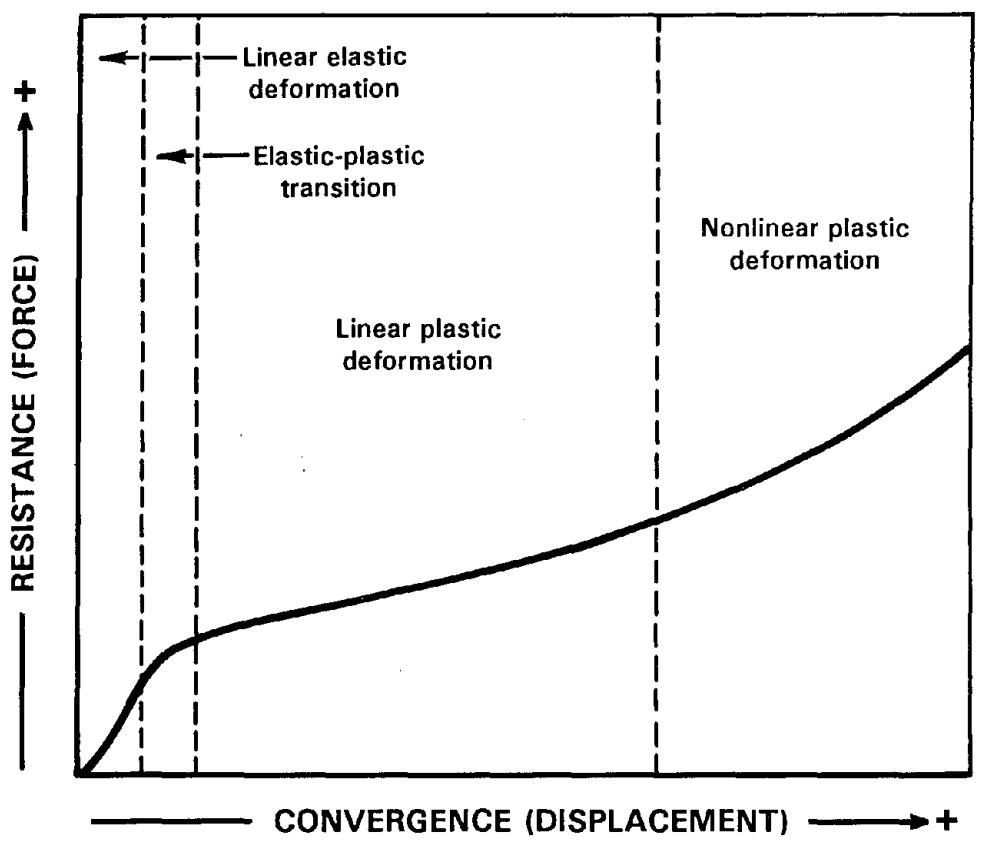

Figure 3.—Generalized force-displacement relationship for wood cribs.

DESIGN CRITERIA AND CONSTRUCTION CONSIDERATIONS

Strength, stiffness, and stability are the criteria that must be met for an acceptable crib design. The strength of a crib is its capacity to support a load. Stiffness is a measure of the resistive force developed to an applied displacement. Stability is a measure of the capability of a structure to maintain equilibrium without sudden or severe loss of load capacity.

Since wood cribs are passive supports and develop resistance through convergence of the mine roof and floor, the stiffness of the crib is the most critical design factor. Wood cribs should have adequate stiffness to provide resistance to roof loads within a displacement that will maintain roof stability. The design parameters that affect crib stiffness are the strength of the wood, the interlayer contact area, the number of timbers per layer, and the height of the structure. Crib stiffness is maximized by increasing timber width, increasing the number of timbers per layer, and using a high-strength wood.

Stability depends most on the buckling of the crib structure. Wood cribs should remain stable without loss of load capacity through a displacement compatible with the convergence of the mine opening. Design factors that influence stability are the aspect ratio (height-to-width ratio) and the moment of inertia of the crib structure. Buckling becomes more dominant at larger strains. Selection of the proper aspect ratio will ensure the stability of most cribs through 20-pct strain.

The strength of a crib is determined primarily by the compressive strength of the wood and the interlayer contact area. Wood cribs should have sufficient capacity to support the weight of rock masses that become detached from stable roof structures. Data on the compressive strength and hardness of many wood species are reported by the U.S. Department of Agriculture's Forest Service (*3*) and the American Society for Testing and Materials (*4*). Compressive strength and hardness values for wood species commonly used for mine timbers are indicated in table 1.

Factors to consider in wood crib design are summarized below.

TIMBER DIMENSIONS

Timber cross sections may be square or rectangular. With rectangular cross sections, maximum stiffness is attained when the timbers are stacked to maximize the interlayer contact area. The placement of just a single layer of timbers with the smaller dimension in contact with the adjacent layers reduces the stiffness of the crib structure.

Timber length is another important consideration. The aspect ratio is the height of the crib divided by the distance between the contact centers at the corners of the crib structure. The aspect ratio decreases as timber length increases. The effect of the timber length on crib performance is shown in figure 4. Generally, a reduction in the aspect ratio by using longer timbers increases the stability of the crib structure by increasing its resistance to buckling. This increase in stability preserves maximum crib stiffness.

Table 1.—Properties of common wood species used for mine timbers

Wood species	Compressive strength[1]		Average hardness[2]	
	N/cm^2	psi	N	lb
Hardwood:				
Yellow birch[3]	498	723	4,537	1,020
Rock elm	698	1,012	5,026	1,130
Black locust	1,300	1,886	7,272	1,635
Black maple[3]	687	997	4,492	1,010
Red maple	473	686	3,670	825
Northern red oak[3]	681	987	5,093	1,145
Pin oak	813	1,179	5,738	1,290
White oak	765	1,109	5,383	1,210
Yellow poplar	324	470	2,180	490
Softwood:				
Douglas fir	533	773	3,816	585
Western larch	597	867	2,980	670
Jack pine	396	575	2,157	485
Lodgepole pine[3]	305	443	1,801	405
Ponderosa pine	412	597	1,735	390
Tamarack	482	699	2,157	485

[1]Unseasoned wood at 0.1016 cm (0.04 in) of displacement.
[2]Average of dry and unseasoned values.
[3]Species used for model development.

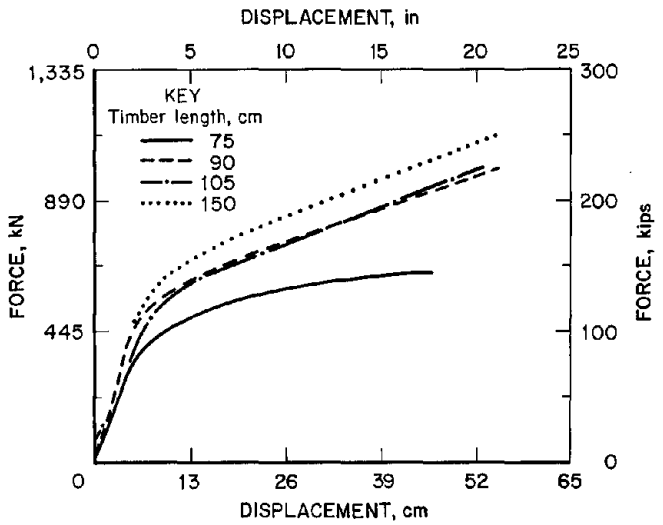

Figure 4.—Effect of timber length as a measure to control crib aspect ratio.

MINING HEIGHT

An increase in crib height reduces both stiffness and stability. These effects can be minimized by controlling the aspect ratio of the crib, as depicted in figure 4. The aspect ratio should be less than 4.3 to provide stable crib performance with linear plastic behavior through 20-pct strain. Cribs constructed with aspect ratios of less than 2.5 use more wood than is necessary to provide effective mine roof support.

TIMBER CONSTRUCTION

Wood cribs perform better when constructed with overhanging timbers. When the crib is constructed without overhanging timbers, the load is applied to the end of the timber. This reduces the strength of the timber and stiffness of the structure. Additionally, crib constructions without overhanging timbers are more susceptible to local shear failures of individual timbers (figure 5). These failures create unequal loading at the weakened layer and contribute to buckling of the crib structure. Overhanging timbers interlock when compressed, thereby reducing the effects of shear failures. Figure 6 shows that cribs constructed with overhanging timbers provide a 10- to 15-pct increase in crib resistance. The performance improvement is accomplished even though the aspect ratio is increased slightly. An overhang length of one-half the width of the timber is recommended.

NUMBER OF TIMBERS PER LAYER

The number of contact points in a crib construction equals the square of the number of timbers per layer.

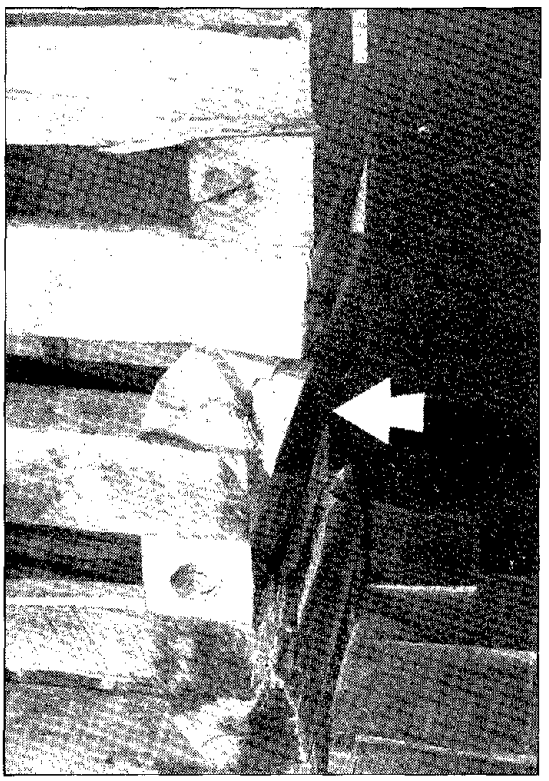

Figure 5.—Arrow indicates shear failure of a timber in a crib construction without overhanging timbers.

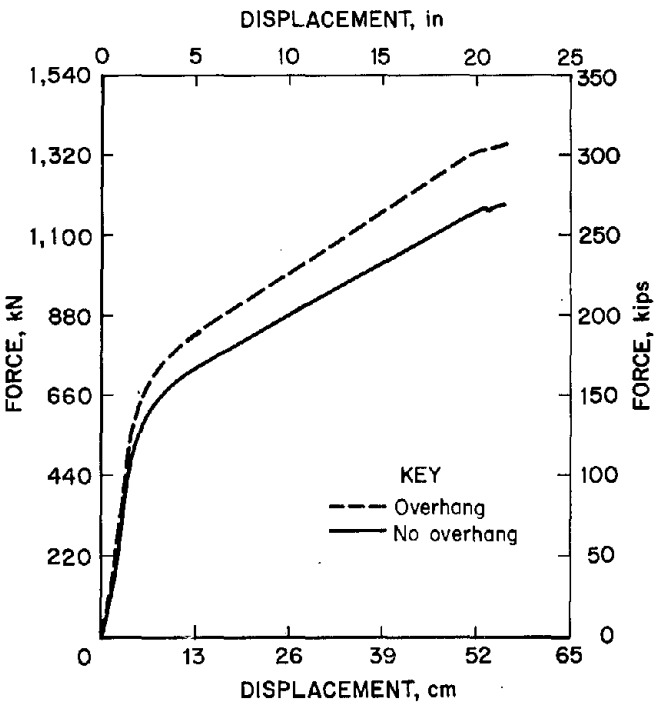

Figure 6.—This graph indicates the improved performance of cribs constructed with overhanging timbers.

Theoretically, the resulting increase in contact area will increase the capacity and the stiffness of the crib proportionately. However, a reduction in timber stiffness from this expectation is observed in multitimbered crib constructions when more than two timbers per layer are used. This reduction stems from the increase in the percentage of loaded area and the reduced distance between the contact areas, which reduces the volume of unstressed wood that provides confinement to loaded sections.

WOOD CRIB PERFORMANCE MODEL

Equation 1 represents the characteristic equation developed to predict the force-displacement behavior of wood cribs.[5] The compressive strength (perpendicular to the grain) and hardness of the wood species are the foundation of the Wood Crib Performance Model. The compressive strength coefficient (A) and the exponential term of the equation represent the capacity of the crib during the linear elastic phase of deformation. The linear elastic crib performance also depends on the height of the structure. The plastic stiffness coefficient (K_p) represents the stiffness of the crib structure during the linear plastic phase of deformation and is based on wood hardness. Adjustments in crib performance also include factors pertaining to (1) percentage of timber contact area, (2) aspect ratio, and (3) timber construction.

$$F_{Crib} = A \times OHFCT \times PCTFCT \times (1 - e^{-HTFCT \times \delta}) + PCTFCT \times ARFCT \times K_p \times \delta, \quad (1)$$

where F_{Crib} = crib resistance, kN,

A = compressive strength coefficient, kN,

K_p = plastic stiffness coefficient, kN/cm,

δ = displacement, cm,

OHFCT = overhanging timber factor,

HTFCT = height factor,

PCTFCT = percentage of contact area factor,

and ARFCT = aspect ratio factor.

The information required to apply the Wood Crib Performance Model is as follows: (1) the wood species, (2) the compressive strength and hardness of the wood, (3) the dimensions of the timbers, (4) the number of layers in the structure, (5) the number of timbers per layer, and (6) whether the crib is to be constructed with or without overhanging timbers.

Some values of compressive strength are reported at the proportional limit, while other values are reported at 0.1016-cm (0.04-in) deflection. Values for green wood reported at the proportional limit must be converted to the equivalent value at 0.1016-cm (0.04-in) deflection to be used in the model by using equation 2.

$$CS_{0.1016} = 1.589 \times CS_{PL} + 29.26, \quad (2)$$

where $CS_{0.1016}$ = compressive strength at 0.1016-cm (0.04-in) deflection,

and CS_{PL} = compressive strength at proportional limit.

Application of the Wood Crib Performance Model is described below. An example of the procedure is provided in appendix A of this paper.

1. Determine the interlayer contact area by multiplying the area per contact by the number of contacts per layer.

$$AREA_{Layer} = AREA_{Contact} \times CONTACTS, \quad (3)$$

where $AREA_{Layer}$ = interlayer contact area, cm^2,

$AREA_{Contact}$ = area per contact, cm^2,

and CONTACTS = number of contacts per layer.

2. Multiply the interlayer contact area by the compressive strength of the wood species to determine the compressive strength coefficient.

$$A = STRENGTH \times AREA_{Layer} \times 10^{-3}, \quad (4)$$

where A = compressive strength coefficient, kN,

STRENGTH = compressive strength of wood, N/cm^2,

and $AREA_{Layer}$ = interlayer contact area, cm^2.

[5]The equations presented throughout this paper are restated in U.S. customary units in appendix B of this paper.

3. Determine the modulus of plasticity for the wood using the wood hardness (table 1) in equation 5a (with overhang) or equation 5b (without overhang).

$$E_p = 0.7178 \times \text{HARDNESS} - 730.9$$

(with overhang) (5a)

$$E_p = 0.6898 \times \text{HARDNESS} - 965.3$$

(without overhang) (5b)

where E_p = modulus of plasticity of mine timber, N/cm^2,

and HARDNESS = wood hardness, N.

4. Determine the plastic stiffness of a single timber by multiplying the area of a single interlayer contact by the modulus of plasticity, then dividing by the timber thickness.

$$K_t = \frac{E_p \times \text{AREA}}{\text{THICKNESS}} \times 10^{-3}, \quad (6)$$

where K_t = plastic stiffness of mine timber, kN/cm,

E_p = modulus of plasticity of mine timber, N/cm^2,

AREA = area per contact, cm^2,

and THICKNESS = timber thickness, cm.

5. Determine the stiffness of the crib structure during plastic deformation by multiplying the number of contacts per layer by the timber stiffness, then dividing by the number of layers.

$$K_p = \frac{K_t \times \text{CONTACTS}}{\text{LAYERS}}, \quad (7)$$

where K_p = plastic deformation crib stiffness, kN/cm,

K_t = timber stiffness, kN/cm,

CONTACTS = number of contacts per layer,

and LAYERS = number of layers in crib.

6. Determine the adjustment factors for height, percentage of timber contact area, aspect ratio, and construction without overhanging timbers. These factors reduce the performance of the crib when certain thresholds are exceeded as described below. A value of 1.0 is used when crib performance is not significantly affected by these parameters.

Height Factor (HTFCT)

$$\text{HTFCT} = 0.6378 - 1.8134 \times 10^{-3} \times \text{Crib Height} \quad (8)$$

where Crib Height = Height of crib, cm.

Percentage of Timber Contact Area Factor (PCTFCT)

$$\text{PCTFCT} = 0.9 \text{ when } \text{AREA}_{pct} \geq 55 \quad (9a)$$

$$\text{PCTFCT} = 1 \text{ when } \text{AREA}_{pct} < 55 \quad (9b)$$

$$\text{AREA}_{pct} = \frac{\frac{\text{AREA}_{Layer}}{\text{CONTACTS}} \times \text{TIMBERS}}{\text{TW} \times \text{TL}} \times 100 \quad (10a)$$

$$\text{AREA}_{pct} = \frac{\text{TW} \times \text{TIMBERS}}{\text{TL}} \times 100, \quad (10b)$$

where AREA_{pct} = timber contact area, pct,

AREA_{Layer} = interlayer contact area, cm^2,

CONTACTS = number of contacts per layer,

TIMBERS = number of timbers per layer,

TW = timber width, cm,

and TL = timber length, cm.

Aspect Ratio Factor (ARFCT)

$$\text{ARFCT} = 2.41 - (0.33 \times \text{AR}) \text{ when } \text{AR} > 4.3 \quad (11a)$$

$$\text{ARFCT} = 1 \text{ when } \text{AR} \leq 4.3 \quad (11b)$$

$$\text{AR} = \frac{\text{HEIGHT}}{\text{TL} - (2 \times \text{OVERHANG}) - \text{TW}}, \quad (12)$$

where AR = aspect ratio,

HEIGHT = crib height, cm,

OVERHANG = overhang distance, cm,

TL = timber length, cm,

and TW = timber width, cm.

Overhanging Timber Construction Factor (OHFCT)

OHFCT = 0.9 *without* overhanging timbers (13a)

OHFCT = 1 *with* overhanging timbers (13b)

7. The crib force-displacement relationship is determined from equation 1.

MODEL LIMITATIONS

This mathematical model to predict wood crib performance is based on data from tests conducted under controlled laboratory conditions. The variables that were controlled during the investigation were the loading rate, wood species, timber length, structure height, number of timbers per layer, and whether the crib was constructed with or without overhanging timbers. When all of these parameters are known, the force-displacement relationship of open-box crib designs can be predicted within a 10-pct error through 20-pct strain. The accuracy of the prediction is limited by variation of these and other parameters.

MIXED WOOD SPECIES

When cribs are constructed from mixed wood species, the model should be applied using the lowest compressive strength and hardness values of the wood species used. This approach will provide a conservative estimate of crib performance.

STABILITY FACTORS

The stability of an open-box wood crib depends on several factors, of which the aspect ratio is the most significant. The model can successfully predict the performance of cribs with aspect ratios between 2 and 6; however, it is recommended that aspect ratios be controlled to a range of 2.5 to 4.3 in crib design. The aspect ratio can be controlled by selecting a timber length that is compatible with the crib height.

Construction of a crib without overhanging timbers also affects stability. Crib construction with contact established at the ends of the timbers decreases the aspect ratio, and will decrease the effective strength and stiffness of the timbers. Furthermore, this type of construction is susceptible to shear failure of the timbers, resulting in instability. The model does not predict the effect of shear failure instabilities.

LOAD APPLICATION

The effects of time-dependent properties of wood are not predicted by the model. The conditions of load application can significantly affect the performance of wood cribs. Different rates of load application, static loads, and static displacements all result in different crib responses.

Generally, crib resistance decreases as the rate of loading decreases. The model was developed from data where a constant rate of displacement of 1.27 cm (0.5 in)/min was applied to the crib structure. Tests on full-scale cribs at 0.127 cm (0.05 in)/min showed little difference from tests conducted at 1.27 cm (0.5 in)/min. However, underground convergence rates in coal mines of 0.0254 cm (0.01 in)/h to 0.0004318 cm (0.00017 in)/min have been associated with unstable mine roof conditions. Load application rates on this order may diminish the resistance provided by wood crib supports.

When a static load is applied to a wood crib, the crib will continue to deform (creep) to approximately twice the initial displacement. The rate of deformation is a function of the load on the structure. When the load is below the elastic limit of the wood, the rate of creep is very slow. When the load exceeds the elastic limit of the wood, the rate of creep increases.

When a displacement is applied to a wood crib, the initial resistive force can be predicted by the model. However, relaxation of the wood causes the resistance to decrease with time. The resistive force can be reduced by 30 pct after 1 h and by 50 pct after 48 h.

NONLINEAR BEHAVIOR

The model does not predict nonlinear plastic behavior. For typical crib configurations, plastic deformation will become nonlinear at strains between 20 and 30 pct, depending on the moment of inertia and the aspect ratio of the structure. Generally, nonlinear plastic behavior will begin sooner if the moment of inertia is increased or if the aspect ratio is reduced. The model will maintain the 10-pct error limit through 20-pct strain if the aspect ratio is between 2 and 6.

SUPPORT SYSTEM DESIGN AND EMPLOYMENT

The goal in support system design is to select a crib configuration and placement strategy. The support system must resist strata loading within a displacement that will ensure the integrity of the immediate roof in the mine opening. Criteria for support design and employment are summarized below.

1. Crib stiffness and capacity.—Cribs should have sufficient stiffness and capacity to preserve the integrity of the mine roof and floor. This requires that the cribs develop sufficient capacity within a displacement that will offset strata loading and prevent deflection of the immediate roof beam to failure (figure 7). Critical beam loading and deflection can be estimated from equations 14 and 15, respectively. Strata loading is measured per centimeter of entry and is computed as the weight of material within the pressure arch surrounding the opening (figure 7). These estimates should be tempered by knowledge of caving height (roof fall cavities) and roof sag to more accurately identify force and displacement criteria for crib design. The maximum required capacity occurs when the immediate mine roof has no strength and the full weight of strata that are detached from stable roof structures must be supported by the crib.

$$F_{Critical} = \frac{4 \times t^2 \times \sigma}{3 \times L} \times 10^{-3}, \qquad (14)$$

where $F_{Critical}$ = critical loading of the roof beam, kN/cm,

t = thickness of immediate roof beam, cm,

σ = tensile strength of roof rock, N/cm^2,

and L = length of roof beam, cm.

$$\delta_{Critical} = \frac{5 \times \sigma \times L^2}{24 \times E \times t}, \qquad (15)$$

where $\delta_{Critical}$ = critical displacement of roof beam, cm,

σ = tensile strength of the roof rock, N/cm^2,

L = length of roof beam, cm,

E = modulus of elasticity of roof rock, N/cm^2,

and t = thickness of immediate roof beam, cm.

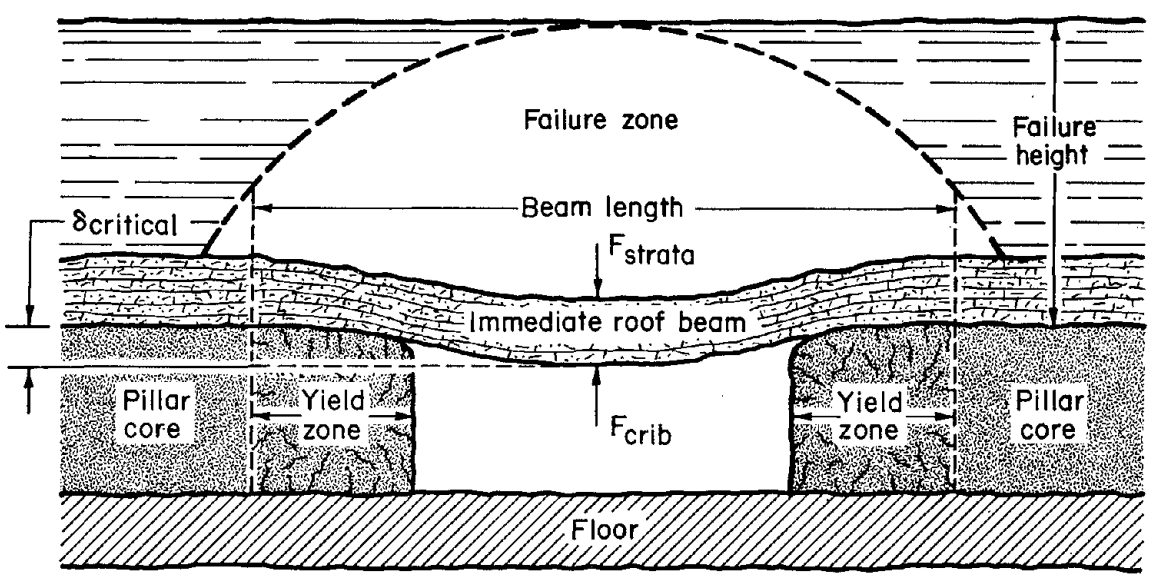

Figure 7.—Crib-strata interaction involving deflection of the immediate roof beam. $\delta_{critical}$ = critical displacement of roof beam, F_{strata} = imposed strata load, and F_{crib} = crib resistance.

2. *Stability requirements.*—Cribs should remain stable and provide support through a displacement that includes roof deflection, coal pillar deformation, and floor heave. Crib stability is ensured by selecting the proper timber length for the mining height to maintain an aspect ratio of less than 4.3.

3. *Roof and floor contact pressures.*—The cribs should have adequate contact area to provide roof and floor contact pressures that are compatible with the strength of the immediate roof and floor. Contact pressure can be estimated by dividing the crib load by twice the interlayer contact area. Full timber length should not be used as an estimate of contact area, since the load distribution is not uniform along the timber.

4. *Crib spacing and employment cost.*—The cost of the support system will depend largely on how far apart the cribs can be spaced. Crib spacing is measured as the distance between cribs. It is determined by the roof load per centimeter of entry and the roof strength as a function of the critical displacement of the immediate roof in relation to the stiffness and capacity of the crib design. Each crib must support a section of roof within a displacement that will control the integrity of the roof. These requirements are expressed in equation 16. This spacing is limited by the capability of the roof to span without support.

$$\text{SPACE } (\delta_c) = \frac{F_{\text{Crib}}\ (\delta_{\text{Critical}})}{F_{\text{Strata}} - F_{\text{Critical}}} - \text{TL}, \quad (16)$$

where SPACE (δ_c) = crib spacing, cm,

$F_{\text{Crib}}\ (\delta_{\text{Critical}})$ = capacity of a single crib at the critical roof deflection $(\delta_{\text{Critical}})$, kN,

F_{Strata} = imposed strata load, kN/cm,

F_{Critical} = critical beam load, kN/cm,

and TL = timber length, cm.

The employment cost is the material and labor costs required for the support system installation measured in dollars per centimeter of entry. It is calculated by adding the material and labor costs, then dividing by the crib spacing plus the timber length (see equation 17).

$$\text{EMPLOY COST} = \frac{\text{CONS COST}}{\text{SPACING} + \text{TL}}, \quad (17)$$

where EMPLOY COST = employment cost, $ per cm of entry,

CONS COST = cost to construct a crib, $,

SPACING = crib spacing, cm,

and TL = timber length, cm.

The equivalent cost spacing is the spacing that provides the same employment cost for all crib designs. It is determined from equation 18. Placement of cribs at distances greater than the equivalent cost spacing will provide savings in the cost of employment. The equivalent cost spacing is useful in comparing the advantages of multitimbered configurations to 2×2 crib designs.

$$\text{EQ (COST) SPACE} = \frac{\text{CONS COST} - (\text{TL} \times \text{EMPLOY COST})}{\text{EMPLOY COST}}, \quad (18)$$

where EQ (COST) SPACE = equivalent cost spacing, cm,

CONS COST = construction cost for single crib, $,

TL = timber length, cm,

and EMPLOY COST = employment cost per centimeter of entry, $/cm.

The equivalent force spacing, where the support system resistance per centimeter of entry is equal, can be computed using equation 19. This equation can be used to compare alternative crib designs with a current support system.

$$\text{EQ (FORCE) SPACE} = \frac{F_{\text{Crib}} - (\text{TL} \times F_{\text{Supsys}})}{F_{\text{Supsys}}}, \quad (19)$$

where EQ (FORCE) SPACE = equivalent force spacing, cm,

F_{Crib} = individual crib resistance at critical displacement, kN,

F_{Supsys} = crib resistance per cm of mine entry, kN/cm,

and TL = timber length, cm.

CONCLUSIONS AND RECOMMENDATIONS

The design and utilization of wood cribs can be optimized if the load-carrying characteristics of the crib and the load conditions imposed by the mine environment are understood. The importance of the stiffness of the support structure should be carefully considered in designing wood cribs. Often, too much attention is given to the capacity of the support without recognizing the stiffness. It is the development of the support capacity within a specified displacement that is crucial to ground control. Therefore, efforts to maximize crib stiffness should be a design priority.

Proper construction methods are necessary to ensure optimum performance from crib support systems. Recommendations to maximize crib efficiency are summarized below.

1. Wood cribs should be constructed with overhanging timbers. The minimum recommended overhang distance is one-half the width of the timber. Overhang construction enhances crib stability and provides a 10- to 15-pct increase in crib capacity.
2. Wood cribs should be constructed from wood of the same species or those with similar compressive strength and hardness. This helps prevent differential compression of timbers in a single layer, which can contribute to buckling-induced failure.
3. The aspect ratio (height-to-width ratio) for wood crib construction should be between 2.5 and 4.3 to ensure stability through 20-pct strain and for efficient use of the wood timbers. Timber lengths should increase as the mining height increases to maintain an aspect ratio in this range.
4. Wood cribs should be constructed to maximize the interlayer contact area. Therefore, the wide side of the timber should be placed horizontally in the crib construction. This construction will provide maximum stability and support capacity.
5. The stiffness of wood cribs can be increased by increasing the number of timbers per layer or by increasing the width of the timber. Increasing the width of the timber should be given first priority, since additional timbers per layer will increase the labor costs for construction. The increased stiffness will provide greater resistance at less displacement, which will improve ground control.

Application of the Wood Crib Performance Model has led to recommendations for wood crib utilization. These recommendations are summarized below.

1. Most wood crib systems in longwall gate roads employ one or two rows of 2×2 wood crib constructions placed 1.52 m (5 ft) apart. The example discussed in this report demonstrates that 3×3 and 4×4 crib configurations are more cost-effective than 2×2 configurations, provided they can be spaced at distances commensurate with their higher capacity advantage.
2. The equivalent cost spacing of a 3×3 and a 4×4 configuration compared with a 2×2 configuration on a 1.52-m (5-ft) spacing in a 2-m (80-in) thick coal seam is 2.7 m (8.7 ft) and 3.8 m (12.5 ft), respectively. Installation of the 3×3 or 4×4 configurations at greater distances than the equivalent cost spacing will provide a cost savings.
3. A single 3×3 wood crib will provide more capacity at less cost than a double row of 2×2 wood cribs. Therefore, a single row of 3×3 cribs should be used if the mine roof is sufficiently competent to remain stable. When the supported area needs to be increased owing to poor roof quality, consideration should be given to a rectangular 3×3 design where the long axis is employed across the entry. The rectangular design will increase roof coverage while preserving the capacity enhancements of the 3×3 configuration.
4. The stiffness of wood cribs increases as the height decreases. Therefore, if the mining height changes significantly, the crib spacing or design should be adjusted accordingly.

Wood cribs are likely to continue to be used extensively to improve ground control in underground coal mining. The information presented in this paper will enhance the efficient utilization of these support systems and will lead to a safer underground environment for mineworkers.

REFERENCES

1. Barczak, T. M., and C. Tasillo. Evaluation of Multitimbered Wood Crib Supports. USBM RI 9341, 1991, 11 pp.

2. Barczak, T. M., D. E. Schwemmer, and C. L. Tasillo. Practical Considerations in Longwall Face and Gate Road Support Selection and Utilization. USBM IC 9217, 1989, 22 pp.

3. U.S. Department of Agriculture. Wood Handbook: Wood as an Engineering Material. Section on Mechanical Properties of Wood, Forest Products Laboratory. Agricultural Handbook 72, 1987, p. 4-3.

4. Standard Methods of Testing Small Clear Specimens of Timber. ASTM Designation 143, 1983, p. 55.

APPENDIX A.—WOOD CRIB DESIGN AND EMPLOYMENT EXAMPLES

EXAMPLE 1: WOOD CRIB PERFORMANCE MODEL

The example below calculates the load-displacement relationship for a 203.2-cm (80-in) high, 3×3 crib constructed from northern red oak timbers with overhanging ends. The timber size is 13×15×76 cm (5×6×30 in). The compressive strength (perpendicular to the grain) and hardness for the northern red oak are 680.5 N/cm^2 (987 psi) and 5,093 N (1,145 lb), respectively (see table 1).

1. The interlayer contact area is determined from equation 3.

$$AREA_{Layer} = (15.24 \times 15.24)\ cm^2$$

$$\times (3\times3)\ CONTACTS = 2{,}090\ cm^2 \quad (A\text{-}1)$$

2. The compressive strength coefficient is computed using equation 4.

$$A = 680.5\ N/cm^2 \times 2{,}090\ cm^2 \times 10^{-3} = 1{,}422\ kN \quad (A\text{-}2)$$

3. The crib is constructed with overhanging ends, so equation 5a is used to convert the wood hardness value to the plastic modulus for the mine timber.

$$E_p = 0.7178 \times 5{,}093\ N - 730.87 = 2{,}925\ N/cm^2 \quad (A\text{-}3)$$

4. The plastic timber stiffness for one contact area is computed from equation 6.

$$K_t = \frac{2{,}925\ N/cm^2 \times (15.24 \times 15.24)\ cm^2}{12.70\ cm}$$

$$\times 10^{-3} = 53.5\ kN/cm \quad (A\text{-}4)$$

5. The plastic stiffness coefficient (K_p) is computed using equation 7.

$$K_p = \frac{53.5\ kN/cm \times 9\ CONTACTS}{16\ LAYERS}$$

$$= 30.1\ kN/cm \quad (A\text{-}5)$$

6. Determine the adjustment factors for height, percentage of timber contact area, aspect ratio, and construction without overhanging timbers.

Height Factor (HTFCT)

The height factor is computed as 0.269 using equation 8.

$$HTFCT = 0.6378 - 1.8134 \times 10^{-3} \times 203.2\ cm$$

$$= 0.269 \quad (A\text{-}6)$$

Percentage of Timber Contact Area Factor (PCTFCT)

The percentage of timber contact area is computed from equation 10b as 60 pct for the 3×3 configuration using 13×15×76-cm (5×6×30-in) timbers. Since this is greater than 55 pct, PCTFCT equals 0.9.

$$AREA_{pct} = \frac{15.24 \times 3}{76.2} \times 100 = 60\ pct \quad (A\text{-}7)$$

$$PCTFCT = 0.9 \quad (A\text{-}8)$$

Aspect Ratio Factor (ARFCT)

The aspect ratio for the 203-cm (80-in) high crib constructed from 76-cm (30-in) long timbers with 7.62 cm (3 in) of overhang on each end is computed as 4.44, which makes ARFCT equal to 0.94.

$$AR = \frac{203.2}{76.2 - (2 \times 7.62) - 15.24} = 4.44 \quad (A\text{-}9)$$

$$ARFCT = 2.41 - (0.33 \times 4.44) = 0.94 \quad (A\text{-}10)$$

Overhanging Timber Construction Factor (OHFCT)

Since the crib is constructed with overhanging timbers, OHFCT equals 1. Therefore, the following equation represents the force-displacement relationship for this crib. Figure A-1 compares the Wood Crib Performance Model prediction to a full-scale test of a 3×3 crib in the mine roof simulator at the USBM's Pittsburgh Research Center.

$$F_{Crib}\ (3\times3) = 1{,}422 \times 1 \times 0.9 \times (1 - e^{-0.269 \times \delta})$$

$$+ 0.9 \times 0.94 \times 30.1 \times \delta\ kN \quad (A\text{-}11)$$

$$F_{Crib}\ (3\times3) = 1{,}278.9 \times (1 - e^{-0.269 \times \delta})$$

$$+ 25.5 \times \delta\ kN \quad (A\text{-}12)$$

EXAMPLE 2: EMPLOYMENT ANALYSIS

This example compares 3×3 and 4×4 crib designs to a mine's 2×2 crib system and determines the optimum placement of these alternative systems. The 2×2 design is constructed from 12.7×15.24×76.2-cm (5×6×30-in) northern red oak timbers and is employed in single-row arrangement at 152.4-cm (5-ft) spacing in a 203.2-cm (80-in) coal seam. Mine experience has shown that roof sag (deflection) must be controlled to less than 6.1 cm (2.4 in) to maintain roof stability.

The force-displacement relationship for the 2×2 crib construction is computed from the Wood Crib Performance Model. The resistive force provided by the crib at 6.1 cm (2.4 in) of displacement is 587.1 kN (132 kips), which translates to 2.57 kN per cm (17.6 kips per ft) of entry for a 152.4-cm (5-ft) crib spacing.

$$F_{Crib}\,(2\times2) = 632.1 \times (1 - e^{-0.269\times\delta}) + 12.6\times\delta \quad \text{(A-13)}$$

Choosing the timber length is the first priority for the 3×3 and 4×4 designs. The optimum timber length is that which is least expensive while maintaining an aspect ratio between 2.5 and 4.3 for the crib structure. On this basis, 76.2-cm (30-in) timber length is selected.

The model equations for the 3×3 and 4×4 configurations are shown below and compared with the 2×2 design in figure A-2. Using these equations to compute the crib resistance at 6.1 cm (2.4 in) of displacement, it is found from equation 19 that the 3×3 crib design can be spaced at 384 cm (12.6 ft) and provide the same resistance to roof loading as the current 2×2 design. Likewise, the 4×4 design can be spaced at 744 cm (24.4 ft) and provide equal resistance.

$$F_{Crib}\,(3\times3) = 1{,}278.9 \times (1 - e^{-0.269\times\delta}) + 25.5\times\delta \quad \text{(A-14)}$$

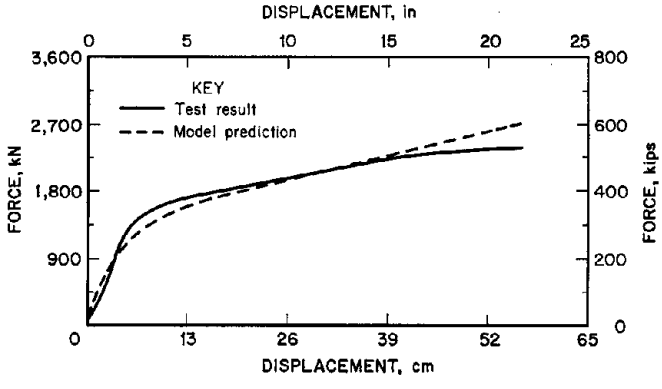

Figure A-1.—Comparison of Wood Crib Performance Model prediction with full-scale testing of 3×3 crib in the USBM's mine roof simulator.

$$F_{Crib}\,(4\times4) = 2{,}276 \times (1 - e^{-0.269\times\delta}) + 45.5\times\delta \quad \text{(A-15)}$$

$$\text{EQ (FORCE) SPACE } (3\times3) = \frac{1{,}183.2 - (76.2 \times 2.57)}{2.57}$$

$$= 384 \text{ cm} \quad \text{(A-16)}$$

$$\text{EQ (FORCE) SPACE } (4\times4) = \frac{2{,}108.4 - (76.2 \times 2.57)}{2.57}$$

$$= 744 \text{ cm} \quad \text{(A-17)}$$

Since 305 cm (10 ft) is considered the maximum acceptable unsupported roof span, the 3×3 design at 305-cm (10-ft) spacing is chosen as the optimum crib design and employment. This design will provide a cost savings of 10 pct with over 20 pct more support force.

$$\text{EMPLOY COST } (2\times2) = \frac{44}{152.4 + 76.2}$$

$$= \frac{\$0.1926}{\text{cm}} \quad \text{(A-18)}$$

$$\text{EMPLOY COST } (3\times3) = \frac{66}{304.8 + 76.2}$$

$$= \frac{\$0.1732}{\text{cm}} \quad \text{(A-19)}$$

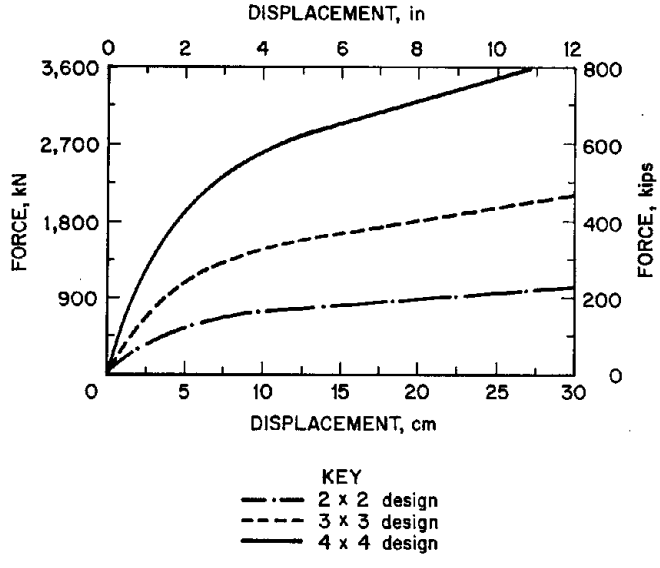

Figure A-2.—Comparison of 2×2, 3×3, and 4×4 wood crib performances.

APPENDIX B.—EQUATIONS IN U.S. CUSTOMARY UNITS

Restated below are the equivalent equations from the main body of this paper in U.S. customary units.

$$F_{Crib} = A \times OHFCT \times PCTFCT \times (1 - e^{-HTFCT \times \delta}) + PCTFCT \times ARFCT \times K_p \times \delta \quad \text{(B-1)}$$

$$CS_{0.04} = 1.589 \times CS_{PL} + 42.44 \quad \text{(B-2)}$$

$$AREA_{Layer} = AREA_{Contact} \times CONTACTS \quad \text{(B-3)}$$

$$A = STRENGTH \times AREA_{Layer} \times 10^{-3} \quad \text{(B-4)}$$

$$E_p = 4.63 \times HARDNESS - 1{,}060 \quad \text{(with overhang)} \quad \text{(B-5a)}$$

$$E_p = 4.45 \times HARDNESS - 1{,}400 \quad \text{(without overhang)} \quad \text{(B-5b)}$$

$$K_t = \frac{E_p \times AREA}{THICKNESS} \times 10^{-3} \quad \text{(B-6)}$$

$$K_p = \frac{K_t \times CONTACTS}{LAYERS} \quad \text{(B-7)}$$

$$HTFCT = 1.62 - 0.0117 \times \text{Crib Height} \quad \text{(B-8)}$$

$$PCTFCT = 0.9 \text{ when } AREA_{pct} \geq 55 \text{ pct} \quad \text{(B-9a)}$$

$$PCTFCT = 1 \text{ when } AREA_{pct} < 55 \text{ pct} \quad \text{(B-9b)}$$

$$AREA_{pct} = \frac{\frac{AREA_{Layer}}{CONTACTS} \times TIMBERS}{TW \times TL \times 12} \times 100 \quad \text{(B-10a)}$$

$$AREA_{pct} = \frac{TW \times TIMBERS}{TL \times 12} \times 100 \quad \text{(B-10b)}$$

$$ARFCT = 2.41 - (0.33 \times AR) \text{ when } AR > 4.3 \quad \text{(B-11a)}$$

$$ARFCT = 1 \text{ when } AR \leq 4.3 \quad \text{(B-11b)}$$

$$AR = \frac{HEIGHT}{(TL \times 12) - (2 \times OVERHANG) - TW} \quad \text{(B-12)}$$

$$OHFCT = 0.9 \textit{ without} \text{ overhanging timbers} \quad \text{(B-13a)}$$

$$OHFCT = 1 \textit{ with} \text{ overhanging timbers} \quad \text{(B-13b)}$$

$$F_{Critical} = \frac{4 \times t^2 \times \sigma}{3 \times L} \times 12 \times 10^{-3} \quad \text{(B-14)}$$

$$\delta_{Critical} = \frac{5 \times \sigma \times L^2}{24 \times E \times t} \quad \text{(B-15)}$$

$$SPACE\ (\delta_c) = \frac{F_{Crib}\ (\delta_{Critical})}{F_{Strata} - F_{Critical}} - TL \quad \text{(B-16)}$$

$$EMPLOY\ COST = \frac{CONS\ COST}{SPACING + TL} \quad \text{(B-17)}$$

$$EQ\ (COST)\ SPACE = \frac{CONS\ COST - (TL \times EMPLOY\ COST)}{EMPLOY\ COST} \quad \text{(B-18)}$$

$$EQ\ (FORCE)\ SPACE = \frac{F_{Crib} - (TL \times F_{Supsys})}{F_{Supsys}} \quad \text{(B-19)}$$

Use ft for: SPACE (δ_c), SPACING, EQ (COST) SPACE, and EQ (FORCE) SPACE.

Use inches for: δ, THICKNESS, Crib Height, TW, TL, HEIGHT, OVERHANG, t, L, and $\delta_{Critical}$.

Use in^2 for: $AREA_{Layer}$, $AREA_{Contact}$, and AREA.

Use kips for: F_{Crib} and $F_{Crib}\ (\delta_{Critical})$.

Use kips/ft for: F_{Strata}, $F_{Critical}$, and F_{Supsys}.

Use kips/in for: K_p and K_t.

Use lb for: HARDNESS.

Use psi for: CS_{PL}, STRENGTH, E_p, σ, and E.

Use $/ft for: EMPLOY COST.

EFFECTIVE MONITORING TECHNIQUES FOR ASSESSING STRUCTURAL STABILITY

By Hamid Maleki[1]

ABSTRACT

Roof, pillar, and floor instability have long influenced mine safety, ventilation, productivity, and resource recovery. Based on decades of measurements in ten U.S. mines, suitable measurement techniques and preliminary stability evaluation criteria are proposed for prudent structural stability assessments. Three methods that use the changes in rock deformation, fracturing, and stress conditions are shown to be useful and effective for routine stability evaluations and show potential for improving safety in underground excavations.

INTRODUCTION

During the life of underground mines, more than 100 km of entries are excavated to access and extract the ore. Since both geologic and stress conditions may vary across a mine (Maleki and others, 1994), there is a good possibility that every mine experiences stability problems sometime during its life. From a practical point of view, stability problems are those influencing the capability of an entry to provide safe access, efficient ventilation, and sufficient space for material transport. Thus, mine roof falls, significant rib dilation (as a result of pillar failure), and significant floor heave are considered to be stability problems in the context of this paper.

Historically, the mining industry has depended on quick observations of strata deformation and failure (Maleki, 1988a), bolt failure, and lithologic changes (Hilbert, 1978) to evaluate stability. These preliminary evaluations sometimes have been used to make significant changes in mine layout and support systems, which may affect the economics of a mine. Because of the subjectivity involved in these visual observations, the mining process is slowed, creating inefficiencies and safety concerns during the time a decision is being reached.

The U.S. Bureau of Mines (USBM) has made significant contributions to the development of innovative measurement techniques for prudent stability assessment. Unlike observational techniques, these measurements are quantitative and enhance both an understanding of the failure process and the decisionmaking process.

Following a review of common coal mine stability problems and monitoring techniques, case studies are presented to demonstrate the application of these techniques to detect imminent stability problems. New developments in the application of geophysical techniques are emphasized, for such techniques show great potential for quantifying abnormal fracturing and stresses that lead to ground failure.

[1]Mining engineer, Spokane Research Center, U.S. Bureau of Mines, Spokane, WA.

REVIEW OF STABILITY PROBLEMS

Stability problems in sedimentary mines are influenced by variations in lithology, structure, hydrology, and stress conditions (table 1). Roof and floor instabilities are influenced by both strength and stress regime. Unconsolidated carbonaceous shales and underclays are known to detach from other strata, contributing to mine roof falls and floor heave. Similarly, discontinuities adversely influence rock mass strength.

Table 1.—Factors affecting stability in coal-measure rocks

Factor	*Example*
Lithologic:	
Unconsolidated, uncohesive rock.	Carbonaceous shale, underclay.
Laminated, low-friction planes	Thin-bedded strata.
Nonuniform lithology	Channels, riders.
Structural:	
Unfavorable discontinuities ..	Joints, faults, dikes, cleats, slickensided joints.
Hydrologic and gaseous:	
Hydrostatic and/or gas pressures.	Channels, bumps.
Chemical decomposition	Underclays.
Stress-related:	
Roof failure	Cutters, kinks, delamination.
Pillar failure	Squeezes, bumps.
Floor failure	Buckling, squeezing.

Both groundwater and gas trapped within rock strata assert significant pressure within mine structures. The margins of sandstone channels, for example, can be influenced by both saturated groundwater head and depositional effects that can reduce rock mass strength because of differential compaction.

Excessive far-field horizontal stresses can enhance deformation along laminated rock interfaces and may form cutters and kinks in brittle material (Maleki and others, 1994) depending on strength and stiffness of mine strata. High stresses can also contribute to buckling of floor strata (Aggson, 1978) and squeeze of underclays.

Changes in vertical stresses as a result of topographic changes and/or secondary mining may cause coal pillar stability problems. Pillar failure mechanisms in U.S. coal mines are described by Maleki (1992a) and consist of gradual rib dilation, pillar failure in a panel (squeeze), and violent failure in the form of coal bumps. Coal bumps are influenced by the stiffness of the mine loading system (Wawersik and Fairhurst, 1970).

From this review, it is evident that stability problems are complex and influenced by strength, stiffness, and stress. There are, however, changes in rock conditions that occur during the failure process that can be used to evaluate stability. Because failure is physically associated with deformation, dilation, microcracking, fracturing, and destressing, measurement techniques that monitor changes in these properties can be effective tools for assessing structural stability.

REVIEW OF MONITORING TECHNIQUES

To monitor stability, changes in two physical properties may be measured: (1) deformation and fracturing and (2) stress conditions. Stability assessment is generally accomplished by comparing measurements between initial (or expected) conditions and predetermined critical levels for the material under investigation. For example, if changes in seismic velocities reach a critical level of 17%, the mine roof is expected to behave inelastically and would benefit from supplementary support (Maleki, 1993b).

Measurements of deformation and fracturing have been used extensively to assess mine roof stability (Maleki, 1988a, 1993a) and yield pillar performance. These measurements are inexpensive, simple, and reliable. Deformation measurements are obtained with extensometers and roof-to-floor convergence meters and are supplemented by borescope observations of fracture development within boreholes. Development of failure zones in coal pillars is similarly associated with rib fracturing and dilation, which is measured with dilation points and tape extensometers (Maleki, 1988b).

Fracture initiation has been monitored using microseismic emissions (Repsher and Steblay, 1985), and fracture density has been studied recently using a controlled source and tomographic techniques (Maleki and others,

1993). The latter approach has allowed changes in roof stability to be compared with roof deformation and fracturing, which can significantly influence dynamic properties such as velocity, attenuation, Young's modulus, and Poisson's ratio. These measurements are available from recent studies at three sites and have great potential for widespread use in assessing stability problems and evaluating sites in detail.

Controlled source techniques have also been used to identify fracture zones and zones of high stress in pillars (Jung and others, 1991; Friedel and others, 1993; Westman, 1993). The latter is based on experimental evidence showing an increase in seismic velocity with stress increase.

Figure 1 illustrates typical geometries used in a controlled-source tomographic survey to evaluate mine roof and floor stability. Pillar surveys are similar except that there is usually access to all sides of a pillar, while contact is limited to three sides (two source boreholes and the roof) for roof or floor surveys. The impact source is generally some sort of hammer that transmits energy to the rock within source boreholes or directly to the pillar. Accelerometers are attached to the mine roof, floor, or pillar to receive the signal generated by the impact. These techniques quantify wave velocity within a volume of rock (see "area of interest" in figure 1) in contrast to obtaining point measurements when using sagmeters.

The principle of crosshole seismic tomography is shown in figure 2, where the structure under investigation is surveyed by a high density of waves traveling between sources and receivers. This is analogous to the use of a computerized axial tomography (CAT) scan of the human body, but sound waves are generated instead of x-rays. Nonlinear (curved) rays are used to accommodate ray bending, which occurs when changes in geologic conditions cause significant velocity differences.

Inverse iterative calculation methods are used to calculate a two-dimensional picture of velocity distribution in the mine structure bounded by the receivers and amplifiers. Since seismic velocity is influenced by fracturing and stresses, these seismic profiles can provide snapshots of variations in fractures, stress patterns, and stability of the structure under investigation (Maleki and others, 1993).

The components of a crosshole seismic survey developed for routine underground applications are shown in figure 3. A PC-based, 13-channel system with programmable gains capable of acquiring up to 150,000 samples per second was used for data acquisition. This system utilized an analog digital board, amplifiers, filters, and a trigger unit (Maleki and others, 1992).

Stress measurements can also provide an assessment of structural stability, particularly when these measurements are compared with expected stress profiles based on numerical models. Overcoring techniques and borehole deformation gauges developed by the USBM are among the most direct and reliable methods of determining stress (Bickel, 1993; Maleki and others, 1994) and are routinely used for mine layout design.

The above methods are most suitable for monitoring changes in rock mass deformation and stress conditions. There are other useful measurements that indicate strata movement, but do not directly lend themselves to evaluations of structural stability. Measurements of bolt tension (Maleki, 1992b), for example, provide indirect indications of roof movements, but data analysis is complex because of the interaction of rock and support elements.

APPLICATION RESULTS

Typical results from long-term measurements in U.S. sedimentary mines are presented to examine the application of these measurements and existing criteria for structural stability evaluations. Three examples are presented using deformation, seismic velocity, and overcoring stress measurements for assessment of mine roof stability problems.

ROOF DEFORMATION HISTORY

Measurements of amount and rate of roof deformation have been extensively used in both longwall and room-and-pillar retreat mining systems (Maleki, 1993a, 1988a). Because there is a large database involving a variety of geologic and stress conditions, there are preliminary criteria for the routine use of this technique in underground coal mines.

Measurements in seven U.S. mines have indicated that most coal-measure rocks deform 2 to 7 cm prior to roof collapse, then accelerate to a critical velocity called the critical rate. Between the initiation of the critical rate and the actual mine roof fall, a period of time elapses that is called time-to-caving.

The rate of roof movement is a good indicator of roof stability, for it indicates a change in the stability of the whole mining system. A change from a steady rate of

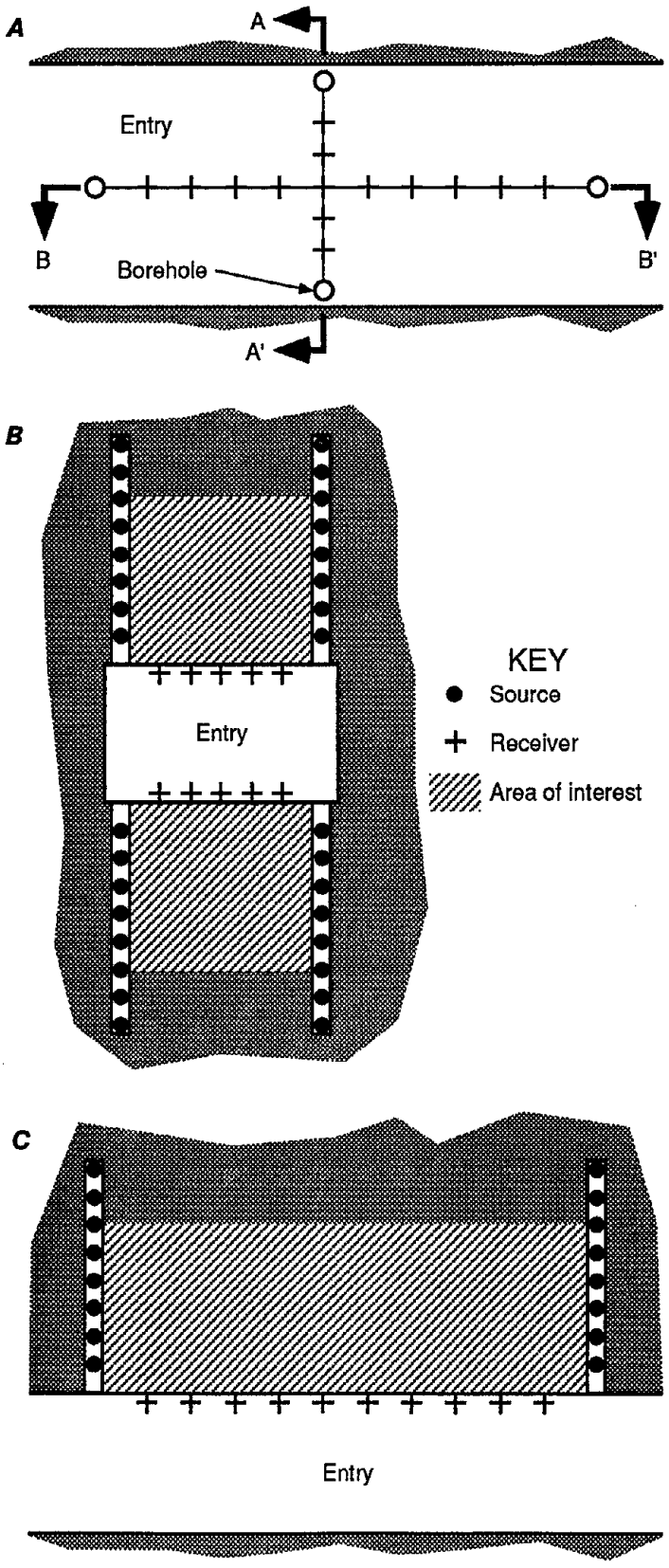

Figure 1.—Typical three-sided seismic surveys of mine roofs and floors. *A*, Plan view; *B*, cross section along A-A′; *C*, cross section along B-B′.

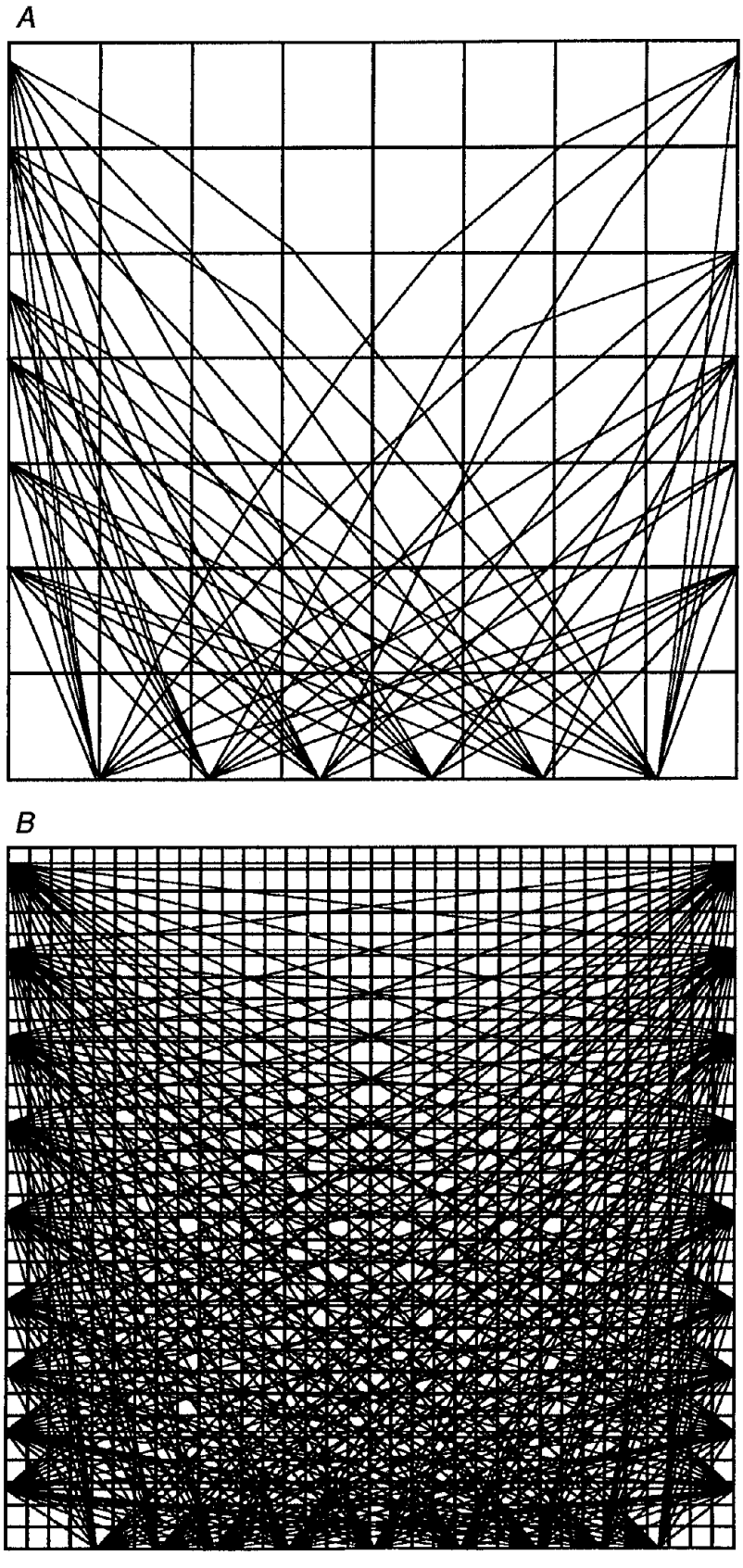

Figure 2.—Typical ray path for three-sided seismic survey in (*A*) mine roof or floor and (*B*) coal pillar.

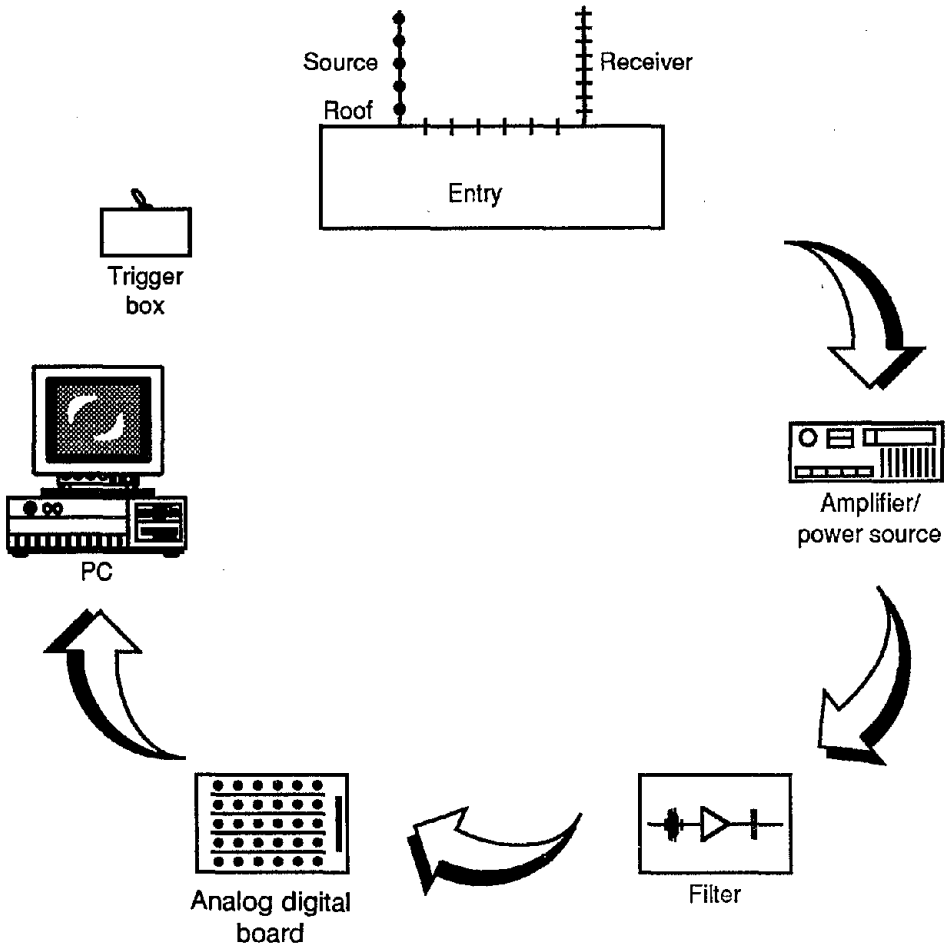

Figure 3.—Data acquisition system.

movement to a high (critical) rate can indicate roof block detachment, loss of support effectiveness, roof shearing by pillars, or impending coal pillar failure.

A history of relative roof deformation is presented in figure 4 for the middle entry of a longwall headgate. The span was 6 m; the immediate mine roof consisted of mudstone overlain by a sandstone channel, and the primary support was 1.2-m-long mechanical bolts and straps.

Roof deformation was monitored by two wire sagmeters, with anchors 1 (at 2.5 m) and 2 (at 1 m) positioned above and below the bolt anchor horizon, respectively. Relative roof movements were calculated. The difference between the two curves in figure 4 reflects bed separation in the mine roof.

After development, roof movements reached 0.05 cm/d, resulting in roof flaking. Installation of posts reduced the rate of roof movement, but did not stop bed separation at the sandstone contact. As the longwall face approached within 100 m of the instrument, bed separation and rate of roof movement significantly increased. Installation of additional support slowed movement, but another accelerated roof movement and bed separation cycle occurred as the longwall face came within 30 m of the instrument. This was followed by a mine roof fall that occurred approximately 4 days after the last accelerated roof movement.

The critical rate of roof movement and the time-to-caving are best established by actually monitoring unstable mine roofs. A critical rate of roof sag of 0.05 cm/d was

determined based on a total of 142 measurements in 3 mines with 6-m spans and stable pillars (table 2). This critical rate was based on roof sag measurements along the gate roads of five panels where no secondary support had been installed. Installation of secondary supports generally stabilized roof movements; therefore, measurements taken near secondary supports were excluded from the study. Maleki (1993a) has established these same caving parameters for another four pillar-pulling operations where spans are gradually increased to 15 m and pillars crush to residual strength.

Table 2.—Critical rate of roof sag for three mines using 6-m spans

Mine	Critical rate, cm/d	Time-to-caving, days	Number of measurements
1	0.06	2- 8	115
2	[1]0.08	NAp	24
3	0.05	9-11	3

NAp Not applicable.
[1]No failure was recorded, but area was stable.

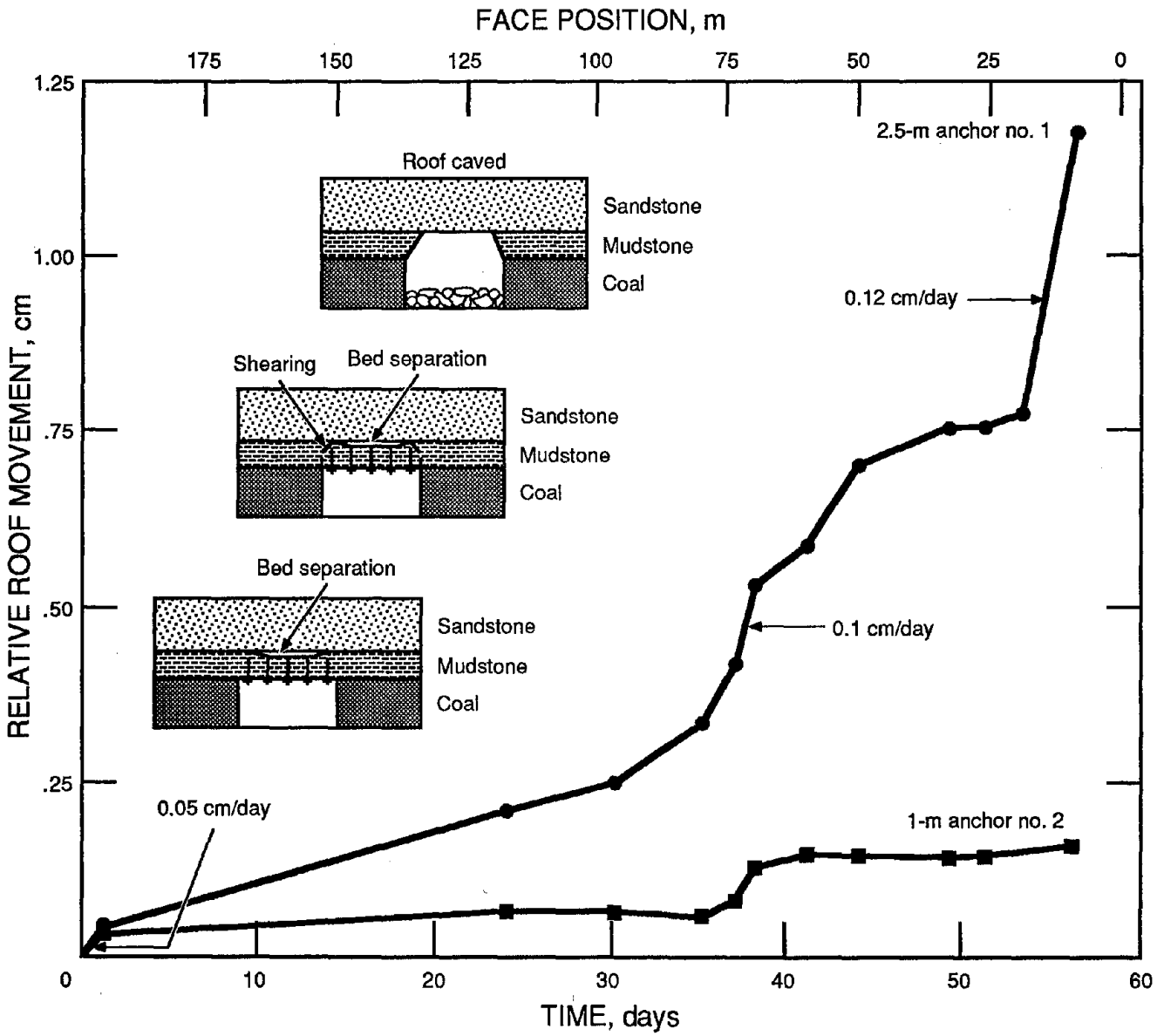

Figure 4.—Relative mine roof movement history for a longwall gate road.

SEISMIC VELOCITY AND ROOF DEFORMATION

A detailed instrumentation plan was developed to measure changes in seismic velocity patterns in mine roofs and to relate these measurements to roof stability and support requirements. These measurements were completed in a shaley mine roof. The plan consisted of—

- Crosshole seismic surveys at 1-month intervals,
- Biweekly deformation measurements in the mine roof, pillar, and floor,
- Biweekly stress change measurements within the seam, and
- Mapping, corehole observations, and core testing in the mine roof either during monthly monitoring or at the beginning and end of the monitoring program.

The instruments were installed in a three-entry development system using 5.2- by 13.4-m pillars and 5.2-m spans at depths of 430 m. Figure 5 shows the instrument layout, mining geometry, and crosshole seismic layout. Accelerometers were attached to the mine roof and installed in a receiver hole using a setting device. An impact unit was used as the seismic source. A tomographic image of velocity patterns in mine roof was constructed along section B-B′.

An array of extensometers was installed in the test area to measure relative mine roof movements. The extensometers were anchored 1.8 and 3.1 m above the roof. In addition, borehole observations were made at locations B and B′ (figure 5) with a borescope to map fracture propagation in the roof and to observe changes in roof moisture during the monitoring period. Two cores were obtained from the roof so that physical properties at the beginning and end of the monitoring program could be compared. Roof appearance was also mapped to monitor development of fracture patterns.

Seam instruments consisted of vibrating wire stressmeters placed in the coal pillars and the solid block, and rib dilatation pins anchored 0.6, 1.2, 2.1, and 2.7 m into the pillar. These measurements were taken to monitor pillar yielding, but are excluded from this discussion.

Significant changes in seismic wave velocities, amount of roof separation, and number of roof fractures occurred during the monitoring period. Supplementary support, consisting of 2.4-m-long fully grouted resin bolts and straps to control roof deformation, was installed on day 80. Roof and floor movements and pillar dilation were all large, indicating rock failure and complex strata interactions around the mining excavation.

Wave velocities were reduced by 22% at the B intersection and by 15% at midpillar during the 120-day monitoring period. Figure 6 and table 3 demonstrate the calculated changes in dynamic properties and relative roof deformation.

Table 3.—Calculated changes in dynamic properties

Factor	*Change, %*
Seismic velocity	21
Maximum amplitude	22
Dominant frequency	48
Deformation modulus	51
Poisson's ratio	125

A preliminary relationship between velocity changes and supplementary support requirements may be established for this mine using these measurements. On day 80, wave velocities were reduced by approximately 17% at the intersection because of increased fracturing and possible roof destressing (Maleki, 1993b). The roof had deformed 60 mm since development. Changes in wave velocity greater or equal to 15% may be used as a criterion for allocating supplementary support.

ROOF STRESS PATTERN

Stress measurements can be a valuable technique for analyzing stress concentrations, destressing, and failure zones in a mine roof when these measurements are compared with expected stress patterns calculated with elastic models. Recent overcoring stress measurements in two vertical holes drilled in a coal mine roof illustrate the use of full stress measurement profiles to assess failure zones and support requirements (Maleki and others, 1994). This analysis differed from conventional measurements for the quantification of the stress field.

The measurements were taken along the main entries of a Colorado mine under a high horizontal stress field. Failure in the mine roof is influenced by both stress concentrations in the mine roof and variations in strength and stiffness of roof rocks. The roof consists of thinly bedded siltstones; massive, fine-grained sideritic siltstones that grade laterally to dark gray limestone; and sandstones.

Figure 7 presents expected stress conditions in (*A*) an elastic mine roof and (*B*) a roof with both elastic and inelastic (brittle and delamination) zones. These generic

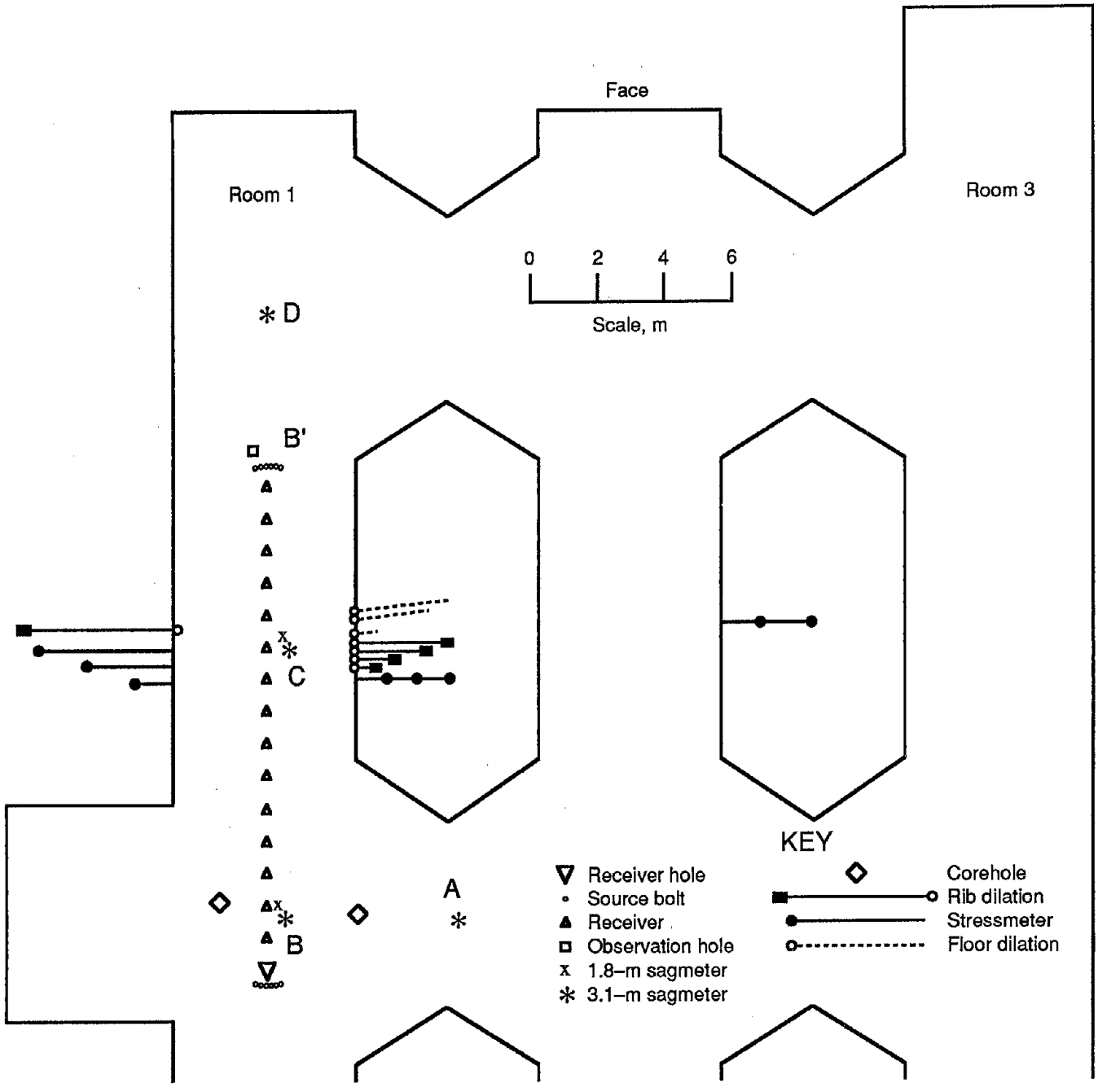

Figure 5.—Instrument layout and face position for mine roof seismic application.

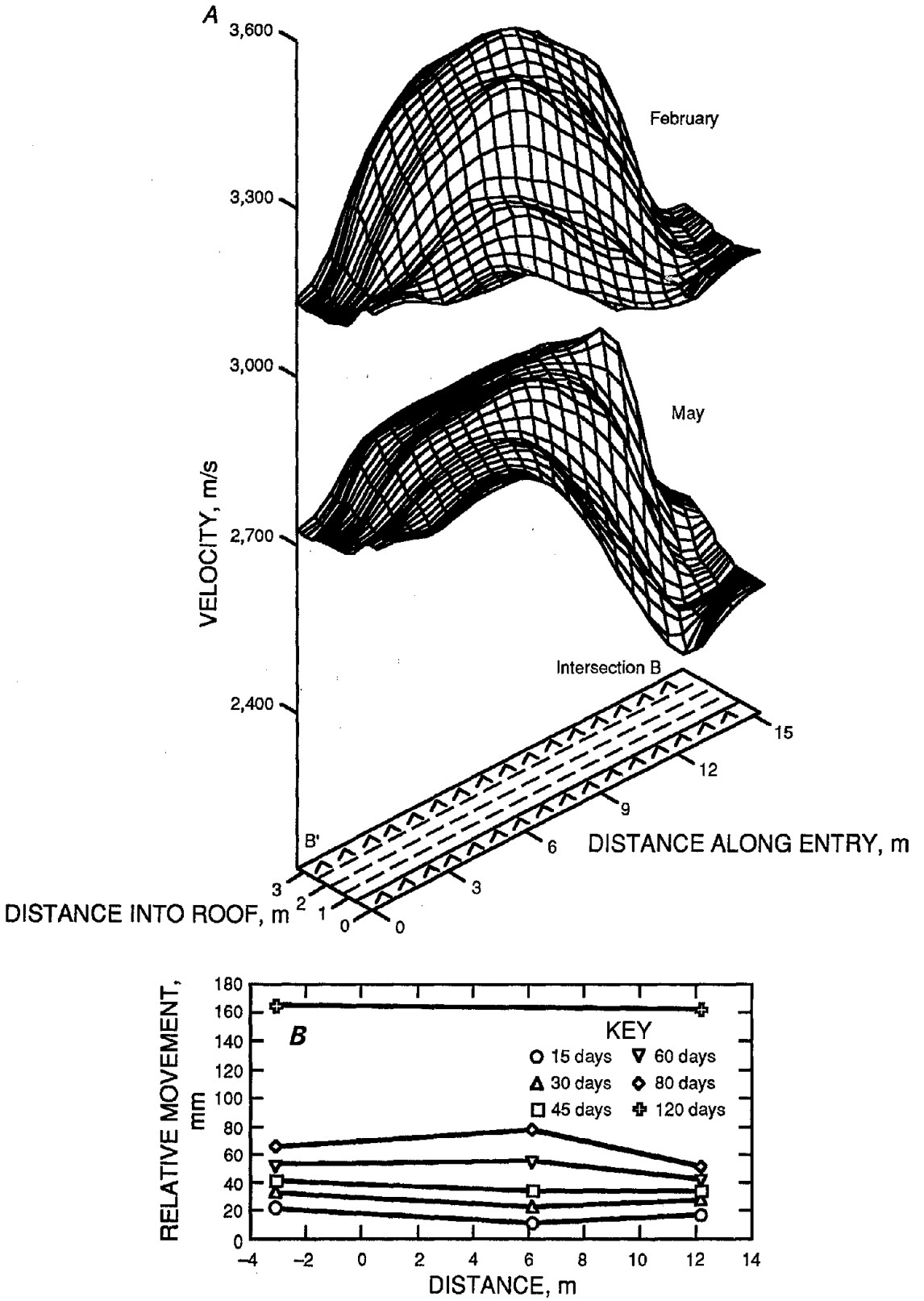

Figure 6.—History of roof velocity and deformation along B-B′ during 120-day monitoring period. *A*, Velocity; *B*, deformation.

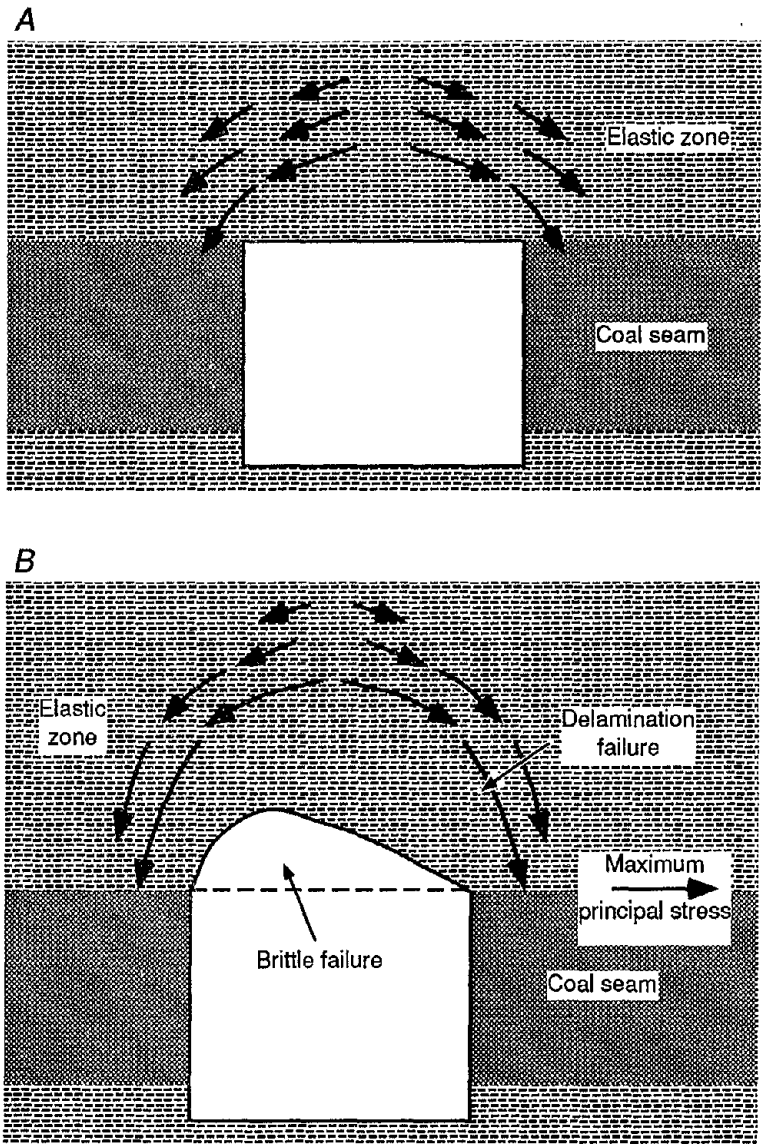

Figure 7.—Principal stresses in mine roof for (*A*) elastic and (*B*) inelastic strata conditions.

models were developed using underground observations, stress measurements, and comparison of the results to numerical models with both elastic and inelastic material behaviors. In the elastic roof (*7A*), the principal stresses concentrate near the immediate mine roof, whereas within the brittle/laminated roof (*7B*), the stresses shift deeper into the roof as a result of failure and partial destressing. Figure 8 presents the maximum (P) and minimum (Q) measured horizontal stress profiles in the mine roof, supporting the generalized models of figure 7. Figure 8*B* suggests that partial failure in the mine roof extends to a distance of 3 m. This zone requires support and reinforcement to prevent time-dependent collapse of the immediate roof.

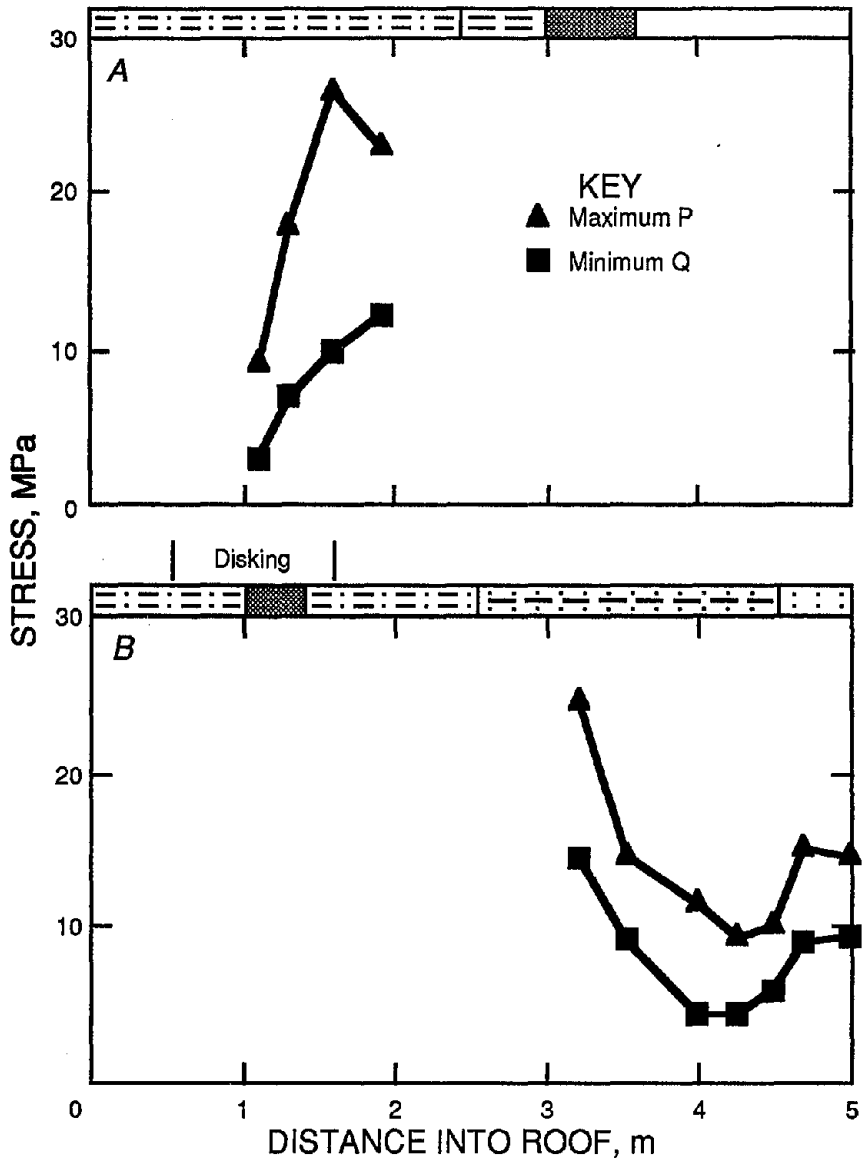

Figure 8.—Measured horizontal stress profiles in mine roof. *A*, Elastic roof; *B*, inelastic immediate roof.

CONCLUSIONS

Practical applications of three methods of evaluating structural stability are presented. Preliminary stability criteria were developed using extensive measurements obtained during the last decade from ten U.S. mines. These methods involve measuring changes in deformation, fracturing, and stress conditions to infer structural stability.

Obtaining deformation measurements is simple, inexpensive, and reliable. These measurements can be used quickly to assess structural stability, thereby enhancing mine safety and improving the decisionmaking process. Measurements of dynamic properties can provide a precise assessment of rock fracturing and support requirements along the entire length of an area of interest. Obtaining these measurements is more costly than obtaining deformation measurements. Therefore, this method is most suitable for detailed structural stability evaluations. Stress profiling can be achieved simply during measurement of far-field horizontal stresses, providing helpful information on strata inelastic behavior and support requirements. This method is most useful for mines experiencing stress-induced stability problems.

REFERENCES

Aggson, J. R. Coal Mine Floor Heave in the Beckley Coalbed, An Analysis. USBM RI 8274, 1978, 32 pp.

Bickel, D. L. Rock Stress Determinations From Overcoring—An Overview. USBM Bull. 694, 1993, 146 pp.

Friedel, M. J., M. J. Jackson, D. R. Tweeton, and M. S. Olson. Application of Seismic Tomography for Assessing Yield Pillar Stress Conditions. Paper in Proceedings of the 12th Conference on Ground Control in Mining, ed. by S. S. Peng (Morgantown, WV, Aug. 3-5, 1993). Dept. of Min. Eng., WV Univ., Morgantown, WV, 1993, pp. 292-296.

Hilbert, D. The Classification, Evaluation, and Projection of Coal Mine Roof Rocks in Advance of Mining. Pres. at Annu. Meet. AIME, 1978, 27 pp. Available from H. Maleki, USBM Spokane Research Center, Spokane, WA.

Jung, Y., A. Ibrahim, and D. Born. Mapping Fracture Zones in Salt. Geophysics: The Leading Edge of Exploration, Apr. 1991, pp. 37-39.

Maleki, H. The Application of Deformation Measurements for Roof Stability Evaluation. Soc. Min. Eng. AIME preprint 93-197, 1993a, 7 pp.

_____. Case Study of the Inelastic Behavior of Strata Around Mining Excavations. Rock Mechanics in the 1990s. Paper in Proceedings of the 34th U.S. Symp. on Rock Mechanics, ed. by B. Haimson (Madison, WI, June 27-30, 1993). Geol. Eng. Prog., Univ. WI—Madison, v. 2, 1993b, pp. 717-720.

_____. Detection of Stability Problems by Monitoring Rate of Roof Movements. Coal Age, Dec. 1988a, pp. 34-38.

_____. Ground Response to Longwall Mining. CO Sch. Mines Q., v. 83, No. 3, 1988b, 14 pp.

_____. In Situ Pillar Strength and Failure Mechanisms for U.S. Coal Seams. Paper in Proceedings of the Workshop on Coal Pillar Mechanics and Design. USBM IC 9315, 1992a, pp. 73-77.

_____. Significance of Bolt Tension in Ground Control. Paper in Rock Support in Mining and Underground Construction: Proceedings of the Int. Symp. on Rock Support, ed. by P. K. Kaiser and D. R. McCreath (Sudbury, Ontario, Canada, June 16-19, 1992). A. A. Balkema, 1992b, pp. 439-449.

Maleki, H., W. Ibrahim, Y. Jung, and P. A. Edminster. Development of an Integrated Monitoring System for Evaluating Roof Stability. Paper in Proceedings of the Fourth Conf. on Ground Control for Midwestern U.S. Coal Mines, ed. by Y. P. Chugh and G. A. Beasley (Mt. Vernon, IL, Nov. 2-4, 1992). Dept. of Min. Eng., Southern IL Univ., 1992, pp. 255-271.

Maleki, H., Y. Jung, P. A. Edminster, and W. Ibrahim. Application of a Static and Geophysical Monitoring System for Detection of Stability Problems. Paper in Proceedings of the 12th Conference on Ground Control in Mining, ed. by S. S. Peng (Morgantown, WV, Aug. 3-5, 1993). Dept. of Min. Eng., WV Univ., Morgantown, WV, 1993, pp. 125-132.

Maleki H., R. W. McKibbin, and F. M. Jones. Stress Variations and Stability in a Western U.S. Coal Mine. Pres. at Soc. Min. Eng. AIME Annu. Meet., Albuquerque, NM, Feb. 14-17, 1994, 10 pp. Available from H. Maleki, USBM Spokane Research Center, Spokane, WA.

Repsher, R. C., and B. Steblay. Structure Stability Monitoring Using High Frequency Microseismics. Paper in Research and Engineering Applications in Rock Masses. Proceedings of the 26th U.S. Symp. on Rock Mechanics, ed. by Eileen Ashworth (SD Sch. Mines and Tech., Rapid City, SD, June 26-28, 1985). A. A. Balkema, v. 2, 1985, pp. 707-713

Wawersik, W. R., and C. Fairhurst. A Study of Brittle Rock Fracture in Laboratory Compression Experiments. Int. J. Rock Mech. and Min. Sci., v. 7, No. 5, 1970, pp. 561-575.

Westman, E. C. Characterization of Structural Integrity and Stress State Via Seismic Methods: A Case Study. Paper in Proceedings of the 12th Conference on Ground Control in Mining, ed. by S. S. Peng (Morgantown, WV, Aug. 3-5, 1993). Dept. of Min. Eng., WV Univ., Morgantown, WV, 1993, pp. 322-327.

AUTOMATED MONITORING AND GEOTECHNICAL EVALUATION FOR GROUND CONTROL IN LONGWALL MINING

By John P. McDonnell,[1] Robert M. Cox,[1] and John P. Dunford[2]

ABSTRACT

The U.S. Bureau of Mines (USBM), utilizing commercially available monitoring system technology, is developing computer-assisted processing and analysis techniques for near real-time evaluation of underground coal mine ground conditions. The combination of existing mine monitoring system and sensor technology with automated computer analysis techniques enhances the acquisition, analysis, and display of geostructural data from high-production longwall mining operations.

Underground monitoring system instrumentation networks have been installed at three longwall operations (one in western Colorado and two in central Utah) to collect ground control information to aid in evaluating ground conditions along high-production longwall faces and surrounding gate road entries. The data typically consist of pillar, panel, and shield pressure changes, and strata movements.

Samples of monitoring system results presented in this paper, which combine mine structure data with other information, such as geologic conditions, have provided near real-time information on stress transfer, mine structure pressure buildup, and strata movement associated with several ground control events. The monitoring system network provides the mine operator with information to rapidly identify and manage potentially hazardous ground conditions while mining is in progress.

INTRODUCTION

Ground control is a critical factor in maintaining the safety and efficiency of modern, highly mechanized, and productive underground coal mines. Advancements in the mechanization of underground production equipment have resulted in increased longwall production and panel retreat rates. Rapidly changing ground and stress conditions that accompany high mining rates challenge mine operators to maintain safe working conditions.

The design, implementation, and management of ground control systems are difficult due to (1) the large number of parameters affecting the stability of coal mine openings, (2) the variation of parameters throughout the mine, and (3) the lengthy time required to thoroughly analyze ground conditions and support requirements (*1*).[3] Mine management seldom has sufficient time or resources to review all possible control techniques, and controls are often implemented too late to prevent major problems. The USBM is conducting research to improve the management of ground control systems by combining minewide monitoring technology with automated analysis techniques.

Advances in sensor technology and monitoring systems have improved remote acquisition of underground mining information. Minewide monitoring systems, used to manage many diverse mining activities such as conveyor and ventilation systems, are becoming commonplace in U.S. mines and are improving safety and productivity (*2*).

[1]Mining engineer, Denver Research Center, U.S. Bureau of Mines, Denver, CO.

[2]Mining engineer, Spokane Research Center, U.S. Bureau of Mines, Spokane, WA.

[3]Italic numbers in parentheses refer to items in the list of references at the end of this paper.

Real-time data acquisition, coupled with automated processing, provides important decisionmaking tools for mine management (*3-4*).

The USBM research effort to automate the acquisition and analysis of ground control information is to utilize existing monitoring and sensor technology for data collection, storage, and processing. Data acquisition and analysis are being accomplished using commercially available monitoring system components, instrumentation, and software packages and custom software routines.

This paper provides a general overview of the in-mine application of the monitoring system technology and presents several examples of monitoring system data collection and processing results related to ground control events.

MONITORING SYSTEM COMPONENTS

The instrumentation networks were designed to provide real-time ground control information and data from operating longwall mines for subsequent automated analysis and evaluation tasks. The monitoring system also served as a test facility to evaluate the effectiveness of various instruments and sensors for measuring ground control parameters. The entire system is comprised of commercially available equipment, and all underground components located in return airways are approved by the U.S. Mine Safety and Health Administration (MSHA).

Discussion of the monitoring system components will focus mainly on the instrumentation network installed in the Colorado mine because of the magnitude of the system demonstration there. The data from the Colorado mine, where the USBM has its own monitoring network separate from the mine, are monitored remotely from the mine surface and the Denver Research Center (DRC) mine monitoring laboratory. Computers linked to the DRC system process the mine structure data and generate graphics displays to permit near real-time detailed evaluation of strata control information. The instrumentation networks at the two Utah mines are connected to the respective mine's monitoring system, where the data are collected and stored on the mine's own monitoring and computing equipment (*5*).

The primary ground control parameters measured are shield-leg pressures, ground pressures in the gate road structure (pillars and panels), and strata movements (roof-bed separation and gate road entry closure). Figure 1 shows a generalized schematic of the monitoring system network. The instrumentation layout was designed to continuously monitor shield loading on the longwall face, and ground pressure and strata movement changes at several longwall gate road sites having different pillar configurations and geologic conditions. The numbers of sensors, locations of various monitoring system components, and cable routes and lengths were adjusted throughout the monitoring program as necessary, depending on the specific instrumentation layout (*1*).

COMPUTER CONTROLS

The main computer control station, shown in figure 2, is located at DRC and consists of a Conspec Model 400 Mine Monitoring System computer linked to various graphics and data processing computers. The DRC computer controls communication with the sensors at the mine via a dedicated phone line and displays sensor status. Coupled with the primary computer is a graphics system installed both on a separate computer at DRC and a computer at the mine surface. The graphics computers provide real-time color displays of sensor data and alarm conditions, permanent storage of data on magnetic disk, and printing of detailed reports.

The mine surface installation consists of two modems, a communication monitoring switch, and a secondary computer system for data display and storage. The modems control communication between DRC, the mine surface, and the underground control station (UCS).

UNDERGROUND COMPONENTS

The UCS consists of trunk barriers for the various gate road sites, trunk extenders that supply power to the individual trunk cables, a modem for communication to the mine surface, and an intelligent area controller (IAC). The IAC allows personnel to access sensor information while underground during installation and troubleshooting operations. The UCS is generally located at the outby end of the panel being mined, near or in the main entries, and near an available power supply.

Sensors are connected to the monitoring network through an electronic interface (accessor), which converts the analog signals to digital form for communication and data transmission over trunk cables to the UCS. Each accessor is mounted adjacent to the sensor, as shown in figure 3, to reduce sensor cable signal loss and to minimize damage to sensor cabling. The accessors communicate with the UCS over four-conductor shielded trunk cables

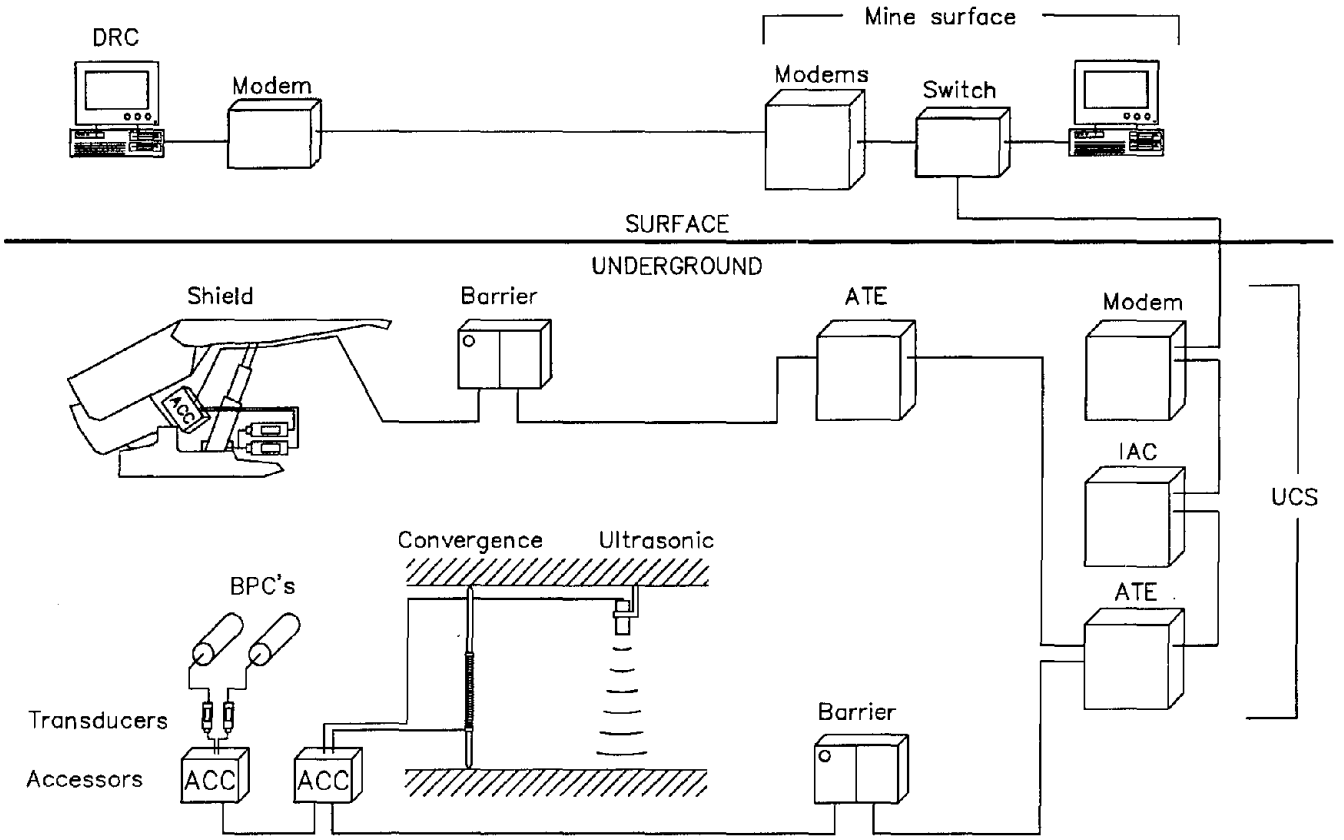

Figure 1.—Schematic of underground monitoring system instrumentation network.

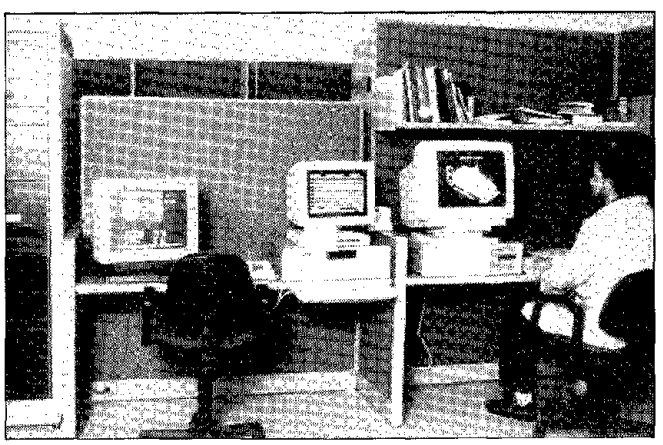

Figure 2.—Main computer control station at the Denver Research Center.

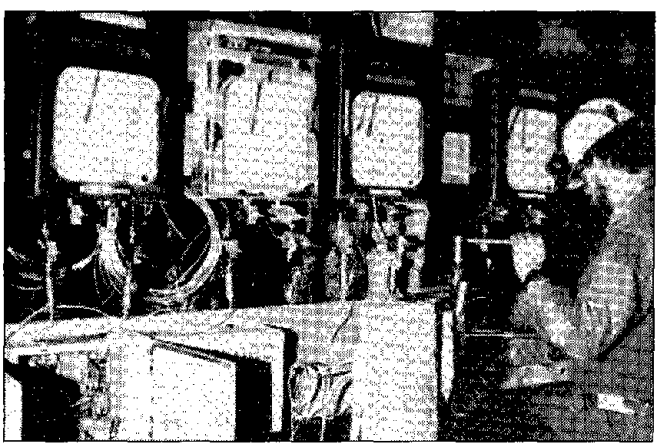

Figure 3.—Gate road instrumentation site showing accessors, transducers, and chart recorders.

that supply power to the accessors and sensors, and transmit bidirectional digital information. Each accessor is individually addressed to permit communication with specific instruments or sensors.

Since all instrumentation sites were eventually located in return airways, the trunk cables along the longwall face and to the instrumentation sites were connected through power barriers that limit both voltage and current to satisfy MSHA permissibility requirements. Limiting the power to each trunk line reduced the number of instruments that could be monitored on a single trunk cable. Consequently, separate trunk cables were required to monitor each test site and the longwall face.

Various geotechnical sensors and instruments (pressure transducers, convergence meters, position transducers, and ultrasonic distance meters) were tested for compatibility with the system. The different sensors are compatible with the monitoring system, using both currently available and custom-designed accessors. In general, the sensors are powered by the trunk line (24 V in fresh air, 14 V in permissible areas) and provide either a voltage or current signal that is converted to 8-bit digital form by the accessor. Sensors being considered for use underground should be durable, have low power consumption, and be classified as permissible. Results from various instrument and sensor types are described later.

MINE DEMONSTRATION

Figure 4 shows a layout of the Colorado mine and the general locations of the monitoring system components and gate road instrumentation sites. Figure 5 shows the barrier pillar test area in one of the two Utah mines.

The instrumentation plans were designed to continuously monitor ground behavior during the high-speed extraction of successive longwall panels under different geologic conditions and different pillar arrangements.

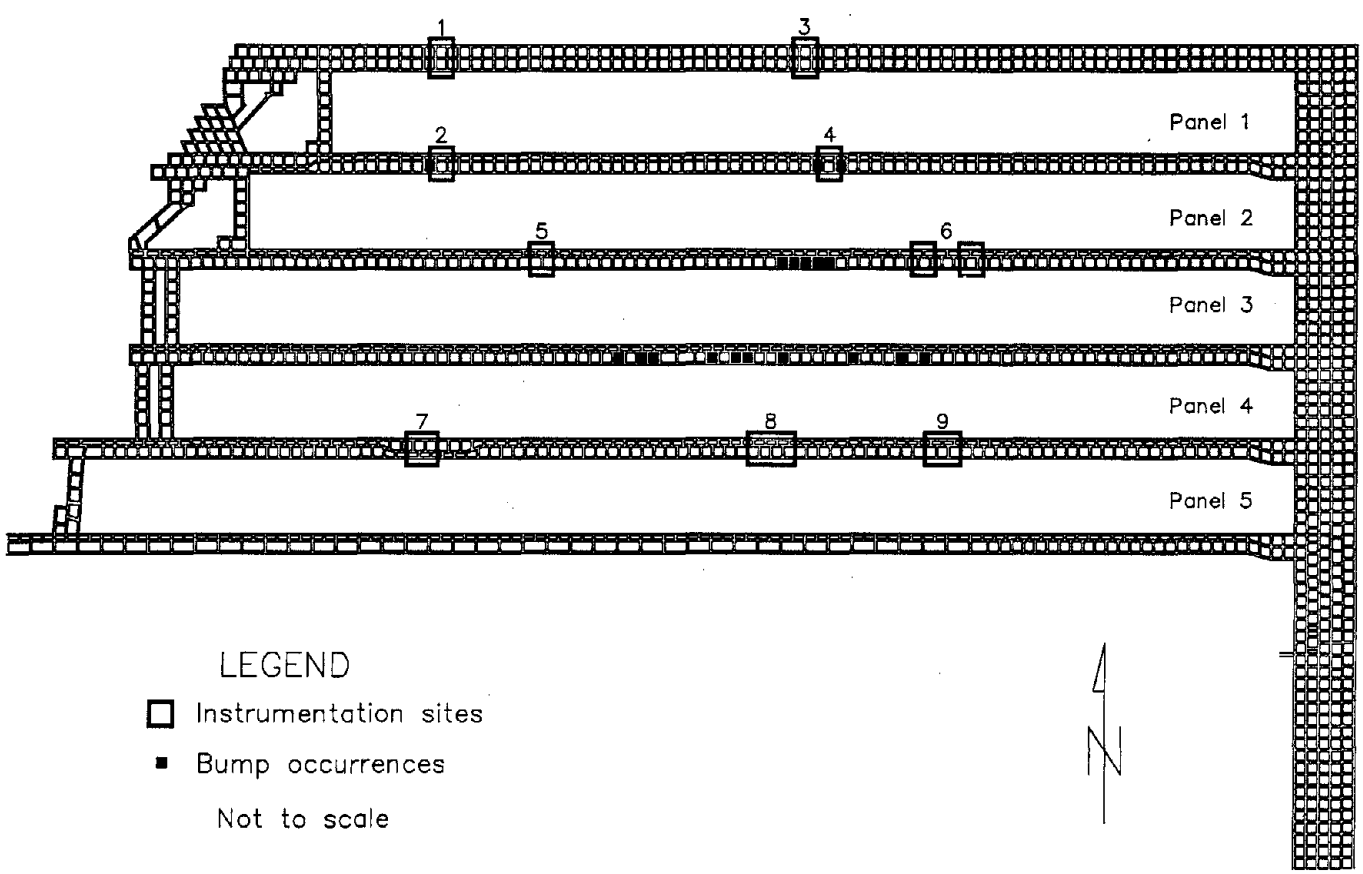

Figure 4.—General mine layout at the Colorado longwall mine.

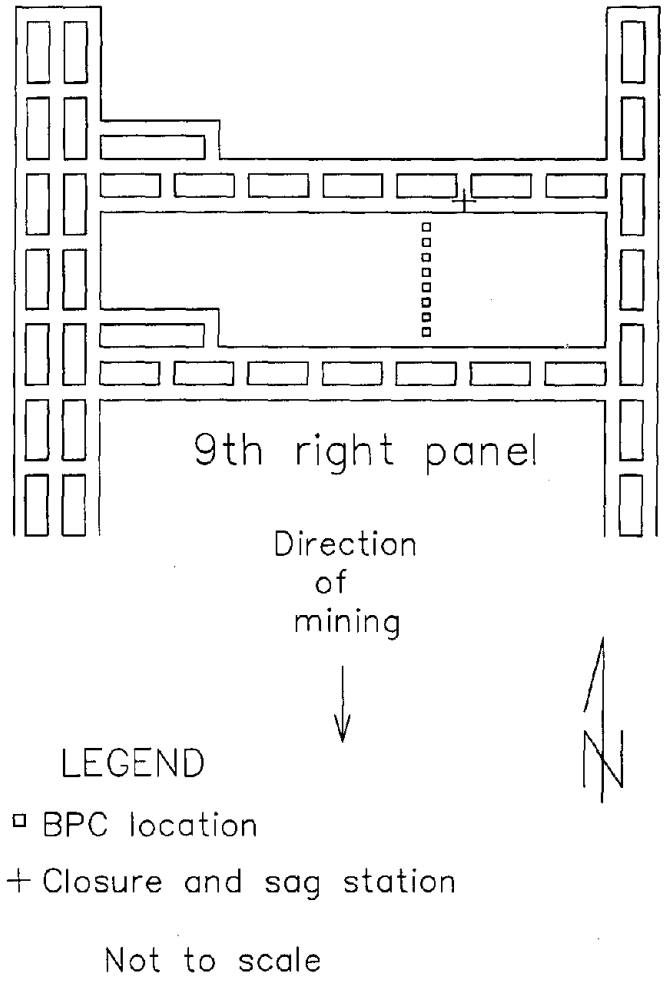

Figure 5.—Layout of barrier pillar test area in a Utah mine.

At the Colorado mine, data have been monitored continuously throughout panels 1 through 5 mining. A total of nine gate road instrumentation sites have been monitored during the extraction of the five longwall panels. Shield-leg pressure data from the longwall faces were collected to analyze shield loading behavior along the longwall face, relative pressure behavior between adjacent shields, and near-tailgate loading related to observed caving conditions. Data from the underground instrumentation network were continuously transmitted via phone modem to computers located at the mine surface and the main control station at the DRC mine monitoring laboratory.

The field site at the Utah mine was instrumented to characterize load transfer to the barrier pillar and bleeder system during longwall mining. No shields were connected to the monitoring network at the Utah mines. Data from the underground test area were transmitted through the mine's monitoring network to the mine surface, where the data were collected and stored on the mine computer. The data were not transmitted directly to the DRC monitoring laboratory (*5*).

SHIELD INSTRUMENTATION

Figure 6 shows the location of monitored shields for each of the five panels in the Colorado longwall mine. Each of the longwall panels were about 195 m (640 ft) wide by 3,050 m (10,000 ft) long and had approximately 130 shields along each face. The location of monitored shields varied from panel to panel to evaluate the influence on shield pressure from the cycling operations of neighboring shields and to assess the pressure changes along the longwall face. The monitored shield concentration near the tailgate was increased as subsequent panels were mined to better define the shield pressure response to tailgate ground control conditions and near-tailgate roof caving behavior.

GATE ROAD INSTRUMENTATION

Pressure transducers were attached to hydraulic borehole pressure cells (BPC's) installed in the gate road structures at the various instrumentation sites. Convergence rods and position transducers were also installed to measure entry closure and strata movements when the respective longwall faces were near the various test areas. Initially, mechanical chart recorders to measure pressure were installed along with the monitoring system pressure sensor components to verify the data obtained from the monitoring system. These were discontinued when it became evident that the monitoring system provided superior data collection accuracy, reliability, and analysis capabilities.

SYSTEM RELIABILITY

An uninterrupted flow of data is crucial for conducting trend analyses and correlating monitored data with field observations. Special modifications were made to the equipment to ensure system reliability, such as encasing the trunk cable on the longwall face in reinforced hose, fabricating custom enclosures for the components on the longwall face, relocating accessor enclosures to less hazardous areas on the lemniscate assembly of the shields, upgrading and eliminating wiring connectors, and applying waterproofing coatings to accessor cards.

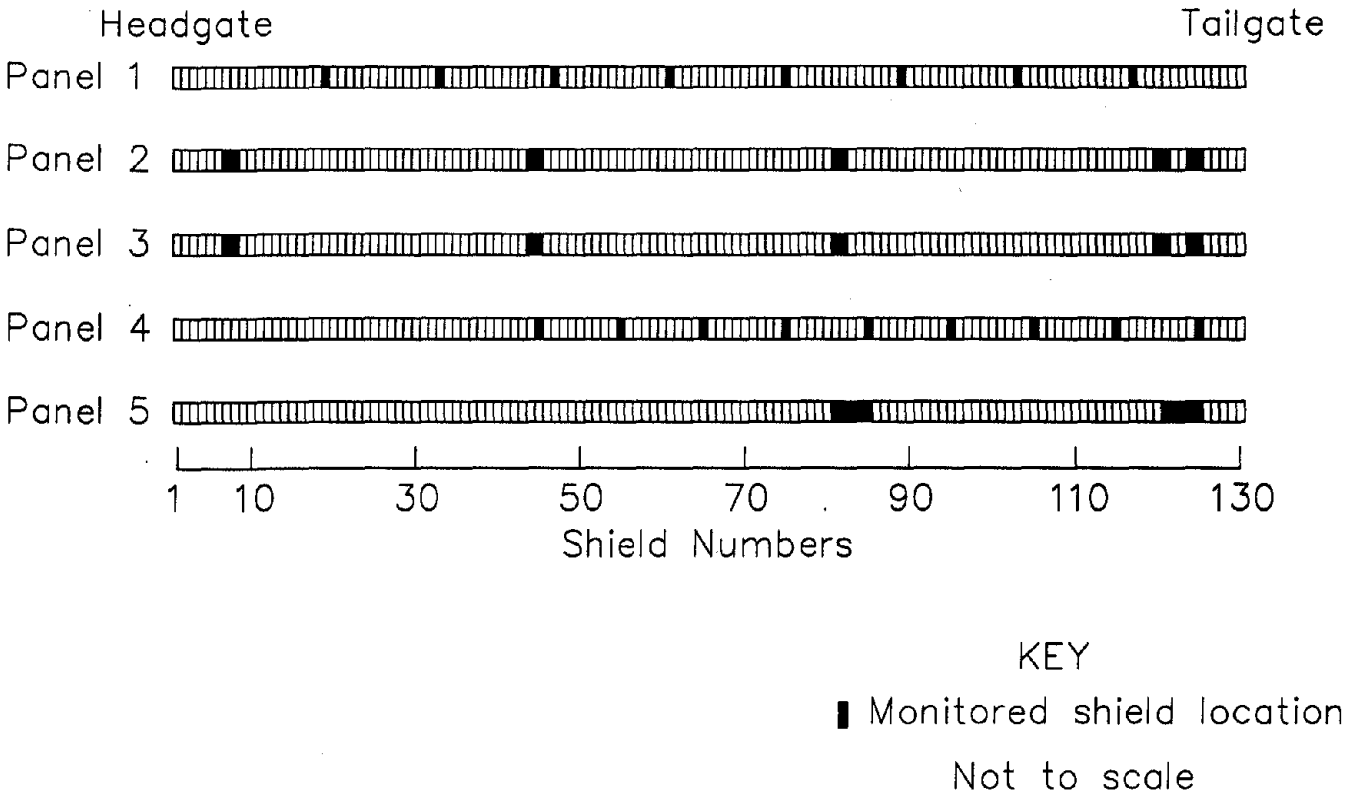

Figure 6.—Shield monitor locations for panels 1 through 5 at the Colorado longwall mine.

Overall reliability of the monitoring system, including downtime from both external sources (telephone and power) and internal sources (cables, components, and sensors), is approximately 85%. Data collection reliability of the BPC, convergence, and roof sag instrumentation sites, which are located away from the moving machinery in the active face areas, has generally exceeded 90%.

DATA PROCESSING AND EVALUATION

The continuous evaluation and management of ground control hazards associated with high-production mechanized longwall mining depends on the ability to monitor, process, and analyze geotechnical data in real-time. This section will discuss techniques developed for managing and analyzing the large quantities of information supplied by the monitoring network.

The processing and analysis operations have been performed using a variety of commercial and custom software. Figure 7 illustrates the general sequence of data management and analysis. The data collected from the underground instrumentation network are combined with other pertinent information, such as face position and geologic conditions, and analyzed using various techniques.

An advantage provided by the automated monitoring systems over conventional data collection methods is the real-time display and conversion of sensor data to engineering units, which permits timely viewing by the mine engineering and operations staff. Significant or anomalous ground behavior changes can be rapidly identified to alert the mine operator in sufficient time to implement any necessary remedial action. With manual data collection techniques (mechanical recorders, dataloggers, etc.), the data records must physically be collected from the measurement site (retrieving charts and/or storage modules, manually reading instruments, taking measurements, etc.), digitized, and inputted to the computer (or manually plotted) before analysis can begin. With the automated

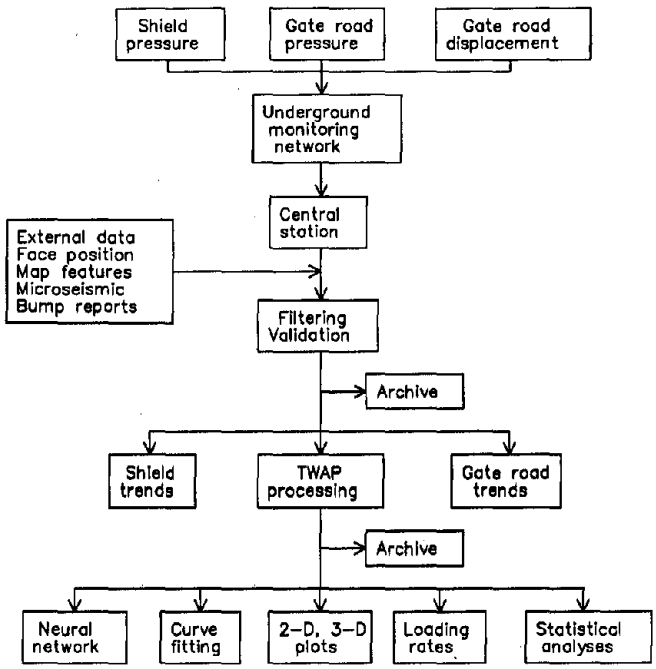

Figure 7.—Data management flowchart. TWAP = time-weighted-average pressure.

data collection system, large quantities of information and data are collected and processed automatically and continuously.

Management of the monitored data consisted of evaluation of the quality of the data through inspections of trend plots, conversion of the binary data to formats more suitable for analysis, and archiving of the data for future use. In addition, external data were digitized to enable inclusion of geologic data, bump occurrences, and longwall face positions into the analyses.

DATA MANAGEMENT SOFTWARE

The main control station computer at the DRC mine monitoring laboratory and the secondary computer system at the mine surface provide a permanent record of the monitored data as stored binary files. Because of the many pressure changes that occur during shield cycling activities, data files for 1 day occupy approximately 2.5 megabytes of disk space. Managing the large volume of shield pressure data required custom software routines to automate the data processing and editing functions.

Data management primarily involves reducing data file size to minimize data storage space requirements and to facilitate more rapid data processing during subsequent analysis procedures. Under normal operating conditions, the shield-leg pressure data have continual small pressure changes, approximately 0.1 to 1 MPa (14.5 to 145 psi), owing to the shield operation characteristics. Data file size is reduced by ignoring pressure changes less than 0.28 MPa (40 psi).[4] Additionally, periods of sensor and/or monitoring system communication interruption of less than 1 min are also eliminated from the data file storage. The resulting data files occupy only about 10% of the original file storage space. The file size is further reduced for storage using commercial data compression software.

Most of the analysis programs require input data in the form of text files, listing the data in engineering units for selected instruments at specific time intervals. Custom software was written to convert the binary data files into an appropriate format, and a commercial spreadsheet was also used to reformat the data and to combine the monitored data with external data, such as face positions. Data management also involved digitizing mine layout and geologic maps to generate base maps for plotting analysis results.

DATA DISPLAY CAPABILITIES

The monitoring system software package provides graphical displays of data in two formats, real-time and trend, for rapid visual analysis. Real-time displays access the monitored data directly and are updated during each scan interval. The color graphics displays depict data in either numeric form or as bar graphs and can be customized by the operator. The trend displays access data files stored on computer disk and permit examining trends from any prior monitoring period.

The capabilities for processing and displaying geotechnical data are best demonstrated by examples. Real-time displays of shield pressure data illustrate some of the parameters being considered for ground control applications. Figure 8, an actual display of shield pressure data from panel 2, shows shield-leg pressures on all eight monitored shields as bars and numeric values (figure 8*A*), and trends of the preceding 30-min interval (figure 8*B*). Examination of this shield data display provides information on shield-leg pressure magnitude and uniformity, rate of pressure increase, and pressure distribution along the face. Once the operator is familiar with the "normal" appearance of the display and shield pressure profiles, any unusual conditions, such as excessive or unequal pressures, can be easily identified. The continuously updated trends shown in figure 8*B* provide plots of shield pressure behavior; the rate and uniformity of shield cycling and the relative sequence of cycling for all monitored shields can be readily observed (*6*). For example, referring to the shield 44 trend plot in figure 8*B*, the unchanging low

[4]0.28 MPa (40 psi) corresponds to one digitizing interval of the monitoring system using 0 to 70-MPa (0 to 10,000-psi) pressure sensors.

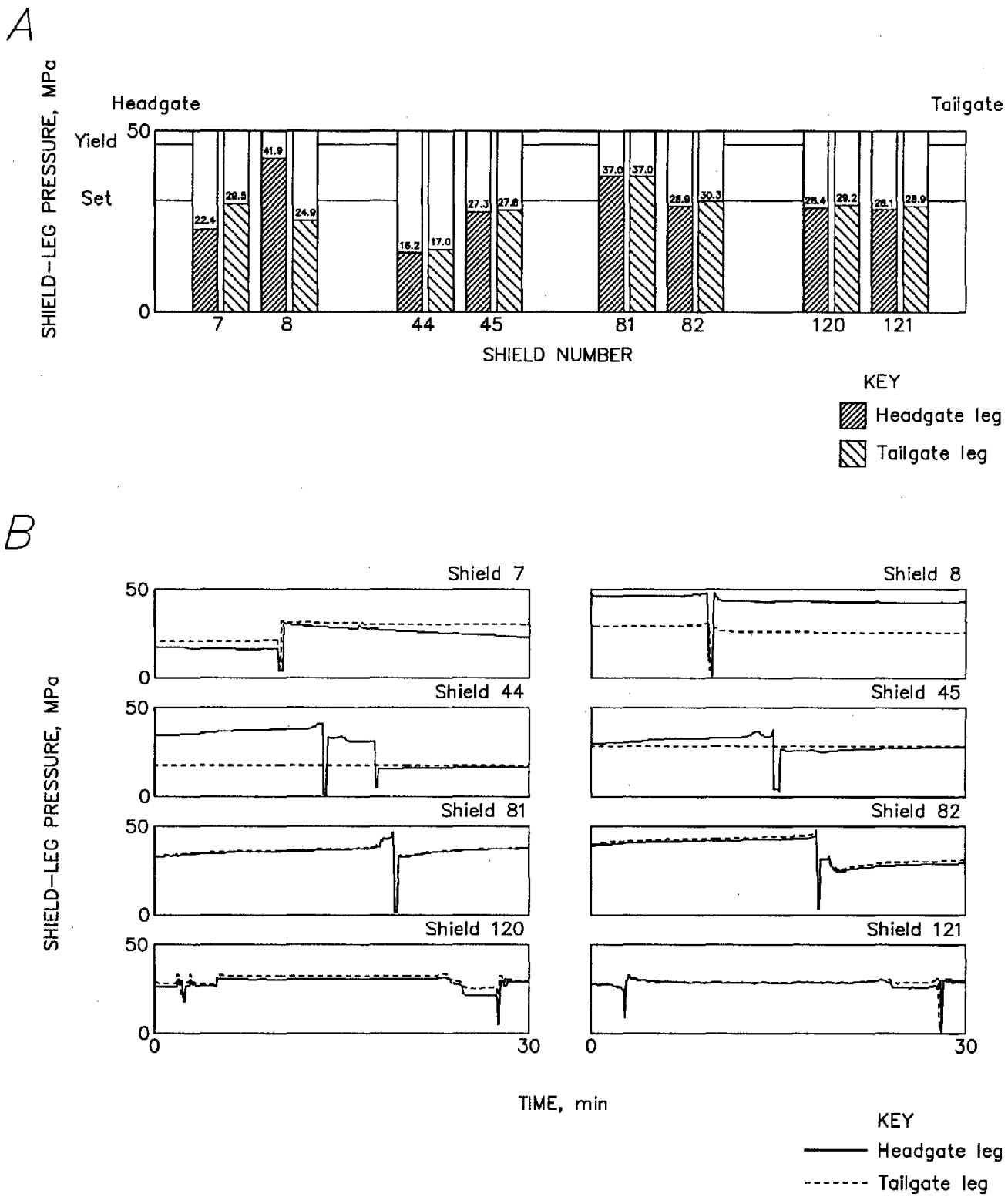

Figure 8.—Display of real-time shield data from panel 2. *A*, Bar graph display with shield-leg pressures. *B*, 30-min trend display.

pressure on the tailgate leg that does not appear to cycle along with the headgate leg could indicate a malfunctioning monitoring system component (sensor or accessor). Again, referring to figure 8*B*, the trend plot for shield 8 indicates uneven leg pressures which may indicate either malfunctioning shield operation or monitoring system components.

Typical shield loading variations during a production shift are shown in figure 9 (*7*). The time scale of the trend displays can be easily varied to examine specific sensor information during any specified time interval. The trend plots are used to evaluate unusual loading conditions that can be examined in greater detail. In addition, the quality of the data can be assessed by identifying abnormal data values caused by malfunctioning instruments, sensors, or other equipment. To identify abnormal data, the operator looks for large differences in headgate versus tailgate leg pressures, unchanging shield pressures in one shield leg during obvious production periods, etc.

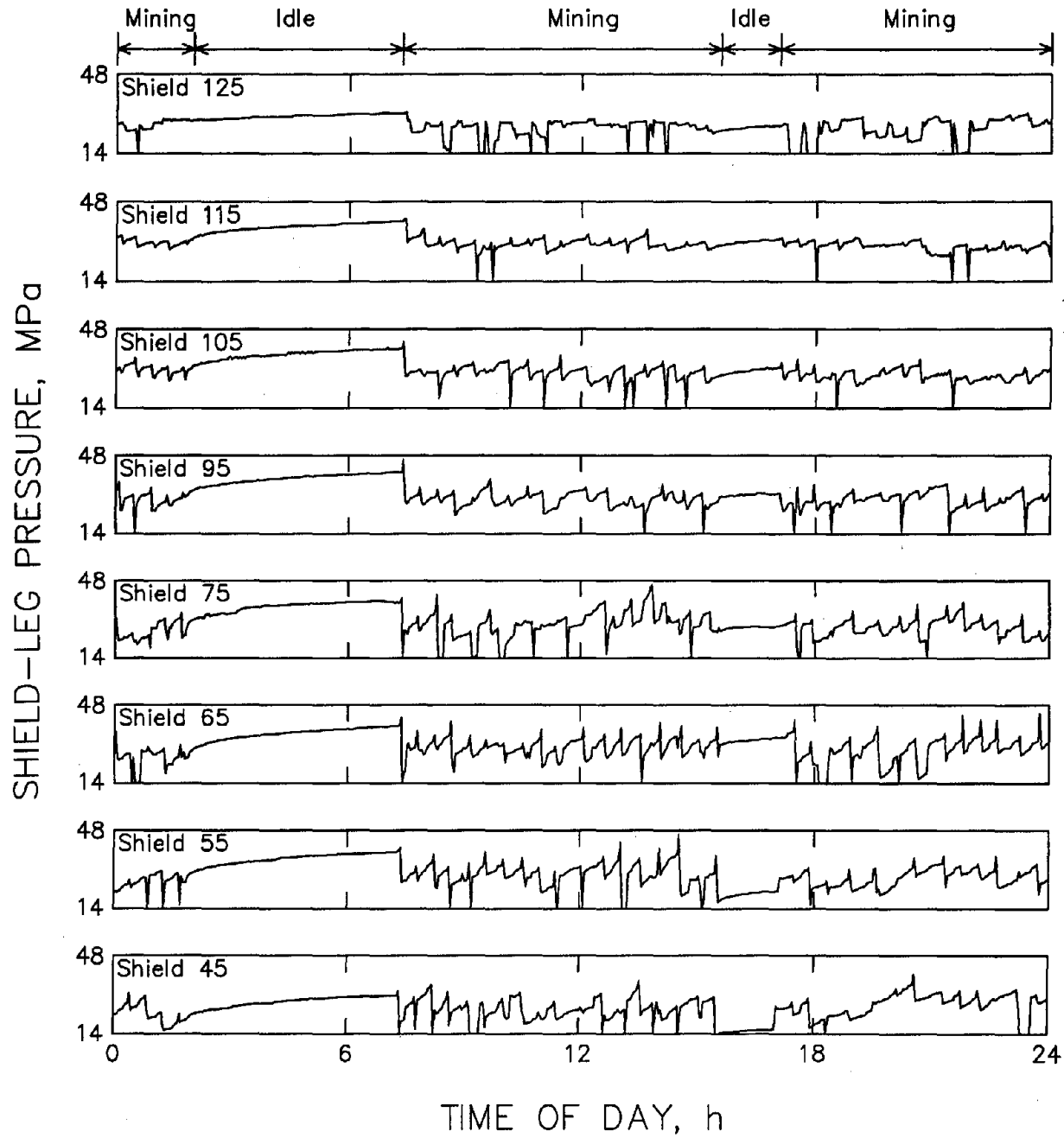

Figure 9.—Shield load variations during a production shift.

DATA ANALYSIS SOFTWARE

Shield data analysis has been primarily concerned with evaluating shield-leg pressure behavior using various parameters calculated from individual shield cycles. Shield data files, obtained from the system software, are processed using custom software to determine the time-weighted-average pressure (TWAP), setting pressure (SP), cycle length (CL), and maximum pressure (MP) for each shield cycle (*1*). Shield data analysis tasks have been handled primarily by a commercial spreadsheet program. Text files containing the shield TWAP information are combined with face position information from the mine production reports and other shield cycle information to evaluate periodic shield loading conditions and load distributions. The TWAP information is compared to the SP and CL values to evaluate the average load changes experienced by the shields during each loading cycle. To provide a consistent basis for comparison, the TWAP data are further processed to remove the effects of long cycle times, low setting pressures, and other conditions associated with operating procedures, rather than changes in ground conditions.

Gate road pressure and strata movement data are also imported into the spreadsheets to evaluate pillar yielding, load transfer behavior, mine roof stability, and entry convergence relative to longwall face position. Several utility programs were developed to improve the efficiency of data importing, editing, and calculation steps. The spreadsheet data are also used to further process and graphically display the data to assist in analysis and presentation.

Additional commercial software includes programs to plot two-dimensional data sets and generate surfaces and contours of three-dimensional data sets. The three-dimensional plots are being used to examine the relationship between high shield pressures, local geological features, and zones of ground control problems. A sample three-dimensional plot, shown in figure 10, illustrates shield TWAP results for panels 2 and 3. In general, the data reveal higher shield pressures toward the tailgate end of the longwall faces.

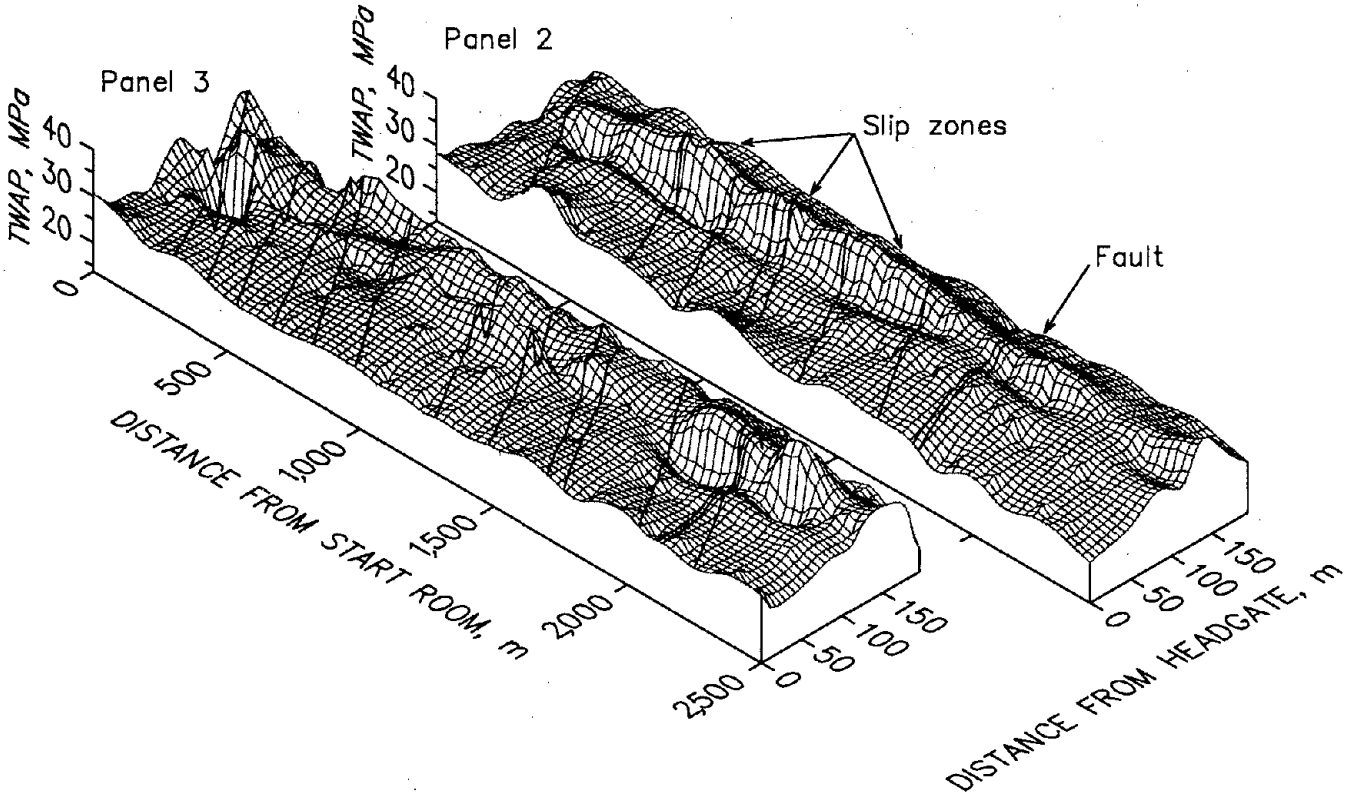

Figure 10.—Comparison of panels 2 and 3 TWAP results with geologic slip zones.

EVALUATION OF GROUND CONDITIONS

The detection and management of ground control hazards associated with high-speed mechanized longwall mining requires real-time monitoring and analysis of geotechnical data combined with a detailed knowledge of the geostructural conditions around the longwall panels. The geotechnical data alone are insufficient to anticipate ground control problems. Geostructural characteristics of the mine site play a significant role in determining ground stability and need to be evaluated along with the geotechnical information (*7*).

Data from the monitoring system network are analyzed to evaluate rock mass behavior during longwall panel mining, with particular emphasis placed on comparing data patterns to observed ground conditions and local geologic settings. Ground conditions at various locations around the longwall panels were investigated through a review of sensor and site data, and in-mine observations. A typical ground control hazard evaluation map was developed, as shown in figure 11 (*7*). The hazard map superimposes contour plots of shield TWAP results for panels 2 and 3

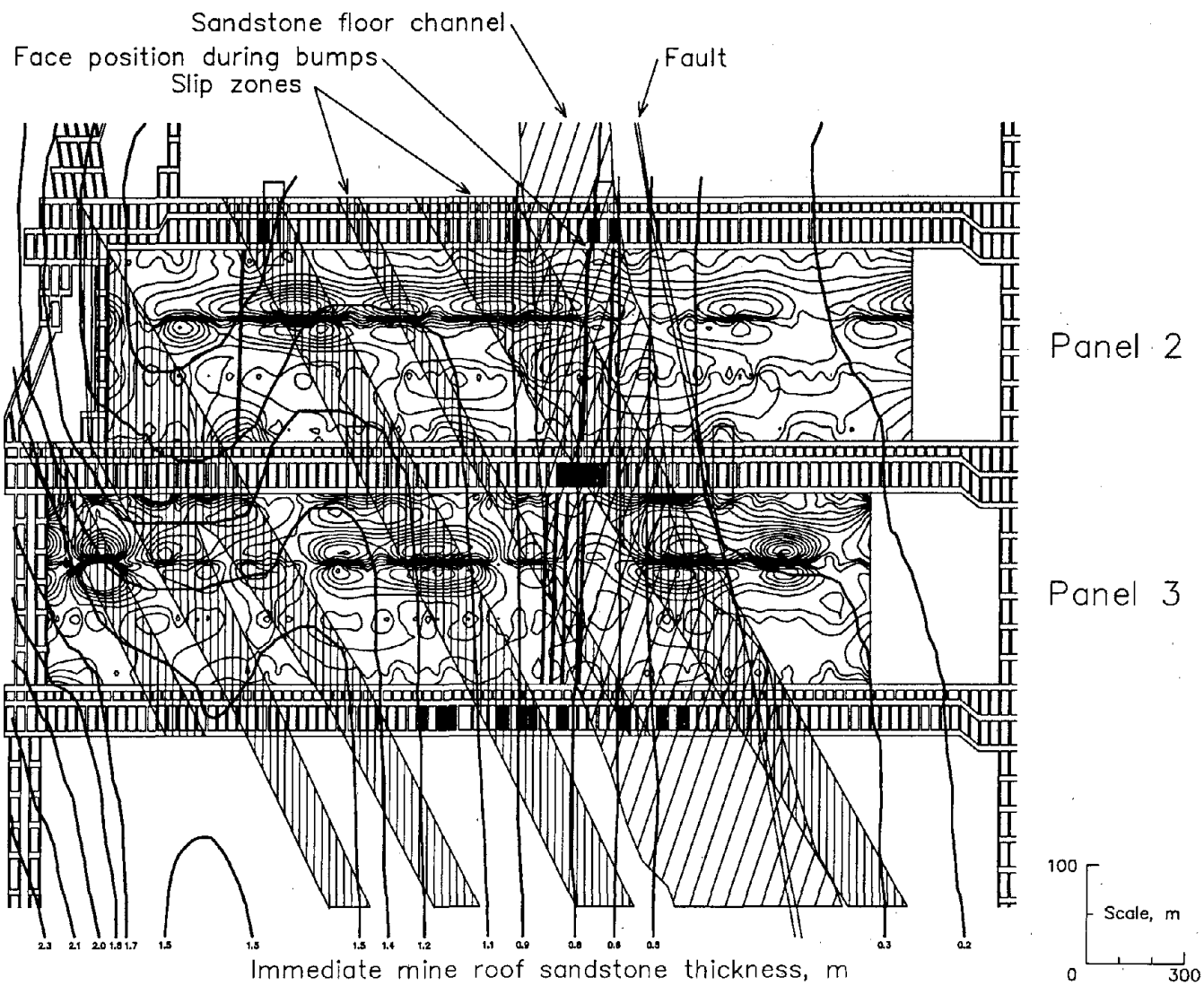

Figure 11.—Ground control hazard evaluation map showing geology, bump locations, and processed shield TWAP data.

along with locations of geologic slip zones and an isopach of the sandstone member thickness in the immediate mine roof. Based on discussions with mine personnel, the local geologic conditions and roof member structure were the most important parameters affecting gate road ground stability. This type of plot, using monitoring system results along with geologic information, provided the mine operator with information to evaluate anomalous pressure behavior associated with specific geostructural conditions. The hazard map, once developed, can be updated in near real-time with monitoring system results for rapid assessment by mine personnel. Appropriate ground control procedures, such as selecting stress control methods or alternative support types for expected recurring problem areas, can then be implemented if necessary.

The following discussion provides additional examples of near real-time data collection, analysis, and results to demonstrate the capabilities and application of the monitoring system to specific ground control events.

GATE ROAD PILLAR AND STRATA BEHAVIOR

Analysis of BPC data is most readily accomplished through examination of the trend plots. Figure 12 is a plot of yield pillar pressure cell readings at site 4 (location of site 4 is noted in figure 4) over a 4-day period as the panel 1 face mined to a position approximately 122 m (400 ft) past the pillar site. The data plotted in figure 12 illustrate progressive pressure decrease (possible pillar yielding) of the pillar edges (cells 1 and 3) coincident with a pressure

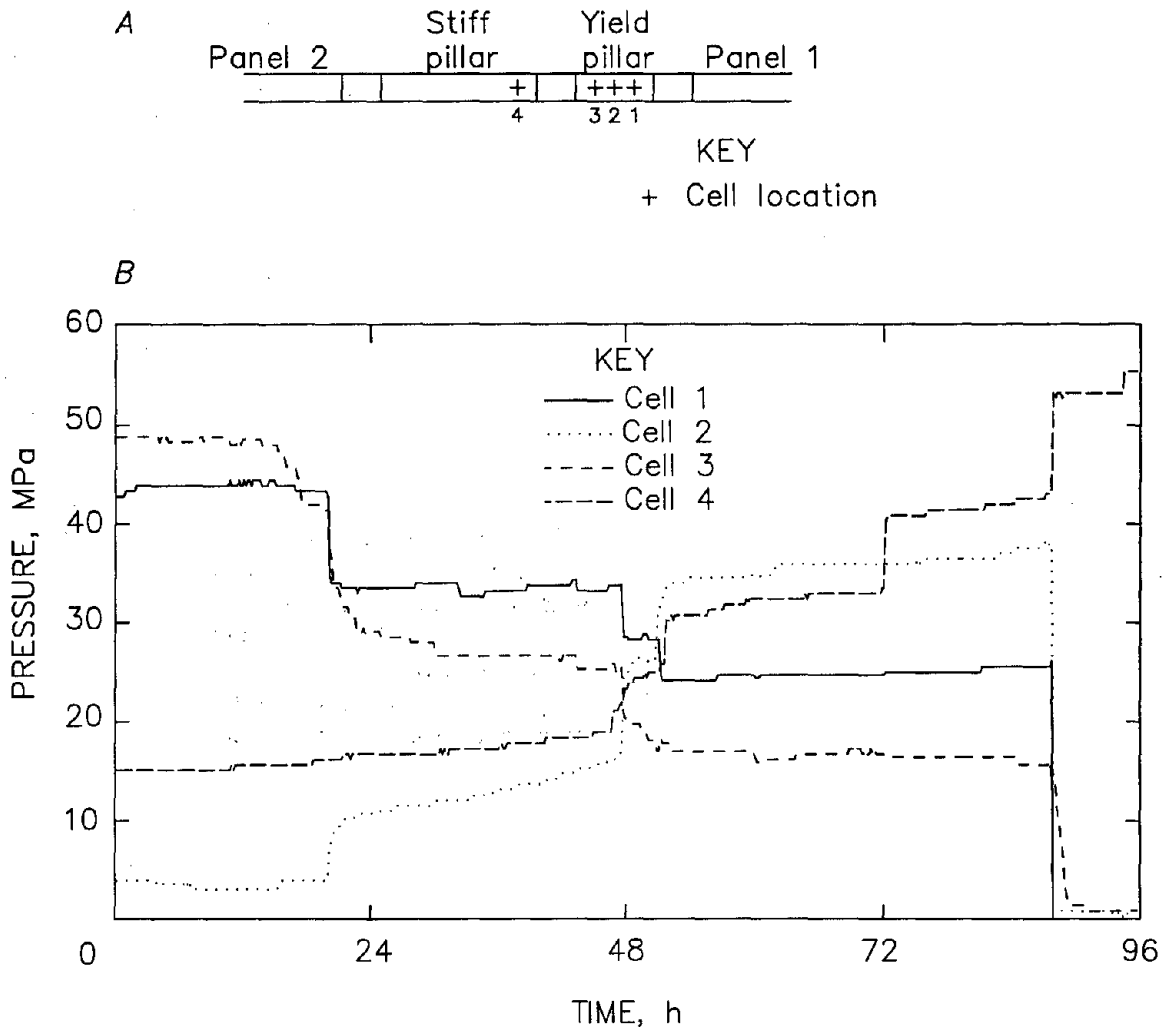

Figure 12.—Yield pillar pressure cell results. *A*, General mine layout showing cell location. Yield pillar width = 10.7 m (35 ft); stiff pillar width = 24 m (80 ft). *B*, BPC pressure results.

increase at the center of the pillar (cell 2). Also, the figure shows an apparent load transfer to the adjacent stiff pillar (cell 4) while pressures were dropping on the yield pillar. All of the pressure and load transfer data are transmitted continuously to the mine surface for rapid assessment by mine engineering and operations personnel.

Other information such as entry closure and roof-bed separation is demonstrated through monitoring system results from the barrier pillar test area at the Utah mine. Figures 13 and 14 illustrate strata movement results during longwall mining operations as the longwall face mined away from the barrier pillar. Rates of closure and roof-bed separation (indicators of changing ground stability) were continually monitored and displayed for the mine operations personnel. At this instrumentation site, no significant ground movement or control problems were encountered. The data are merely presented to illustrate the additional capabilities with various sensors.

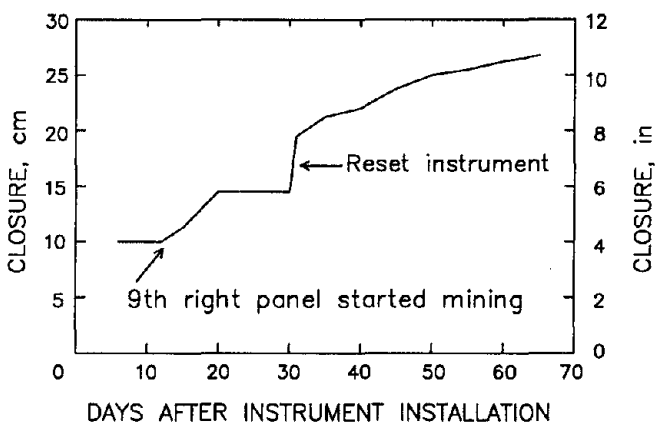

Figure 13.—Convergence results.

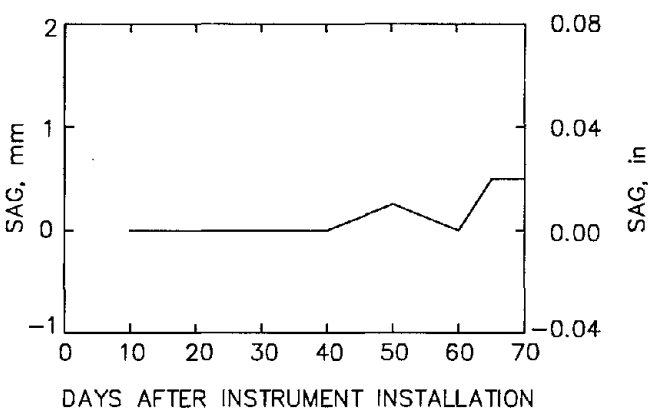

Figure 14.—Roof-bed separation results.

SHIELD LOADING BEHAVIOR

Shield loading analysis has primarily involved identifying anomalous patterns of individual shield cycles. Trends of the shield pressure data have been used to evaluate shield and face loading conditions (*6*). The first example of anomalous shield-leg pressure increases occurred while monitoring the initial caving of panel 2. The leg pressures on the four midpanel shields increased rapidly to yield pressure during two consecutive cycles. Figure 15, a 16-h detail plot of these cycles, shows the rapid pressure increases that occurred in midcycle (about 2.7 h after the start of the plot) and, once again, 1.4 h later. At that time, another large pressure increase occurred. According to mine personnel working at the face, a major roof cave occurred as noted on figure 15 approximately 2 h after the second major pressure increase (*6*).

Rapid pressure increases were also observed on several occasions that coincided with rapid tailgate floor heaves immediately outby the face during panels 2, 3, and 4 mining. Figure 16, a plot of both shield and pillar pressures during a bump at the Colorado longwall mine, displays pressure trend information from the panel 2 shields and from BPC's installed in the tailgate of panel 2 at site 2. Shields 120 and 121, within 12.1 m (40 ft) of the tailgate edge of panel 2, experienced sharp pressure increases in midcycle. The shield pressure increase coincides precisely with similar pressure increases in the BPC's installed in the tailgate stiff pillar at site 2. Approximately 1 m (3 ft) of floor heave occurred adjacent to the tailgate end of the panel 2 longwall face at approximately the same time as the rapid pressure increases in the shields and the stiff pillar. Shields 81 and 82 on the panel 2 face showed no corresponding pressure increase, suggesting that the influence of this tailgate event extended no more than about 61 m (200 ft) into the panel.

Additional tailgate ground control events during panels 2, 3, and 4 (locations shown in figure 4) coincided with rapid shield-leg pressure increases on the near-tailgate shields. Rapid pressure increases of 1.4 to 13.8 MPa (200 to 2,000 psi) occurred in the shield legs in only one scan interval, less than 6 s. Normally, the shield-leg pressure increases by approximately 3.4 to 13.8 MPa (500 to 2,000 psi) over the entire shield cycle, almost 30 min. No corresponding pressure increases were observed on the shields at the center or headgate end of the panel during any of the near-tailgate events. The tailgate events typically involved pillar sloughage, extensive floor heave, and mine roof problems for a distance up to 45.7 m (150 ft) outby the face.

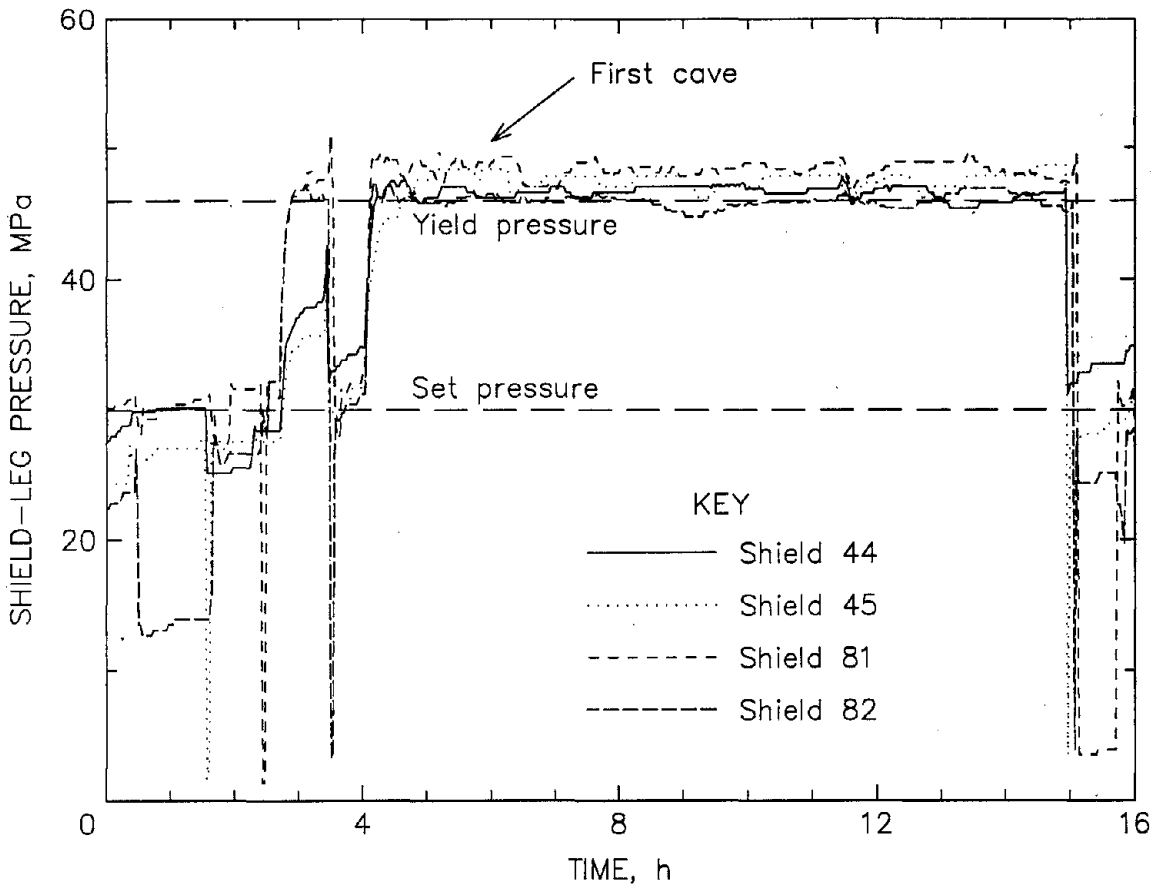

Figure 15.—Shield-leg pressure results during panel 2 first cave.

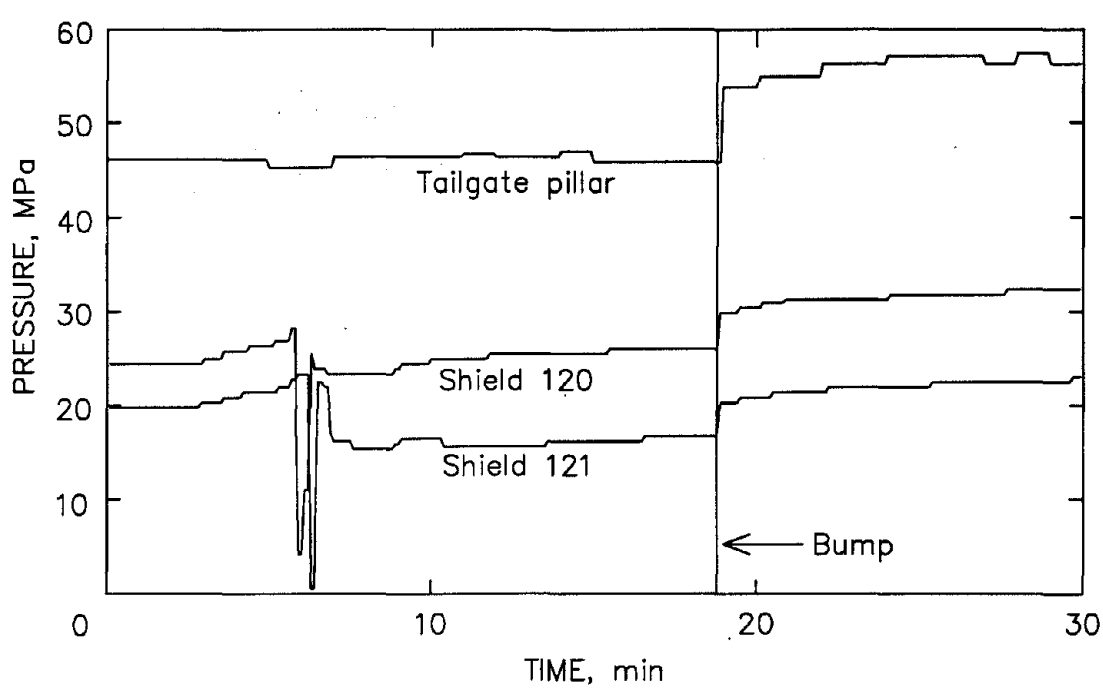

Figure 16.—Simultaneous shield and pillar pressure increases.

SUMMARY AND CONCLUSIONS

The development of an automated monitoring system for coal mine ground control evaluation has greatly improved data quality, access time, and speed of analysis over conventional monitoring methods. Continuous real-time acquisition of underground mine structure information (strata movement and pressure), coupled with automated processing and evaluation of ground conditions, has been demonstrated and has proved valuable in assessing mine structure behavior during longwall production mining. Combining mine structural behavior data with other information, such as local geological conditions, within an automated monitoring and data processing system has provided information on stress transfer and pressure buildup associated with several ground control events. Shield-leg and ground pressure changes, along with strata movement monitoring results, have been used to identify and assess abnormal changes in ground conditions. Real-time stress transfer information, coupled with mine opening convergence and structure deformation information, provides the potential for rapidly and effectively evaluating underground conditions as mining progresses. The monitoring system information, when combined with direct observations by mine personnel, permits a more rapid and complete near real-time evaluation of face area hazardous conditions. As a result, the mine operator can make critical decisions related to coal mine ground control with more information in a more timely manner.

ACKNOWLEDGMENTS

The authors thank David P. Conover of DRC for his significant assistance in the successful installation and operation of the monitoring system networks at the Colorado longwall mining operation and the DRC mine monitoring laboratory. His computer expertise has been utilized to create nearly all of the data displays and analysis capabilities that are now used regularly by numerous research and mine personnel.

REFERENCES

1. Conover, D., K. Hanna, and T. Muldoon. Mine-Wide Monitoring Applications in Ground Control Research. Paper in Proceedings of the 9th Conference on Ground Control in Mining, ed. by S. S. Peng (Morgantown, WV, June 4-10, 1990). Dept. of Min. Eng., WV Univ., Morgantown, WV, 1990, pp. 135-141.

2. Hanna, K., K. Haramy, and T. R. Ritzel. Automated Longwall Mining for Improved Health and Safety at the Foidel Creek Mine. SME Annual Meeting, Denver, CO, Feb. 25-28, 1991, preprint 91-165, 8 pp.

3. Jackson, D. Deserado Gains Edge Through Computer Monitoring. Coal Mining, Dec. 1987, v. 24, No. 12, 3 pp.

4. Zaburunov, S. A., and A. P. Sanda. Mine Monitoring in America. Coal, June 1988, v. 25, No. 6, pp. 34-40.

5. Dunford, J. P., and M. O. Serbousek. Case Studies Using Mine-Wide Monitoring Systems for Geotechnical Evaluations. Paper in Proceedings of the 12th Conference on Ground Control in Mining, ed. by S. S. Peng (Morgantown, WV, Aug. 3-5, 1993). Dept. of Min. Eng., WV Univ., Morgantown, WV, 1993, pp. 152-158.

6. Conover, D., and K. Hanna. Shield Pressure Monitoring To Detect Longwall Ground Control Hazards. Paper in Proceedings of the 4th Conference on Ground Control for Midwestern U.S. Coal Mines, Southern IL Univ., Mt. Vernon, IL, Nov. 2-4, 1992, pp. 217-226.

7. Hanna, K., and R. Cox. Automated Ground Control Management System for Coal Mine Hazard Detection. Paper in Proceedings of the 2nd Int. Conf. on Mine Mechanization and Automation, Luleå, Sweden, June 7-10, 1993, Balkema, pp. 681-689.

* U.S. GOVERNMENT PRINTING OFFICE: 1994-509-021/05000